UNIVERSITÉ DE GENÈVE
Section de Mathématiques
Section de Mathématiques

FACULTÉ DES SCIENCES
Professeur Hugo Duminil-Copin
Professeur Stanislav Smirnov

Universality of the Random-Cluster Model and Applications to Quantum Systems

THÈSE

Présentée à la Faculté des Sciences de l'Université de Genève
pour obtenir le grade de Docteur ès Sciences, mention Mathématiques

par

Jhih-Huang LI
de
Taïpei (Taïwan)

Thèse N°5155

GENÈVE
Atelier d'impression ReproMail
2017

UNIVERSITÉ
DE GENÈVE

FACULTÉ DES SCIENCES

DOCTORAT ÈS SCIENCES, MENTION MATHEMATIQUES

Thèse de Monsieur Jhih-Huang LI

intitulée :

«Universality of the Random-Cluster Model and Applications to Quantum Systems»

La Faculté des sciences, sur le préavis de Monsieur S. SMIRNOV, professeur ordinaire et directeur de thèse (Section de mathématiques), Monsieur H. DUMINIL-COPIN, professeur ordinaire et codirecteur de thèse (Section de mathématiques), Monsieur Y. VELENIK, professeur ordinaire (Section de mathématiques) et Monsieur V. BEFFARA, docteur (Institut Fourier, Université Grenoble Alpes, Saint-Martin-d'Hères, France), autorise l'impression de la présente thèse, sans exprimer d'opinion sur les propositions qui y sont énoncées.

Genève, le 12 décembre 2017

Thèse - 5155 -

Le Doyen

N.B. - La thèse doit porter la déclaration précédente et remplir les conditions énumérées dans les "Informations relatives aux thèses de doctorat à l'Université de Genève".

學而不思則罔，思而不學則殆。

孔子

Abstract

This thesis is divided into two parts: the first part being dedicated to the universality of the random-cluster model and the second to its quantum counterpart and, in particular, to the quantum Ising model.

The random-cluster model is a generalization of Bernoulli percolation, the Ising model and the q-color Potts model. It can be seen as a reweighted Bernoulli percolation with an additional (real) weight parameter $q \geqslant 1$, which is also the number of colors in the Potts model when it is an integer.

These models have been widely studied on planar regular graphs, especially on the square lattice. Critical parameters are known and behaviors at the criticality and away from the criticality are also fairly well understood. Moreover, for the Ising model, by means of the parafermionic observable, we can prove the conformal invariance of interfaces separating different connected components.

In the thesis, we study the random-cluster model on a wider family of (planar) graphs, called isoradial, by proving that the same properties also hold. This family of graphs is interesting due to the following reasons. A parafermionic observable can be defined on such graphs for our model of interest and nice combinatorial properties can be deduced. Along with the complex analysis on isoradial graphs, we may also get some exact relations at the discrete level. Moreover, under star-triangle transformations, the main tool that we introduce in the thesis, random-cluster measures are preserved. This allows us to transport properties, even only conjecturally known, from the square lattice to other isoradial graphs. In particular, results using methods which are specific to the square lattice (such as the transfer matrix formulation) can be obtained on isoradial graphs in this way.

A $(d+1)$-dimensional quantum model consists of d dimensions in space and 1 dimension in time, representing evolution of a quantum state under the action of a Hamiltonian. If we represent both the space and time dimensions graphically, a $(1+1)$-quantum model has a planar representation, and thus, we expect to find the same properties as its planar counterpart.

We define the quantum version of the aforementioned random-cluster model, then compute its critical parameters and determine its behavior at the criticality and away from it. This is an application of the previous part: the quantum random-cluster model can be seen as the limit of its discrete counterpart defined on more and more flattened isoradial graphs. Then, by proving uniform probability bounds on crossing events, we obtain the same properties for the quantum model.

To conclude the thesis, we prove, for the $(1 + 1)$-dimensional quantum Ising model, a classical result of the 2D Ising model: the conformal invariance. We work directly in the quantum setting; in other words, on the semi-discrete lattice $\mathbb{Z} \times \mathbb{R}$.

Résumé

Cette thèse comprend deux parties : la première portant sur l'universalité du modèle de random-cluster et la seconde sur sa version quantique, et plus précisément, sur le modèle d'Ising quantique.

Le modèle de random-cluster est une généralisation de la percolation de Bernoulli, le modèle d'Ising et le modèle de Potts à q couleurs. Ce modèle peut être vu comme une percolation de Bernoulli pondérée à l'aide d'un paramètre supplémentaire $q \geqslant 1$, qui est aussi le nombre de couleurs dans le modèle de Potts lorsque ce dernier est un entier.

Ces modèles ont été beaucoup étudiés sur les graphes réguliers, dont le réseau carré en particulier. Les paramètres critiques sont connus et les comportements au point critique et en dehors du point critique sont plutôt bien compris. De plus, l'observable fermionique pour le modèle d'Ising nous permet de prouver l'invariance conforme des interfaces qui séparent des composantes connexes distinctes.

Dans cette thèse, nous étudions le modèle de random-cluster sur une famille de graphes (planaires) plus large, appelés isoradiaux et nous démontrons que les mêmes propriétés sont aussi satisfaites. Cette famille de graphes ont un intérêt particulier pour les raisons suivantes. Une observable parafermionique peut être définie sur de tels graphes pour les modèles qui nous intéressent et à partir de celle-ci, on peut déduire de bonnes propriétés combinatoires. De plus, avec la théorie de l'analyse complexe sur ces graphes, nous obtenons aussi des relations exactes au niveau discret. Nous introduisons aussi les transformations triangle-étoile, qui jouent le rôle central dans cette thèse. Ce sont des transformations qui préservent les mesures de random-cluster qui transportent des propriétés, même si elles sont seulement conjecturales, du réseau carré à n'importe quel autre graphe isoradial. Ce qui est particulièrement intéressant est que les résultats qui découlent des méthodes propres au réseau carré (les matrices de transfert par exemple) peuvent aussi être obtenus de cette manière.

Un modèle quantique de dimension $(d+1)$ contient d dimensions en espace et une en temps, qui représente l'évolution d'un état quantique sous l'action d'un Hamiltonien. Si nous représentons l'espace et le temps graphiquement, un modèle quantique de dimension $(1+1)$ admet une représentation planaire, et nous nous attendons à trouver sur ce dernier les mêmes propriétés que son homologue planaire.

Nous définissons le modèle de random-cluster quantique, calculons ses paramètres critiques et déterminons ses comportements au point critique et en dehors du point critique. Ceci est une application de la partie précédente : le modèle quantique peut être vu comme la limite du modèle discret défini sur des graphes isoradiaux de plus en plus plats. Nous établis-

sons des bornes uniformes sur les probabilités de croisement afin d'étudier les comportements mentionnés ci-dessus.

Pour conclure cette thèse, nous démontrons un résultat classique du modèle d'Ising planaire pour le modèle d'Ising quantique de dimension $(1 + 1)$: l'invariance conforme. Nous travaillons directement dans le cadre quantique, en d'autres termes, sur le réseau semi-discret $\mathbb{Z} \times \mathbb{R}$.

Remerciements

Partir loin de chez soi pour les études n'est pas une chose facile. Aller dans un pays où l'on comprend à peine la langue et la culture, y construire une vie et en être content, c'est encore moins évident. Tout cela sans parler de l'apprentissage mathématique, une chose qui demande de la patience et beaucoup de réflexion. Ces neuf ans et demi à l'étranger, durant lesquels se sont passés d'innombrables événements inoubliables, se sont envolés comme le vent. J'aimerais dédier ce paragraphe de la thèse à ces personnes avec qui j'ai partagé ces moments précieux et je demande aussi pardon à ceux que j'aurais oubliés par erreur.

L'aboutissement de cette thèse n'aurait pas été possible sans l'aide de mes directeurs de thèse, Hugo Duminil-Copin et Stanislav Smirnov. Je les remercie pour leur disponibilité, leur patience, et leur connaissance mathématique, dont j'ai encore beaucoup à apprendre. Je suis également reconnaissant envers Vincent Beffara, qui a dirigé mon mémoire de master et qui m'a initié au domaine de la physique statistique. J'aimerais aussi remercier Ioan Manolescu, avec qui j'ai fait une grande partie de cette thèse et grâce à qui j'ai appris la rigueur mathématique dans la rédaction après de nombreuses corrections et réécritures. Mes remerciements vont également à Yvan Velenik, qui a accepté de faire partie du jury et qui m'a aidé à plusieurs reprises au cours de mon doctorat. Il ne faut pas non plus oublier d'autres membres du groupe de probabilités à Genève avec qui j'ai eu des discussions mathématiques enrichissantes : Maxime, Sébastien, Roma, Matan, Eveliina, Hao, Sasha, Vincent, Marcelo, Aran, Misha, Dasha et Marianna.

Les enseignants que j'ai eus en classe préparatoire m'ont donné la première motivation pour la recherche mathématique. Je tiens à remercier Monsieur Dupont et Monsieur Duval pour leur pédagogie ainsi que la culture générale mathématique qu'ils m'ont apportée. Je pense aussi à Henri Guenancia pour son apport et son encadrement au cours de mon projet TIPE ; Gabriel Scherer et Irène Walspurger pour les colles d'informatiques et mathématiques qui m'ont été très utiles. Mon tuteur Thierry Bodineau a joué un rôle important durant mes années d'ENS, qui m'a encouragé et m'a donné des informations sur les conférences de mécanique statistique. Je tiens aussi à mentionner Jean-François Le Gall, Wendelin Werner et Raphaël Cerf pour leurs cours, leurs conseils professionnels et leurs disponibilités pendant mon année de M2. Je n'oublie pas non plus Sébastien Martineau, qui a partagé avec moi sa passion des mathématiques, plus précisement de la vulgarisation mathématique, et avec qui j'ai pu réaliser quelques petites expériences intéressantes.

N'étant pas né francophone, je suis reconnaissant à ceux qui ne se sont jamais montrés impatients avec mon français et qui m'ont aidé à l'améliorer. Merci à mon professeur de français et amie épistolaire Angélique pour ses encouragements et ses petits mots ainsi qu'à deux

autres professeurs de l'Institut français de Taïpei, Sonia et Thierry, pour m'avoir beaucoup poussé durant les heures de cours intensifs. Je mentionne également les familles Autebert, Filipiak et Scherer qui m'ont toujours accueilli comme si je faisais partie de leurs familles. J'aimerais remercier chaleureusement les amis de Louis-le-Grand, en particulier Alexandre (育青), Alexandre, Alicia, Benoît, Corinne, Céline, Étienne, Julia, Malek et Miguel, sans qui je n'aurais pas fait de progrès en français.

Pendant les années d'ENS, j'ai rencontré de nombreuses personnes de différents horizons qui m'ont ouvert les yeux. Ce sont des gens qui sont à la fois intelligents et ouverts d'esprit. Je tiens à remercier les enseignants du cours d'arabe Zaïd et Houda qui m'ont fait découvert la langue et les cultures du monde arabe ; Maxime pour le voyage linguistique en Égypte et les heures où on se faufilait dans les ruelles du Caire ; Fathi pour m'avoir rappelé des mots en arabe quand je les oubliais ; Chaïma pour le tandem linguistique. Merci également à Marie pour m'avoir aidé pour le français et surtout, pour m'avoir appris à cuisiner français.

Après les cours, le C3 représentait cette maison où l'on vivait comme une famille. Les repas d'étage composés de délicieux mets de toute origine, les fêtes et les anniversaires, sans votre présence, la vie n'aurait pas été aussi remplie de joie et de bonheur. Je remercie David, Diego, Joël, Maxime, Thibault, Aude, Gabriel, Hongzhou (泓州), Yichao (逸超), Mégane (蓮梅), Léon (泳龍), Médéric, Florian, Florence et Silvia.

Grâce à l'échange que j'ai effectué en Inde, j'ai pu faire de belles découvertes sur ce pays immense et fascinant. Les Indiens ont été tellement chaleureux et prêts à m'aider, un étranger un peu désorienté qui parlait un franglais incompréhensible, m'ont fait chaud au cœur. Je pense en particulier à Devashish, un scientifique-philosophe, qui se pose des tas de questions métaphysiques et me défie avec ses points de vue originaux ; Biman, petit, généreux, aventureux et toujours plein d'énergie, qui me remonte le moral quand j'en ai besoin ; Parul, ma cobureau, une fille indienne hors du commun et cherche à éviter les règles injustes de la société imposées aux femmes ; Akash et Yajnaseni pour m'avoir initié à l'hindi. Je voudrais aussi remercier BV Rao, Siva Athreya et Amitabha Bagchi, professeurs de probabilités avec qui j'ai eu des conversations mathématiques intéressantes et qui m'ont très bien accueilli lors de mon séjour. Tout cela sans oublier les amis qui sont partis en échange avec moi : Grégoire et Pierre-Yves, arrivés deux mois avant moi et qui m'ont transmis leurs expériences locales et Weikun (偉鯤), avec qui j'ai partagé deux mois au quotidien.

Je n'oublie pas les amis de Genève, qui m'ont été vraiment importants pendant mes années de doctorat. Je remercie Wanda et Claude, botaniste et géologue passionnée et spéologue, pour m'avoir fait découvrir de jolis coins dans les Alpes et m'avoir initié à la spéologie ; Xavier pour ses potagers, ses fraises et ses prunes ; 阿發, 宜儒, 婉郁 pour les moments nostalgiques et les petites soirées taïwanaises ; le chœur de l'Université, en particulier le chef Sébastien et ses membres Caterina, Máté, Dominik, Shaula et Flavio, pour les moments musicaux et les sorties de vélo à Dardagny ; Ziemowit, un couchsurfer polonais qui travaille au CERN, de qui j'ai appris de nombreuses choses sur la vie ; Paul-Henry pour les week-ends au Salève sur les sentiers périlleux ; Marco, passionné des langues et de l'histoire, qui m'a raconté plein de choses sur le christianisme et l'Italie et avec qui j'ai partagé de nombreuses heures dans la cuisine ; Tommaso pour les excursions en vélo à Piedicavallo et au sanctuaire d'Oropa ; Mayank, Pratik, Basundhara et Aurélie pour le tandem d'hindi et Lina pour celui d'allemand ; Anna et Tiziano pour les pierogis, les lasagnes et Tchini ; l'UPCGE pour ses cours de langues, les enseignants Ursula, Elena et Africa ainsi que les camarades Munir et Rémi.

J'ai aussi eu la chance de vivre en colocation avec de différentes personnes : Aglaia, Frédéric, Hanno, Hiro, Audrey, Francesco et Marina, avec qui j'ai partagé des repas et des week-end

ensemble. Je pense aussi à la famille de Hongler, qui m'a toujours reçu chaleureusement, en particulier Isadora et Clément, pour les séminaires raviolis à Lausanne. Je remercie en outre les collègues de la section sans qui les pauses et les moments de frustration auraient été moins sympas : Adrien, Anthony, Corina, Eiichi, Fayçal, Giulio, Guillaume, Hanna, Ibrahim, Jérémy, Máté, Minh, Mucyo, Parisa et Soheil. J'ai aussi apprécié les personnes que j'ai croisées dans des conférences pour les discussions fructifiantes : Sanjay, Antoine, Hugo, Igor, Linxiao (林曉), Loïc, Lorène, Nicolas et Thomas.

Avant de finir, un grand merci à mes amis taïwanais qui sont venus en France avec le même programme que moi ainsi que certains d'autres qui sont ailleurs en Europe que le destin m'a fait croiser. Grâce à vous, j'ai toujours pu trouver quelqu'un qui me montre l'exemple et qui me soutient :學庸, 紘翎, 駿祥, 鈺霖, 嘉蔓, 力明, 癸安, 恩宏, 莉雯, 悅寧, 依輯 et 婕瑄. J'aimerais aussi mentionner les amis avec qui depuis trois ans j'écris *Aurore Formosane*, un magazine trimestriel francophone sur Taïwan : 有蓉, 皆安, 杰森 et 驊庭.

上尾了，我擱愛感謝我家己的父母佮小妹，佇這段時間來，恬恬佇背後共我支持，雖然無佇我身軀邊，毋過是我感覺上虧欠的人。

Contents

Abstract iii

Résumé v

Remerciements vii

Contents x

Introduction xiii

1 Definition of models 1
- 1.1 The random-cluster model on finite graphs . . . 1
  - 1.1.1 Definition . . . 1
  - 1.1.2 Edward-Sokal coupling . . . 2
  - 1.1.3 Boundary conditions . . . 3
  - 1.1.4 Dual model . . . 4
  - 1.1.5 Loop representation . . . 5
  - 1.1.6 Domain Markov property . . . 6
  - 1.1.7 Positive association . . . 7
  - 1.1.8 Infinite-volume measure . . . 10
  - 1.1.9 Finite-energy property . . . 12
  - 1.1.10 Russo-Seymour-Welsh property . . . 13
  - 1.1.11 Known results . . . 14
- 1.2 Quantum random-cluster model . . . 14
  - 1.2.1 Semi-discrete lattice and domain . . . 14
  - 1.2.2 Quantum Bernoulli percolation . . . 17
  - 1.2.3 Quantum random-cluster model . . . 17
  - 1.2.4 Limit of the discrete random-cluster model . . . 18
  - 1.2.5 Critical quantum model: loop representation . . . 20

2 Isoradial graphs and star-triangle transformation 23
- 2.1 Isoradial graphs . . . 23
  - 2.1.1 Definition . . . 23
  - 2.1.2 Bounded-angles property . . . 24
  - 2.1.3 Track systems . . . 25

2.2 Isoradial square lattices . . . 26
2.3 Doubly-periodic isoradial graphs . . . 27
2.3.1 Asymptotic direction . . . 27
2.3.2 Square-grid property . . . 28
2.4 Random-cluster model on isoradial graphs . . . 29
2.4.1 Definition . . . 29
2.4.2 Loop representation . . . 30
2.4.3 Uniqueness of the measure for doubly-periodic isoradial graphs . . . 31
2.5 Known results . . . 33
2.6 Star-triangle transformation . . . 34
2.6.1 Abstract star-triangle transformation . . . 34
2.6.2 Star-triangle transformation on isoradial graph . . . 36
2.7 Observable on isoradial graphs . . . 38
2.7.1 Discrete complex analysis . . . 38
2.7.2 Observable on Dobrushin domains . . . 39
2.7.3 Behavior under star-triangle transformations in the Ising model . . . 39

3 Universality of the random-cluster model 43
3.1 Results . . . 43
3.2 Switching between isoradial graphs . . . 45
3.2.1 From regular square lattice to isoradial square lattice . . . 45
3.2.2 From isoradial square lattices to general graphs . . . 53
3.3 Proofs for $1 \leqslant q \leqslant 4$ . . . 55
3.3.1 Notations and properties . . . 55
3.3.2 Isoradial square lattices . . . 56
3.3.2.1 RSW: an alternative definition . . . 57
3.3.2.2 Transporting RSW: proof of Proposition 3.11 . . . 60
3.3.2.3 Sketch of proof for Propositions 3.15 and 3.16 . . . 62
3.3.3 Doubly-periodic isoradial graphs . . . 68
3.3.4 Tying up loose ends . . . 71
3.3.5 Universality of arm exponents: Theorem 3.4 . . . 72
3.4 Proofs for $q > 4$ . . . 75
3.4.1 Isoradial square lattices . . . 79
3.4.2 Doubly-periodic isoradial graphs . . . 84
3.4.3 Conclusion . . . 87

4 Behavior of the quantum random-cluster model 89
4.1 Results . . . 89
4.2 Discretisation . . . 90
4.3 The case $1 \leqslant q \leqslant 4$ . . . 92
4.3.1 The case $q > 4$ . . . 101

5 Semi-discrete complex analysis 105
5.1 Basic definitions . . . 105
5.1.1 Derivatives . . . 105
5.1.2 Integration on primal and dual lattices . . . 107
5.1.3 Integration of a product of functions . . . 109
5.2 Brownian motion, harmonic measure and Laplacian . . . 110
5.3 Dirichlet boundary problem . . . 115

5.4 Green's function . . . 116
5.4.1 Construction and properties . . . 117
5.4.2 Link with Brownian motion . . . 121
5.5 Harnack Principle and convergence theorems . . . 123
5.6 Convergence to continuous Dirichlet problem . . . 127
5.7 S-holomorphicity . . . 128

6 Scaling limit of the quantum Ising model 131
6.1 The quantum random-cluster model . . . 131
6.1.1 Semi-discretization of a continuous domain . . . 131
6.1.2 Main result . . . 132
6.2 Observable and properties . . . 132
6.2.1 Definition and illustration . . . 132
6.2.2 Relations and holomorphicity . . . 134
6.2.3 Primitive of $\mathcal{F}_\delta^2$ . . . 137
6.3 Boundary-value problems . . . 141
6.3.1 Boundary modification trick . . . 141
6.3.2 Riemann-Hilbert boundary value problem . . . 142
6.4 RSW on the quantum model . . . 143
6.4.1 RSW property: second-moment method . . . 143
6.5 Convergence of the interface . . . 148
6.5.1 Convergence theorem . . . 148
6.5.2 Conclusion: proof of the Main Theorem . . . 151
6.5.3 Going further: quantum random-cluster model . . . 151

A Computation of residues 153

B RSW theory and applications 157

C Proof of phase transition for $1 \leqslant q \leqslant 4$: Theorem 3.1 and Corollary 3.3 163

D Separation Lemma and Consequences 165

Bibliography 173

Introduction

Definition of models

In statistical mechanics, one is interested in systems of particles which are described at microcopic level and observed at macroscopic level. Usually, the model could be a particle moving on a discrete lattice or a collection of interacting particles. At the microscopic level, the system could be hard to study due to the huge amount of local information, but at the macroscopic level, only the dominating behavior will remain because fluctuations that are too small will disappear, which simplifies the analysis.

In this thesis, we are interested in planar models from statistical mechanics. These models are usually described by one (or more) parameters, which could be interpreted in physical systems as pressure, temperature, porosity or strength of interaction, for instance. When a parameter varies, the system may exhibit different macroscopic behaviors, which are called *phases*. A value below which and above which one observes different macroscopic properties is called *critical* and we say that a phase transition occurs at this point. At the critical point, the model has non-trivial behaviors which are of particular interest. Before going further for detailed analysis, let us see a few examples of such models.

The *Bernoulli percolation* on $\mathbb{Z}^2$ is a model of statistical mechanics that can be defined in a few words. Fix a parameter $p \in [0,1]$, consider the infinite graph $\mathbb{Z}^2$ and remove each of its edges one by one independently with probability $1-p$. The random outcome thus obtained is the object of our interest, called *Bernoulli percolation of parameter* p. One can see a configuration as a function on edges, which takes 0 if it is removed (also called a *closed edge*) and 1 if it is kept (also called an *open edge*). As such, a configuration is also an element ω in $\{0,1\}^E$, where E is the edge set of $\mathbb{Z}^2$.

One can easily observe that when $p = 0$, all the edges are removed and one ends up with a graph with only isolated vertices. When $p = 1$, all the edges are kept so the final graph is still the whole $\mathbb{Z}^2$ itself. In other words, when $p = 0$, the graph has a lot of small finite connected components while when $p = 1$, the model has a unique infinite connected component. For intermediate values of p, the situation is less trivial. One may have a look at Figure 1 for an illustration. The value $p = \frac{1}{2}$ is the self-dual point [1] and is actually the critical point of the model in the following sense.

[1] The dual graph of $\mathbb{Z}^2$ is $(\mathbb{Z}+\frac{1}{2})^2$. With a configuration ω on the edge set of $\mathbb{Z}^2$, one can associate a dual configuration ω^* on the edge set of $(\mathbb{Z}+\frac{1}{2})^2$ by letting $\omega^*(e^*) = 1-\omega(e)$, where e^* is the dual edge of e. By *self-dual* point we mean that ω^* and ω have the same distribution.

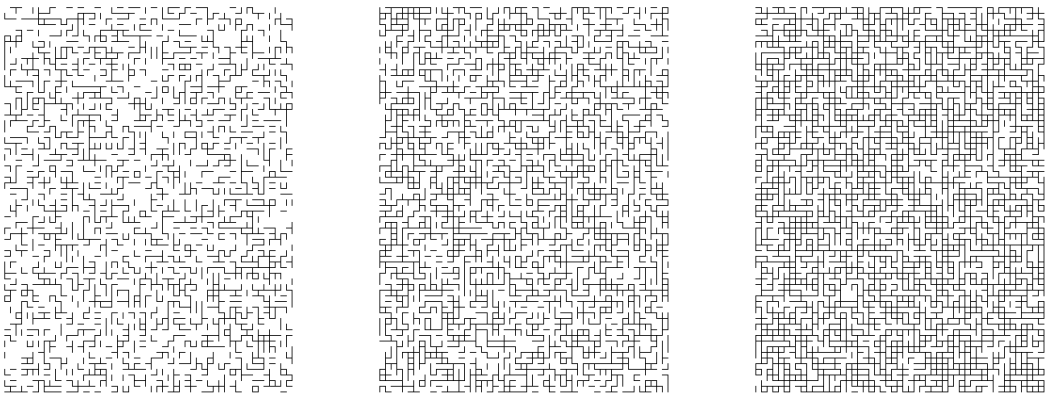

Figure 1 – Simulations of Bernoulli percolation with parameters $p = 0.35$ (subcritical), $p = 0.5$ (critical) and $p = 0.65$ (supercritical).

When $p < \frac{1}{2}$, there is no infinite connected component (or *infinite cluster*) almost surely; whereas when $p > \frac{1}{2}$, almost surely such an infinite cluster exists and is unique. Moreover, in the latter case, the complement of the unique infinite cluster consists only of finite-size connected components. These two regimes are called *subcritical* and *supercritical* respectively. In the subcritical regime, when one zooms out, these small islands of finite-size connected components all disappear; whereas in the supercritical regime, the connected components in the complement disappear.

At the critical point $p = \frac{1}{2}$, one observes a less trivial phenomenon: no matter how one scales the model, one observes "more or less the same picture" and one obtains similar "connection properties" [2]. In particular, this suggests some self-similar behaviors of the critical model. This property characterizes the critical point $p = \frac{1}{2}$ and is called the *Russo-Seymour-Welsh property* (RSW property) [3]. A more precise and mathematical way of describing this property will be given in Section 1.1.10. Readers are referred to Figure 2 for a simulation.

A possible approach to describe the property of the self-similarity is to use a concept, called "renormalization group", proposed by theoretical physicists. This consists of a "renormalization map", which changes the scale at which we study the model. In other words, this map *fusions* neighboring vertices into blocks, which we call *defocusing* or *coarse-graining*, and results roughly in the same model but with a different parameter.

Let us look at Figure 3 for some simulations of the (site) Bernoulli percolation. The procedure is as follows: we sample the Bernoulli percolation with parameter p and the renormalization maps consists of replacing each 3×3 block by a block of the dominating state (close or open site). The picture thus obtained can still be described by a site percolation model with a different parameter [4].

In the subcritical phase, for example at $p = 0.35$, after zooming out by a factor of 3, we see "less" open edges: this would correspond to a percolation model with a smaller parameter. In the supercritical phase, for example at $p = 0.65$, one observes something opposite.

[2] For example, the probability that there is an open path between the left and the right side of a rectangle of size $n \times (n+1)$ is $\frac{1}{2}$ for all integer n.

[3] We note that at $p = 0$ and $p = 1$, the model is also self-similar, but since these cases are degenerated, we do not need to care much.

[4] If the original model is the site Bernoulli percolation with parameter p, then the resulting model is with parameter $p' = \sum_{k=5}^{9} \binom{9}{k} p^k (1-p)^{9-k}$. By solving $p' = p$, one obtains $p = 0, \frac{1}{2}, 1$ as solutions.

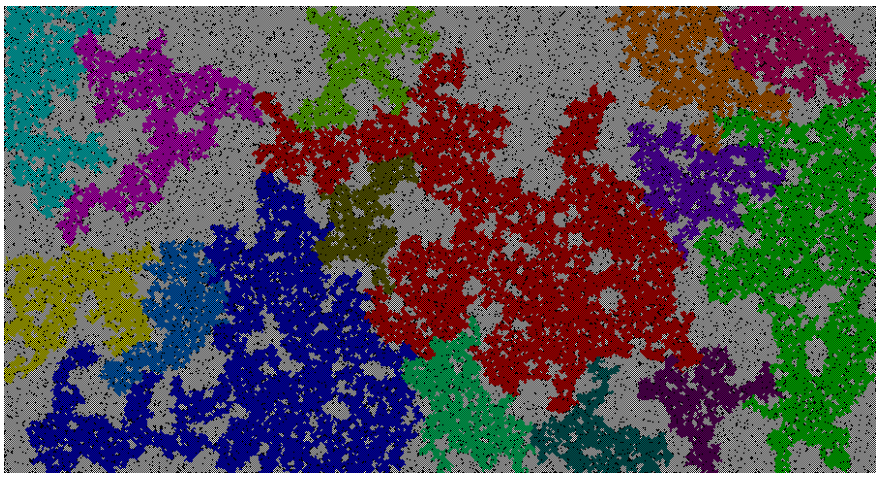

Figure 2 – A simulation of Bernoulli percolation at criticality. Closed edges are in black and open edges in white. The ten largest connected components are drawn in various colors in decreasing order: red, blue, green, etc.

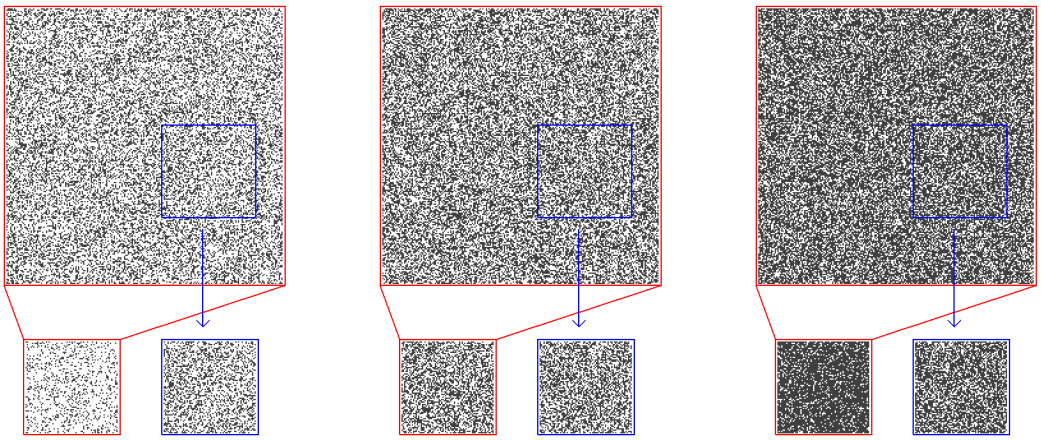

Figure 3 – Simulations of the site Bernoulli percolation with parameters $p = 0.35$ (subcritical), $p = 0.5$ (critical) and $p = 0.65$ (supercritical). On the bottom, the blue windows correspond to a portion observed in the model and the red windows correspond to the observation made after a "renormalization map" which scales out by factor 3, replacing each 3×3 block by a block with the dominating color. At the critical point, the red and the blue windows have the same "statistics" (correlations are the same).

After zooming out by a factor of 3, we see "more" open edges and this would correspond to a percolation model with a larger parameter. Finally, we examine the behavior of this "renormalization map" at the critical point $p = 0.5$, before and after scaling. What we observe from the simulation is that the two realizations look pretty much the same.

Therefore, a fixed point of the renormalization map, or the self-similarity of the model, would provide us with the critical model. Readers are referred to [Car96, ZJ07] and the references therein.

Another well-known model is the Ising model. It was invented by Wilhelm Lenz [Len20] to understand the phenomenon of ferromagnetism. It was studied by his student Ernst Ising

in his PhD thesis [Isi25] who proved that the model does not exhibit any phase transition in one dimension and wrongly generalized this result to all higher dimensions.

Here, we only define the Ising model on a finite subgraph $G = (V, E)$ of $\mathbb{Z}^2$, where V is the vertex set and E the edge set. We note that more care is needed to define the model on an infinite graph such as $\mathbb{Z}^2$, which will be done by means of weak limits in Chapter 3. Fix a parameter $\beta > 0$ which can be seen as the inverse of the temperature. A spin is usually denoted by $\uparrow / \downarrow$ or ± 1 and a spin configuration σ is a function associating a spin with each vertex, i.e., σ is an element of $\{-1, +1\}^V$.

Given a spin configuration $\sigma \in \{-1, +1\}^V$, define its Hamiltonian to be

$$H(\sigma) = -\sum_{\langle u,v\rangle \in E} \sigma_u \sigma_v, \tag{0.1}$$

where the sum is taken over all the edges $\langle u, v\rangle$ in E. Then, the probability of a particular spin configuration $\sigma \in \{-1, +1\}^V$ is given by

$$\mathbb{P}_\beta[\sigma] = \frac{\exp(-\beta H(\sigma))}{Z_\beta}, \tag{0.2}$$

where $Z_\beta = \sum_{\sigma'} \exp(-\beta H(\sigma'))$ sums over all possible spin configurations and is called the *partition function*.

A simple observation allows us to say that in a configuration, the more the neighbours agree with each other, the lower is the Hamiltonian. Thus, such configurations occur with higher probabilities.

When β goes to 0 (temperature goes to infinity), the exponential term in the numerator does not differ too much between different spin configurations and as a consequence, they are all "more or less" equiprobable. This is called a *disordered* phase. On the other side, when β goes to infinity (temperature goes to zero), only two configurations have much higher weights than the others: one with only plus spins and the other one with only minus spins. This phase is called *ordered*.

On $\mathbb{Z}^2$, the existence of phase transition can be shown by using Peierls argument [Pei36]. The idea is to expand $e^{-\beta H}$ in two different ways, called *low- and high- temperature expansions*. They are rewritings of the exponential terms $e^{\sigma_u \sigma_v}$ using combinatorics arguments. In this way, one can prove that there is a value $\beta_c \in (0, \infty)$, called *critical value* of the inverse temperature, such that for $\beta < \beta_c$, the model is in the disordered phase; and for $\beta > \beta_c$, it is in the ordered phase.

Hendrik Kramers and Gregory Wannier computed the critical value by duality [KW41] and the fact that at the critical point, the model should be self-dual. Later, an analytic description of the model was given by Lars Onsager [Ons44] where this was solved by means of transfer-matrix and the critical value was computed to be $\beta_c = \frac{1}{2}\ln(\sqrt{2}+1)$. Later, by using differential inequalities, Aizenman, Barsky and Fernández proved that the phase transition is sharp [ABF87], which, combined with Kramers-Wannier argument, provided a new approach to compute the critical value.

The main model studied in this thesis, the *random-cluster model*, or *Fortuin-Kasteleyn percolation* (FK-percolation), was introduced by Fortuin and Kesteleyn [FK72] to unify the aforementioned Bernoulli percolation, the theory of electrical network and the Potts model. Like the Ising model, this model presents a lot of dependency and cannot be defined directly on an infinite graph. Thus, we describe it for a finite subgraph $G = (V, E)$ of $\mathbb{Z}^2$ and a precise definition of the infinite-volume measure is postponed to Chapter 3.

Fix $p \in [0,1]$ and $q \geqslant 1$, called the *cluster-weight*. Let $\omega \in \{0,1\}^E$ be an edge configuration and let

$$\varphi_{G,p,q}[\omega] = \frac{p^{o(\omega)}(1-p)^{c(\omega)}q^{k(\omega)}}{Z_{G,q}}, \tag{0.3}$$

be a measure where $Z_{G,p,q} = \sum_{\omega'} p^{o(\omega')}(1-p)^{c(\omega')}q^{k(\omega')}$ sums over all possible edge configurations $\omega' \in \{0,1\}^E$. Here, $o(\omega)$, $c(\omega)$ and $k(\omega)$ denote respectively the number of open edges, closed edges and connected components in ω, and $Z_{G,p,q}$ is called the *partition function*. The measure $\varphi_{G,p,q}$ is a probability measure called the random-cluster measure on G.

The model on the square lattice $\mathbb{Z}^2$ is now pretty well understood. The critical value p_c was computed by Vincent Beffara and Hugo Duminil-Copin [BDC12], which is given by $p_c = \frac{\sqrt{q}}{1+\sqrt{q}}$ (see also [DCM16, DRT16, DRT17]). In the same paper, it is also shown that the distribution of the size of finite clusters has exponential tails when the model is non-critical. Also, the phase transition of the model is continuous [5] if the cluster-weight q belongs to $[1,4]$ [DCST17] and discontinuous if it is greater than 4 [DGH+16].

For integer cluster-weights, the model can be coupled with the Potts model via the so-called *Edwards-Sokal coupling* [ES88], also see Section 1.1.2. The Potts model is a generalization of the Ising model: instead of having spins ± 1 on vertices, we associate with each vertex a "color" which is described by an integer in $\{1,\dots,q\}$. Also note that the configurations of the Potts model are defined on vertices whereas those of the random-cluster model are defined on edges. In particular, for the cluster-weight $q = 2$, the Edwards-Sokal coupling gives the Ising model; and the critical value from [BDC12] gives again the critical parameter $\beta_c = \frac{1}{2}\ln(\sqrt{2}+1)$ for the Ising model.

Criticality and conformal invariance

A *conformal map* between two simply-connected open sets of $\mathbb{C}$ is a biholomorphic map between them. Such a map is $\mathbb{C}$-differentiable, hence at infinitesimal scale, it is the composition of a scaling and a rotation [6]. Translations, scalings, rotations and Möbius transformations are examples of such maps. Informally speaking, a mathematical object (a stochastic process for example) is said to be *conformally invariant* if under the transformation of such maps, the resulting object remains of the same nature (in distribution) as the initial one.

At criticality, the aforementioned RSW property implies the infinite correlation length of the model (i.e., the correlation decreases in power laws with respect to the distance). And the models having an infinite correlation length are conjectured to be conformally invariant in the scaling limit. In other words, when one zooms out such models, or "observes them from very far away", we should see an object which is conformally invariant.

This idea first aorse in seminal papers by Belavin, Polyakov and Zamolodchikov [BPZ84a, BPZ84b] by introducing the notion of *conformal field theory*, which consists of the study of scaling limits of quantum fields, containing all information of planar models of statistical mechanics, and allowing us to explain non-rigorously many of their phonemena at criticality.

However, in mathematical terms, this notion still needs to be defined rigorously, and one of the possible ways, for example, is to look at some interface (one-dimensional curve) arising

[5] Roughly speaking, a phase transition is said to be *continuous* if the free energy is continuous by differentiation with respect to the parameter at the critical point; and *discontinuous* otherwise.

[6] Let U and V be two simply-connected sets of $\mathbb{C}$, f be a conformal map and $z \in U$. One may write $f'(z)$ in the polar coordinates $f'(z) = re^{i\theta}$, where $r > 0$ and $\theta \in \mathbb{R}$. At the infinitesimal scale around z, f acts as a scaling of factor r composed with a rotation of angle θ.

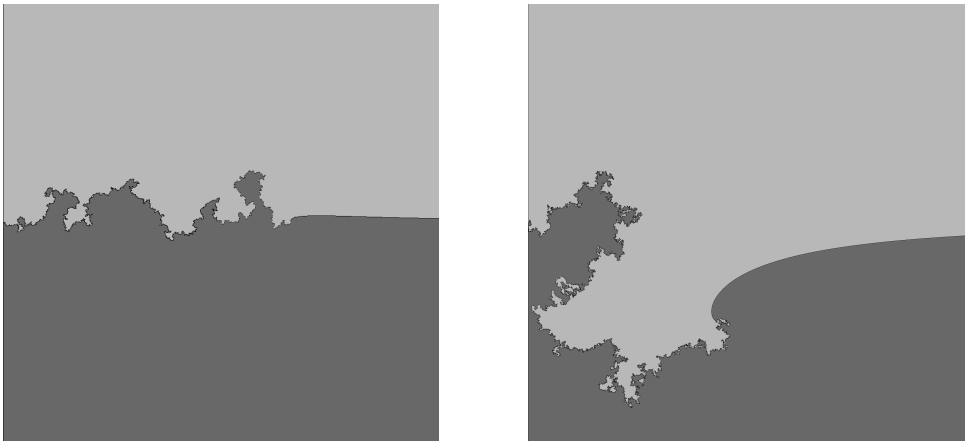

Figure 4 – Simulations of SLE curves of parameter $\kappa = 2$ et $\kappa = 3.5$. (Courtesy of Vincent Beffara)

from the model. A good candidate for the scaling limit of such an interface is the *(chordal) Schramm-Löwner Evolution* (or SLE) which is a one-parameter family of processes that can be described by the following stochastic differential equation:

$$\partial g_t(z) = \frac{2}{g_t(z) - W_t}, \quad z \in \mathbb{H},$$

where $W_t = \sqrt{\kappa} B_t$ is the driving function. In the previous definition, $\kappa > 0$ is the parameter of the SLE process and $(B_t)_{t \geqslant 0}$ the standard two-dimensional Brownian motion. These are self-similar fractal curves and some simulations are shown in Figure 4. For all values of κ, the process satisfies the domain Markov property and conformal invariance; and conversely, as long as we have a stochastic process satisfying these two properties, it can be described by an SLE curve. This was first introduced by Oded Schramm [Sch00] and a lot of planar models have been shown or are conjectured to have interfaces described in the limit by some SLE curves.

Let us discuss some results of this kind concerning the aforementioned models at the critical point. We start from the site percolation model.

Let Ω be a simply connected open set of $\mathbb{C}$. Consider the triangular lattice $\mathbb{T}$ on which we define the site percolation with parameter $p = \frac{1}{2}$, i.e., instead of having open and closed edges, we have open and closed vertices, each with equal probability. By duality, this can also be seen as the face percolation on the hexagonal lattice. For $\delta > 0$, write Ω_δ for the discretization of Ω by $\delta\mathbb{T}$. We do not need to worry too much about the way we discretize and we can therefore take for example Ω_δ to be the largest subgraph of $\delta\mathbb{T}$ which is entirely contained in Ω. We pick up four points a, b, c and d on the boundary $\partial\Omega$ in counterclockwise order and we write a_δ, β_δ, c_δ and d_δ for their discrete counterparts: for example, $\sharp_\delta$ stands for the closest vertex to $\sharp$ in Ω_δ for $\sharp \in \{a, b, c, d\}$. See Figure 5 for an illustration. We are interested in the probability that the arc $(a_\delta b_\delta)$ is connected to $(c_\delta d_\delta)$ by an open path of percolation. The Cardy formula predicts that the limit of this probability, when δ goes to 0, is given by a simple formula which is conformally invariant [Car92].

Let $\triangle$ be any equilateral triangle embedded in $\mathbb{C}$. Due to the Riemann mapping theorem, we can find a unique conformal map Φ which sends Ω to $\triangle$ such that $\Phi(a)$, $\Phi(b)$ and $\Phi(c)$ are vertices of $\triangle$ in the counterclockwise order. Therefore, the image $\Phi(d)$ is between $\Phi(c)$

and $\Phi(a)$. Stanislav Smirnov proved that Cardy's formula is true [Smi01]:

$$\lim_{\delta \to 0} \mathbb{P}_\delta\Big[(a_\delta b_\delta) \text{ is connected to } (c_\delta d_\delta)\Big] = \frac{\left|\overrightarrow{\Phi(c)\Phi(d)}\right|}{\left|\overrightarrow{\Phi(a)\Phi(c)}\right|}.$$

This limit only depends on the images of the initial data under the unique conformal map satisfying the properties mentioned above. Thus we say that the connection probability between arcs (ab) and (cd) is *conformally invariant*.

Cardy's formula along with the "locality property" [7] of the percolation process concludes that the scaling limit of the percolation interface coincides with SLE_6 [Smi01]. We point out that this result is still unknown for other lattices and for bond-percolation on any lattice. This remains an important open conjecture of the domain.

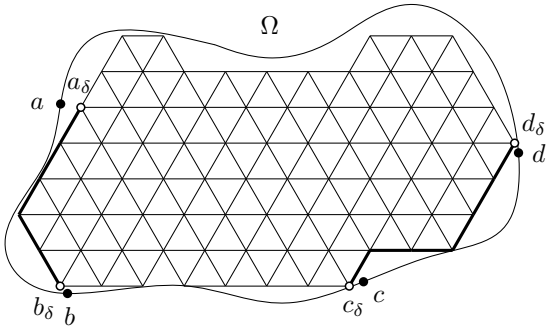

Figure 5 – The simply connected open domain Ω and its δ-discretization Ω_δ. The vertices a_δ, β_δ, c_δ and d_δ are drawn in white and the arcs $(a_\delta b_\delta)$ and $(c_\delta d_\delta)$ are drawn with thick lines.

The Ising model is the model for which we have the best understanding. By means of a fermionic observable, Smirnov showed that, on the square lattice, the interface of the spin-representation of the Ising model converges to SLE_3, and the one of the FK-representation to $SLE_{16/3}$ [Smi10, CDCH$^+$14] (we refer to [DS12] for a review). Later, using fermionic spinor, Hongler and Smirnov proved the conformal invariance of the energy density in the planar Ising model [HS13]. Chelkak, Hongler and Izyurov showed that the magnetization and multi-spin correlations are conformally invariant in the scaling limit [CHI15]. Recently, Kemppainen and Smirnov showed in a series of two papers that the collection of critical FK-Ising loops converges to CLE(16/3), the Conformal Loop Ensemble of parameter 16/3 [KS15, KS16], by looking at what they call an exploration tree. Almost at the same time, Benoist and Hongler gave a proof that the collection of critical spin-Ising loops converges to CLE(3) [BH16]. Some other recent progress relating the conformal field theory (or its representation as a Virasoro algebra) to the discrete level of the model can be found in [GHP16, HVK17, CHI15].

Universality and isoradial graphs

Following the discussion on the conformal invariance, the conformal field theory also suggests that when we "look at the model from far away", the local property of the lattice struc-

[7] This term will not be made precise in this thesis, that is why we put quotation marks around.

ture should not be relevant. In other words, no matter the underlying discrete lattice on which the model is defined, its scaling limit should be given by the same object.

An easy example to explain is the (planar) Brownian motion. We start with a random walk that moves at each step according to a random vector given by a random variable. It turns out that when scaled out correctly [Don51, Don52], in the limit, it converges to a two-dimensional Brownian motion (with drift). This limiting object is universal in the sense that only the expectation and the variance of the random vector characterize the resulting Brownian motion. In particular, one can consider the simple random walk on a regular lattice such as the square lattice, the triangular lattice or the hexagonal lattice, and it turns out that the limiting object is as described above.

Moreover, the trajectory of the Brownian motion is conformally invariant, meaning that it is still the trajectory of the Brownian motion under conformal transformations, up to time-change. In other words, the Brownian motion is a stochastic process which is preserved under conformal maps up to time-change. To sum up, the Brownian motion is not only the universal limit (under some condition on the expectation and the variance of its displacements) of random walks, but it is also a stochastic process satisfying pretty restrictive properties, such as the conformal invariance.

In our context, we will be interested in the universality of the models on a family of graphs called *isoradial*. A planar embedded graph $G = (V, E)$ is said to be *isoradial* if all of its faces are inscribed in circles of the same radius. See Figure 6 for an illustration. Note that such graphs should always be infinite since otherwise, the exterior face would not be able to be inscribed in a circle of finite radius. This family of graphs is huge and contains the classical periodic graphs such as the square lattice, the triangular lattice, the hexagonal lattice, etc. There are a few good reasons and motivation to study the universality on such graphs:

- The star-triangle transformations which transform one isoradial graph to another, see Section 2.6.
- The robust theory of discrete complex analysis on isoradial graphs developed in [Ken02, Mer01, CS11].

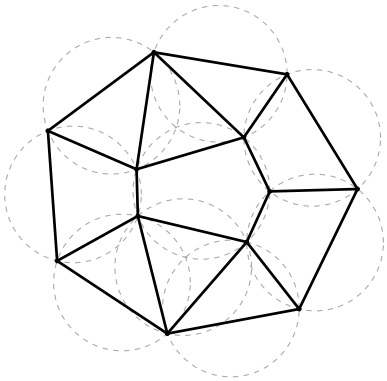

Figure 6 – An example of isoradial graph. All the faces are inscribed in circles of the same radius.

The universality result on (bond) Bernoulli percolation was first obtained by Geoffrey Grimmett and Ioan Manolescu [GM13a, GM13b, GM14]. They used *star-triangle transformations* to transform one isoradial graph into another, by preserving the percolation measure in such a way that the connection properties in different isoradial graphs do not differ too

much in probability. This method did not only allow them to determine the critical parameters of the random-cluster model, but also showed the behavior at the critical point, such as the sharpness of the phase transition, the correlation length, the critical exponents, etc.

In the first part of this thesis, we will show advances in this direction. We are interested in the universal behavior of the random-cluster model for $q \geqslant 1$ at criticality. We proceed in a similar way as in [GM14] with the difference that the random-cluster model with parameter $q > 1$ is a model with a lot of dependancy between edges, which demands more care while we perform star-triangle transformations.

More precisely, for an isoradial graph $G = (V, E)$, let $p_e(\beta)$ be the probability parameter associated with the edge $e \in E$ and $\beta > 0$ be an additional parameter that we introduce. Note that β here is different from the inverse temperature in the Ising model. The probability parameter is an increasing function in β and is defined by $p_e(\beta) = \frac{y_e(\beta)}{1+y_e(\beta)}$, where

$$\begin{aligned}
\text{if } 1 \leqslant q < 4, \quad & y_e(\beta) = \beta\sqrt{q} \cdot \tfrac{\sin(r(\pi-\theta_e))}{\sin(r\theta_e)}, \quad \text{where } r = \tfrac{1}{\pi}\cos^{-1}\left(\tfrac{\sqrt{q}}{2}\right), \\
\text{if } q = 4; \quad & y_e(\beta) = \beta \cdot \tfrac{2(\pi-\theta_e)}{\theta_e}, \\
\text{if } q > 4; \quad & y_e(\beta) = \beta\sqrt{q} \cdot \tfrac{\sinh(r(\pi-\theta_e))}{\sinh(r\theta_e)}, \quad \text{where } r = \tfrac{1}{\pi}\cosh^{-1}\left(\tfrac{\sqrt{q}}{2}\right),
\end{aligned}$$

where θ_e is the subtended angle of e, as shown in Figure 7. Moreover, we will prove that at $\beta = 1$, the model is critical; for $\beta < 1$, the model is subcritical and for $\beta > 1$, supercritical.

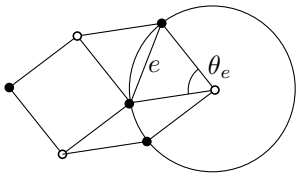

Figure 7 – The primal edge e has subtended angle θ_e.

Let us come back to what we said previously about the conformal invariance.

A universality result on the conformal invariance was proven for the Ising model by Dmitry Chelkak and Stanislav Smirnov [CS12, CDCH+14]. They proved the convergence of the interface of the Ising model on isoradial graphs to SLE_3 (spin-Ising) and to $SLE_{16/3}$ (FK-Ising), which are the scaling limits of the same model on the square lattice proved a few years earlier.

In the case of the Bernoulli percolation, the only result we know on the scaling limit of the interface is in the case of the site percolation on the triangular lattice. As mentioned in the previous section, this converges to SLE_6. Such a result is still unknown for the site percolation on other regular lattices or isoradial graphs, not to mention for the bond percolation, no result on the scaling limit is known so far.

It was conjectured by Oded Schramm [Sch07] that the interface of the random-cluster model with parameter $1 \leqslant q \leqslant 4$ should converge to the Schramm-Loewner Evolution of parameter $\kappa = 4\pi/\arccos(-\sqrt{q}/2)$, which should be independent of the underlying isoradial graph, as for the Ising model. We note that for $q = 1$ (Bernoulli percolation) and $q = 2$ (Ising model), we find the values $\kappa = 6$ and $\kappa = \frac{16}{3}$ mentioned above.

Up to the present, we are still far from understanding the scaling limit of the interfaces arising from the random-cluster model. From the fermionic observable used to show the conformal invariance of the Ising model, Smirnov also conjectured [Smi06] the existence of a parafermionic observable which might allow us to prove the convergence of the interface

in the random-cluster model. This observable works well for the Ising model because at the discrete level, one has full Cauchy-Riemann relations whereas for the general random-cluster model, unfortunately, one has only half of them.

The universality results that we will show in Chapter 3 may lead us further, although they are not strong enough to tell us about the scaling limit of the interface. In the second part of this thesis, we will discuss the (1+1)-dimensional [8] quantum random-cluster model, which is believed to behave in the same way as the planar random-cluster model. As a consequence of these universality results, we will show that some connection properties are the same for the quantum model in Chapter 4.

The quantum random-cluster model

A special case of the isoradial lattice is the flattened square lattice $\mathbb{Z} \times (\varepsilon\mathbb{Z})$, as shown in Figure 8. As before, we can define a planar model on edges or vertices of this flattened lattice. In the limit $\varepsilon \to 0$, this model converges to a quantum model on the semi-discrete lattice $\mathbb{Z} \times \mathbb{R}$ (Figure 9a). Without any surprise, this model also possesses the same properties at criticality as its discrete counterpart due to the universality result on isoradial graphs.

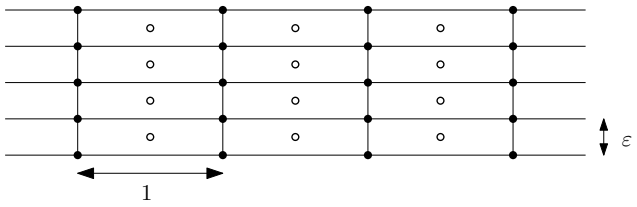

Figure 8 – A piece of the flattened square lattice.

Let us briefly describe the quantum random-cluster model here. Its link with the discrete model will be discussed later in Section 1.2.4.

In $\mathbb{R}^2$, we consider the collection of vertical real lines indexed by $\mathbb{Z}$, which we denote by $\mathbb{Z} \times \mathbb{R}$ below, it is called the *(primal) semi-discrete lattice*. We put independent Poisson point processes with parameter $\lambda > 0$ on each of these real lines. The points of these processes are called *cut points*. Similarly, we consider the dual of $\mathbb{Z} \times \mathbb{R}$ which is $(\mathbb{Z} + \frac{1}{2}) \times \mathbb{R}$. It can also be seen as a collection of vertical real lines, this time indexed by $\mathbb{Z} + \frac{1}{2}$. We also put independent Poisson point processes on each of these lines, with parameter $\mu > 0$. These points are called *bridges* and we draw at the same level a horizontal segment connecting the two neighboring vertical (primal) lines. See Figure 9b and 9c for an example. Moreover, these two families of Poisson point processes are taken to be independent of one another.

Consider a random configuration given by the above Poisson point processes and define the notion of *connectivity*. Two points x and y in the semi-discrete lattice are said to be connected if one can go from one to the other using only primal lines and horizontal bridges without crossing any cuts. The *cluster* of a point x is the largest subgraph containing x which is connected in this sense.

Having this notion of connectivity, we can define the quantum random-cluster model using the number of connected components as in (0.3). The model also has a *loop representation*, which is obtained by interfaces separating clusters in both the primal and dual lattices, see Figure 9d.

[8] A d-dimensional discrete model corresponds to a $(d+1)$-dimensional quantum model with an additional dimension describing the time evolution.

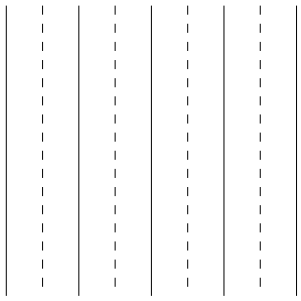

(a) A piece of the semi-discrete lattice $\mathbb{Z} \times \mathbb{R}$.

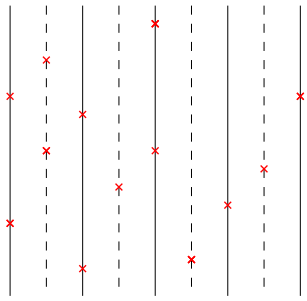

(b) Red points represent the Poisson point processes on primal (parameter λ) and dual (parameter μ) lines.

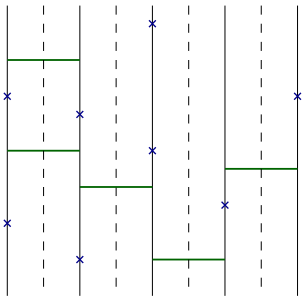

(c) Poisson points on primal lines are transformed into cuts and those on dual lines into bridges.

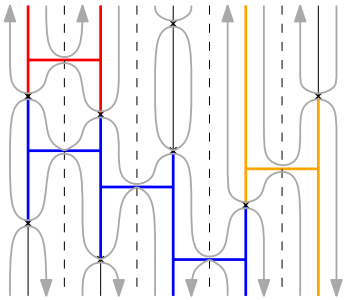

(d) The loop representation obtained by interfaces separating connected components.

Figure 9 – The random-cluster model on the semi-discrete lattice with different representations.

Fix a parameter $q \geqslant 1$. The measure of the quantum random-cluster model is given as follows,

$$\mathrm{d}\mathbb{P}_{\lambda,\mu}(D,B) \propto q^{k(D,B)}\mathrm{d}\mathbb{P}_{\lambda,\mu}(D,B)$$

where $\mathbb{P}_{\lambda,\mu}$ is the law of Poisson point processes described above with parameters λ on primal lines and μ on dual lines. Here, D and B are locally finite sets of cuts and bridges respectively. Given a configuration of Poisson points (D,B), the quantity $k(D,B)$ denotes the number of clusters in the configuration (on the primal lattice). Using the self-duality at criticality, i.e., the set of parameters (λ,μ) such that $\mu/\lambda = q$, one can show the following relation

$$\mathrm{d}\mathbb{P}_{\lambda,\mu}(D,B) \propto q^{k(D,B)}\mathrm{d}\mathbb{P}_{\lambda,\mu}(D,B) \propto \sqrt{q}^{l(D,B)}\mathrm{d}\mathbb{P}_{\rho,\rho}(D,B),$$

where $\rho = \sqrt{\lambda\mu}$ and $l(D,B)$ denotes the number of loops in the loop representation.

At the end of the first part of this thesis, we will discuss some properties of the quantum model at criticality derived from its discrete counterpart.

The quantum Ising model

For $q = 2$, the quantum random-cluster model described above can also be obtained from the quantum Ising model via the Edwards-Sokal coupling as in the discrete setting. We recall

that the random-cluster representation is also called FK-representation sometimes. In this section, we quantize the Hamiltonian (0.1) in the classical setting with an additional external field then explain how to obtain different representations of the model, among which the FK-representation.

The quantum Hamiltonian we define later is an operator acting on the Hilbert space $\bigotimes_{\mathbb{Z}} \mathbb{C}^2$, which is the tensor product of Hilbert spaces indexed by $\mathbb{Z} = (V, E)$. More precisely, with each $x \in \mathbb{Z}$, we associate a Hilbert space of spin configurations $\mathbb{C}^2 \cong \mathrm{Span}(|+\rangle, |-\rangle)$, where we identify $|+\rangle$ with $(1,0)$ and $|-\rangle$ with $(0,1)$, for instance. Then, we define the quantum Hamiltonian to be

$$H = -\mu \sum_{\langle x,y\rangle \in E} \sigma_x^{(3)} \sigma_y^{(3)} - \lambda \sum_{x \in V} \sigma_x^{(1)}.$$

In the previous definition, λ and μ are two positive parameters, where μ is the interaction term between particles at neighboring sites and λ is the intensity of the transverse field. The Pauli matrices are given by

$$\sigma^{(1)} = \begin{pmatrix} 0 & 1 \\ 1 & 0 \end{pmatrix}, \quad \sigma^{(3)} = \begin{pmatrix} 1 & 0 \\ 0 & -1 \end{pmatrix}$$

and act on $\mathbb{C}^2$, which we recall is the space of spin configurations. The operators $\sigma_x^{(1)}$ is defined by the tensor product which takes the Pauli matrix $\sigma^{(1)}$ at coordinate x and identity operator elsewhere; the same applies to $\sigma_x^{(3)}$. As consequence, the operator H makes sense and acts effectively on $\bigotimes_{\mathbb{Z}} \mathbb{C}^2$.

The quantum Ising model (with a transverse field) on $\mathbb{Z}$ is given by the operator $e^{-\beta H}$, where $\beta > 0$. This may also be seen as the quantization of the Gibbs measure given earlier in (0.2). It is mentioned in [Pfe70] that it is an exactly solvable one-dimensional quantum model.

Moreover, this model can also be seen as a space-time evolution of a spin configuration via the "path integral" method. Roughly speaking, we interprete the parameter $\beta > 0$ as the time parameter and expand the exponential operator $e^{-\beta H}$ in different ways. For $\nu \in \mathbb{R}$, we may consider $e^{-\beta(H+\nu)}$ instead of $e^{-\beta H}$ because $e^{-\beta \nu}$ is just a constant factor of renormalization. Then, we write

$$e^{-\beta(H+\nu)} = [e^{-\Delta(H+\nu)}]^{\beta/\Delta},$$

where we choose $\Delta > 0$ such that $\beta/\Delta \in \mathbb{N}$. For $\Delta > 0$ small enough, we may expand $e^{-\Delta(H+\nu)}$ up to order $\mathcal{O}(\Delta)$ in different ways, which provide us with the FK-representation (along with the loop representation) mentioned above, and also the random-current representation. Readers may have a look at [Iof09] for a nice and complete exposition on this topic. These representations are useful in interpreting results from the classical Ising model [GOS08, BG09, Bjö13].

In the second part of this thesis, we are interested in proving a result of conformal invariance as mentioned earlier for the discrete Ising model.

In order to state the theorem, let us recall a few more important notions. We consider a Dobrushin domain (Ω, a, b), i.e., an open, bounded and simply connected set with two marked points on the boundary a and b. For every positive δ, we can semi-discretize it by a Dobrushin domain $(\Omega_\delta, a_\delta, b_\delta)$ which is a subgraph of the semi-discrete medial lattice $\frac{\delta}{2}\mathbb{Z} \times \mathbb{R}$ with the so-called *Dobrushin boundary conditions*, consisting of wired boundary conditions on the arc $(a_\delta b_\delta)$ and free boundary conditions on the arc $(b_\delta a_\delta)$. In this case, the loop representation gives rise to a collection of loops and one interface connecting a_δ to b_δ, separating the (primal) cluster connected to the wired arc and the (dual) cluster connected to the free arc.

We will prove the conformal invariance of the quantum Ising model in the following sense: the limit of interfaces when δ goes to 0 is conformally invariant. This is the first quantum model proved to have such a property. The informal statement of our main theorem is given below, while the more precised version will be given in Theorem 6.1.

Theorem. *Let (Ω, a, b) be a Dobrushin domain. For all $\delta > 0$, let $(\Omega_\delta, a_\delta, b_\delta)$ be its semi-discretized counterpart. Define the FK-representation of the quantum Ising model on $(\Omega_\delta, a_\delta, b_\delta)$ and denote by γ_δ the interface separating the (primal) wired boundary and the (dual) free boundary. When δ goes to zero, the interface γ_δ converges to the chordal Schramm-Löwner Evolution of parameter 16/3 in (Ω, a, b).*

The proof is made possible by the similarity between the FK-representations of the quantum and the classical Ising models. The FK-representation and the loop representation of the quantum model can be interpreted as the same representations of the classical model living on a more and more flattened rectangular lattice $\mathbb{Z} \times \varepsilon\mathbb{Z}$. Thus, the proof almost comes from the same arguments as in the so-called isoradial case, except that some notions need to be adapted to the semi-discrete case.

Intuitively, using the universality of the classical Ising model [CS12] on isoradial graphs would require an inversion of limits:

- On one hand, the universality result says that the classical FK-Ising model on $\delta(\mathbb{Z} \times \varepsilon\mathbb{Z})$, the flattened isoradial rectangular lattice of mesh size δ, has an interface which is conformally invariant in the limit $\delta \to 0$, provided that ε is kept unchanged. In this first approach, the lattice "converges" to the whole plane uniformly in all directions.
- On the other hand, if we put the classical FK-Ising on $\delta(\mathbb{Z} \times \varepsilon\mathbb{Z})$ with flatter and flatter rectangles by making ε go to 0, we would get continuous lines in the vertical direction, and the model we obtain is exactly the FK-representation of the quantum Ising model. Therefore, to get the conformal invariance of the interface in the quantum FK-Ising, we would need to make δ go to 0 afterwards, which is the distance between two neighboring vertical lines. In this second approach, the lattice "converges" to the whole plane first in the vertical direction, then in the horizontal one.

The heuristic described above strongly suggests that the FK-representation of the quantum Ising model should also be conformally invariant in the limit, and that the interface in the limit should be the same as in the classical case. However, making this argument mathematically rigorous is far from immediate, and that is why we work directly in the semi-discrete case.

To this end, some classical notions need to be adapted and new tools be constructed. We will define the Green's function on the semi-discrete lattice, give the notion of s-holomorphicity, show that the fermionic observable is s-holomorphic and give a proof of the RSW property by the second-moment method. Everything is defined directly in the semi-discrete setting. Among all the notions and properties, it is worth mentioning that the construction of the Green's function is not totally trivial even though the method and the main idea are pretty similar to the case of the isoradial setting [Ken02].

Other results mentioned earlier concerning the conformal invariance from the classical Ising model are also expected to have their counterparts in the quantum case, such as the energy density and multi-spin correlations.

Organization of this thesis

This thesis consists of three parts. The first chapter is introductive in which we introduce the basic notions required for the lecture of this thesis. The second and the thrid chapters deal with the random-cluster model on isoradial graphs and the universality of the model. The last three chapters deal with the quantum random-cluster model, or more specifically, the quantum FK-Ising model, and the convergence of its interface to $SLE_{16/3}$. More precisely, this thesis is divided as follow:

- Chapter 1: introduction to the classical and the quantum random-cluster model along with their useful properties.
- Chapter 2: presentation of isoradial graphs and the star-triangle transformations, which are the key transformations towards universality.
- Chapter 3: theorems on the universality of the random-cluster model.
- Chapter 4: consequences of the previous universality results on the quantum random--cluster model.
- Chapter 5: introduction to the semi-discrete complex analysis, which is the main tool to proving the convergence of the FK-Ising interface.
- Chapter 6: the proof of the convergence.

Chapter 1

Definition of models

In this chapter, we will give a precise definition of the random-cluster model. We first define the model on finite graphs with boundary conditions, then discuss its properties such as the FKG property and the domain Markov property. This will turn out to be useful when we come to the definition of the model on infinite graphs, which can be seen as weak limits of measures on larger and larger finite graphs.

We fix a constant $q \geqslant 1$ once for all, which is the *cluster-weight* of the random-cluster model.

1.1 The random-cluster model on finite graphs

1.1.1 Definition

Consider a finite graph $G = (V, E)$ and a family of weights $\boldsymbol{p} = (p_e)_{e \in E} \in [0,1]^E$ indexed by its edges. A *configuration* of the random-cluster model on G is an element ω of $\Omega := \{0,1\}^E$. Given a configuration ω, we say that an edge $e \in E$ is *open* if $\omega(e) = 1$; and *close* otherwise. An equivalence relation on vertex set V can be defined via open edges. We say that x and y are equivalent if there exists a sequence of vertices $(x_i)_{0 \leqslant i \leqslant n}$ such that x_i and x_{i+1} are connected to each other by an open edge, $x_0 = x$ and $x_n = y$. Then, we denote by $k(\omega)$ the number of its *connected components* (or *clusters*), which is the number of equivalence classes induced by this equivalence relation. Thus, we can assign to each configuration a weight defined by

$$c_{G,\boldsymbol{p},q}(\omega) = \prod_{e \in E} p_e^{\omega(e)} (1 - p_e)^{1 - \omega(e)} q^{k(\omega)}. \tag{1.1}$$

Finally, we define the measure of the random-cluster model on Ω to be the probability measure given by

$$\varphi_{G,\boldsymbol{p},q}[\omega] = \frac{c_{G,\boldsymbol{p},q}(\omega)}{Z_{G,\boldsymbol{p},q}},$$

where $Z_{G,\boldsymbol{p},q}$ is called the *partition function* and is defined by $Z_{G,\boldsymbol{p},q} = \sum_{\omega'} c_{G,\boldsymbol{p},q}(\omega')$ where the sum is taken over Ω. In other words, we define the random-cluster model to be propor-

tional to

$$\varphi_{G,\boldsymbol{p},q}[\omega] \propto \prod_{e\in E} p_e^{\omega(e)}(1-p_e)^{1-\omega(e)} q^{k(\omega)}$$
$$\propto \prod_{e\in E} y_e^{\omega(e)} q^{k(\omega)},$$

where we write $y_e = \frac{p_e}{1-p_e}$ for $e \in E$ for convenience. Here, the symbol $\propto$ indicates that the two quantities on the left-hand and the right-hand sides are equal up to a multiplicative constant which is independent from ω.

The random-cluster model is a generalization of the two following models. When $q = 1$, the dependence on the number of clusters is removed, thus we have a model in which all the edges are independently open or close with probability p_e and $1 - p_e$, which is exactly the Bernoulli percolation. When $q \geqslant 1$ is an integer, we obtain the q-color Potts model via the standard Edward-Sokal coupling (Section 1.1.2). In particular, for $q = 2$, we get the random--cluster representation (or FK-representation) of the Ising model.

1.1.2 Edward-Sokal coupling

Given a finite graph $G = (V, E)$, a family of edge weights $J = (J_e)_{e\in E} \in (0,\infty)^E$ and an integer $q \geqslant 1$. The *q-color Potts model* is some random distribution of q colors on vertices of G. With a configuration $\sigma \in \{1,\dots,q\}^V$, we associate the Hamiltonian

$$H_{G,\boldsymbol{J}}(\sigma) = -\sum_{e=\langle x,y\rangle\in E} J_e \mathbb{1}_{\sigma_x=\sigma_y},$$

where for $e \in E$, J_e can be seen as the strength of interaction between two vertices of e. Then, the measure of the q-color Potts model is defined to be equal to

$$\mathbb{P}_{G,\boldsymbol{J}}(\sigma) = \frac{\exp(-H_{G,\boldsymbol{J}}(\sigma))}{Z_{G,\boldsymbol{J}}}, \quad \text{where} \quad Z_{G,\boldsymbol{J}} = \sum_{\sigma'} \exp(-H_{G,\boldsymbol{J}}(\sigma')).$$

Now, we are ready to explain the Edward-Sokal bijection.

Given a random-cluster configuration $\omega \in \{0,1\}^E$ and a Potts configuration $\sigma \in \{1,\dots,q\}^V$, we say that the couple (ω,σ) is *compatible* if $\omega_e = 1$, then $\sigma_x = \sigma_y$ for $e = \langle x, y\rangle$.

Given a Potts configuration $\sigma \in \{1,\dots,q\}^V$, we associate a random-cluster configuration $\omega \in \{0,1\}^E$ as follows. For $e = \langle x, y\rangle \in E$,

- if $\sigma_x \neq \sigma_y$, then we set $\omega_e = 0$;
- if $\sigma_x = \sigma_y$, then we set $\omega_e = 1$ with probability p_e and $\omega_e = 0$ with probability $1 - p_e$.

We denote the joint law of (σ,ω) defined as above by $\mathbb{P}_1$.

Conversely, given a random-cluster configuration $\omega \in \{0,1\}^E$, we associate a Potts configuration $\sigma \in \{1,\dots,q\}^V$ by choosing uniformly a random color in $\{1,\dots,q\}$ for each cluster of ω. We denote the joint law of (σ,ω) defined as above by $\mathbb{P}_2$.

It can be easily check that the couple of configurations (ω,σ) is compatible in both directions.

To show that we can couple the random-cluster measure and the Potts measure, we need to show that the associated joint measures $\mathbb{P}_1$ and $\mathbb{P}_2$ via these two bijections have the same law.

We have,

$$\begin{aligned}\mathbb{P}_1(\omega,\sigma) &\propto \prod_{\substack{e\in E\\ \sigma_x=\sigma_y}} e^{J_e} p_e^{\omega_e}(1-p_e)^{1-\omega_e}\\ &\propto \prod_{\substack{e\in E\\ \sigma_x=\sigma_y}} e^{J_e} y_e^{\omega_e}(1-p_e),\end{aligned}$$

and

$$\begin{aligned}\mathbb{P}_2(\omega,\sigma) &\propto \prod_{e\in E} y_e^{\omega_e}\cdot q^{k(\omega)}\cdot\left(\frac{1}{q}\right)^{k(\omega)}\\ &\propto \prod_{e\in E} y_e^{\omega_e} = \prod_{\substack{e\in E\\ \sigma_x=\sigma_y}} y_e^{\omega_e},\end{aligned}$$

where we use the fact that (ω,σ) is compatible in the last line. Thus,

$$\frac{\mathbb{P}_1(\omega,\sigma)}{\mathbb{P}_2(\omega,\sigma)} \propto \prod_{\substack{e\in E\\ \sigma_x=\sigma_y}} e^{J_e}(1-p_e).$$

Therefore, by taking $J_e = -\ln(1-p_e)$, the product in the previous line equals 1. Since $\mathbb{P}_1$ and $\mathbb{P}_2$ are both probability measures, we have $\mathbb{P}_1(\omega,\sigma) = \mathbb{P}_2(\omega,\sigma)$ for all (ω,σ).

1.1.3 Boundary conditions

For a finite graph $G=(V,E)$, we call *boundary conditions* a partition of its boundary vertices. In other words, boundary conditions ξ can be written as $P = P_1 \sqcup \cdots \sqcup P_m$ where P is the set of the boundary vertices. This induces an equivalence relation: two vertices of P are said to be *equivalent* if they belong to the same subset of the partition P_i. In terms of the graph structure, vertices in the same equivalence class are connected to each other via edges which are always open (or fusion them into a vertex).

Consider a finite graph $G=(V,E)$ with boundary conditions ξ. We take a family of parameters indexed by its edges $\mathbf{p}\in[0,1]^E$. We write $\Omega=\{0,1\}^E$ for the associated probability space. The weight of a configuration $\omega\in\Omega$ is modified from (1.1) as follows

$$c^{\xi}_{G,\boldsymbol{p},q}(\omega) = \prod_{e\in E} p_e^{\omega(e)}(1-p_e)^{1-\omega(e)} q^{k^{\xi}(\omega)}, \tag{1.2}$$

where $k^{\xi}(\omega)$ denotes the number of connected components in ω with respect to the boundary conditions ξ. A connected component (in ω) is a maximal subgraph (in G induced by ω) for the inclusion. Then, we write $\varphi^{\xi}_{G,\boldsymbol{p},q}$ for the probability measure of the random-cluster model on G with parameters $\boldsymbol{p}$ and q and boundary conditions ξ by

$$\varphi^{\xi}_{G,\boldsymbol{p},q}[\omega] = \frac{c^{\xi}_{G,\boldsymbol{p},q}(\omega)}{Z^{\xi}_{G,\boldsymbol{p},q}}, \quad \text{where } Z^{\xi}_{G,\boldsymbol{p},q} = \sum_{\omega'\in\{0,1\}^E} c^{\xi}_{G,\boldsymbol{p},q}(\omega')$$

is the partition function.

For $q > 1$, this model depends highly on connection properties between vertices. Thus, the boundary conditions turn out to be important. Furthermore, at $\boldsymbol{p}$ fixed, configurations with more connected components are more favoured due to the additional weight $q^{k^\xi(\omega)}$.

In this thesis, we are particularly interested in the following boundary conditions: free and wired boundary conditions. The free boundary conditions represent the partition of boundary points into unit sets, meaning that the boundary points are all disconnected; whereas the wired one represents the partition into only one set containing all the boundary vertices, meaning that all the boundary points are connected. Another way to interprete this is to add a ghost vertex v_g to the graph and edges connecting v_g to all the vertices on the boundary, which are always declared closed for the free boundary conditions and open for the wired boundary conditions. For simplicity, we may write $\xi = 0$ for the free boundary conditions and $\xi = 1$ for the wired one. Then, the random-cluster measures resulting from these boundary conditions are denoted $\varphi^0_{G,\boldsymbol{p},q}$ and $\varphi^1_{G,\boldsymbol{p},q}$.

In mathematical terms, define the augmented graph $\widetilde{G} = (\widetilde{V}, \widetilde{E})$ which is given by $\widetilde{V} = V \cup \{v_g\}$ and $\widetilde{E} = E \cup \{(v_g, v), v \in \partial G\}$. For $\xi = 0, 1$, we define the graph G with boundary conditions ξ, denoted G^ξ, to be the graph $\widetilde{G}$ whose admissible configurations are $\omega \in \{0,1\}^{\widetilde{E}}$ such that $\omega(e) = \xi$ for all $e \in \widetilde{E} \backslash E$. Note that we have $\varphi^\xi_{G,\boldsymbol{p},q} = \varphi^0_{G^\xi,\boldsymbol{p},q} = \varphi_{G^\xi,\boldsymbol{p},q}$.

1.1.4 Dual model

Consider a finite graph $G = (V, E)$ which is locally finite. We define its dual graph $G^* = (V^*, E^*)$ as follows. The vertex set V^* consists of the centers of the faces of G and the edge set E^* consists of the edges connecting the vertices of V^*, corresponding to adjacent faces in G. Here, both the primal and dual graphs are considered as combinatorial objects without any embedding. Therefore, the graphs $(G^*)^*$ and G have the same graph structure. See Figure 1.1 for an illustration.

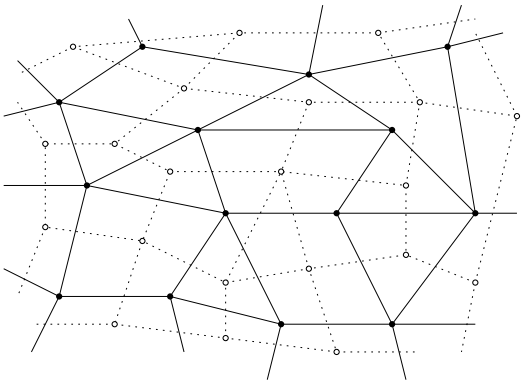

Figure 1.1 – Black vertices with solid segments represent the primal graph and white vertices with dotted segments represent the dual graph.

Given a random-cluster measure $\varphi^\xi_{G,\boldsymbol{p},q}$, we want to make sense of its dual measure, which is coupled with the original measure but defined on the dual graph G^*. Since there are boundary conditions on G, we should also take this into account.

We denote by G^ξ the graph G with boundary conditions $\xi = 0$ or 1. Its dual graph is then defined by $(G^\xi)^* := (\widetilde{G}^*)^{1-\xi}$, where $\widetilde{G}$ is the augmented graph defined in the previous section. By abuse of notation, we may also write $(G^*)^{1-\xi}$ for this.

Then, with a configuration $\omega \in \{0,1\}^{\widetilde{E}}$, we associate the canonical dual configuration $\omega^* \in \{0,1\}^{(\widetilde{E})^*}$ by

$$\omega^*(e^*) = 1 - \omega(e), \quad \forall e \in \widetilde{E}, \tag{1.3}$$

where e^* is the dual edge of e.

Given $\boldsymbol{p} = (p_e)_{e\in E}$ and $\boldsymbol{p}^* = (p_{e^*})_{e^*\in E^*}$ two families of probability parameters associated with the primal edges and the dual edges of G. Define $y_e = \frac{p_e}{1-p_e}$ for $e \in E$ and $y_{e^*} = \frac{p_{e^*}}{1-p_{e^*}}$ for $e^* \in E^*$. Let $q \geqslant 1$ be the cluster-weight of the random-cluster model. The following proposition gives a criterion for $\varphi^{\xi}_{G,\boldsymbol{p},q}$ and $\varphi^{1-\xi}_{G^*,\boldsymbol{p}^*,q}$ to be "dual" one to another.

Proposition 1.1. *Let ω be a configuration sampled according to the law of $\varphi^{\xi}_{G,\boldsymbol{p},q}$. Define the dual configuration ω^* as in (1.3). Moreover, assume that $y_e y_{e^*} = q$ for all $e \in E$. Then, ω^* has the same law as $\varphi^{1-\xi}_{G^*,\boldsymbol{p}^*,q}$.*

Proof. Consider $\omega \in \{0,1\}^{\widetilde{E}}$ and define ω^* as in (1.3). We first state the Euler formula which can be shown by induction on the number of vertices:

$$|\widetilde{V}| - o^{\xi}(\omega) + f^{\xi}(\omega) - k^{\xi}(\omega) = 1, \tag{1.4}$$

where $|\widetilde{V}|$ is the cardinal of the vertex set of $\widetilde{G}$, $o^{\xi}(\omega)$ the number of open edges, $f^{\xi}(\omega)$ the number of faces and $k^{\xi}(\omega)$ the number of clusters induced by the configuration ω with the boundary conditions ξ.

We are going to rewrite $\varphi^{\xi}_{G,\boldsymbol{p},q}(\omega)$ in terms of ω^*. In the following steps, we might get some additional multiplicative factors, but since they do not depend on ω, we just say that different quantities are proportional to each other using the symbol $\propto$. We find

$$\begin{aligned}
\varphi^{\xi}_{G,\boldsymbol{p},q}[\omega] &\propto \prod_{e\in E} y_e^{\omega(e)} q^{k^{\xi}(\omega)} \\
&\propto \prod_{e\in E} y_e^{\omega(e)} q^{f^{\xi}(\omega) - o^{\xi}(\omega)} \\
&\propto \prod_{e\in E} \left(\frac{y_e}{q}\right)^{\omega(e)} q^{f^{\xi}(\omega)} \\
&\propto \prod_{e\in E} \left(\frac{q}{y_e}\right)^{\omega(e^*)} q^{k^{1-\xi}(\omega^*)} \\
&\propto \prod_{e\in E} (y_{e^*})^{\omega(e^*)} q^{k^{1-\xi}(\omega^*)},
\end{aligned}$$

where we apply (1.4) in the second line, use the fact that $f^{\xi}(\omega) = k^{1-\xi}(\omega^*)$ in the fourth line and the hypothesis $y_e y_{e^*} = q$ in the last line. This shows that $\varphi^{\xi}_{G,\boldsymbol{p},q}[\omega]$ and $\varphi^{1-\xi}_{G^*,\boldsymbol{p}^*,q}[\omega^*]$ are proportional to each other for all ω, thus are equal since both are probability measures. In conclusion, the law of ω^* is described by $\varphi^{1-\xi}_{G^*,\boldsymbol{p}^*,q}$ if ω is sampled according to $\varphi^{\xi}_{G,\boldsymbol{p},q}$. □

1.1.5 Loop representation

Consider a finite graph $G = (V, E)$, boundary conditions $\xi = 0$ or 1 and two families of parameters $(y_e)_{e\in E}$ and $(y_{e^*})_{e^*\in E^*}$ as in Proposition 1.1. Due to the duality in law of $\varphi^{\xi}_{G,\boldsymbol{p},q}$

and $\varphi^{1-\xi}_{G^*,\boldsymbol{p}^*,q}$, we can write, for any configuration $\omega \in \{0,1\}^E$,

$$\begin{aligned}\varphi^{\xi}_{G,\boldsymbol{p},q}[\omega] &= \sqrt{\varphi^{\xi}_{G,\boldsymbol{p},q}[\omega]\varphi^{1-\xi}_{G^*,\boldsymbol{p}^*,q}[\omega^*]} \\ &\propto \prod_{e\in E} y_e^{\omega(e)/2}(y_{e^*})^{\omega^*(e^*)/2}\cdot\sqrt{q}^{k^{\xi}(\omega)+k^{1-\xi}(\omega^*)} \\ &\propto \prod_{e\in E} y_e^{\omega(e)/2}(y_{e^*})^{\omega^*(e^*)/2}\cdot\sqrt{q}^{l^{\xi}(\omega)} \\ &\propto \prod_{e\in E}\Big(\frac{y_e}{y_{e^*}}\Big)^{\omega(e)/2}\cdot\sqrt{q}^{l^{\xi}(\omega)} \end{aligned} \tag{1.5}$$

where $l^{\xi}(\omega)$ is the number of loops in the configuration ω, which depends only on ω. A loop in a configuration ω is a path in $\mathbb{R}^2$ separating different clusters. See Figure 1.2 for an illustration.

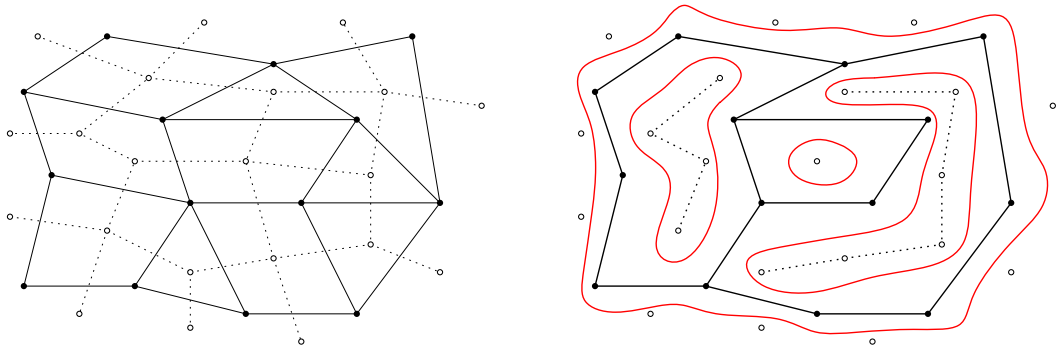

Figure 1.2 – **Left:** A primal graph G^1 (in solid lines) along with its dual graph $(G^*)^0$ (in dotted lines). **Right:** A primal configuration (in solid line) with its coupled dual configuration (in dotted line) and the loop representation (in red).

The probability measure in (1.5), expressed in terms of weights (y_e), (y_{e^*}) and the number of loops $l^{\xi}(\omega)$, is called the *loop representation* of the random-cluster model.

1.1.6 Domain Markov property

We say that $F \subset G$ is a *subgraph* of G if the edge set $\mathcal{E}(F)$ is a subset of $\mathcal{E}(G)$ with the vertex set $\mathcal{V}(F)$ given by the vertices of $\mathcal{V}(E)$ who are an endpoint of some edge in $\mathcal{E}(F)$.

Let $F \subset G$ be a subset of G and ξ boundary conditions of G. Consider $\psi \in \{0,1\}^{\mathcal{E}(G)\setminus\mathcal{E}(F)}$, a configuration on edges outside of F. We define ξ^{ψ} the induced boundary conditions of F given by ξ and ψ: two boundary vertices of F are in the same equivalence class if they are connected in $\mathcal{E}(G)\setminus\mathcal{E}(F)$ with the boundary conditions ξ on G.

Proposition 1.2 (Domain Markov Property)**.** *Let A be a measurable set of $\{0,1\}^{\mathcal{E}(F)}$. We have*

$$\varphi^{\xi}_{G,\boldsymbol{p},q}[A \mid \omega(e) = \psi(e), \forall e \in \mathcal{E}(G)\setminus\mathcal{E}(F)] = \varphi^{\xi^{\psi}}_{F,\boldsymbol{p},q}[A]. \tag{1.6}$$

Proof. We prove this by induction on the cardinal of $\mathcal{E}(G)\setminus\mathcal{E}(F)$. Assume that $F = G\setminus\{e\}$ for some edge $e \in \mathcal{E}(G)$. Let ξ be boundary conditions on G and write ξ^e for the induced boundary conditions on F by ξ with the edge e open. Let $\omega \in \{0,1\}^{\mathcal{E}(G)}$ be a configuration

and write ω^e for the configuration ω with the edge e open. We have

$$\begin{aligned}\varphi^{\xi}_{G,\boldsymbol{p},q}[\omega \mid \omega(e)=1] &= \frac{\varphi^{\xi}_{G,\boldsymbol{p},q}[\omega^e]}{\varphi^{\xi}_{G,\boldsymbol{p},q}[\omega(e)=1]} \\ &= \frac{\prod_{f\in\mathcal{E}(G)} p_f^{\omega^e(f)}(1-p_f)^{1-\omega^e(f)} q^{k^{\xi}(\omega^e)}}{\sum_{\omega'\in\{0,1\}^{\mathcal{E}(G)},\omega'(e)=1}\prod_{f\in\mathcal{E}(G)} p_f^{\omega'(f)}(1-p_f)^{1-\omega'(f)} q^{k^{\xi^e}(\omega')}} \\ &= \frac{\prod_{f\in\mathcal{E}(F)} p_f^{\omega(f)}(1-p_f)^{1-\omega(f)}\cdot p_e q^{k^{\xi}(\omega^e)}}{\sum_{\omega'\in\{0,1\}^{\mathcal{E}(F)}}\prod_{f\in\mathcal{E}(F)} p_f^{\omega'(f)}(1-p_f)^{1-\omega'(f)}\cdot p_e q^{k^{\xi^e}(\omega')}} \\ &= \varphi^{\xi^e}_{F,\boldsymbol{p},q}[\omega_{|\mathcal{E}(F)}],\end{aligned}$$

where we use the fact that $k^{\xi}(\omega^e) = k^{\xi^e}(\omega)$. □

As an application, consider a subgraph $F \subset G$ such that $G\backslash F$ is connected. Define $\psi(e) = 1$ for all $e \in \mathcal{E}(G)\backslash\mathcal{E}(F)$. Then, no matter the boundary conditions ξ on G, ξ^{ψ} always corresponds to the wired boundary conditions on F. Equation (1.6) can be rewritten as

$$\varphi^{\xi^{\psi}}_{G,\boldsymbol{p},q}[A] = \varphi^{\xi}_{G,\boldsymbol{p},q}[A \mid \omega(e)=1, \forall e\in\mathcal{E}(G)\backslash\mathcal{E}(F)] = \varphi^{1}_{F,\boldsymbol{p},q}[A].$$

Similarly, if $\psi(e) = 0$ for all $e \in \mathcal{E}(G)\backslash\mathcal{E}(F)$. Then, for any boundary conditions ξ on G, ξ^{ψ} corresponds to the free boundary conditions on F. Equation (1.6) can be rewritten as

$$\varphi^{\xi^{\psi}}_{G,\boldsymbol{p},q}[A] = \varphi^{\xi}_{G,\boldsymbol{p},q}[A \mid \omega(e)=0, \forall e\in\mathcal{E}(G)\backslash\mathcal{E}(F)] = \varphi^{0}_{F,\boldsymbol{p},q}[A].$$

This also justifies why we write 1 for the wired boundary conditions and 0 for the free ones.

1.1.7 Positive association

The set $\Omega = \{0,1\}^E$ can be seen as the set consisting of all binary functions on the edges of a graph $G = (V, E)$. We can define a partial order on Ω as follows. For $\omega, \omega' \in \{0,1\}^E$, we write $\omega \leqslant \omega'$ if $\omega(e) \leqslant \omega'(e)$ for all $e \in E$. A function $f : \{0,1\}^E \to \mathbb{R}$ is said to be *increasing* if it is increasing for this partial order; and *decreasing* if $-f$ is increasing.

Let A be an event in $\{0,1\}^E$. We say that A is increasing if $\mathbb{1}_A$ is an increasing function; decreasing if A^c is increasing. This can also be interpreted as follows: for $\omega \leqslant \omega'$, if $\omega \in A$ then $\omega' \in A$, meaning that the operation of opening edges is stable in A.

To compare two different probability measures, we talk about *stochastic domination*. Given two probability measures μ_1 and μ_2, we say that μ_1 dominates μ_2 stochastically, denoted by $\mu_1 \geqslant \mu_2$, if for all increasing events A, we have $\mu_1(A) \geqslant \mu_2(A)$.

To know whether a probability measure dominates another, here is an useful criterion.

Theorem 1.3 (Holley criterion [Hol74]). *Let μ_1, μ_2 be two probability measures on $\{0,1\}^E$. If the following inequality is satisfied*

$$\mu_1(\omega\vee\eta)\mu_2(\omega\wedge\eta) \geqslant \mu_1(\omega)\mu_2(\eta) \tag{1.7}$$

for all $\omega, \eta \in \{0,1\}^E$, then μ_1 dominates μ_2 stochastically.

Proof. The idea is to find a coupling $(\omega_1, \omega_2) \sim \mathbb{P}$ with marginals $\omega_1 \sim \mu_1$ and $\omega_2 \sim \mu_2$ such that $\mathbb{P}(\omega_1 \geqslant \omega_2) = 1$. Then, for an increasing event A, we obtain

$$\mu_1(A) = \mathbb{P}(\omega_1 \in A) = \mathbb{P}(\omega_1 \in A, \omega_1 \geqslant \omega_2) \geqslant \mathbb{P}(\omega_2 \in A) = \mu_2(A).$$

The measure $\mathbb{P}$ is constructed as the stationary measure of some Markov chain. See [Hol74] for details. □

For a configuration $\omega \in \{0,1\}^E$ and an edge $e \in E$, write ω^e (respectively ω_e) for the configuration which coincides with ω everywhere except that its value at e is set to 1 (respectively 0).

We note that to show the previous stochastic domination, instead of the condition (1.7), it is actually sufficient to check that for any $\omega \in \{0,1\}^E$ and $e \neq f \in E$,

$$\mu_1(\omega^e)\mu_2(\omega_e) \geqslant \mu_1(\omega_e)\mu_2(\omega^e) \tag{1.8}$$

$$\text{and} \quad \mu_1(\omega^{ef})\mu_2(\omega_{ef}) \geqslant \mu_1(\omega_e^f)\mu_2(\omega_f^e). \tag{1.9}$$

Reders are referred to [Gri06, Thm. 2.3] for more details.

An important application of Holley criterion is the property called *positive associativity* on the random-cluster model. It is also known as *Fortuin-Kasteleyn-Ginibre inequality* (shortened as *FKG inequality*).

Definition 1.4 (FKG inequality)**.** Let $\mathbb{P}$ be a probability measure on the probability space $\Omega = \{0,1\}^E$. We say that $\mathbb{P}$ satisfies the FKG inequality (or is a positively correlated measure) if one of the following equivalent statements is true.

- For any increasing measurable sets A and B, we have $\mathbb{P}(A \cap B) \geqslant \mathbb{P}(A)\mathbb{P}(B)$.
- For any increasing functions $f, g : \{0,1\}^E \to \mathbb{R}$, we have $\mathbb{E}(fg) \geqslant \mathbb{E}(f)\mathbb{E}(g)$.

This is actually equivalent to the same inequalities with both A and B decreasing events or both f and g decreasing functions. The first part can be done by considering the complements and the second point by considering the opposites.

Theorem 1.5 (FKG lattice condition)**.** *Given a finite graph $G = (V, E)$ and a positive measure μ on $\{0,1\}^E$. If for any configuration $\omega \in \{0,1\}^E$ and $e \neq f \in E$, we have*

$$\mu(\omega^{ef})\mu(\omega_{ef}) \geqslant \mu(\omega_e^f)\mu(\omega_f^e), \tag{1.10}$$

then for any increasing events A and B,

$$\mu(A \cap B) \geqslant \mu(A)\mu(B). \tag{1.11}$$

Proof. Consider an increasing event A and measures defined by $\mu_1 = \mu(\cdot \mid A)$ and $\mu_2 = \mu$. We need to show that μ_1 stocastically dominates μ_2. To do so, we need to check inequalities (1.8) and (1.9) for μ_1 and μ_2. Fix a configuration ω and $e \neq f$. We have

$$\mathbb{1}_{\omega^e \in A}\mu(\omega^e)\mu(\omega_e) \geqslant \mathbb{1}_{\omega_e \in A}\mu(\omega_e)\mu(\omega^e),$$

since A is increasing. Dividing by $\mu(A)$, we get

$$\mu(\omega^e \mid A)\mu(\omega_e) \geqslant \mu(\omega_e \mid A)\mu(\omega^e),$$

which is exactly (1.8). For (1.9), we use the hypothesis (1.10) to obtain

$$\mathbb{1}_{\omega^{ef} \in A}\mu(\omega^{ef})\mu(\omega_{ef}) \geqslant \mathbb{1}_{\omega_e^f \in A}\mu(\omega_e^f)\mu(\omega_f^e).$$

Again, we divide by $\mu(A)$ and get (1.9). □

Proposition 1.6. *For any family of parameters $\boldsymbol{p} = (p_e)_{e\in E}$ and any boundary conditions ξ on G, the random-cluster measure $\varphi^{\xi}_{G,\boldsymbol{p},q}$ satisfies the FKG inequality.*

Proof. It is enough to check the FKG lattice condition (1.10). Let $\omega \in \{0,1\}^E$ be a configuration and $e \neq f$ two edges, we need to check that

$$\prod_{\eta\in E} y_\eta^{o(\omega^{ef})+o(\omega_{ef})} q^{k^\xi(\omega^{ef})+k^\xi(\omega_{ef})} \geqslant \prod_{\eta\in E} y_\eta^{o(\omega_e^f)+o(\omega_f^e)} q^{k^\xi(\omega_e^f)+k^\xi(\omega_f^e)}.$$

The products of y_η simplify on both sides, so we just need to check that $k^\xi(\omega^{ef})+k^\xi(\omega_{ef}) \geqslant k^\xi(\omega_e^f)+k^\xi(\omega_f^e)$. To show this, we discuss whether the two endpoints of f in $E\backslash\{e,f\}$ are connceted or not:

- connected: $k(\omega^{ef}) = k(\omega_f^e)$ and $k(\omega_{ef}) = k(\omega_e^f)$;
- disconnected: $k(\omega^{ef}) \geqslant k(\omega_f^e) - 1$ and $k(\omega_{ef}) = k(\omega_e^f) + 1$.

This concludes the proof. □

The random-cluster measures with different parameters can be shown to have stochastic domination relations. The precise statement is given below.

Proposition 1.7. *Consider a finite graph $G = (V,E)$, two families of parameters $\boldsymbol{p} = (p_e)_{e\in E}$ and $\boldsymbol{p}' = (p'_e)_{e\in E}$ with $\boldsymbol{p} \leqslant \boldsymbol{p}'$, and two cluster-weights q and q'. Also, for $e \in E$, write*

$$y_e = \frac{p_e}{1-p_e} \quad \text{and} \quad y'_e = \frac{p'_e}{1-p'_e}.$$

Moreover, assume that one of the two following conditions is satisfied:

- *$1 \leqslant q' \leqslant q$ and $y'_e \geqslant y_e$ for all $e \in E$;*
- *$q' \geqslant q \geqslant 1$ and $\frac{y'_e}{q'} \geqslant \frac{y_e}{q}$ for all $e \in E$.*

Then, the random-cluster measure $\varphi^{\xi}_{G,\boldsymbol{p}',q'}$ dominates stochastically $\varphi^{\xi}_{G,\boldsymbol{p},q}$ for any boundary conditions ξ. In other words, $\varphi^{\xi}_{G,\boldsymbol{p},q} \leqslant \varphi^{\xi}_{G,\boldsymbol{p}',q'}$.

Proof. For any random variable X, we have

$$\begin{aligned}
\varphi^{\xi}_{G,\boldsymbol{p}',q'}[X] &= \frac{1}{Z'}\sum_\omega X(\omega)\prod_{e\in E}(y'_e)^{\omega(e)}(q')^{k^\xi(\omega)} \\
&= \frac{Z}{Z'}\frac{1}{Z}\sum_\omega X(\omega)Y(\omega)\prod_{e\in E} y_e^{\omega(e)} q^{k^\xi(\omega)} \\
&= \frac{Z}{Z'}\varphi^{\xi}_{G,\boldsymbol{p},q}[XY],
\end{aligned}$$

where Z and Z' are partition functions and Y a random variable defined as follow,

$$\begin{aligned}
Z' &= \sum_\omega \prod_{e\in E}(y'_e)^{\omega(e)}(q')^{k^\xi(\omega)}, \\
Z &= \sum_\omega \prod_{e\in E} y_e^{\omega(e)} q^{k^\xi(\omega)}, \\
Y(\omega) &= \prod_{e\in E}\left(\frac{y'_e}{y_e}\right)^{\omega(e)}\left(\frac{q'}{q}\right)^{k^\xi(\omega)} = \prod_{e\in E}\left(\frac{y'_e/q'}{y_e/q}\right)^{\omega(e)}\left(\frac{q'}{q}\right)^{k^\xi(\omega)+o(\omega)}.
\end{aligned}$$

We claim that under both conditions of the statement, Y is an increasing random variable. Indeed, for the first condition, we have that $\frac{y_e'}{y_e} \geqslant 1$, $\frac{q'}{q} \leqslant 1$, $\omega(e)$ increasing in ω and $k^\xi(\omega)$ decreasing in ω. For the second condition, we have that $\frac{y_e'/q'}{y_e/q} \geqslant 1$, $\frac{q'}{q} \geqslant 1$, $\omega(e)$ increasing in ω and $k^\xi(\omega) + o(\omega)$ also increasing in ω, since each time when we open an edge, $o(\omega)$ increases exactly by 1 and $k^\xi(\omega)$ decreases at most by 1.

Take X to be an increasing random variable. Then we have

$$\varphi^\xi_{G,\boldsymbol{p}',q'}[X] \geqslant \frac{Z}{Z'}\varphi^\xi_{G,\boldsymbol{p},q}[X]\varphi^\xi_{G,\boldsymbol{p},q}[Y] = \varphi^\xi_{G,\boldsymbol{p},q}[X],$$

where $\varphi^\xi_{G,\boldsymbol{p},q}[Y] = \frac{Z'}{Z}$. □

Boundary conditions correspond to a partition of the boundary vertices. On the set of possible partitions, we can define a partial order. Given boundary conditions ξ and ψ, we say that $\xi \leqslant \psi$ if vertices which are in the same equivalence class of ξ are also in the same one for ψ, meaning that ξ is a finer partition than ψ.

Proposition 1.8 (Comparison between two boundary conditions)**.** *Given a finite graph $G = (V, E)$, a family of parameters $\boldsymbol{p} = (p_e)_{e\in E}$ and boundary conditions satisfying $\xi \leqslant \psi$, we have*

$$\varphi^\xi_{G,\boldsymbol{p},q} \leqslant \varphi^\psi_{G,\boldsymbol{p},q}. \tag{1.12}$$

Proof. The boundary conditions ξ correspond to a partition of boundary vertices $P_1 \sqcup \cdots \sqcup P_m$. Construct a new graph $\widetilde{G} = (V, \widetilde{E})$ from G by adding an edge between P_i and P_j with $i \neq j$ such that P_i and P_j are in the same equivalence class in ψ. Then, by the domain Markov property, we have

$$\varphi^\xi_{G,\boldsymbol{p},q}[\cdot] = \varphi^\xi_{\widetilde{G},\boldsymbol{p},q}[\cdot \mid \omega(e) = 0, \forall e \in \widetilde{E}\backslash E],$$
$$\varphi^\psi_{G,\boldsymbol{p},q}[\cdot] = \varphi^\xi_{\widetilde{G},\boldsymbol{p},q}[\cdot \mid \omega(e) = 1, \forall e \in \widetilde{E}\backslash E].$$

For any increasing event A depending only on E, we apply the FKG inequality to get

$$\varphi^\xi_{G,\boldsymbol{p},q}[A] \leqslant \varphi^\xi_{\widetilde{G},\boldsymbol{p},q}[A] \leqslant \varphi^\psi_{G,\boldsymbol{p},q}[A].$$

□

This result is particularly important since it will allow us to define infinite-volume random-cluster measures, which we discuss in the next section.

1.1.8 Infinite-volume measure

From now on, notations associated with infinite graphs will be denoted in bold letters.

Given an infinite graph $\mathbb{G} = (\mathbb{V}, \mathbb{E})$, the random-cluster model has no reason to be well-defined on it, since (i) the number of clusters $k(\omega)$ is infinite for some configurations ω and (ii) the partition function, or normalizing constant, may be infinite. However, it turns out that the positive correlation of the random-cluster measure is useful. More precisely, Proposition 1.8, which is an application of the FKG inequality, allows us to define some random-cluster measures on infinite graphs if we proceed carefully.

Let $\mathbb{G} = (\mathbb{V}, \mathbb{E})$ be an infinite graph with probability parameters $\boldsymbol{p} = (p_e)_{e\in\mathbb{E}}$ and cluster-weight parameter q. A measure $\mathbb{P}$ on $\mathbb{G}$ is an *infinite-volume random-cluster measure*

with parameters $\boldsymbol{p} = (p_e)$ and q if for every finite subgraph $F \subset \mathbb{G}$, any configuration $\xi \in \{0,1\}^{\mathbb{E}\setminus\mathcal{E}(F)}$ and any measurable set A with respect to edges in $\mathcal{E}(F)$, we have the *compatibility condition*,

$$\mathbb{P}[A \mid \omega_{|\mathbb{E}\setminus\mathcal{E}(F)} = \xi] = \varphi^{\xi}_{F,\boldsymbol{p},q}[A],$$

where, by abuse of notation, the configuration ξ is also used to denote the boundary conditions on F induced by ξ.

We say that the sequence of finite graphs $(G_n)_{n\in\mathbb{N}}$ exhausts $\mathbb{G}$ if the two following conditions are satisfied:

- The sequence is increasing: $G_0 \subset G_1 \subset \cdots \subset \mathbb{G}$.
- For all edge $e \in \mathbb{E}$, there exists $n \in \mathbb{N}$ such that $e \in \mathcal{E}(G_n)$.

Proposition 1.9. *Let G to be an infinite graph exhausted by $(G_n)_{n\in\mathbb{N}}$. For an increasing measurable event A which depends only on finitely many edges, we have the following inequalities*

$$\begin{aligned} &\varphi^0_{G_n,\boldsymbol{p},q}[A] \leqslant \varphi^0_{G_{n+1},\boldsymbol{p},q}[A] \\ \text{and} \quad &\varphi^1_{G_n,\boldsymbol{p},q}[A] \geqslant \varphi^1_{G_{n+1},\boldsymbol{p},q}[A], \end{aligned} \tag{1.13}$$

for n large enough.

Proof. Fix an increasing event A depending only on a finite number of edges in $\mathbb{G}$. Assume that k is the smallest integer such that A is measurable with respect to $\mathcal{E}(G_k)$. Take $n \geqslant k$. Set $\widetilde{E}$ to be the set of edges of $\mathcal{E}(G_{n+1})$ which are outside of $\mathcal{E}(G_n)$. Let ω be distributed as $\varphi^0_{G_n,\boldsymbol{p},q}$. Then we can write

$$\varphi^0_{G_n,\boldsymbol{p},q}[A] = \varphi^0_{G_{n+1},\boldsymbol{p},q}[A \mid \omega(e) = 0, \forall e \in \widetilde{E}] \leqslant \varphi^0_{G_{n+1},\boldsymbol{p},q}[A],$$

where we apply the FKG inequality and the fact that $\{\omega(e) = 0, \forall e \in \widetilde{E}\}$ is an decreasing event.

The proof is similar for the wired boundary conditions. □

In consequence, for any increasing event A, the sequences $(\varphi^0_{G_n,\boldsymbol{p},q}[A])$ and $(\varphi^1_{G_n,\boldsymbol{p},q}[A])$ have limits as n goes to infinity. Write $\varphi^0_{\mathbb{G},\boldsymbol{p},q}[A]$ and $\varphi^1_{\mathbb{G},\boldsymbol{p},q}[A]$ for their limits. By inclusion-exclusion principle, we can make sense of $\varphi^0_{\mathbb{G},\boldsymbol{p},q}[A]$ and $\varphi^1_{\mathbb{G},\boldsymbol{p},q}[A]$ for any measurable event A. As a result, we have constructed with success two infinite-volume random-cluster measures on infinite graphs by taking weak limits of finite-volume measures. Henceforth, we can talk about "random-cluster model on an infinite graph".

Proposition 1.10. *The infinite-volume random-cluster measures $\varphi^0_{\mathbb{G},\boldsymbol{p},q}$ and $\varphi^1_{\mathbb{G},\boldsymbol{p},q}$ do not depend on the sequence of finite subgraphs $(G_n)_{n\in\mathbb{N}}$ which exhausts $\mathbb{G}$.*

Proof. Let $(G'_n)_{n\in\mathbb{N}}$ be another sequence of finite graphs exhausting $\mathbb{G}$. Consider an increasing event A depending only on a finite number of edges which are all in G'_k for a certain fixed k. For $n \geqslant k$, since the graph G'_n is finite, we can find a m large enough such that $G'_n \subset G_m$. Thus, by comparing boundary conditions, we have the stochastic domination $\varphi^0_{G'_n,\boldsymbol{p},q}[A] \leqslant \varphi^0_{G_m,\boldsymbol{p},q}[A]$. Taking the limit $n \to \infty$, we obtain the inequality

$$\lim_{n\to\infty} \varphi^0_{G'_n,\boldsymbol{p},q}[A] \leqslant \varphi^0_{\mathbb{G},\boldsymbol{p},q}[A].$$

By exchanging the role of (G'_n) and (G_n), we get the inequality in the other direction. Therefore, we deduce the equality

$$\varphi^0_{\mathbb{G},\boldsymbol{p},q}[A] = \lim_{n\to\infty} \varphi^0_{G'_n,\boldsymbol{p},q}[A].$$

□

Given any infinite-volume random-cluster measure $\mathbb{P}$, we have the following inequality in the sense of stochastic domination,

$$\varphi^0_{\mathbb{G},\boldsymbol{p},q} \leqslant \mathbb{P} \leqslant \varphi^1_{\mathbb{G},\boldsymbol{p},q}.$$

In particular, when the two infinite-volume random-cluster measures $\varphi^0_{\mathbb{G},\boldsymbol{p},q}$ and $\varphi^1_{\mathbb{G},\boldsymbol{p},q}$ coincide, there exists only one unique infinite-volume random-cluster measure.

1.1.9 Finite-energy property

Consider an infinite graph $\mathbb{G} = (\mathbb{V}, \mathbb{E})$ and a family of edge parameters $(p_e)_{e\in\mathbb{E}}$. The finite-energy property says that the probability that a given edge e is open can be bounded away from 0 and 1 if p_e can be bounded away from 0 and 1.

Lemma 1.11. *Let $e \in \mathbb{E}$. Take $\varepsilon > 0$ such that $p_e \in [\varepsilon, 1-\varepsilon]$. Then, there exists $c = c(\varepsilon) > 0$ such that*

$$c \leqslant \varphi^{\xi}_{\mathbb{G},\boldsymbol{p},q}[\omega(e) = 1] \leqslant 1 - c.$$

Proof. We first note that the event $\{\omega(e) = 1\}$ is increasing.

When we condition on the states of the edges different from e, the inducing boundary conditions on the endpoints of e is either free or wired. In consequence, by denoting $G_0 = (V_0, E_0)$ where $E_0 = \{e = \langle u, v\rangle\}$ and $V_0 = \{u, v\}$ and comparing different boundary conditions, we get

$$\varphi^{\xi}_{\mathbb{G},\boldsymbol{p},q}[\omega(e) = 1] \leqslant \varphi^1_{G_0,p_e,q}[\omega(e) = 1] = p_e \leqslant 1 - \varepsilon$$

and

$$\varphi^{\xi}_{\mathbb{G},\boldsymbol{p},q}[\omega(e) = 1] \geqslant \varphi^0_{G_0,p_e,q}[\omega(e) = 1] = \frac{p_e}{p_e + (1-p_e)q} \geqslant \frac{\varepsilon}{\varepsilon + (1-\varepsilon)q}.$$

□

Proposition 1.12. *Let F be a finite subgraph of $\mathbb{G}$. Take $\varepsilon > 0$ such that $p_e \in [\varepsilon, 1-\varepsilon]$ for all $e \in \mathcal{E}(F)$. Then, there exists $c = c(\varepsilon) > 0$ such that for any configuration $\eta \in \{0,1\}^{\mathcal{E}(F)}$ and any boundary condition ξ,*

$$c \leqslant \varphi^{\xi}_{\mathbb{G},\boldsymbol{p},q}[\omega_{|F} = \eta] \leqslant 1 - c.$$

Proof. Enumerate the edges in $F : e_1, \dots e_m$, where $m = |\mathcal{E}(F)|$. Define $F_0 = \varnothing$ and $F_i = \{e_j, j \leqslant i\}$ for $1 \leqslant i \leqslant m$. We write

$$\varphi^{\xi}_{\mathbb{G},\boldsymbol{p},q}[\omega_{|\mathcal{E}(F)} = \eta] = \prod_{i=1}^{m} \varphi^{\xi}_{\mathbb{G},\boldsymbol{p},q}[\omega(e_i) = \eta(e_i) \mid \omega_{|F_{i-1}} = \eta_{|F_{i-1}}].$$

Let c_0 be the constant provided by Lemma 1.11. Then, for all i, we have

$$c_0 \leqslant \varphi^{\xi}_{\mathbb{G},\boldsymbol{p},q}[\omega(e_i) = \eta(e_i) \mid \omega_{|F_{i-1}} = \eta_{|F_{i-1}}] \leqslant 1 - c_0$$

by the FKG inequality and the domain Markov property. Thus, we can take $c = c_0^m$ to conclude. □

Proposition 1.13. *Let F be a finite subgraph of $\mathbb{G}$. Take $\varepsilon > 0$ such that $p_e \in [\varepsilon, 1-\varepsilon]$ for all $e \in \mathcal{E}(F)$. Then, there exists $c = c(\varepsilon) > 0$ such that for any increasing event A depending on edges not in $\mathcal{E}(F)$, any configuration $\eta \in \{0,1\}^{\mathcal{E}(F)}$ and any boundary conditions ξ,*

$$\varphi^{\xi}_{\mathbb{G},\boldsymbol{p},q}[A \cap \{\omega_{|\mathcal{E}(F)} = \eta\}] \geqslant c\varphi^{\xi}_{\mathbb{G},\boldsymbol{p},q}[A].$$

Proof. Let c be as given in the previous proposition. We write

$$\begin{aligned}
&\varphi^{\xi}_{\mathbb{G},\boldsymbol{p},q}[A \cap \{\omega_{|\mathcal{E}(F)} = \eta\}] \\
&\quad = \sum_{\psi \in \{0,1\}^{E\setminus\mathcal{E}(F)}} \varphi^{\xi}_{\mathbb{G},\boldsymbol{p},q}[\{\omega_{E\setminus\mathcal{E}(F)} = \psi\} \cap \{\omega_{\mathcal{E}(F)} = \eta\} \cap A] \\
&\quad = \sum_{\psi \in \{0,1\}^{E\setminus\mathcal{E}(F)}} \varphi^{\xi}_{\mathbb{G},\boldsymbol{p},q}[\{\omega_{E\setminus\mathcal{E}(F)} = \psi\} \cap A]\varphi^{\xi}_{\mathbb{G},\boldsymbol{p},q}[\omega_{\mathcal{E}(F)} = \eta \mid \omega_{E\setminus\mathcal{E}(F)} = \psi] \\
&\quad = \sum_{\psi \in \{0,1\}^{E\setminus\mathcal{E}(F)}} \varphi^{\xi}_{\mathbb{G},\boldsymbol{p},q}[\{\omega_{E\setminus\mathcal{E}(F)} = \psi\} \cap A]\varphi^{\xi^{\psi}}_{\mathbb{G},\boldsymbol{p},q}[\omega_{\mathcal{E}(F)} = \eta] \\
&\quad \geqslant c \sum_{\psi \in \{0,1\}^{E\setminus\mathcal{E}(F)}} \varphi^{\xi}_{\mathbb{G},\boldsymbol{p},q}[\{\omega_{E\setminus\mathcal{E}(F)} = \psi\} \cap A] = c\varphi^{\xi}_{\mathbb{G},\boldsymbol{p},q}[A],
\end{aligned}$$

where in the third line, we drop the conditioning on A because if ψ is not in A, the terms in the second and the third lines are both 0. □

1.1.10 Russo-Seymour-Welsh property

In this section, we define the Euclidean version of the Russo-Seymour-Welsh property. It can also be defined at the lattice level, but actually, it can be proven that the two definitions are equivalent. As mentioned earlier in Introduction, this is a property about self-similarity of the model and is a good criterion to determine the critical point of the random-cluster model. See [DCST17] for more details.

Definition 1.14 (Euclidean RSW property)**.** Let $\mathbb{G} = (\mathbb{V}, \mathbb{E})$ be an infinite planar graph. Take a family of edge parameters $\boldsymbol{p} = (p_e)_{e\in E}$, an cluster-weight parameter $q \geqslant 1$ and boundary conditions $\xi = 0$ or 1. We say that the random-cluster measure $\varphi^{\xi}_{\mathbb{G},\boldsymbol{p},q}$ satisfies the RSW property if for any $\rho > 1$, there exists $c := c(\rho) > 0$ such that for all $n > 0$, we have

$$c \leqslant \varphi^{\xi}_{R'_n,\boldsymbol{p},q}[\mathcal{C}_h(R_n)] \leqslant 1 - c, \tag{1.14}$$

where $R'_n = [-(\rho+1)n, (\rho+1)n] \times [-2n, 2n]$ and $R_n = [-\rho n, \rho n] \times [-n, n]$ denote Euclidean domains; $\varphi^{\xi}_{R'_n,\boldsymbol{p},q}$ denotes the random-cluster measure on $R'_n \cap \mathbb{G}$ whose boundary is given by edges of $\mathbb{G}$ with one endpoint inside R'_n and another one outside; and $\mathcal{C}_h(R_n)$ denotes the event that there is a path in $\omega \cap R_n$ connecting the left-boundary of R_n to its right-boundary. Note that we require the constant $c > 0$ to be uniform in n.

The lattice RSW property can be defined in a similar way. In this case, we would need a coordinate system on the graph to be able to define "rectangles". This can be done for isoradial graphs with the square-grid property, see further in Definition 2.1. By gluing rectangles together, it is not hard to see that these two versions of RSW property are equivalent. More details can be found in Appendix B.

1.1.11 Known results

Here, we discuss the homogeneous random-cluster model on the square lattice $\mathbb{Z}^2$. Fix $p \in [0,1]$, $q \geqslant 1$ and boundary conditions $\xi = 0$ or 1. Consider the random-cluster model on $\mathbb{Z}^2$ with edge parameters $p_e = p$ for all $e \in \mathcal{E}(\mathbb{Z}^2)$. Proposition 1.1 states that for $p = p_{\mathrm{sd}}(q) := \frac{\sqrt{q}}{1+\sqrt{q}}$, the model is self-dual in the following sense: if ω is sampled according to $\varphi^{\xi}_{\mathbb{Z}^2,p_{\mathrm{sd}},q}$, then the dual configuration ω^*, defined via (1.3), follows the law of $\varphi^{1-\xi}_{\mathbb{Z}^2,p_{\mathrm{sd}},q}$. This is due to the equalities $y_{\mathrm{sd}}(q) = \frac{p_{\mathrm{sd}}(q)}{1-p_{\mathrm{sd}}(q)} = \sqrt{q}$ and $y_{\mathrm{sd}}(q)^2 = q$.

For $p \in [0,1]$ and boundary conditions $\xi \in \{0,1\}$, define the *connectivity* to be

$$\theta^{\xi}(p) = \varphi^{\xi}_{\mathbb{Z}^2,p,q}[0 \leftrightarrow \infty].$$

It can be shown that the random-cluster model is *critical* at the self-dual point $p = p_c(q) = p_{\mathrm{sd}}(q) = \frac{\sqrt{q}}{1+\sqrt{q}}$ in the following sense [BD12]:

- for $p < p_c(q)$, $\theta^0(p) = \theta^1(p) = 0$ and
- for $p > p_c(q)$, $\theta^0(p) = \theta^1(p) > 0$.

Moreover, at $p = p_c(q)$, two different cases could happen:

- *continuous* or *second-order* phase transition: $\theta^0(p_c) = \theta^1(p_c) = 0$;
- *discontinuous* or *first-order* phase transition: $\theta^1(p_c) > \theta^0(p_c) = 0$.

In [DCST17], some criteria are given to determine whether the phase transition is continuous or discontinuous. In particular, the existence of the infinite cluster, decay of the connection probability between 0 and the box of size n or the RSW property. As a consequence, they prove that for $q \in [1,4]$, the phase transition is continuous. Later on, using the coupling between the six-vertex model and the q-color Potts model, Duminil-Copin et al. prove that the phase transition is discontinuous for $q > 4$ [DGH+16].

For $q = 2$, the classic Edward-Sokal coupling of the random-cluster measure gives the Ising model. It is proven in [Smi06, CDCH+14] that the interface of this model converges to some conformally invariant limit. This limit can be identified with the SLE curve of parameter 3 for the spin-Ising model and with the SLE curve of parameter 16/3 for the FK-Ising model.

1.2 Quantum random-cluster model

1.2.1 Semi-discrete lattice and domain

The *semi-discrete lattice* is defined by the Cartesian product $\mathbb{Z} \times \mathbb{R}$. It can be seen as a collection of *vertical lines* $\mathbb{R}$ indexed by $\mathbb{Z}$ with *horizontal edges* connecting neighboring vertical lines with the same y-coordinate. In our graphical representation, horizontal edges are not drawn for simplicity.

If we are given a planar graph, we know how to define its dual graph (Section 1.1.4). This will be the same for $\mathbb{Z} \times \mathbb{R}$, using the fact that it can be seen as the "limit" of a more and

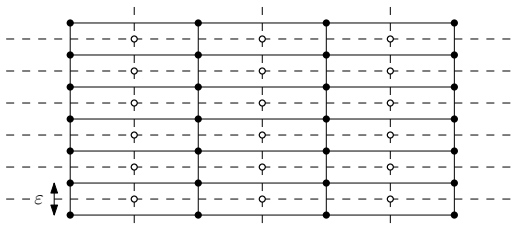

(a) The primal graph is given by black vertices and think edges. The dual graph is given by white vertices and dasehed edges.

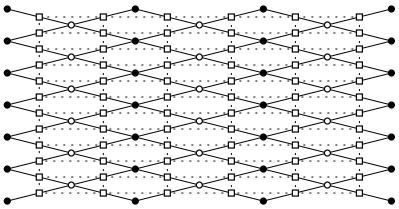

(b) The medial graph is given by black and white vertices along with think edges. The mid-edge graph is given by square vertices and dotted edges.

Figure 1.3 – The primal, dual, medial and mid-edge graphs of (a part of) the flattened square lattice.

more flattened rectangular lattice $\mathbb{Z}\times\varepsilon\mathbb{Z}$ as illustrated in Figure 1.3. The faces are "crushed" together so that vertically, the notion of being neighbors gets degenerated. We will only call neighbors two sites whose x-coordinates differ by 1. More details will be given below in a general setting.

Take $\delta > 0$. We will define here the following notions related to the *semi-discrete lattice with mesh size* δ: primal, dual, medial and mid-edge lattices. Formal definitions are given below and to visualize them, we refer to Figure 1.4.

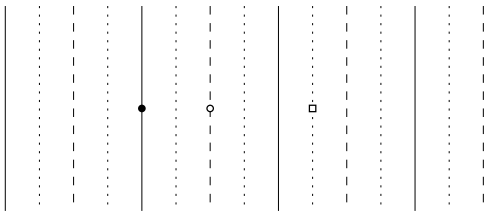

Figure 1.4 – Thick lines represent the primal semi-discrete lattice $\mathbb{L}_\delta$, dashed lines represent the dual semi-discrete lattice $\mathbb{L}_\delta^\star$ and dotted lines represent the mid-edge semi-discrete lattice $\mathbb{L}_\delta^\flat$.

Let $\mathbb{L}_\delta$ be the semi-discrete primal lattice $\delta\mathbb{Z}\times\mathbb{R}$. We denote by $\mathbb{L}_\delta^\star$, the lattice $\delta(\mathbb{Z}+\frac{1}{2})\times\mathbb{R}$ with the same notion of connectivity as $\delta\mathbb{Z}\times\mathbb{R}$, the *dual* of $\mathbb{L}_\delta$. We can notice that the dual lattice is isomorphic to the primal one, by translation of $\frac{\delta}{2}$ in the x-coordinate. As in the discrete setup, the dual lattice is given by the center of faces in the primal lattice, and edges by connecting two primal faces sharing a common edge. Since the faces of $\mathbb{L}_\delta$ are all crushed together vertically, the same happens to vertically-ordered dual vertices, giving us continuous lines isomorphic to $\mathbb{R}$.

Moreover, we define the *medial lattice* by taking $\mathbb{L}_\delta^\diamond = \mathbb{L}_\delta \cup \mathbb{L}_\delta^\star$. It is again isomorphic to the primal or dual lattice by scaling of factor $\frac{1}{2}$.

Finally, we define the *mid-edge lattice* $\delta(\frac{1}{2}\mathbb{Z}+\frac{1}{4})\times\mathbb{R}$, denoted by $\mathbb{L}_\delta^\flat$. The vertices of this lattice are sometimes called *mid-edges*. It is isomorphic to the medial lattice.

In the following graphical presentations, we will draw a filled black dot to represent a vertex on the primal lattice, a filled white dot a vertex on the dual lattice, and a filled white square when it is a vertex on the mid-edge lattice. See Figure 1.4.

We need to define some more notions related to the semi-discrete lattice $\mathbb{L}_\delta$, including segments, paths and domains.

A *primal vertical segment* is denoted by $[\delta k + \mathrm{i}\, a, \delta k + \mathrm{i}\, b] := \{\delta k\} \times [a, b]$, where $k \in \mathbb{Z}$ and $a < b$ are real numbers. A *primal horizontal segment* is denoted by $[\delta k + \mathrm{i}\, a, \delta l + \mathrm{i}\, a] := ([\delta k, \delta l] \times \{a\}) \cap \mathbb{L}_\delta = \{\delta j + \mathrm{i}\, a, k \leqslant j \leqslant l\}$ where $k < l$ are integers and a is a real number. When a primal horizontal segment is of length δ, we call it an *elementary primal segment*.

A sequence of points $(z_i)_{0 \leqslant i \leqslant n}$ on $\mathbb{L}_\delta$ forms a *path* if the consecutive points share the same y-coordinate (forming horizontal segments) or the same x-coordinate (forming vertical segments).

A *primal domain* is a finite region delimited by primal horizontal and vertical segments. More precisely, it is given by a self-avoiding path consisting of $2n+1$ points $z_0, z_1, \ldots, z_{2n}$ on $\mathbb{L}_\delta$ such that

- $[z_{2i}, z_{2i+1}]$ are horizontal segments for $i \in [\![0, n-1]\!]$;
- $[z_{2i+1}, z_{2i+2}]$ are vertical segments for $i \in [\![0, n-1]\!]$;
- these points form a closed path, i.e., $z_0 = z_{2n}$.

The set consisting of segments $\partial = \{[z_{2i} z_{2i+1}], [z_{2i+1}, z_{2i+2}], i \in [\![0, n-1]\!]\}$ separates the plane into two connected *open* components, a bounded one which is simply connected and an unbounded one. The first one is called the *domain* and is usually denoted by Ω_δ. And ∂, or $\partial\Omega_\delta$, is called the *boundary* of Ω_δ. Except otherwise mentioned, the points z_i are ordered counterclockwise.

These same definitions apply to the dual lattice $\mathbb{L}_\delta^\star$ to get a *dual domain*, usually denoted by $\Omega_\delta^\star$, or to the medial lattice to get a *medial domain*, $\Omega_\delta^\diamond$.

The *interior* of a primal domain Ω_δ, denoted by $\operatorname{Int}\Omega_\delta$, is the largest dual domain contained in Ω_δ. It can also be seen as the set of dual vertices in Ω_δ having both (primal) neighbors inside Ω_δ. Similarly, the *interior* of a dual domain $\Omega_\delta^\star$ or a medial domain $\Omega_\delta^\diamond$, denoted by $\operatorname{Int}\Omega_\delta^\star$ or $\operatorname{Int}\Omega_\delta^\diamond$, can also be defined in a similar way by replacing the word "primal" by "dual" or "medial".

Now we define a *semi-discrete Dobrushin domain*, which is a medial domain with so-called *Dobrushin boundary conditions*. This will be useful in studying the interface of the quantum Ising model in Chapter 6. Given $(a_w a_b)$ and $(b_b b_w)$ two horizontal edges, consider a primal path from a_b to b_b and a dual path from b_w to a_w, such that the concatenation of both (first primal then dual) forms a counterclockwise non self-intersecting boundary. We write ∂_{ab} and $\partial_{ba}^\star$ for the primal and dual parts. See Figure 1.5.

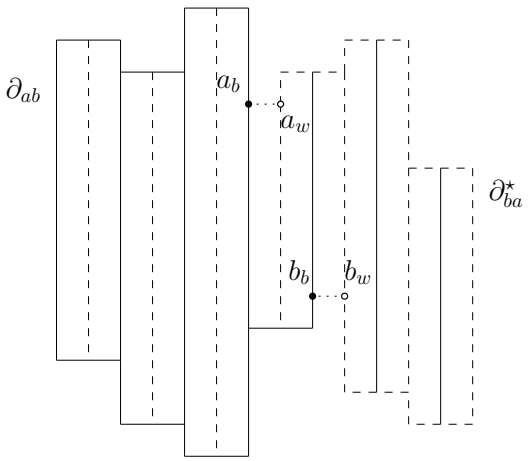

Figure 1.5 – A Dobrushin domain.

1.2.2 Quantum Bernoulli percolation

The quantum Bernoulli percolation model can be defined on the semi-discrete lattice or any semi-discrete primal, dual or medial domain. We start with its definition on the semi-discrete lattice.

Given the mesh size of the lattice $\delta > 0$ and two parameters $\lambda, \mu > 0$. Recall that $\mathbb{L}_\delta$ denotes the collection of primal vertical lines, separated by distance δ one from another; and $\mathbb{L}_\delta^\star$ denotes the collection of dual vertical lines, which are at equal distance between two neighboring vertical primal lines. We consider two independent (one-dimensional) Poisson point processes with parameters λ and μ on $\mathbb{L}_\delta$ and $\mathbb{L}_\delta^\star$ respectively. We denote by (D, B) such a configuration, where D contains the points in $\mathbb{L}_\delta$ and B the points in $\mathbb{L}_\delta^\star$. The points in D are called *cuts*. They cut vertical (primal) lines into disjoint segments. The points in B are called *bridges*. They create horizontal connections between two neighboring vertical segments. See Figure 1.6 for an example. We denote this probability measure by $\mathbb{P}^{(\delta)}_{\mathcal{Q},\lambda,\mu}$ or $\mathbb{P}_{\mathcal{Q},\lambda,\mu}$.

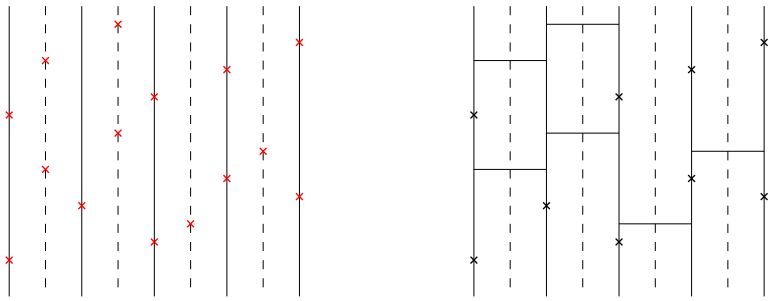

Figure 1.6 – **Left:** Example of a (random) configuration on a part of the semi-discrete lattice. Red crosses are points given by Poisson point processes. **Right:** Representation with cuts and bridges of the configuration on the left-hand side. Red points on primal lines become cuts and those on dual lines become bridges connecting the two neighboring primal vertical lines.

Given a configuration of the quantum Bernoulli percolation (D, B), we can define the notion of *primal (or dual) connectivity* with respect to it.

Two points in the primal domain are said to have a *primal connection* if there is a primal path going from one to another by taking primal vertical segments and horizontal bridges without crossing any cuts. The notion of having a *dual connection* is similar by taking the dual graph, reversing primal and dual segments and the role of cuts and bridges. More precisely, two points in the dual domain are said to have a *dual connection* if there is a path going from one to another by taking dual lines and cuts without crossing any bridges.

In the following, except otherwise mentioned, the connectivity always refers to the primal domain. We call *(primal) connected component of* $v \in \mathbb{L}_\delta$ the maximal subset composed only of connected (primal) vertical lines and bridges. It may also be called *cluster*.

1.2.3 Quantum random-cluster model

To define the quantum random-cluster model on the semi-discrete lattice, we need to be careful with the boundary conditions as in the case of the random-cluster model on infinite graphs (Section 1.1.8). The idea behind is exactly the same: we start by defining the random-cluster model on larger and larger finite domains with wired or free boundary conditions and take the weak limit of this. The details are not given here and in the rest of this chapter,

since the main idea follows as in Section 1.1.8. We will only give a precise definition of the random-cluster measure on finite domains.

Fix one more parameter $q \geqslant 1$, called *cluster-weight*, and boundary conditions $\xi = 0, 1$. We define the random-cluster measure on a primal domain Ω_δ with cluster-weight parameter q and boundary conditions ξ, denoted by $\varphi^\xi_{\mathcal{Q},\Omega_\delta}$, as follows. We write $\mathbb{P}_{\mathcal{Q},\Omega_\delta}$ for the measure of the quantum Bernoulli percolation on Ω_δ, which is the restriction on Ω_δ of the measure of quantum Bernoulli percolation on the semi-discrete lattice $\mathbb{P}_{\mathcal{Q},\lambda,\mu}$. Given a configuration (D, B) on Ω_δ, we define $\mathrm{d}\varphi^\xi_{\mathcal{Q},\Omega_\delta}$ via the following relation of proportionality,

$$\mathrm{d}\varphi^\xi_{\mathcal{Q},\Omega_\delta}(D, B) \propto q^{k^\xi(D,B)} \mathrm{d}\mathbb{P}_{\mathcal{Q},\Omega_\delta}(D, B),$$

where $k^\xi(D, B)$ denotes the number of clusters in the configuration (D, B) with respect to the boundary conditions ξ. When the boundary conditions are wired ($\xi = 1$), one should count all the clusters touching the boundary $\partial\Omega_\delta$ as one; and when the boundary conditions are free ($\xi = 0$), they are all considered as different clusters.

In other words, we write

$$\mathrm{d}\varphi^\xi_{\mathcal{Q},\Omega_\delta}(D, B) = \frac{q^{k^\xi(D,B)}}{Z^\xi_{q,\Omega_\delta}} \mathrm{d}\mathbb{P}_{\mathcal{Q},\Omega_\delta}(D, B). \tag{1.15}$$

In the above definition, we have

$$\begin{aligned} Z^\xi_{q,\Omega_\delta} &= \int q^{k^\xi(D,B)} \mathrm{d}\mathbb{P}_{\mathcal{Q},\Omega_\delta}(D, B) \\ &\leqslant \int q^{|D|} \mathrm{d}\mathbb{P}_{\mathcal{Q},\Omega_\delta} = \sum_{n=0}^{\infty} q^n \frac{(\lambda C)^n}{n!} e^{-\lambda C} = e^{(q-1)\lambda C} < \infty, \end{aligned}$$

where C is the one-dimensional Lebesgue measure of $\Omega_\delta \cap \mathbb{L}_\delta$, which is finite due to the boundedness of Ω_δ.

We mention that the quantum model also has the same properties as the classical one, in particular, the FKG property and the domain Markov property. Hence, as a consequence, we can define infinite-volume measures such as $\varphi^0_{\mathcal{Q}}$ and $\varphi^1_{\mathcal{Q}}$ on the whole semi-discrete lattice by taking weak limits.

1.2.4 Limit of the discrete random-cluster model

From now on, when we talk about the semi-discrete lattice, we assume that $\delta = 1$, which is to say that we consider $\mathbb{Z} \times \mathbb{R}$ as the standard semi-discrete lattice, since up to a scaling factor, they are the same thing.

The semi-discrete lattice $\mathbb{Z} \times \mathbb{R}$ can be viewed as the "graph limit" of $\mathbb{Z} \times \varepsilon\mathbb{Z}$ when ε goes to 0. Moreover, it is also the limit of $\mathbb{G}^\varepsilon$ defined below, which is a better graph to study despite its more complicated definition.

The medial graph of $\mathbb{G}^\varepsilon$ is given by rhombi of size 1 with angles ε and $\pi - \varepsilon$, as shown on the left-hand side of Figure 1.7. The graph is bipartite, we attribute primal and dual vertices alternatively. We can choose an arbitrary primal vertex and set the origin of $\mathbb{R}^2$ at this vertex. The primal graph thus obtained is shown on the right-hand side of Figure 1.7.

Observe that $\mathbb{G}^\varepsilon$ contains two types of edges: those of length $2\sin(\frac{\varepsilon}{2})$ and those of length $2\cos(\frac{\varepsilon}{2})$. As we will take ε to 0, we call the first *short edges* and the latter *long edges*. Write p_ε and $p_{\pi-\varepsilon}$ for the percolation parameters associated with short and long edges respectively.

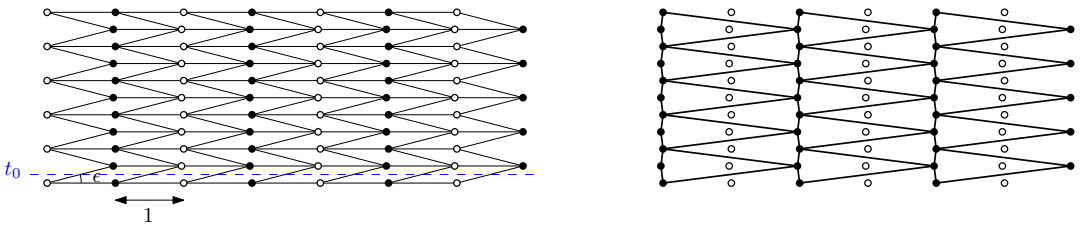

Figure 1.7 – **Left:** The medial lattice of $\mathbb{G}^\varepsilon$. **Right:** The primal lattice with dual vertices.

We remind that they denote the probability that a short or a long edge is open. Assume there exist constants $\lambda_0, \mu_0 > 0$ such that asymptotically, p_ε and $p_{\pi-\varepsilon}$ behave as follows when $\varepsilon \to 0$:

$$p_\varepsilon \sim 1 - \varepsilon\lambda_0 \quad \text{and} \quad p_{\pi-\varepsilon} \sim \varepsilon\mu_0.$$

Write $\varphi^{(\varepsilon)} = \varphi_{\mathbb{G}^\varepsilon}$ for the measure of Bernoulli percolation on $\mathbb{G}^\varepsilon$ with parameters given above. Taking $\varepsilon \to 0$, we obtain in the limit the quantum Bernoulli percolation on $2\mathbb{Z} \times \mathbb{R}$, where the cuts are described by Poisson points with parameter λ_0 on primal lines and the bridges by Poisson points with parameter μ_0 on dual lines.

Note that by a scaling of factor $\frac{1}{2}$, the above model is the same as the quantum Bernoulli percolation on $\mathbb{Z} \times \mathbb{R}$, where the cuts are Poisson points with parameter λ on primal lines and the bridges are Poisson points with parameter μ on dual lines where

$$\lambda = 2\lambda_0 \quad \text{and} \quad \mu = 2\mu_0. \tag{1.16}$$

To see that when ε goes to 0, we obtain the quantum model described above, we may proceed as follows. Consider $L > 0$ and a collection of $N = \frac{L}{\varepsilon}$ consecutive short edges, each of whom is closed with probability $\lambda_0\varepsilon$. Consider a sequence of i.i.d. Bernoulli random variables $(X_i)_{1\leqslant i\leqslant N}$ with parameter $\lambda\varepsilon$: $X_i = 1$ if the i-th edge is closed and $X_i = 0$ otherwise. Set $S = \sum_{i=1}^N X_i$, which counts the number of closed edges in this collection of edges. Then, for any fixed $k \geqslant 0$ and $\varepsilon \to 0$, we have that

$$\begin{aligned}
\mathbb{P}[S = k] &= \binom{N}{k} (\lambda_0\varepsilon)^k (1 - \lambda_0\varepsilon)^{N-k} \\
&\sim \frac{N^k}{k!} (\lambda_0\varepsilon)^k e^{-N\lambda_0\varepsilon} \\
&= e^{-L\lambda_0} \frac{(L\lambda_0)^k}{k!},
\end{aligned}$$

where the quantity in the last line is the probability that a Poisson variable with parameter $L\lambda_0$ takes the value k. As a consequence, when $\varepsilon \to 0$, the N vertical short edges converge to a vertical segment of length L, among which closed edges (at ε scale) give us cuts that can be described by a Poisson point process with parameter λ_0. And the same reasoning also applies to the long edges.

For the quantum random-cluster model, we can proceed in a similar way by taking weak limits of their discrete counterparts.

In Chapter 2, we will see that the graphs $\mathbb{G}^\varepsilon$ are isoradial, and we will study the random-cluster model on such graphs in Chapter 3. In particular, Theorem 3.1 provides us with the

critical value of the model on such graphs, which are

$$p_\varepsilon = \frac{y_\varepsilon}{1+y_\varepsilon} \quad \text{and} \quad p_{\pi-\varepsilon} = \frac{y_{\pi-\varepsilon}}{1+y_{\pi-\varepsilon}},$$

where y_ε and $y_{\pi-\varepsilon}$ are given by (2.2) with $\beta = 1$, where we consider $\theta_e = \varepsilon$ if e is a short edge; $\theta_e = \pi - \varepsilon$ if e is a long edge. A more detailed statement will be given in Proposition 4.2. Here, we just mention that the computation from Section 4.2 gives

$$\begin{aligned} \text{if } 1 \leqslant q < 4, \quad & \lambda_0 = \frac{2r}{\sqrt{q(4-q)}}, && \mu_0 = \frac{2r\sqrt{q}}{\sqrt{4-q}}; \\ \text{if } q = 4, \quad & \lambda_0 = \frac{1}{2\pi}, && \mu_0 = \frac{2}{\pi}; \\ \text{if } q > 4, \quad & \lambda_0 = \frac{2r}{\sqrt{q(q-4)}}, && \mu_0 = \frac{2r\sqrt{q}}{\sqrt{q-4}}. \end{aligned} \tag{1.17}$$

From Theorem 4.1, we deduce the critical parameters for the quantum model, which are given by (λ, μ) such that $\mu/\lambda = q$. The special case of $q = 2$ is what we call the quantum Ising model, which is supposed to have the same behavior as the classical Ising model. In Chapter 6, we study the quantum Ising model and we prove the convergence of its interface to a conformally invariant limit.

1.2.5 Critical quantum model: loop representation

In this section, we explain how to obtain the *loop representation* of the quantum random-cluster model on semi-discrete domains. A *loop* is a simple closed path living on the mid-edge lattice $\mathbb{L}^\flat_\delta$. For our convenience, we may orient it using the following operation: replace the pieces of our domain according to the rules explained in Figure 1.8. Then, loops arise as contours around primal or dual clusters.

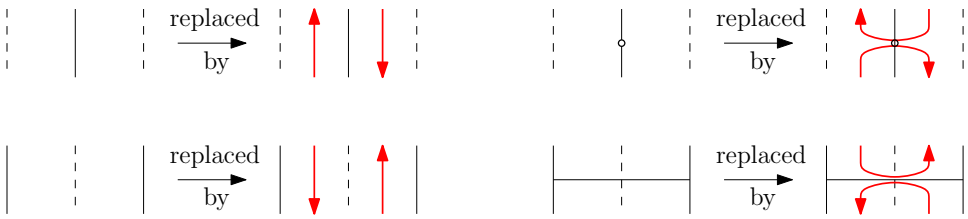

Figure 1.8 – Transformation to get the loop representation of a FK-configuration of the quantum Bernoulli percolation.

We notice that if we work on a Dobrushin domain $(\Omega^\diamond, a, b)$, then we get a collection of loops surrounding either primal or dual connected components together with one interface connecting a to b. This is illustrated in Figure 1.9.

Now, let us come to the quantitative side. We want to rewrite the quantum random-cluster measure in terms of the number of loops. To do so, we couple the quantum random-cluster model with its dual model and look at them together.

Let Ω be a primal domain and we write $\mathbb{P}_{\mathcal{Q},\lambda,\mu}$ for the quantum Bernoulli percolation on Ω. We put boundary conditions $\xi = 0, 1$ on Ω and for $q \geqslant 1$, we write the associated quantum random-cluster measure $\varphi^\xi_{\mathcal{Q},\Omega}$. On the dual graph $\Omega^\star$, we inverse the role of primal and dual lines (by switching primal and dual lines and inversing cuts and bridges), and write $\mathbb{P}^*_{\mathcal{Q},\mu,\lambda}$

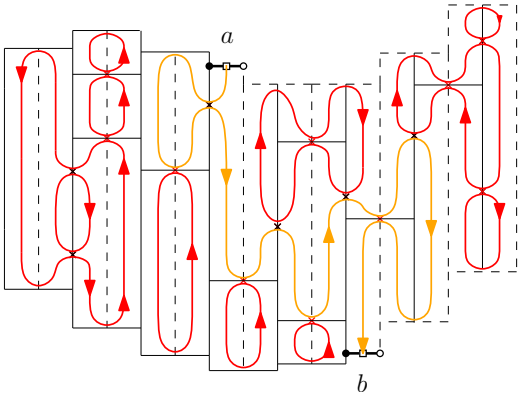

Figure 1.9 – The loop representation corresponding of a configuration on the Dobrushin domain $(\Omega^\diamond, a, b)$.

for the coupled measure of the quantum Bernoulli percolation. In consequence, we have, for any finite sets D of primal vertical lines and B of dual vertical lines, that

$$\mathrm{d}\mathbb{P}_{\mathcal{Q},\mu,\lambda}(D,B) = \mathrm{d}\mathbb{P}^*_{\mathcal{Q},\mu,\lambda}(D^*,B^*),$$

where $D^* = B$ and $B^* = D$.

Given a subset of primal lines of Lebesgue measure a and a subset of dual lines of Lebesgue measure b. Let D be a set of cuts and B a set of bridges of cardinality k and l on these subsets. Fix $\omega = (D,B)$ a configuration. We can calculate the Radon-Nikodym derivative between $\mathrm{d}\mathbb{P}_{\lambda,\mu}(D,B)$ and $\mathrm{d}\mathbb{P}_{\mu,\lambda}(D,B)$,

$$\frac{\mathrm{d}\mathbb{P}_{\lambda,\mu}(D,B)}{\mathrm{d}\mathbb{P}_{\mu,\lambda}(D,B)} = \frac{e^{-\lambda a}\frac{(\lambda a)^k}{k!}e^{-\mu b}\frac{(\mu b)^l}{l!}}{e^{-\mu a}\frac{(\mu a)^k}{k!}e^{-\lambda b}\frac{(\lambda b)^l}{l!}} = e^{-(\lambda-\mu)(a-b)}\left(\frac{\lambda}{\mu}\right)^{k-l}.$$

Thus, by denoting $D^* = B$, $B^* = D$ and $\omega^* = (D^*,B^*)$, and knowing that $\mathrm{d}\mathbb{P}_{\mu,\lambda}(D,B) = \mathrm{d}\mathbb{P}^*_{\lambda,\mu}(D^*,B^*)$, we can write

$$\begin{aligned}
\mathrm{d}\varphi^{1-\xi}_{\mathcal{Q},\Omega^\star}(D^*,B^*) &= \mathrm{d}\varphi^{\xi}_{\mathcal{Q},\Omega}(D,B)\\
&\propto q^{k^\xi(\omega)}\mathrm{d}\mathbb{P}_{\lambda,\mu}(D,B)\\
&\propto q^{k^\xi(\omega)}\left(\frac{\lambda}{\mu}\right)^{|D|-|B|}\mathrm{d}\mathbb{P}_{\mu,\lambda}(D,B)\\
&\propto \left(\frac{q\lambda}{\mu}\right)^{k^\xi(\omega)}\left(\frac{\mu}{\lambda}\right)^{k^{1-\xi}(\omega^*)}\mathrm{d}\mathbb{P}^*_{\lambda,\mu}(D^*,B^*).
\end{aligned}$$

where we use Euler's formula $|D| - |B| + f^\xi(\omega) - k^\xi(\omega) = cst.$ and $f^\xi(\omega) = k^{1-\xi}(\omega^*)$. At criticality, we have $q\lambda/\mu = 1$, thus, the last line gives

$$\mathrm{d}\varphi^{1-\xi}_{\mathcal{Q},\Omega^\star}(\omega^*) \propto q^{k^{1-\xi}(\omega^*)}\mathrm{d}\mathbb{P}^*_{\lambda,\mu}(D^*,B^*).$$

This shows that the model at criticality is self-dual.

We will apply the same technique as in Section 1.1.5 to get the loop representation for the quantum random-cluster model. We have,

$$\mathrm{d}\varphi^{\xi}_{\mathcal{Q},\Omega}(\omega) = \sqrt{\mathrm{d}\varphi^{\xi}_{\mathcal{Q},\Omega}(\omega^*)\mathrm{d}\varphi^{1-\xi}_{\mathcal{Q},\Omega^*}(\omega^*)} = \sqrt{q}^{l(\omega)}\sqrt{\mathrm{d}\mathbb{P}_{\lambda,\mu}(D,B)\mathrm{d}\mathbb{P}_{\mu,\lambda}(D,B)} \tag{1.18}$$

where $l(\omega) = k(\omega) + k(\omega^*)$ is the number of loops in ω (or ω^*). We note that this quantity is symmetric in primal and dual lattice. We should now estimate the square root of two Poisson point processes. Let us denote it by $\mathrm{d}Q_{\lambda,\mu}$. As before, consider a subset of primal axes and a subset of dual axes of Lebesgue measure respectively a and b. Let D and B be the set of cuts and the set of bridges on them. We need to estimate this square root for the event $|D| = k$ and $|B| = l$,

$$\begin{aligned} Q_{\lambda,\mu}(|D| = k, |B| = l) &= \sqrt{\left(e^{-\lambda a}\frac{(\lambda a)^k}{k!}e^{-\mu b}\frac{(\mu b)^l}{l!}\right)\left(e^{-\mu a}\frac{(\mu a)^k}{k!}e^{-\lambda b}\frac{(\lambda b)^l}{l!}\right)} \\ &= e^{-\frac{1}{2}(\lambda+\mu)(a+b)}\frac{(\sqrt{\lambda\mu}a)^k}{k!}\frac{(\sqrt{\lambda\mu}b)^l}{l!} \end{aligned}$$

which is proportional to a Poisson point process of same intensity $\sqrt{\lambda\mu}$ on primal and dual axes, independent on everything.

In consequence, the critical model can be seen in two ways.

1. FK representation: we put independent Poisson point processes on primal and dual axes, with parameters λ on primal axes and μ on dual axes. We weigh configurations by $q^{k(\omega)}$ where $k(\omega)$ is the number of primal connected components in the configuration. The critical model is obtained by setting $\mu/\lambda = q$.
2. Loop representation: we put independent Poisson point processes on primal and dual axes, with the same parameter, and all of them are independent of each other. The weight of a configuration is proportional to $\sqrt{q}^{l(\omega)}$ where q is the parameter and $l(\omega)$ the number of loops in the configuration.

In Chapter 6, we will be particularly interested in the loop representation of the critical quantum FK-Ising model, or the random-cluster model corresponding to the case of $q = 2$. Our goal will be to get a result on conformal invariance of the critical model. The critical parameters of this model are given by (λ, μ) such that the relation $\mu/\lambda = 2$ [Pfe70, BG09] is satisfied. However, to get an isotropic model, we need to consider parameters obtained in (1.17) and the scaling relation 1.16, which give

$$\lambda = \frac{1}{2\delta} \quad \text{and} \quad \mu = \frac{1}{\delta}. \tag{1.19}$$

Using (1.18), the loop representation of the critical quantum FK-Ising measure can be rewritten as follows,

$$\mathrm{d}\mathbb{P}^{QI}_{\lambda,\mu}(D, B) \propto \sqrt{2}^{l(D,B)}\mathrm{d}\mathbb{P}_{\rho,\rho}(D, B), \tag{1.20}$$

where $l(D, B)$ denotes the number of loops in a given configuration (D, B) and $\mathbb{P}_{\rho,\rho}$ a Poisson point process on primal and dual vertical lines with parameter $\rho = \sqrt{\lambda\mu} = \frac{1}{\sqrt{2}\delta}$.

Let Ω be a simply connected domain of $\mathbb{C}^2$ and $a, b \in \partial\Omega$ be two marked boundary points. For $\delta > 0$, write $(\Omega^\diamond_\delta, a_\delta, b_\delta)$ for the δ-approximated semi-discrete Dobrushin domain of (Ω, a, b). We consider the loop representation of the FK-Ising model on the domain $(\Omega^\diamond_\delta, a_\delta, b_\delta)$ to get a collection of loops and an interface going from a_δ to b_δ, denoted γ_δ. We will show that the limiting curve of γ_δ when δ goes to 0 is conformally invariant.

Chapter 2

Isoradial graphs and star-triangle transformation

2.1 Isoradial graphs

In this section, we define the notion of isoradial graphs. They are infinite planar graphs with an embedding to be precised later. This includes a huge class of regular graphs which we are interested in: square lattice, triangular lattice, hexagonal lattice, etc. In Chapter 3, we will study the random-cluster model on such graphs and show the universality of its universal behavior at the critical point. Moreover, on this family of graphs, a theory of complex analysis have been developped [Ken02, CS11], which was used to study the Ising model on isoradial graphs and to prove the conformal invariance of its interface [CS12, CDCH+14]. A similar result is conjectured to hold as well for the random-cluster model [Sch07].

2.1.1 Definition

An embedded planar graph $\mathbb{G} = (\mathbb{V}, \mathbb{E})$ is said to be *isoradial* if it satisfies the three following properties:

- All its faces are inscribed in circles of the same radius.
- The center of each circumcircle is in its own face.
- All its edges are straight segments.

In particular, such a graph should be infinite since otherwise, we would have an infinite face on the exterior which cannot be inscribed in a circle of finite radius. We note that in the first condition, up to scaling, we may assume that the radius of the circumcircles are all equal to 1.

An isoradial graph $\mathbb{G}$ is said to be *doubly-periodic* if it is invariant under translations which form a group action $\Lambda \cong \tau_1\mathbb{Z} \oplus \tau_2\mathbb{Z}$ with $\tau_1/\tau_2 \notin \mathbb{R}$. The complex numbers τ_1 and τ_2 are called *periods* of $\mathbb{G}$. Note that their choice is not unique.

In this thesis, most of the time we will consider doubly-periodic isoradial graphs but actually, some proofs can be adapted without too much difficulty to more general graphs, such as those satisfying the bounded-angles property (Section 2.1.2) and the square-grid property (Definition 2.1).

The canonical way to define the dual graph of an isoradial graph is to take the centers of circumcircles as the set of dual vertices, and to embed all the dual edges to be straight segments. It is not hard to see that the dual graph $\mathbb{G}^* = (\mathbb{V}^*, \mathbb{E}^*)$ embedded in this way is

also isoradial since the distance between a primal (*resp.* dual) vertex and the center of its circumcircle, which is a dual (*resp.* primal) vertex, is a constant over the graph. We notice that by taking twice the isoradial dual $(\mathbb{G}^*)^*$, we obtain exactly $\mathbb{G}$ with the same isoradial embedding.

An isoradial graph gives rise to a *diamond graph* or *quad graph*, denoted $\mathbb{G}^\diamond = (\mathbb{V}^\diamond, \mathbb{E}^\diamond)$, which is defined as follows. The vertex set $\mathbb{V}^\diamond$ consists of all the primal and dual vertices, which means $\mathbb{V}^\diamond = \mathbb{V} \cup \mathbb{V}^*$. The edge set $\mathbb{E}^\diamond$ consists of all the unordered pairs $\langle v, c \rangle$ where v is a primal vertex and c is the center of the circumcircle of a face containing v. These edges are also called *mid-edges*. We also denote by $\mathbb{C}^\diamond$ the set of *rhombi centers*, which are given by intersection between primal and dual edges. We also have $\mathbb{C}^\diamond = (\mathbb{V}^\diamond)^*$. By isoradiality, all these edges are of the same length, which is the radius of the circumcircles mentionned above. Moreoever, all the faces are rhombi, with two vertices in $\mathbb{V}$ and two others in $\mathbb{V}^*$.

We notice that the previous definition is symmetric in $\mathbb{G}$ and $\mathbb{G}^*$, which means that the diamond graphs of $\mathbb{G}$ and $\mathbb{G}^*$ are the same. In other words, we can switch the role of primal and dual vertices to define $\mathbb{G}^\diamond$. Conversely, starting from a rhombi tiling of the plane, we may obtain two isoradial graphs. More precisely, a rhombi tiling is a bipartite graph, thus admits two black-white colorings on its vertices, corresponding to two different isoradial graphs, that are dual of each other. This shows that there is a 2-to-1 correspondance between isoradial graphs and diamond graphs.

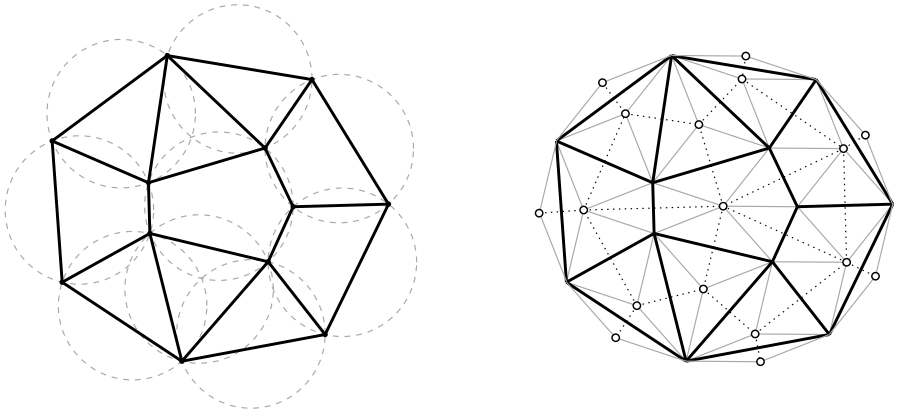

Figure 2.1 – The graph with black vertices and thick edges is (a finite part of) an isoradial graph. **Left:** The isoradial graph with all the circumcircles in dashed gray. **Right:** Its dual embedding and diamond graph in gray.

2.1.2 Bounded-angles property

Let $\mathbb{G}$ be an isoradial graph. Recall that $\mathbb{G}^\diamond$ is the diamond graph associated with $\mathbb{G}$, whose faces are rhombi. Each edge e of $\mathbb{G}$ corresponds to a face of $\mathbb{G}^\diamond$, and the angle θ_e associated to e is one of the two angles of that face. We say that $\mathbb{G}$ satisfies the *bounded-angles property* with parameter $\varepsilon > 0$ if all the angles θ_e of edges of $e \in \mathbb{E}$ are contained in $[\varepsilon, \pi - \varepsilon]$. Equivalently, edges of $\mathbb{G}$ have parameter p_e bounded away from 0 and 1 uniformly. The property also implies that the graph distance on $\mathbb{G}^\diamond$ or $\mathbb{G}$ and the euclidean distance are quasi-isometric.

Write $\mathcal{G}(\varepsilon)$ for the set of double-periodic isoradial graphs satisfying the bounded-angles property with parameter $\varepsilon > 0$.

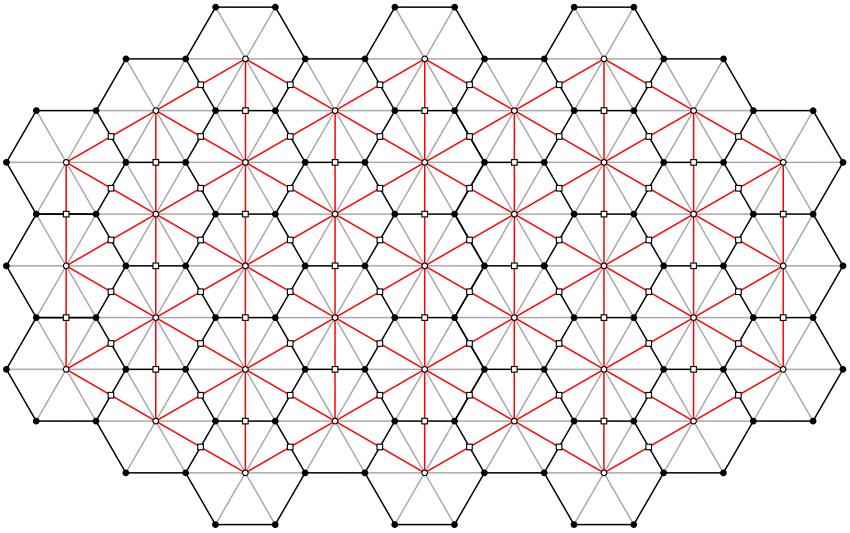

Figure 2.2 – The hexagonal lattice (in black) and the triangular lattice (in red) are dual one to the other. Their rhombic lattice is drawn in gray.

2.1.3 Track systems

If we take the diamond graph representation of an isoradial graph, each edge is shared by exactly two rhombi and each rhombus has exactly four neighboring rhombi. Therefore, we can define *train track* as a double-infinite sequence of rhombi $(r_i)_{i\in\mathbb{Z}}$ if all the intersections $(r_i \cap r_{i+1})_{i\in\mathbb{Z}}$ are non-empty, distinct and parallel segments (Figure 2.3).

A train track as above may also be viewed as an arc in $\mathbb{R}^2$ which connects the midpoints of the edges $(r_i \cap r_{i+1})_{i\in\mathbb{Z}}$. These edges are called the *transverse segments* of the track, and the angle they form with the horizontal line is called the *transverse angle* of the track.

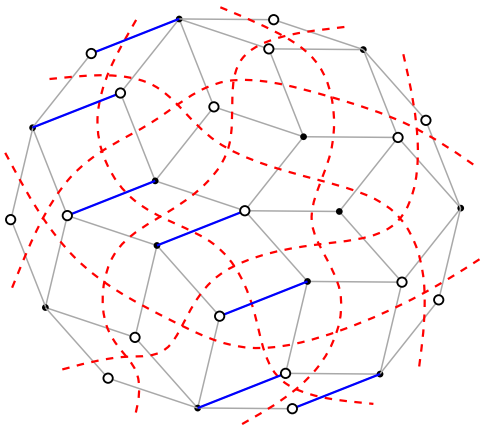

Figure 2.3 – The train track representation (in dotted red lines) of the isoradial graph in Figure 6. Transverse edges of a track are drawn in blue.

Given an isoradial graph $\mathbb{G}$, we write $\mathcal{T}(\mathbb{G})$ the set of its train tracks. We notice that $\mathcal{T}(\mathbb{G}) = \mathcal{T}(\mathbb{G}^*)$ since again, it is a notion associated to the diamond graph, but not to the primal or dual graph.

One can easily check that the rhombi forming a track are distinct, thus a track does not intersect itself. Furthermore, two distinct tracks can only have at most one intersection. A converse theorem has been showned by Kenyon and Schlenker [KS05]. Let $\mathbb{Q}$ be an infinite quad-graph (every face is of degree four) on which we adapt the notion of train tracks from above definition. Moreover, assume that (i) each track does not cross itself and (ii) any two distinct two train tracks may cross each other only at most once. Then $\mathbb{Q}$ can be embedded isoradially.

Each face of $\mathbb{G}^\diamond$ corresponds to an intersection of two train tracks. A hexagon in $\mathbb{G}^\diamond$ (that is a star or triangle in $\mathbb{G}$) corresponds to the intersection of three train tracks, as in Figure 2.9. The effect of a star-triangle transformation is to locally permute the three train tracks involved in the hexagon by "pushing" one track over the intersection of the other two.

Let e be a primal (*resp.* dual) edge, we write θ_e its *subtended angle* with respect to one of the two neighboring dual (*resp.* primal) vertices, as illustrated in Figure 2.4.

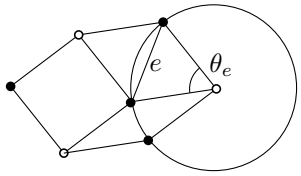

Figure 2.4 – In the figure, the primal edge e has subtended angle θ_e.

Let $\mathbb{G}$ be an isoradial graph and denote by $\mathcal{T}(\mathbb{G})$ the set of its train tracks. We call a *grid* of $\mathbb{G}$ two bi-infinite families of tracks $(s_n)_{n\in\mathbb{Z}}$ and $(t_n)_{n\in\mathbb{Z}}$ of $\mathbb{G}$ with the following properties.

- The tracks within the same family do not intersect each other.
- All tracks of $\mathcal{T}(\mathbb{G})\backslash\{s_n : n \in \mathbb{Z}\}$ intersect all those of $(s_n)_{n\in\mathbb{Z}}$.
- All tracks of $\mathcal{T}(\mathbb{G})\backslash\{t_n : n \in \mathbb{Z}\}$ intersect all those of $(t_n)_{n\in\mathbb{Z}}$;
- The intersections of $(s_n)_{n\in\mathbb{Z}}$ with t_0 appear in order along t_0 (according to some arbitrary orientation of t_0) and the same holds for the intersections of $(t_n)_{n\in\mathbb{Z}}$ with s_0.

The tracks $(s_n)_{n\in\mathbb{Z}}$ are called *vertical* and $(t_n)_{n\in\mathbb{Z}}$ *horizontal*.

Definition 2.1. An isoradial graph $\mathbb{G}$ is said to have the *square-grid property (SQP)* if it has a grid given by $(s_n)_{n\in\mathbb{Z}}$ and $(t_n)_{n\in\mathbb{Z}}$ in the above sense; and it is said to have the *strict square-grid property (SSQP)* if, additionally, the two families $(s_n)_{n\in\mathbb{Z}}$ and $(t_n)_{n\in\mathbb{Z}}$ form a partition of $\mathcal{T}(\mathbb{G})$.

The strict square-grid property of an isoradial graph $\mathbb{G}$ gives rise to a natural coordinate system defined by its grid. Notice that a rhombus is exactly the intersection of two train tracks, so we may write $r_{i,j}$ for the rhombus at the intersection between s_i and t_j. We shall call it the rhombus at position (i, j). The vertex at the bottom-left corner of $r_{i,j}$ (surrounded by tracks s_{i-1}, s_i, t_{j-1} and t_j) is written $x_{i,j}$. This is illustrated in Figure 2.5.

2.2 Isoradial square lattices

An *isoradial square lattice* is encoded by two bi-infinite sequences of angles. Let $\boldsymbol{\alpha} = (\alpha_n)_{n\in\mathbb{Z}}$ and $\boldsymbol{\beta} = (\beta_n)_{n\in\mathbb{Z}}$ be two sequences of angles in $[0, \pi)$ such that

$$\begin{aligned} \sup\{\alpha_n : n \in \mathbb{Z}\} &< \inf\{\beta_n : n \in \mathbb{Z}\}, \\ \inf\{\alpha_n : n \in \mathbb{Z}\} &> \sup\{\beta_n : n \in \mathbb{Z}\} - \pi. \end{aligned} \tag{2.1}$$

Then define $\mathbb{G}_{\boldsymbol{\alpha},\boldsymbol{\beta}}$ to be the isoradial embedding of the square lattice with horizontal train tracks $(s_n)_{n\in\mathbb{Z}}$ with transverse angles $(\alpha_n)_{n\in\mathbb{Z}}$ and vertical train tracks $(t_n)_{n\in\mathbb{Z}}$ with transverse angles $(\beta_n)_{n\in\mathbb{Z}}$. As such, the isoradial graph $\mathbb{G}_{\boldsymbol{\alpha},\boldsymbol{\beta}}$ satisfies $BAP(\varepsilon)$ for $\varepsilon = \inf\{\beta_n - \alpha_m, \alpha_n - \beta_m + \pi : m, n \in \mathbb{Z}\} > 0$. Moreover, an isoradial square lattice satisfies the strict square-grid property and vice versa.

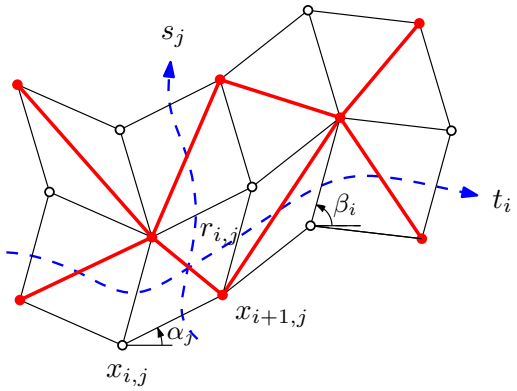

Figure 2.5 – A piece of an isoradial embedding of a square lattice with the associated coordinate system. The square lattice is drawn in red, the diamond graph in black and the tracks in blue.

We will call the *regular square lattice* the embedding corresponding to sequences $\beta_n = \frac{\pi}{2}$ and $\alpha_n = 0$ for all $n \in \mathbb{Z}$.

Note that "having the strict square-grid property" and "being an isoradial square lattice" are two equivalent notions. Therefore, we will rather use the term "isoradial square lattice" since it is more convenient to say.

Next, we will have a closer look at doubly-periodic isoradial graphs and the grid property.

2.3 Doubly-periodic isoradial graphs

Let $\mathbb{G}$ be a doubly-periodic isoradial graph with periods τ_1 and τ_2 ($\tau_1/\tau_2 \notin \mathbb{R}$). We note that $\mathbb{G}$ is in $\mathcal{G}(\varepsilon)$ for some $\varepsilon > 0$. Denote by K a fundamental domain of $\mathbb{G}$. Given $a, b \in \mathbb{Z}$, write $\tau_{a,b}$ for the translation by the vector $a\tau_1 + b\tau_2$. Set $K_{a,b} := \tau_{a,b}K$, the fundamental domain K translated by $\tau_{a,b}$. Note that the sets $(K_{a,b})_{a,b\in\mathbb{Z}}$ are disjoint and cover $\mathbb{G}$.

2.3.1 Asymptotic direction

Lemma 2.2. *For a track s of $\mathbb{G}$, define*

$$H_s = \{(a, b) \in \mathbb{Z}^2, \tau_{a,b}s = s\},$$

which is a subgroup of rank 1 of $\mathbb{Z}^2$. A generator of H_s is called asymptotic direction *s. Moreover, two distinct tracks s and t intersect each other if and only if $H_s \cap H_t = \{0\}$; or in other words, the asymptotic dirctions of s and t are not parallel.*

Proof. The Abelian group $\mathbb{Z}^2$ acts transitively on $\{\tau_{a,b}s \mid a, b \in \mathbb{Z}\}$ and H_s is the stabilizer of s under this action. The track s can also be seen as a closed curve living on the torus, and H_s is exactly its homology class, denoted $[s] \in \mathbb{Z}^2$.

Let s and t be two intersecting train tracks of $\mathbb{G}$ such that $H_s \cap H_t \neq \{0\}$. Write K for a fundamental domain in which s and t intersect each other. Let $(a, b) \in H_s \cap H_t$ and $(a, b) \neq$

$(0,0)$. For any $n \in \mathbb{N}$, the tracks $\tau_{an,bn}s = s$ and $\tau_{an,bn}t = t$ also intersect each other in $K_{an,bn} \neq K$. We just show that s and t have infinitely many intersections, which is not possible for two distinct train tracks.

Let s and t two train tracks of $\mathbb{G}$ which do not intersect each other such that $H_s \cap H_t = \{0\}$. Write $H_s = (a_s, b_s)\mathbb{Z}$ and $H_t = (a_t, b_t)\mathbb{Z}$. Let K_s and K_t be two fundamental domains in which s and t go through respectively. By the definition of stabilizer, s should also go through $\tau_{a_s n, b_s n}K_s$ and t thourgh $\tau_{a_t n, b_t n}K_t$ for all $n \in \mathbb{Z}$. Since the tracks are continuous curves in $\mathbb{R}^2$, they should intersect because (a_s, b_s) and (a_t, b_t) are linearly independent. □

This lemma gives the two following corollaries as consequences. They give a better description of intersections between train tracks of a doubly-periodic isoradial graph $\mathbb{G}$.

Corollary 2.3. *If t and t' are two tracks that intersect each other. Then for any other track s different from t and t', we have one of the following three possibilities in terms of intersection of s with t and t':*

- *s intersects only with t but not with t';*
- *s intersects only with t' but not with t;*
- *s intersects with both t and t'.*

In other words, given three distinct tracks t, t' and t'' in $\mathbb{G}$, we can either have 0, 2 or 3 intersections between them.

Proof. Since t and t' intersect each other, we know that $H_t \cap H_{t'} = \{0\}$. Assume that s does not intersect neither t nor t', which means that $H_s \cap H_t$ and $H_s \cap H_{t'}$ are both subgroups of rank 1 of H_s. Hence, the quotient

$$H_s/(H_s \cap H_t \cap H_{t'}) \cong H_s/(H_s \cap H_t) \oplus H_s/(H_s \cap H_{t'})$$

is finite, which contradicts the fact that $H_t \cap H_{t'} = \{0\}$. □

Corollary 2.4. *If s intersects t, then s also intersects $\tau_{a,b}t$ for all $a, b \in \mathbb{Z}$.*

Proof. If $\tau_{a,b}t = t$, the corollary is clear. Assume that they are different. By Corollary 2.3, $\tau_{a,b}t$ should intersect at least either t or s. But since $H_{\tau_{a,b}t} = H_t$, Lemma 2.2 says that t and $\tau_{a,b}t$ do not intersect each other. As a consequence, $\tau_{a,b}t$ intersects s. □

2.3.2 Square-grid property

Here, we will show the following proposition.

Proposition 2.5. *Let $\mathbb{G}$ be a doubly-periodic isoradial graph. Then $\mathbb{G}$ contains a grid given by $(s_n)_{n\in\mathbb{Z}}$ and $(t_n)_{n\in\mathbb{Z}}$ which are bi-infinite periodic sequences. Moreover, if $\mathbb{G}$ is an isoradial square lattice, then any grid contains all tracks of $\mathbb{G}$.*

Proof. Consider $\mathbb{G}$ a biperiodic isoradial graph with periods τ_1 and τ_2. Take $\widetilde{t_0}$ and $\widetilde{s_0}$ two intersecting tracks of $\mathbb{G}$ and K a fundamental domain of $\mathbb{G}$ containing this intersection. We will then construct two families of tracks by recurrence.

To start with, consider $\widetilde{\mathcal{T}} = \{\widetilde{t_0}\}$ and $\widetilde{\mathcal{T}}' = \{\widetilde{s_0}\}$. For any track s going through K (there is only a finite number of them), when we look at its intersection (in $\mathbb{G}$) with tracks in $\widetilde{\mathcal{T}}$ and those in $\widetilde{\mathcal{T}}'$, we are in one of the following three possible cases by Lemma 2.3.

- If s intersects with some (all) tracks in $\widetilde{\mathcal{T}}$ but not with those in $\widetilde{\mathcal{T}}'$, add s to $\widetilde{\mathcal{T}}'$.
- If s intersects with some (all) tracks in $\widetilde{\mathcal{T}}'$ but not with those in $\widetilde{\mathcal{T}}$, add s to $\widetilde{\mathcal{T}}$.

- If s intersects with some (all) tracks in $\widetilde{\mathcal{T}}$ and some others (all) in $\widetilde{\mathcal{T}}'$, keep s apart.

Finally, let

$$\mathcal{T} = \bigcup_{a,b\in\mathbb{Z}} \tau_{a,b}\widetilde{\mathcal{T}} \quad \text{and} \quad \mathcal{T}' = \bigcup_{a,b\in\mathbb{Z}} \tau_{a,b}\widetilde{\mathcal{T}}'.$$

We claim that the families of tracks $\mathcal{T}$ and $\mathcal{T}'$ form a grid of $\mathbb{G}$.

First, note that in the construction, we can replace "some" by "all" due to Corollary 2.3. Then, by definition, it is easy to see that each translation $K_{a,b}$ of K intersects at least one track of $\mathcal{T}$ and $\mathcal{T}'$ (it intersects $\tau_{a,b}\widetilde{t_0}$ and $\tau_{a,b}\widetilde{s_0}$). Let us check that the tracks in $\mathcal{T}$ do not intersect each other. If there are $t_1, t_2 \in \mathcal{T}$ intersecting each other, then by Corollary 2.4, we can find two tracks $\widetilde{t_1}$ and $\widetilde{t_2}$ both in $\widetilde{\mathcal{T}}$ intersecting each other by translation. This contradicts the construction of $\widetilde{\mathcal{T}}$. The same property holds for the tracks in $\mathcal{T}'$.

Let us check that all the tracks of $\mathbb{G}$ not in $\mathcal{T}$ intersect all those of $\mathcal{T}$. Take t_1 a track not in $\mathcal{T}$ and $t_2 \in \mathcal{T}$. Consider $\widetilde{t_1}$ and $\widetilde{t_2}$ two translations of t_1 and t_2 respectively such that both go through K. Hence, by the construction, they should intersect each other, because otherwise they would have been put both into $\mathcal{T}$. So t_1 and t_2 intersect each other as well by Corollary 2.4. To show that all tracks of $\mathbb{G}$ not in $\mathcal{T}'$ intersect all those of $\mathcal{T}'$, the proof is the same.

Finally, it is always possible to order tracks in $\mathcal{T}$ and those in $\mathcal{T}'$ according to intersections with some referential tracks $s_0 \in \mathcal{T}'$ and $t_0 \in \mathcal{T}$. The periodicity of the tracks follows from the periodicity of the graph $\mathbb{G}$.

For the last part of the lemma, we note that in a square lattice, any three different (horizontal or vertical) tracks have either 0 (3 of the same type) or 2 (2 of one type and 1 of the other type) intersections between them. If there is a grid $(s_n)_{n\in\mathbb{Z}}$ and $(t_n)_{n\in\mathbb{Z}}$ not containing all the tracks of $\mathbb{G}$. Take s which is not one of the s_n or t_n. Then, between s_0, t_0 and s there are three intersections, which is not possible. □

To conclude this part about the construction of a grid in a doubly-periodic isoradial graph (Proposition 2.5), we note that Lemma 2.2 provides us with an alternative. Write $(\rho_i)_{1\leqslant i\leqslant \ell}$ the set of (distinct) asymptotic directions seen as unit complex numbers. There is only a finite number of them due to the double periodicity of $\mathbb{G}$. Denote by $\mathcal{T}^{(\rho_i)}(\mathbb{G})$ the set of tracks whose asymptotic direction is ρ_i. Then it is easy to see that

$$\mathcal{T}(\mathbb{G}) = \bigcup_{i=1}^{\ell} \mathcal{T}^{(\rho_i)}(\mathbb{G}).$$

Pick up two distinct ρ_i and ρ_j, then the families $\mathcal{T}^{(\rho_i)}$ and $\mathcal{T}^{(\rho_j)}$ form a grid of $\mathbb{G}$.

2.4 Random-cluster model on isoradial graphs

2.4.1 Definition

Previously, we defined the random-cluster model on any finite graph and extended the definition to infinite graphs with specific boundary conditions. Here we define the model on (infinite) isoradial graphs with respect to what we call the *isoradial parameters*.

Fix the cluster weight $q \geqslant 1$ and an additional parameter $\beta > 0$. We define the family of edge parameters $\boldsymbol{p}(\beta) = (p_e(\beta))_{e\in E}$ via the relation

$$p_e(\beta) = \frac{y_e(\beta)}{1 + y_e(\beta)},$$

where $y_e(\beta)$ is defined according to the value of q and θ_e, the subtended angle of the edge e as shown earlier in Figure 2.4:

$$\begin{aligned}
\text{if } 1 \leqslant q < 4, \quad & y_e(\beta) = \beta\sqrt{q}\,\frac{\sin(r(\pi-\theta_e))}{\sin(r\theta_e)}, \quad \text{where } r = \frac{1}{\pi}\cos^{-1}\Big(\frac{\sqrt{q}}{2}\Big);\\
\text{if } q = 4, \quad & y_e(\beta) = \beta\,\frac{2(\pi-\theta_e)}{\theta_e};\\
\text{if } q > 4, \quad & y_e(\beta) = \beta\sqrt{q}\,\frac{\sinh(r(\pi-\theta_e))}{\sinh(r\theta_e)}, \quad \text{where } r = \frac{1}{\pi}\cosh^{-1}\Big(\frac{\sqrt{q}}{2}\Big).
\end{aligned} \tag{2.2}$$

The parameters $\boldsymbol{p}$ defined by these formulae are called *isoradial probability parameters*. The associated infinite-volume random-cluster measure will be denoted by $\varphi^{\xi}_{\mathbb{G},\beta,q}$, where the boundary conditions ξ can be either 0 (free) or 1 (wired), as given in the previous sections.

Proposition 2.6. *We have the following duality relations for the random-cluster model:*

$$\varphi^{\xi}_{\mathbb{G},\beta,q} \overset{(d)}{=} \varphi^{1-\xi}_{\mathbb{G}^*,1/\beta,q}, \quad \textit{where} \quad \xi = 0,1.$$

In particular, at $\beta = 1$, the random-cluster model is self-dual up to the boundary conditions, that is $\varphi^{0}_{\mathbb{G},1,q} \overset{(d)}{=} \varphi^{1}_{\mathbb{G}^*,1,q}$ and $\varphi^{1}_{\mathbb{G},1,q} \overset{(d)}{=} \varphi^{0}_{\mathbb{G}^*,1,q}$.

Proof. According to Proposition 1.1, it is enough to check that $y_\theta(\beta)y_{\pi-\theta}(\frac{1}{\beta}) = q$. This is immediate by (2.2). □

2.4.2 Loop representation

The loop representation was already mentioned in Section 1.1.5 for any finite graph. Here, we give a more precise description for isoradial graphs.

Given a finite graph $G = (V, E)$ and a random-cluster configuration $\omega \in \{0,1\}^E$ on it, we connect midpoints of edges in $\mathbb{E}^\diamond$ by avoiding intersection with the edges given by ω. In other words, we connect midpoints to separate vertices in $\mathbb{V}$ and $\mathbb{V}^*$ and thus create interface between different connected components. Figure 2.6 illustrates how this is done locally for each rhombus. In consequence, we obtain the *loop representation* of the model.

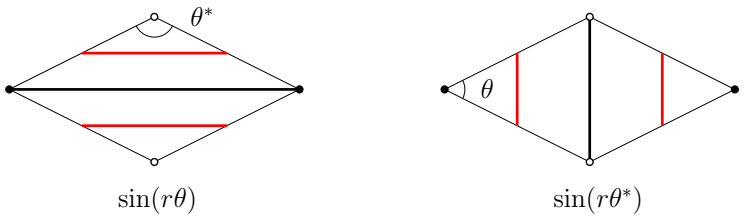

Figure 2.6 – The local lines connecting midpoints of edges of $\mathbb{E}^\diamond$ are drawn in red. On the left, the primal edge is open and on the right, the dual one is open.

We continue the calculation from (1.5). We have

$$\begin{aligned}\varphi^{\xi}_{\mathbb{G},1,q}[\omega] &\propto \prod_{e\in E}\left(\frac{y_e}{y_{e^*}}\right)^{\omega(e)/2}\cdot\sqrt{q}^{l^{\xi}(\omega)}\\ &\propto \prod_{e\in E}\left(\frac{\sin(r\theta^*)}{\sin(r\theta)}\right)^{\omega(e)}\cdot\sqrt{q}^{l^{\xi}(\omega)}\\ &\propto \prod_{e\in E}\sin(r\theta^*)^{\omega(e)}\sin(r\theta)^{\omega^*(e^*)}\cdot\sqrt{q}^{l^{\xi}(\omega)},\end{aligned}$$

where $\theta^* = \pi - \theta$, as indicated in Figure 2.6. This is the *loop representation* of the random--cluster model on the isoradial graph $\mathbb{G}$.

We note that when we are on the quare lattice, we have $\theta = \theta*$, which means that $\varphi^{\xi}_{\mathbb{G},1,q}[\omega]$ is proportional to $\sqrt{q}^{l^{\xi}(\omega)}$.

2.4.3 Uniqueness of the measure for doubly-periodic isoradial graphs

Here, we will determine some conditions under which we can deduce the uniqueness of the infinite-volume random-cluster measure. From what precedes, without any further information, we could have more than one infinite-volume random-cluster measures. However, using the same techniques as for the square lattice [Gri06], we can show that this measure is actually unique, except for a set of parameters which is at most countable, for any doubly-periodic isoradial graph.

Proposition 2.7. *There exists a subset $\mathcal{D}_q$ of $(0,+\infty)$ at most countable such that if $\beta \notin \mathcal{D}_q$, then $\varphi^0_{\mathbb{G},\beta,q} = \varphi^1_{\mathbb{G},\beta,q}$. Thus, the infinite-volume random-cluster measure is unique for values of β outside of a countable set.*

Before showing the proposition, we need to introduce the notion of the *free energy*.

Proposition 2.5 provides us with two families of train tracks $(s_n)_{n\in\mathbb{Z}}$ and $(t_n)_{n\in\mathbb{Z}}$ which form a grid. Due to the periodicity of $\mathbb{G}$, there exist $M, N \in \mathbb{N}$ such that the region $K = [0,M)\times[0,N)$ is a fundamental domain of $\mathbb{G}$. Moreover, the number of edges on its boundary can be bounded $|\partial_E K| \leqslant c(M+N)$ for some $c > 0$.

For $k \in \mathbb{N}$, let $G_k = [-2^k M, 2^k M)\times[-2^k N, 2^k N)$ and write V_k and E_k its vertex set and edge set. Note that $|\partial G_k| \leqslant 2^{k+1}c(M+N)$ and that G_{k+1} contains four copies of G_k with edges connecting them, thus $|E_{k+1}| = 4|E_k|$.

For $k \in \mathbb{N}$, $\xi = 0,1$ and $\beta > 0$, define the following quantities

$$Z^{\xi}_k(\beta) := \widetilde{Z}^{\xi}_{G_k,\beta,q} = \sum_{\omega\in\{0,1\}^{E_k}}\prod_{e\in E_k} y_e(\beta)^{\omega(e)} q^{k^{\xi}(\omega)}, \tag{2.3}$$

$$f^{\xi}_k(\beta) = \frac{1}{|E_k|}\ln Z^{\xi}_k(\beta). \tag{2.4}$$

Lemma 2.8. *For all $\beta > 0$, the limits $f^0_k(\beta)$ and $f^1_k(\beta)$ exist and coincide when $k \to \infty$. Write $f(\beta) = \lim f^0_k(\beta) = \lim f^1_k(\beta)$. Moreoever, the function $\beta \mapsto f(\beta)$ is convex.*

Proof. Cut G_{k+1} into four disjoint copies of G_k, denoted by G^1_k, G^2_k, G^3_k and G^4_k and let F be the set of edges connecting boundaries of different G^i_k. We can bound Z^0_{k+1} from below by taking into account only the configurations with all the edges in F closed. Given such

a configuration $\omega \in \{0,1\}^{E_{k+1}}$, write $k^{0,i}(\omega)$ for the number of clusters in G_k^i, then we have $k^0(\omega) = k^{0,1}(\omega) + k^{0,2}(\omega) + k^{0,3}(\omega) + k^{0,4}(\omega)$. This gives,

$$Z_{k+1}^0(\beta) \geqslant Z_k^0(\beta)^4.$$

Hence, $f_k^0(\beta)$ is an increasing function in k, its limit exists in $(-\infty, \infty]$. Denote it by $f(\beta)$.

Notice that we have the relation $k^0(\omega) \geqslant k^1(\omega) \geqslant k^0(\omega) - |\partial G_k|$. Since $|\partial G_k|/|V_k| \to 0$, we deduce that $\lim f_k^0(\beta) = \lim f_k^1(\beta) = f(\beta)$.

For $\xi = 0, 1$, we are going to show that $\beta \mapsto f_k^\xi(\beta)$ is a convex function for all $k \in \mathbb{N}$. Then, the statement of the lemma follows because the pointwise limit of convex functions is still convex. Due to the continuity of the functions $\beta \mapsto f_k^\xi(\beta)$ (polynomial in β), it is sufficient to show that their derivatives are increasing in β.

We start by writing $Z_k^\xi(\beta)$ differently,

$$Z_k^\xi(\beta) = \sum_{\omega \in \{0,1\}^{E_k}} \exp\Big[\sum_{e \in E_k} \omega(e)\pi_e(\beta)\Big] q^{k^\xi(\omega)},$$

where $\pi_e(\beta) = \ln y_e(\beta)$. Then, we compute the derivative of $f_k^\xi(\beta)$ with respect to β,

$$\begin{aligned}
\frac{\mathrm{d}f_k^\xi(\beta)}{\mathrm{d}\beta} &= \frac{1}{|E_k|}\frac{1}{Z_k^\xi(\beta)}\frac{\mathrm{d}Z_k^\xi(\beta)}{\mathrm{d}\beta} \\
&= \frac{1}{|E_k|}\frac{1}{Z_k^\xi(\beta)}\frac{1}{\beta}\sum_{\omega \in \{0,1\}^{E_k}} \Big(\sum_{e \in E_k} \omega(e)\Big) \cdot \exp\Big[\sum_{e \in E_k} \omega(e)\pi_e(\beta)\Big] q^{k^\xi(\omega)} \\
&= \frac{1}{\beta}\frac{1}{|E_k|}\varphi_{k,\beta}^\xi\Big[\sum_{e \in E_k} \omega(e)\Big] \\
&= \frac{1}{\beta}\frac{1}{|E_k|}\sum_{e \in E_k} \varphi_{k,\beta}^\xi[e \text{ is open}] \geqslant 0,
\end{aligned} \tag{2.5}$$

where we use the fact that $\frac{\mathrm{d}\pi_e(\beta)}{\mathrm{d}\beta} = \frac{1}{\beta}$ in the second line. Moreover, since $\beta \mapsto p_e(\beta)$ is increasing for all $e \in E_k$, from Proposition 1.7, the last term is also increasing in β. The proof is complete. □

For $\xi = 0, 1$, define

$$h^\xi(\beta) = \frac{1}{|E_0|}\sum_{e \in E_0} \varphi_\beta^\xi[e \text{ is open}].$$

Note that here we use the infinite-volume measure φ_β^ξ to define $h^\xi(\beta)$. By translational invariance of the measure by periods of $\mathbb{G}$, we also have, for all $k \in \mathbb{N}$,

$$h^\xi(\beta) = \frac{1}{|E_k|}\sum_{e \in E_k} \varphi_\beta^\xi[e \text{ is open}].$$

The following proposition gives a criterion in terms of h^ξ for the uniqueness of the infinite-volume measure.

Lemma 2.9. *If $h^1(\beta) = h^0(\beta)$, then $\varphi_\beta^1 = \varphi_\beta^0$ and the infinite-volume random-cluster measure is unique.*

Proof. Knowing that for all $k \geqslant 0$, the measure $\varphi^1_{k,\beta}$ dominates $\varphi^0_{k,\beta}$ stochastically. There exists a coupling $\mathbb{P}_k$ with marginals $\omega_0 \sim \varphi^0_{k,\beta}$, $\omega_1 \sim \varphi^1_{k,\beta}$ and $\mathbb{P}_k(\omega_0 \leqslant \omega_1) = 1$. Take the weak limits and we have a coupling $\mathbb{P}$ with marginals $\omega_0 \sim \varphi^0_\beta$ and $\omega_1 \sim \varphi^1_\beta$ such that $\mathbb{P}(\omega_0 \leqslant \omega_1) = 1$.

Then, for an increasing event A depending on a finite set of edges, say F, and for k large enough such that $F \subset E_k$, we have

$$\begin{aligned}
0 \leqslant \varphi^1_\beta(A) - \varphi^0_\beta(A) &= \mathbb{P}(\omega_1 \in A, \omega_0 \notin A) \\
&\leqslant \sum_{e \in F} \mathbb{P}(\omega_1(e) = 1 \text{ and } \omega_0(e) = 0) \\
&= \sum_{e \in F} [\mathbb{P}(\omega_1(e) = 1) - \mathbb{P}(\omega_0(e) = 1)] \\
&= \sum_{e \in F} \left[\varphi^1_\beta[\omega(e) = 1] - \varphi^0_\beta[\omega_0(e) = 1]\right] \\
&\leqslant |F||E_0|[h^1(\beta) - h^0(\beta)] = 0.
\end{aligned}$$

Thus, we obtain the equality $\varphi^1_\beta(A) = \varphi^0_\beta(A)$ for all increasing events A depending on finitely many edges. From the construction of these two infinite-volume measures as mentioned in Section 1.1.8, we conclude that φ^1_β and φ^0_β are equal. □

Now we are ready to prove Proposition 2.7.

Proof of Proposition 2.7. A standard argument says that a convex function is differentiable at all but countably many points. Moreover, from the limit given by Lemma 2.8, at $\beta > 0$ where f is differentiable, its derivative is given by the limit of $(f_k^\xi)'(\beta)$, $\xi = 0$ or 1. From (2.5),

$$\begin{aligned}
(f_k^1)'(\beta) &= \frac{1}{\beta}\frac{1}{|E_k|}\sum_{e \in E_k} \varphi^1_{k,\beta}[e \text{ is open}] \\
&\geqslant \frac{1}{\beta}\frac{1}{|E_k|}\sum_{e \in E_k} \varphi^1_{\beta}[e \text{ is open}] = h^1(\beta) \\
&\geqslant \frac{1}{\beta}\frac{1}{|E_k|}\sum_{e \in E_k} \varphi^0_{\beta}[e \text{ is open}] = h^0(\beta) \\
&\geqslant \frac{1}{\beta}\frac{1}{|E_k|}\sum_{e \in E_k} \varphi^0_{k,\beta}[e \text{ is open}] = (f_k^0)'(\beta).
\end{aligned}$$

This shows that at points of differentiability of f, since $\lim(f_k^1)'(\beta) = \lim(f_k^0)'(\beta)$, we should also have $h^1(\beta) = h^0(\beta)$, which implies uniqueness of the infinite-volume measure at β according to Lemma 2.9. Moreover, the convexity of f implies that it is not differentiable at most on a countable set. □

2.5 Known results

It is shown in [GM14] that the percolation on isoradial graphs is critical for parameters defined in (2.2) at $\beta = 1$. The main idea is based on the star-triangle transformations which are going to be introduced in the next section. In Section 3, we generalize this method to the random-cluster model with cluster-weight $q \geqslant 1$ to show the criticality is also at $\beta = 1$.

When it comes to critical behaviors, the interface of the Ising model on isoradial Dobrushin domains converges to a conformally invariant limit as mentioned before for the case of $\mathbb{Z}^2$. This result is given in [CS12, CDCH+14] and the authors use the discrete complex analysis developped in [Ken02, CS11].

2.6 Star-triangle transformation

In this section, we introduce the main tool of the first part of the thesis: the *star-triangle transformation*, also known as the *Yang-Baxter relation*. This transformation was first discovered by Kennelly in 1899 in the context of electrical networks [Ken99]. Then, it was discovered to be a key relation in different models of statistical mechanics [Ons44, Bax82] indicative of the integrability of the system.

2.6.1 Abstract star-triangle transformation

For a moment, we consider graphs as combinatorial objects without any embedding. Consider the triangle graph $\triangle = (V, E)$ and the star graph $\curlyvee = (V', E')$ shown in Figure 2.7; the boundary vertices of both graphs are $\{A, B, C\}$. Write $\Omega = \{0,1\}^E$ and $\Omega' = \{0,1\}^{E'}$ for the two spaces of percolation configurations associated to these two graphs. Additionally, consider two triplets of parameters, $\boldsymbol{p} = (p_a, p_b, p_c) \in (0,1)^3$ for the triangle and $\boldsymbol{p'} = (p'_a, p'_b, p'_c) \in (0,1)^3$ for the star, associated with the edges of the graph as indicated in Figure 2.7. For boundary conditions ξ on $\{A, B, C\}$, denote by $\varphi^{\xi}_{\triangle,\boldsymbol{p},q}$ (and $\varphi^{\xi}_{\curlyvee,\boldsymbol{p'},q}$) the random-cluster measure on $\triangle$ (and $\curlyvee$, respectively) with cluster-weight q and parameters $\boldsymbol{p}$ (and $\boldsymbol{p'}$, respectively). For practical reasons write

$$y_i = \frac{p_i}{1-p_i} \quad \text{and} \quad y'_i = \frac{p'_i}{1-p'_i}.$$

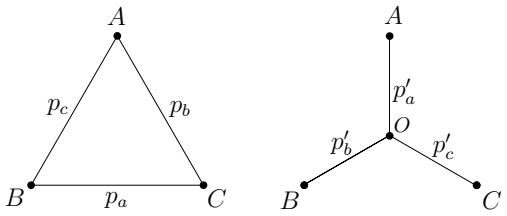

Figure 2.7 – Triangle and star graphs with parameters indicated on edges.

The two measures are related via the following relation.

Proposition 2.10 (Star-triangle transformation)**.** *Fix a cluster weight $q \geqslant 1$ and suppose the following conditions hold:*

$$y_a y_b y_c + y_a y_b + y_b y_c + y_c y_a = q, \tag{2.6}$$

$$y_i y'_i = q, \qquad \forall i \in \{a, b, c\}. \tag{2.7}$$

Then, for any boundary conditions ξ, the connections between the points A, B, C inside the graphs $\triangle$ and $\curlyvee$ have same law under $\varphi^{\xi}_{\triangle,\boldsymbol{p},q}$ and $\varphi^{\xi}_{\curlyvee,\boldsymbol{p'},q}$, respectively.

Remark 2.11. In light of (2.7), the relation (2.6) is equivalent to

$$y'_a y'_b y'_c - q(y'_a + y'_b + y'_c) = q^2. \tag{2.8}$$

The proof of the proposition is a straightforward computation of the probabilities of the different possible connections between A, B and C in the two graphs.

Proof. The probabilities of the different possible connections between A, B and C in $\triangle$ and $\curlywedge$ with different boundary conditions are summarized in the following tables. For ease of notation, the probabilities are given up to a multiplicative constant; the multiplicative constant is the inverse of the sum of all the terms in each column. Different tables correspond to different boundary conditions; each line to one connection event. We exclude symmetries of boundary conditions. It is straightforward to check that the corresponding entries in the two columns of each table are proportional, with ratio (right quantity divided by the left one) $q^2/y_a y_b y_c$ each time. □

$\{\{A,B\},C\}$	In $\triangle$	In $\curlywedge$
all disconnected	q	$q(q+y'_a+y'_b+y'_c)$
$A \leftrightarrow B \nleftrightarrow C$	$y_c q$	$y'_a y'_b q$
$B \leftrightarrow C \nleftrightarrow A$	y_a	$y'_b y'_c$
$C \leftrightarrow A \nleftrightarrow B$	y_b	$y'_c y'_a$
$A \leftrightarrow B \leftrightarrow C$	$y_a y_b + y_b y_c + y_c y_a + y_a y_b y_c$	$y'_a y'_b y'_c$

$\{A,B,C\}$	In $\triangle$	In $\curlywedge$
all disconnected	1	$q+y'_a+y'_b+y'_c$
$A \leftrightarrow B \nleftrightarrow C$	y_c	$y'_a y'_b$
$B \leftrightarrow C \nleftrightarrow A$	y_a	$y'_b y'_c$
$C \leftrightarrow A \nleftrightarrow B$	y_b	$y'_c y'_a$
$A \leftrightarrow B \leftrightarrow C$	$y_a y_b + y_b y_c + y_c y_a + y_a y_b y_c$	$y'_a y'_b y'_c$

$\{\{A\},\{B\},\{C\}\}$	In $\triangle$	In $\curlywedge$
all disconnected	q^2	$q^2(y'_a+y'_b+y'_c+q)$
$A \leftrightarrow B \nleftrightarrow C$	$y_c q$	$y'_a y'_b q$
$B \leftrightarrow C \nleftrightarrow A$	$y_a q$	$y'_b y'_c q$
$C \leftrightarrow A \nleftrightarrow B$	$y_b q$	$y'_c y'_a q$
$A \leftrightarrow B \leftrightarrow C$	$y_a y_b + y_b y_c + y_c y_a + y_a y_b y_c$	$y'_a y'_b y'_c$

Table 2.1 – Probabilities of different connection events with different boundary conditions.

In light of Proposition 2.10, the measures $\varphi^{\xi}_{\triangle,\boldsymbol{p},q}$ and $\varphi^{\xi}_{\curlywedge,\boldsymbol{p}',q}$ may be coupled in a way that preserves connections. For the sake of future applications, we do this via two random maps T and S from $\{0,1\}^{\curlywedge}$ to $\{0,1\}^{\triangle}$, and conversely. These random mappings are described in Figure 2.8; when the initial configuration is such that the result is random, the choice of the resulting configuration is done independently of any other randomness.

Proposition 2.12 (Star-triangle coupling). *Fix $q \geqslant 1$, boundary conditions ξ on $\{A,B,C\}$ and triplets $\boldsymbol{p} \in (0,1)^3$ and $\boldsymbol{p}' \in (0,1)^3$ satisfying (2.6) and (2.7). Let ω and ω' be configurations chosen according to $\varphi^{\xi}_{\triangle,\boldsymbol{p},q}$ and $\varphi^{\xi}_{\curlywedge,\boldsymbol{p}',q}$, respectively. Then,*

1. *$S(\omega)$ has the same law as ω',*
2. *$T(\omega')$ has the same law as ω,*

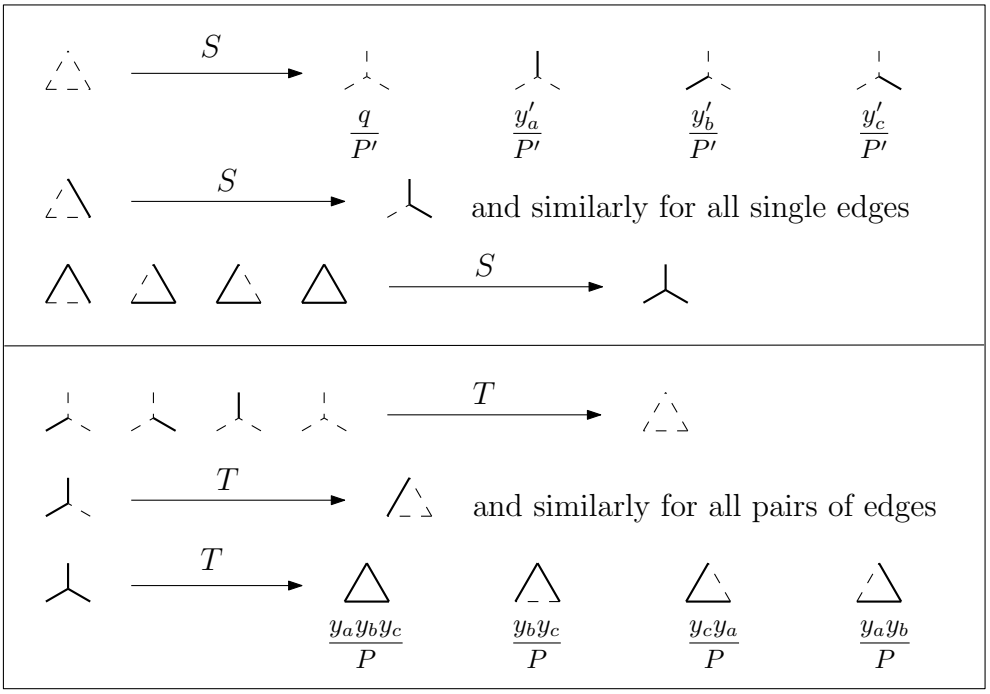

Figure 2.8 – The random maps T and S. Open edges are represented by thick segments, closed edges by dashed ones. In the first and last lines, the outcome is random: it is chosen among four possibilities with probabilities indicated below. The normalizing constants are $P' = q + y'_a + y'_b + y'_c = y'_a y'_b y'_c / q$ and $P = y_a y_b y_c + y_a y_b + y_b y_c + y_c y_a = q$.

3. *for $x, y \in \{A, B, C\}$, $x \overset{\triangle,\, \omega}{\longleftrightarrow} y$ if and only if $x \overset{\perp,\, S(\omega)}{\longleftrightarrow} y$,*
4. *for $x, y \in \{A, B, C\}$, $x \overset{\perp,\, \omega'}{\longleftrightarrow} y$ if and only if $x \overset{\triangle,\, T(\omega')}{\longleftrightarrow} y$.*

Proof. The points 3 and 4 are trivial by Figure 2.8. Points 1 and 2 follow by direct computation from the construction of S and T, respectively, with the crucial remark that the randomness in S and T is independent of that of ω and ω', respectively. □

2.6.2 Star-triangle transformation on isoradial graph

Next, we study the star-triangle transformation for isoradial graphs. We will see that when star-triangle transformations are applied to isoradial graphs with the random-cluster measure given by isoradiality when $\beta = 1$, what we get is exactly the random-cluster measure on the resulting graph.

Proposition 2.13. *Fix $q \geqslant 1$ and $\beta = 1$. Then, the random-cluster model is preserved under star-triangle transformations in the following sense.*

- *For any triangle ABC contained in an isoradial graph, the parameters y_{AB}, y_{BC} and y_{CA} associated by (2.2) with the edges AB, BC and CA, respectively, satisfy (2.6). Moreover, there exists a unique choice of point O such that, if the triangle ABC is replaced by the star $ABCO$, the resulting graph is isoradial and the parameters associated with the edges CO, AO, BO by (2.2) are related to y_{AB}, y_{BC} and y_{CA} as in (2.7).*
- *For any star $ABCO$ contained in an isoradial graph, the parameters y_{OC}, y_{OA} and y_{OB} associated by (2.2) with the edges CO, AO and BO, respectively, satisfy (2.6). Moreover,*

if the star $ABCO$ is replaced by the triangle ABC, the resulting graph is isoradial and the parameters associated with the edges AB, BC, CA by (2.2) are related to y_{OC}, y_{OA} and y_{OB} as in (2.7).

Proof. We only give the proof of the first point; the second may be obtained by considering the dual graph. Let ABC be a triangle contained in an isoradial graph G. Write a, b, c for the angles subtended to the edges BC, AC, AB, respectively. Then, $a+b+c = 2\pi$. A straightforward trigonometric computation shows that then $y_a y_b y_c + y_a y_b + y_b y_c + y_c y_a - q = 0$.

Permute the three rhombi of $G^\diamond$ corresponding to the edges AB, BC, CA as described in Figure 2.9 and let O be their common point after permutation. Let $\widetilde{G}$ be the graph obtained from G by adding the vertex O and connecting it to A, B and C and removing the edges AB, BC, CA. Since $\widetilde{G}$ has a diamond graph (as depicted in Figure 2.9), it is isoradial. Moreover, the angles subtended by the edges OA, OB and OC are $\pi - a$, $\pi - b$ and $\pi - c$, respectively. It follows from (2.2) that the parameters of the edges OA, OB and OC are related to those of the edges AB, BC and CA by (2.7). □

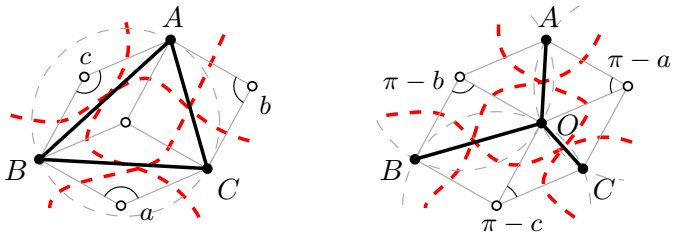

Figure 2.9 – A local triangle subgraph with corresponding subtended angles a, b and c. Note that $a + b + c = 2\pi$. The order of crossing of the three tracks involved is changed.

Triangles and stars of isoradial graphs correspond to hexagons formed of three rhombi in the diamond graph. Thus, when three such rhombi are encountered in a diamond graph, they may be permuted as in Figure 2.9 using a star-triangle transformation. We will call the three rhombi the *support* of the star-triangle transformation.

Let ω be a configuration on some isoradial graph G and σ a star-triangle transformation that may be applied to G. When applying σ to G, the coupling of Proposition 2.12 yields a configuration that we will denote by $\sigma(\omega)$.

Consider an open path γ in ω. Then, define $\sigma(\gamma)$ the image of γ under σ to be the open path of $\sigma(\omega)$ described as follows.

- If an endpoint of γ is adjacent to the support of σ, then we set $\sigma(\gamma)$ to be γ plus the additional possibly open edge if the latter has an endpoint on γ, which is given by the first line of Figure 2.8.
- If γ does not cross (and is not adjacent to) the support of σ, we set $\sigma(\gamma) = \gamma$.
- Otherwise, γ intersects the support of σ in one of the ways depicted in the first two lines of Figure 2.10. Then, we set $\sigma(\gamma)$ to be identical to γ outside the support of σ. And in the support of star-triangle transformation, since σ preserves connections, the part of γ inside may be replaced by an open path as in the same figure. Notice the special case when γ ends in the centre of a star and the corresponding edge is lost when applying σ (third line of Figure 2.10).

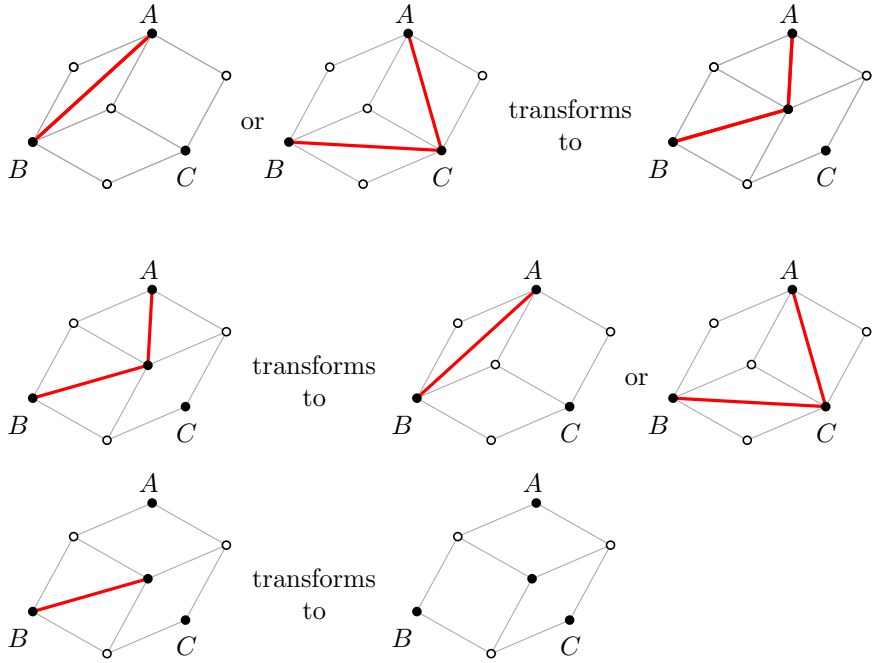

Figure 2.10 – The effect of a star-triangle transformation on an open path. In the second line, the second outcome is chosen only if the edge AB is closed. The fact that the result is always an open path is guaranteed by the coupling that preserves connections. In the last case, the open path may loose one edge.

2.7 Observable on isoradial graphs

2.7.1 Discrete complex analysis

A function $F : \mathbb{C}^\diamond \to \mathbb{C}$ defined on the rhombi centers of the rhombic lattice $\mathbb{G}^\diamond = (\mathbb{V}^\diamond, \mathbb{E}^\diamond)$ is said to be *s-holomorphic* if for each pair of neighboring centers z_1 and z_2, we have the following projection relation,

$$\mathrm{Proj}[F(z_1); \ell(e)] = \mathrm{Proj}[F(z_2); \ell(e)] \tag{2.9}$$

where $e = [wb] = [z_1 z_2]^* \in \mathbb{E}^\diamond$, b and w the closest primal and dual vertices to both z_1 and z_2 and $\ell(e) = [\mathrm{i}(w-b)]^{-\frac{1}{2}}$. See Figure 2.11 for notations.

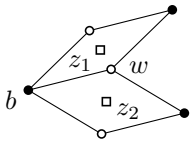

Figure 2.11 – Notations used to define s-holomorphicity in (2.9).

In a rhombus, write b_1, w_1, b_2 and w_2 its four vertices indexed in counterclockwise order, where b_1 and b_2 are primal, w_1 and w_2 are dual. Given a s-holomorphic function F defined on $\mathbb{C}^\diamond$, define a function G on the edges of the rhombic lattice $\mathbb{E}^\diamond$ by

$$G(e) = \mathrm{Proj}[F(z); \nu(e)], \tag{2.10}$$

where $e = [wb]$ is a mid-edge and z the center of one of the two lozenges sharing e as commun edge. The function G is well-defined due to the s-holomorphicity relation (2.9)

Conversely, a function G defined on mid-edges satisfying the two following properties also gives rise to a s-holomorphic function on the rhombic lattice:

1. $G(e) /\!\!/ \nu(e)$ for all mid-edges $e = [wb]$.
2. For any rhombus given by b_1, w_1, b_2 and w_2, we have $G([b_1w_1]) + G([b_2w_2]) = G([w_1b_2]) + G([w_2b_1])$.

We simply set $F(z) = G([b_1w_1]) + G([b_2w_2])$ for all $z \in \mathbb{C}^\diamond$, surrounded by vertices b_1, w_1, b_2 and w_2. We also call such a function *s-holomorphic* (on mid-edges).

2.7.2 Observable on Dobrushin domains

An isoradial *Dobrushin domain* is the data $(\Omega^\diamond, a^\diamond, b^\diamond)$ where $\Omega^\diamond \subset \mathbb{G}^\diamond$ is a simply-connected domain of $\mathbb{G}^\diamond$ containing

- inner rhombi $z \in \operatorname{Int}\Omega^\diamond$;
- boundary half-rhombi $\zeta \in \partial\Omega^\diamond$;
- two marked boundary edges $[a_w^\diamond a_b^\diamond], [b_w^\diamond b_b^\diamond] \in \mathbb{E}^\diamond$ with centers $a^\diamond$ and $b^\diamond$,

such that the arc (with counterclockwise orientation) $\partial = [b_b^\diamond a_b^\diamond]$ contains only vertices in $\mathbb{V}$ and the arc $\partial^* = [a_w^\diamond b_w^\diamond]$ contains only vertices in $\mathbb{V}^*$. See Figure 2.12 for an example. A configuration of the random-cluster model on $\Omega^\diamond$ is an element $\omega \in \{0,1\}^{\mathcal{E}(\operatorname{Int}\Omega^\diamond)}$, which is equivalent to choosing the primal or the dual connection in each of the rhombi of $\operatorname{Int}\Omega^\diamond$.

The *Dobrushin boundary conditions* on $\Omega^\diamond$ is the mixed boundary condition with wired on ∂ and free boundary condition on ∂^*. In other words, we connect primal vertices on the arc ∂ and dual vertices on the arc ∂^*. For $q \geqslant 1$ and $\beta > 0$, we write $\varphi^{\mathrm{Dob}}_{\Omega^\diamond,\beta,q}$ for the random-cluster measure on $\Omega^\diamond$ with the Dobrushin boundary condition.

The loop representation of the random-cluster model on isoradial graphs was described in Section 2.4.2. In the case or regular boundary condition such as wired or free boundary condition, we only get loops separating connected components; whereas in the case of the Dobrushin boundary condition, we get not only loops but also an extra interface going from a to b. It separates the primal connected component connected to ∂ and the dual connected component connected to ∂^*. We denote this interface by γ. See Figure 2.12 for an example.

For $1 \leqslant q \leqslant 4$, we define the *parafermionic observable* as follows. Given a mid-edge $e = [bw]$, with b primal and w dual, the parafermionic observable at e is defined by

$$F(e) := F_{\Omega^\diamond,\beta,q}(e) = \varphi_{\Omega^\diamond,\beta,q}\Big[\exp\left(-\mathrm{i}\,\sigma\, W(a^\diamond, e)\right)\mathbb{1}_{e\in\gamma}\Big], \quad \text{where } \sigma = \frac{2}{\pi}\arcsin\Big(\frac{\sqrt{q}}{2}\Big). \tag{2.11}$$

In the previous definition, $W(a^\diamond, e)$ denotes the winding of the interface γ going from $a^\diamond$ to e. Note that for different configurations, this value differs by a multiple of 2π.

2.7.3 Behavior under star-triangle transformations in the Ising model

When star-triangle transformations are performed locally, the observable defined on mid-edges is only modified locally since the random-cluster measure is preserved (Proposition 2.13). In particular, when $q = 2$, we are in the case of the FK-Ising model and the parafermionic observable given in (2.11) can be rewritten as

$$F(e) := F_{\Omega^\diamond,\beta,q}(e) = \varphi_{\Omega^\diamond,\beta,q}\Big[\exp\Big(-\frac{\mathrm{i}}{2}W(a^\diamond, e)\Big)\mathbb{1}_{e\in\gamma}\Big], \tag{2.12}$$

which is called *fermionic observable* because σ evaluates to $\frac{1}{2}$. The fermionic observable is s-holomorphic [CS12] and actually, this can be translated into a local linear relation between

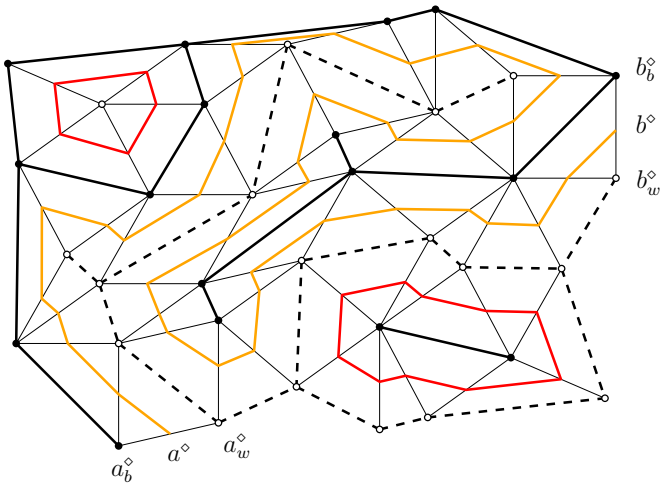

Figure 2.12 – A configuration on a Dobrushin domain. Solid lines represent primal open edges and dashed lines represent dual open edges. Loops separating different clusters are drawn in red and the interface separating the primal cluster connected to ∂ and the dual cluster connected to ∂^* is drawn in orange.

the observable before and after a local star-triangle transformation, independently of the boundary condition.

To be more precise, let us consider the notations as in Figure 2.13. On the left, we have the star graph $\star$ and on the right, the triangle graph $\triangle$. Since the star-triangle transformation preserves the random-cluster measure outside of this hexagon, the observable takes the same values on the boundary of both $\star$ and $\triangle$.

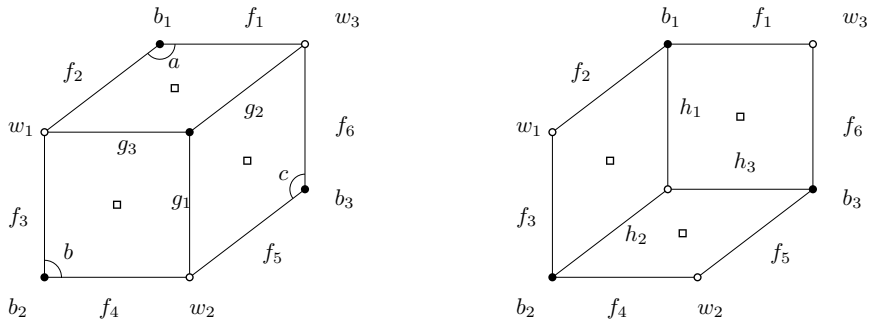

Figure 2.13 – A local star-triangle transformation with notations that we use in Propositions 2.14.

Proposition 2.14. *Write $G = (g_1, g_2, g_3)^T$ and $H = (h_1, h_2, h_3)^T$ two column matrices consisting of the values of the observable at the triangle mid-edges and the star mid-edges (cf. Figure 2.13). There exist two 3×3 matrices P and Q such that*

$$H = PG \quad \text{and} \quad G = QH.$$

Moreover, we have $P = Q$ which are given by the following formula

$$P = Q = \frac{1}{s_a s_b s_c} \begin{pmatrix} s_a c_b c_c & c_a s_b \nu_c & c_a s_c \overline{\nu}_b \\ c_b s_a \overline{\nu}_c & s_b c_c c_a & c_b s_c \nu_a \\ c_c s_a \nu_b & c_c s_b \overline{\nu}_a & s_c c_a c_b \end{pmatrix} \tag{2.13}$$

where $c_\sharp = \cos(\frac{\sharp}{2})$ *and* $s_\sharp = \cos(\frac{\sharp}{2})$ *for* $\sharp \in \{a, b, c\}$.

Proof. We apply Lemma 2.15. Write $F = (f_1, f_2, f_3, f_4, f_5, f_6)^T$, then in the star graph $\star$, we can write the vector F in terms of G; in the triangle graph $\triangle$, we can write F in terms of H. These relations are given by the explicit relation $F = DMG = D'M'H$, where

$$D = \mathrm{i}\cdot\mathrm{Diag}(s_a^{-1}, s_a^{-1}, s_b^{-1}, s_b^{-1}, s_c^{-1}, s_c^{-1}), \qquad D' = \mathrm{i}\cdot\mathrm{Diag}(s_b^{-1}, s_c^{-1}, s_c^{-1}, s_a^{-1}, s_a^{-1}, s_b^{-1}),$$

$$M = \begin{pmatrix} 0 & \overline{\nu}_a & -c_a \\ 0 & c_a & -\nu_a \\ -c_b & 0 & \overline{\nu}_b \\ -\nu_b & 0 & c_b \\ \overline{\nu}_c & -c_c & 0 \\ c_c & -\nu_c & 0 \end{pmatrix}, \qquad M' = \begin{pmatrix} -\nu_b & 0 & c_b \\ \overline{\nu}_c & -c_c & 0 \\ c_c & -\nu_c & 0 \\ 0 & \overline{\nu}_a & -c_a \\ 0 & c_a & -\nu_a \\ -c_b & 0 & \overline{\nu}_b \end{pmatrix}.$$

Also let

$$N = \frac{1}{2}\begin{pmatrix} 0 & 0 & c_b & -\overline{\nu}_b & \nu_c & -c_c \\ \nu_a & -c_a & 0 & 0 & c_c & -\overline{\nu}_c \\ c_a & -\overline{\nu}_a & \nu_b & -c_b & 0 & 0 \end{pmatrix}.$$

We note that $N\cdot(-D^2)\cdot M = I_3$, thus we have $G = QH$ where $Q = -NDD'M'$. A computation shows that Q is of the form (2.13). To conclude, we use the fact that Q is invertible and is an involution. □

Lemma 2.15. *Let f be a s-holomorphic function defined on mid-edges. Given a rhombus whose vertices are denoted by v_1, v_2, v_3 and v_4 (two are primal and two others are dual) in the counterclockwise order with angle α between $\overrightarrow{v_1v_2}$ and $\overrightarrow{v_1v_4}$. Let $f_i = f([v_{i-1}v_i])$ for $i = 1, 2, 3, 4$ with $v_0 = v_4$. Then, for the both possible ways of choosing primal and dual vertices, we can write f_3 and f_4 in terms of f_1 and f_2,*

$$f_3 = \frac{\mathrm{i}}{s_\alpha}(\overline{\nu}_\alpha f_2 - c_\alpha f_1) \quad \text{and} \quad f_4 = \frac{\mathrm{i}}{s_\alpha}(c_\alpha f_2 - \nu_\alpha f_1),$$

where $c_\alpha = \cos(\frac{\alpha}{2})$, $s_\alpha = \sin(\frac{\alpha}{2})$ and $\nu_\alpha = \exp(\mathrm{i}\frac{\alpha}{2}) = c_\alpha + \mathrm{i}s_\alpha$.

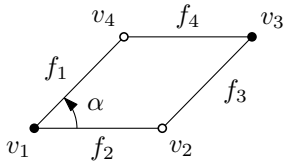

Figure 2.14 – A rhombus

Proof. We just need to show one of the possible way of choosing primal and dual vertices. Say, v_1 and v_3 are primal and v_2 and v_4 are dual as shown in Figure 2.14. Let $f = f_1 + f_3 = f_2 + f_4$ which is the corresponding value of the function f at the center of the rhombus. Write $\theta = \arg(\mathrm{i}(v_2 - v_1))$. Then, we have

$$f_1 = \mathrm{Proj}\Big[f, \ell([v_1v_4])\Big] = \frac{1}{2}(f + \overline{f}e^{-\mathrm{i}(\theta+\alpha)}),$$
$$f_2 = \mathrm{Proj}\Big[f, \ell([v_1v_2])\Big] = \frac{1}{2}(f + \overline{f}e^{-\mathrm{i}\theta}).$$

This gives a formula of f in terms of f_1 and f_2,

$$f = \frac{\mathrm{i}}{s_\alpha}(\overline{\nu}_\alpha f_2 - \nu_\alpha f_1).$$

Then, we use the fact that $f_3 = f - f_1$ and $f_4 = f - f_2$ to conclude. □

Chapter 3

Universality of the random-cluster model

3.1 Results

The square lattice embedded so that each face is a square of side-length $\sqrt{2}$ is an isoradial graph. We will denote it abusively by $\mathbb{Z}^2$ and call it the *regular square lattice*. The edge-weight associated to each edge of $\mathbb{Z}^2$ by (2.2) is $\frac{\sqrt{q}}{1+\sqrt{q}}$. This was shown in [BD12] to be the critical parameter for the random-cluster model on the square lattice. Moreover, the phase transition of the model was shown to be continuous when $q \in [1,4]$ [DCST17] and discontinuous when $q > 4$ [DGH+16]. The following two theorems generalise these results to periodic isoradial graphs.

Theorem 3.1. *Fix a doubly-periodic isoradial graph $\mathbb{G}$ and $1 \leqslant q \leqslant 4$. Then,*

- $\varphi^1_{\mathbb{G},1,q}[0 \leftrightarrow \infty] = 0$ *and* $\varphi^0_{\mathbb{G},1,q} = \varphi^1_{\mathbb{G},1,q}$;
- *there exist $a, b > 0$ such that for all $n \geqslant 1$,*

$$n^{-a} \leqslant \varphi^0_{\mathbb{G},1,q}\Big[0 \leftrightarrow \partial B_n\Big] \leqslant n^{-b};$$

- *for any $\rho > 0$, there exists $c = c(\rho) > 0$ such that for all $n \geqslant 1$,*

$$\varphi^0_{R,1,q}\Big[\mathcal{C}_h(\rho n, n)\Big] \geqslant c,$$

where $R = [-(\rho+1)n, (\rho+1)n] \times [-2n, 2n]$ and $\mathcal{C}_h(\rho n, n)$ is the event that there exists a path in $\omega \cap [-\rho n, \rho n] \times [-n, n]$ from $\{-\rho n\} \times [-n, n]$ to $\{\rho n\} \times [-n, n]$.

The last property is called the *strong RSW property* (or simply RSW property) and may be extended as follows: for any boundary conditions ξ,

$$c \leqslant \varphi^{\xi}_{R,1,q}\Big[\mathcal{C}_h(\rho n, n)\Big] \leqslant 1 - c, \tag{3.1}$$

for any $n \geqslant 1$ and some constant $c > 0$ depending only on ρ. In words, crossing probabilities remain bounded away from 0 and 1 uniformly in boundary conditions and in the size of the box (provided the aspect ratio is kept constant). For this reason, in some works (e.g. [GM14]) the denomination *box crossing property* is used.

The strong RSW property was known for Bernoulli percolation on the regular square lattice from the works of Russo and Seymour and Welsh [Rus78, SW78], hence the name. The

term strong refers to the uniformity in boundary conditions; weaker versions were developed in [BD12] for the square lattice. Hereafter, we say the model has the strong RSW property if (3.1) is satisfied.

The strong RSW property is indicative of a continuous phase transition and has numerous applications in describing the critical phase. In particular, it implies the first two points of Theorem 3.1. It is also instrumental in the proofs of mixing properties and the existence of certain critical exponents and subsequential scaling limits of interfaces. We refer to [DCST17] for details.

Theorem 3.2. *Fix a doubly-periodic isoradial graph* $\mathbb{G}$ *and* $q > 4$. *Then,*

- $\varphi^1_{\mathbb{G},1,q}[0 \leftrightarrow \infty] > 0$;
- *there exists* $c > 0$ *such that for all* $n \geqslant 1$, $\varphi^0_{\mathbb{G},1,q}[0 \leftrightarrow \partial B_n] \leqslant \exp(-cn)$.

Note that the above result is also of interest for regular graphs such as the triangular and hexagonal lattices. Indeed, the transfer matrix techniques developed in [DGH+16] are specific to the square lattice and do not easily extend to the triangular and hexagonal lattices.

The strategy of the proof for Theorems 3.1 and 3.2 is the same as in [GM14]. There, Theorem 3.1 was proved for $q = 1$ (Bernoulli percolation). The authors explained how to transfer the RSW property from the regular square lattice model to more general isoradial graphs by modifying the lattice step by step. The main tool used for the transfer is the star-triangle transformation.

In this article, we will follow the same strategy, with two additional difficulties:

- The model has long-range dependencies, and one must proceed with care when handling boundary conditions.
- For $q \leqslant 4$, the RSW property is indeed satisfied for the regular square lattice (this is the result of [DCST17]), and may be transferred to other isoradial graphs. This is not the case for $q > 4$, where a different property needs to be transported, and some tedious new difficulties arise.

The results above may be extended to isoradial graphs which are not periodic but satisfy the so-called *bounded angles property* and an additional technical assumption termed the *square-grid property* in [GM14]. We will not discuss this generalisation here and simply stick to the case of doubly-periodic graphs. Interested readers may consult [GM14] for the exact conditions required for $\mathbb{G}$; the proofs below adapt readily.

A direct corollary of the previous two theorems is that isoradial random-cluster models are critical for $\beta = 1$. This was already proved for $q > 4$ in [BDCS15] using different tools.

Corollary 3.3. *Fix* $\mathbb{G}$ *a doubly-periodic isoradial graph and* $q \geqslant 1$. *Then, for any* $\beta \neq 1$, *one has* $\varphi^1_{\mathbb{G},\beta,q} = \varphi^0_{\mathbb{G},\beta,q}$ *and*

- *when* $\beta < 1$, *there exists* $c_\beta > 0$ *such that for any* $x, y \in \mathbb{V}$,

$$\varphi^1_{\mathbb{G},\beta,q}[x \leftrightarrow y] \leqslant \exp(-c_\beta \|x - y\|);$$

- *when* $\beta > 1$, $\varphi^0_{\mathbb{G},\beta,q}[x \leftrightarrow \infty] > 0$ *for any* $x \in \mathbb{V}$.

For $1 \leqslant q \leqslant 4$, arm exponents at the critical point $\beta = 1$ are believed to exist and to be universal (that is they depend on q and the dimension, but not on the structure of the underlying graph). Below we define the arm events and effectively state the universality of the exponents, but do not claim their existence.

Fix $k \in \{1\} \cup 2\mathbb{N}$. For $N > n$, define the *k-arm event* $A_k(n,N)$ to be the event that there exists k disjoint paths $\mathcal{P}_1, \dots, \mathcal{P}_k$ in counterclockwise order, contained in $[-N,N]^2 \setminus (-n,n)^2$, connecting $\partial[-n,n]^2$ to $\partial[-N,N]^2$, with $\mathcal{P}_1, \mathcal{P}_3, \dots$ contained in ω and $\mathcal{P}_2, \mathcal{P}_4, \dots$ contained in ω^*. Note that this event could be void if n is too small compared to k; we will always assume n is large enough to avoid such degenerate situations.

For continuous phase transitions (that is for $q \in [1,4]$) it is expected that,

$$\varphi^0_{R,1,q}[A_k(n,N)] = \left(\frac{n}{N}\right)^{\alpha_k + o(1)},$$

for some $\alpha_k > 0$ called the *k-arm exponent*. The RSW theory provides such polynomial upper and lower bounds, but the exponents do not match.

The one-arm exponent of the model describes the probability for the cluster of a given point to have large radius under the critical measure; the four-arm exponent is related to the probability for an edge to be pivotal for connection events.

Theorem 3.4 (Universality of arm exponents). *Fix $\mathbb{G}$ a doubly-periodic isoradial graph and $1 \leqslant q \leqslant 4$. Then, for any $k \in \{1\} \cup 2\mathbb{N}$, there exists a constant $c > 0$ such that, for all $N > n$ large enough,*

$$c\,\varphi^0_{\mathbb{Z}^2,1,q}[A_k(n,N)] \leqslant \varphi^0_{\mathbb{G},1,q}[A_k(n,N)] \leqslant c^{-1}\varphi^0_{\mathbb{Z}^2,1,q}[A_k(n,N)].$$

Section 2.6 contains background on the star-triangle transformation and how it acts on isoradial graphs. It also sets up the strategy for gradually transforming the regular square lattice into general isoradial graphs. This is done in two stages: first the regular square lattice is transformed into general isoradial square lattices, then into bi-periodic isoradial graphs. This two-stage process is repeated in each of the following two sections.

The proofs of Theorems 3.1 and 3.4 are contained in Section 3.3, while that of Theorem 3.2 in Section 3.4. The reason for this partition is that the tools in the case $1 \leqslant q \leqslant 4$ and $q > 4$ are fairly different. Chapter 4 contains the adaptation to the quantum case (Theorem 4.1).

Several standard computations involving the random-cluster model and the RSW technology are necessary. Details are given in appendixes.

3.2 Switching between isoradial graphs

As explained in the introduction, the strategy of the proof is to transform the regularly embedded square lattice into arbitrary doubly-periodic isoradial graphs using star-triangle transformations. This will enable us to transfer estimates on connection probabilities from the former to the latter. Below, we explain the several steps of the transformation.

3.2.1 From regular square lattice to isoradial square lattice

In this section we recall the definition of isoradial embeddings of the square lattice from Section 2.2. As described in [GM14], a procedure based on *track exchanges* transforms one isoradial embedding of the square lattice into a different one. In addition to [GM14], the effect of boundary conditions needs to be taken into account; a construction called *convexification* is therefore required.

Isoradial embeddings of the square lattice may be encoded by two doubly-infinite sequences of angles. Let $\boldsymbol{\alpha} = (\alpha_n)_{n\in\mathbb{Z}}$ and $\boldsymbol{\beta} = (\beta_n)_{n\in\mathbb{Z}}$ be two sequences of angles in $[0,\pi)$ such that Equation 2.1 is satisfied. Then, define $\mathbb{G}_{\boldsymbol{\alpha},\boldsymbol{\beta}}$ to be the isoradial embedding of the

square lattice with vertical train tracks $(s_n)_{n\in\mathbb{Z}}$ with transverse angles $(\alpha_n)_{n\in\mathbb{Z}}$ and horizontal train tracks $(t_n)_{n\in\mathbb{Z}}$ with transverse angles $(\beta_n)_{n\in\mathbb{Z}}$. Condition (2.1) ensures that $\mathbb{G}_{\boldsymbol{\alpha},\boldsymbol{\beta}}$ satisfies the bounded-angles property for $\varepsilon = \inf\{\beta_n - \alpha_m, \alpha_n - \beta_m + \pi : m, n \in \mathbb{Z}\} > 0$.

In the following, we mainly consider doubly-periodic isoradial graphs, hence periodic sequences $(\alpha_n)_{n\in\mathbb{Z}}$ and $(\beta_n)_{n\in\mathbb{Z}}$. The bounded-angles property is then automatically ensured if it is satisfied for a period of (α_n) and (β_n).

The same notation may be used to denote "rectangular" finite subgraphs of isoradial square lattices. Indeed, for finite sequences $\boldsymbol{\alpha} = (\alpha_n)_{M_-\leqslant n\leqslant M_+}$ and $\boldsymbol{\beta} = (\beta_n)_{N_-\leqslant n\leqslant N_+}$, define $G_{\boldsymbol{\alpha},\boldsymbol{\beta}}$ to be a (finite) isoradial square lattice with $M_+ - M_- + 1$ vertical tracks and $N_+ - N_- + 1$ horizontal tracks. We will think of this graph as part of an infinite isoradial graph, thus we call the right boundary of $G_{\boldsymbol{\alpha},\boldsymbol{\beta}}$ the vertices to the right of s_{M_+}, the left boundary those to the left of s_{M_-}, the top boundary the vertices above t_{N_+} and the bottom boundary those below t_{N_-}. The term rectangular refers to the diamond graph rather than to $G_{\boldsymbol{\alpha},\boldsymbol{\beta}}$; the boundary denominations are also used for $G^\diamond_{\boldsymbol{\alpha},\boldsymbol{\beta}}$.

The *regular square lattice* is the embedding corresponding to sequences $\beta_n = \frac{\pi}{2}$ and $\alpha_n = 0$ for all $n \in \mathbb{Z}$.

Track exchange Let us start by describing a simple but essential operation composed of star-triangle transformations, which we call *track exchange*. In the language of transfer matrices, this amounts to that the transfer matrices associated with two adjacent rows commute with each other, which is the usual formulation of the Yang-Baxter transformation.

Let G be a finite rectangular subgraph of an isoradial square lattice and t and t' be two parallel adjacent horizontal train tracks. Suppose that we want to switch their positions using star-triangle transformations. That is, we would like to perform a series of star-triangle transformations that changes the graph G into an identical graph, with the exception of the train tracks t and t' that are exchanged (or equivalently that their transverse angles are exchanged). We will suppose here that the transverse angles of t and t' are distinct, otherwise the operation is trivial.

Since t and t' do not intersect, no star-triangle transformation may be applied to them. Suppose however that G contains one additional rhombus (gray in Figure 3.1) at either the left or right end of t and t' that corresponds to the intersection of these two tracks. (Depending on the transverse angles of the tracks, there is only one possible position for this rhombus.) Then, a series of star-triangle transformations may be performed as in Figure 3.1. In effect, these transformations "slide" the gray rhombus from one end of the tracks to the other, and exchange the two tracks in the process.

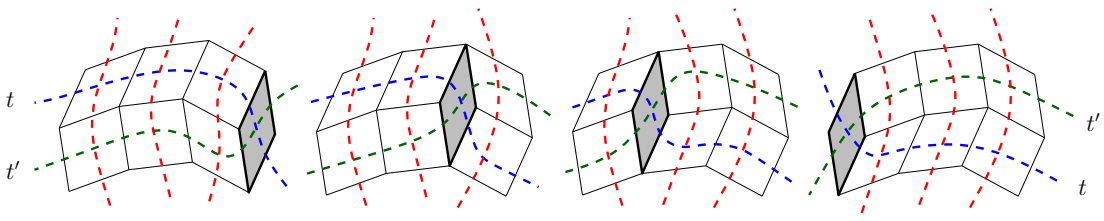

Figure 3.1 – We move the gray rhombus from the right to the left by a sequence of star-triangle transformation. Observe that these transformations only affect the tracks t and t', and that their ultimate effect is to exchange them.

As seen in Section 2.6.2, each star-triangle transformation of an isoradial graph preserves the random-cluster measure and connection properties. Thus, the procedure above, which

we call a *track exchange*, allows us to deduce connection properties of the resulting graph from those of the initial graph.

In [GM14], the gray rhombus was added before exchangin the tracks and removed afterwards. Thus, the track exchange could be perceived as a measure- and connection-preserving transformation between isoradial square lattices. By repeating such track exchanges, blocks of tracks of a square lattice were exchanged, and RSW-type estimates were transported from one block to another.

In the present context, adding a rhombus (and hence an edge) to a graph affects the random-cluster measure of the entire graph. We therefore prefer to "prepare" the graph by adding all necessary gray rhombi for all the track exchanges to be performed at once. The operation is called the *convexification* of a finite part of a square lattice.

Convexification Consider a finite rectangular portion $G = G_{\boldsymbol{\alpha},\boldsymbol{\beta}}$ of an isoradial square lattice, with $\boldsymbol{\alpha}$ and $\boldsymbol{\beta}$ two finite sequences of angles. Suppose that $\boldsymbol{\beta} = (\beta_n)_{0\leqslant n\leqslant N}$ for some $N > 0$. We call the vertices below t_0 (in the present case the bottom boundary) the *base level* of G.

We say that $\widetilde{G}$ is a *convexification* of $G = G_{\boldsymbol{\alpha},\boldsymbol{\beta}}$ if

- G is a subgraph of $\widetilde{G}$ and $\widetilde{G}$ has no other tracks than those of G;
- the top and bottom boundary of $G^\diamond$ are also boundaries of $\widetilde{G}^\diamond$;
- as we follow the boundary of $\widetilde{G}^\diamond$ in counterclockwise direction, the segment between the top and bottom boundaries (which we naturally call the left boundary) and that between the bottom and top boundaries (called the right boundary) are convex.

The second condition may be read as follows: in $\widetilde{G}$, the vertical tracks (s_n) only intersect the horizontal tracks (t_n); however, additionally to G, $\widetilde{G}$ may contain intersections between horizontal tracks.

The third condition is equivalent to asking that all horizontal tracks of G with distinct transverse angles intersect in $\widetilde{G}$. Indeed, the left and right boundaries of $\widetilde{G}^\diamond$ are formed of the transverse segments of the horizontal tracks of G, each track contributing once to each segment of the boundary. That both the left and right boundaries of $\widetilde{G}^\diamond$ are convex means that the transverse segments of two tracks t_i, t_j with distinct transverse angles appear in alternative order along the boundary of $\widetilde{G}^\diamond$, when oriented in counterclockwise direction. Hence, they necessarily intersect in $\widetilde{G}$. The converse may also be easily checked.

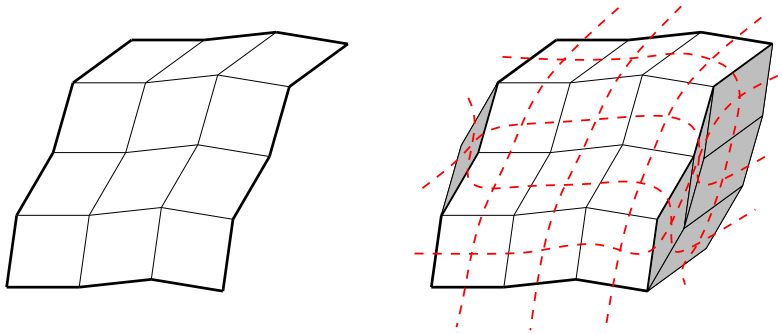

Figure 3.2 – An isoradial square lattice and a convexification of it. Only the diamond graph is depicted.

Below, we will sometimes call G the *square lattice block* of $\widetilde{G}$; $\widetilde{G} \setminus G$ is naturally split into a left and a right part.

The following two simple lemmas will come in useful when performing track exchanges.

Lemma 3.5. *For any adjacent horizontal tracks t, t' of G with distinct transverse angles, there exists a convexification $\widetilde{G}$ of G in which the rhombus corresponding to the intersection of t and t' is adjacent to $G^\diamond$.*

Lemma 3.6. *For any two convexifications $\widetilde{G}$ and $\widetilde{G}'$ of G, there exists a sequence of star-triangle transformations that transforms $\widetilde{G}$ into $\widetilde{G}'$ and that does not affect any rhombus of $G^\diamond$.*

Proof of Lemma 3.5. We start by describing an algorithm that constructs a convexification of G. Let $\langle , \rangle$ be the scalar product on $\mathbb{R}^2$.

1. Set $H = G$, which is the graph to be convexified.
2. Orient the edges on the right boundary of $H^\diamond$ above the base level upwards and denote the corresponding unit vectors by $\overrightarrow{e_0}, \dots, \overrightarrow{e_N}$.
3. If there exists j such that $\langle \overrightarrow{e_{j+1}} - \overrightarrow{e_j}, (1,0) \rangle > 0$, fix such a value j and proceed to Step 4. Otherwise, go to the Step 5.
4. Add a rhombus to $H^\diamond$ whose boundary is given by $\overrightarrow{e_j}$, $\overrightarrow{e_{j+1}}$, $-\overrightarrow{e_j}$ and $-\overrightarrow{e_{j+1}}$ to the right of the edges $\overrightarrow{e_j}$, $\overrightarrow{e_{j+1}}$. Set H to be the graph thus obtained, and go back to Step 2.
5. Proceed the same for the left boundary of G.

Each rhombus added in Step 4 corresponds to an intersection of two horizontal tracks of G. As such, only a finite number of such rhombi may be added, which shows that the algorithm necessarily terminates. Moreover, it is obvious to see that when it terminates, the resulting graph, which we denote by $\widetilde{G}$, is indeed a convexification of G.

The construction of $\widetilde{G}$ does not ensure that the successive tracks t and t' intersect in $\widetilde{G}$ adjacently to G. However, we may choose j corresponding to the index of t the first time the algorithm arrives at Step 3 for either the right or left boundary. If such choice is made, the intersection of the tracks t and t' in the resulting graph $\widetilde{G}$ will be adjacent to G. □

Proof of Lemma 3.6. By symmetry, it is sufficient to show that there exists a sequence of star--triangle transformations that transforms the right part (call it G_r) of $\widetilde{G} \backslash G$ into the right part of $\widetilde{G}' \backslash G$ (which we call G'_r) without affecting any rhombus of $G^\diamond$. Notice that $G_r^\diamond$ and $(G'_r)^\diamond$ have the same boundary. Indeed, the left boundaries of $G_r^\diamond$ and $(G'_r)^\diamond$ coincide both with the right boundary of $G^\diamond$. Their right boundaries are both formed of the segments of length 1, with angles $\boldsymbol{\beta}$, arranged in increasing order. Then, [Ken93, Thm. 5] ensures the existence of the transformations as required. □

Consider a finite rectangular region G of an isoradial square lattice and consider any of its convexification $\widetilde{G}$. Using the previous two lemmas, one can switch the transverse angles of any two neighbouring horizontal train tracks by a sequence of star-triangle transformations. A more precise statement is given below.

Corollary 3.7. *Let $G = G_{\alpha,\beta}$ be as above and let t and t' be two adjacent horizontal train tracks with distinct transverse angles. Then, for any convexification $\widetilde{G}$ of G, there exists a sequence of star-triangle transformations $\sigma_1, \dots, \sigma_k$ that may be applied to $\widetilde{G}$ with the following properties:*

- *there exists $0 \leqslant \ell < k$ such that the transformations $\sigma_1, \dots, \sigma_\ell$ only affect either the right or the left side of $\widetilde{G} \setminus G$;*
- *in $(\sigma_\ell \circ \cdots \circ \sigma_1)(\widetilde{G})$, the tracks t and t' intersect at a rhombus adjacent to G;*

- *the transformations $\sigma_{\ell+1},\dots,\sigma_k$ applied to $(\sigma_\ell\circ\cdots\circ\sigma_1)(\widetilde{G})$ are "sliding" the intersection of t and t' from one side of G to the other, as described in Figure 3.1.*

Write $\Sigma_{t,t'}=\sigma_k\circ\cdots\circ\sigma_1$. If τ denotes the transposition of the indices of tracks t and t', then $\Sigma_{t,t'}(G)$ is a convexification of $G_{\boldsymbol{\alpha},\tau\boldsymbol{\beta}}$.

Proof. Suppose for simplicity that the tracks t and t' intersect in $\widetilde{G}$ to the right of G (which is to say that the transverse angle of the lower track is greater than that of the above).

Write $\widetilde{G}'$ for a convexification of G in which the tracks t, t' intersect in a rhombus adjacent to $G^\diamond$ (as given by Lemma 3.5). It is obvious that the left side of $\widetilde{G}'$ may be chosen identical to that of $\widetilde{G}$, and we will work under this assumption.

Let $\sigma_1,\dots,\sigma_\ell$ be a sequence of star-triangle transformations as that given by Lemma 3.6 that affects only the right side of $\widetilde{G}$ and that transforms $\widetilde{G}$ into $\widetilde{G}'$. Let $\sigma_{\ell+1},\dots,\sigma_k$ be the series of star-triangle transformations that slides the intersection of t and t' from right to left of G, as in Figure 3.1. Then, $\sigma_1,\dots,\sigma_k$ obviously satisfies the conditions above. □

In the following, we will apply repeated line exchanges Σ_{t_i,t_j} to a convexification $\widetilde{G}$ of some finite portion of a square lattice. Thus, we will implicitly assume Σ_{t_i,t_j} is a series of star-triangle transformations as in the lemma above, adapted to the convexification to which it is applied. When t_i and t_j have same transverse angles, we will simply write Σ_{t_i,t_j} for the empty sequence of transformations. We note that tracks are indexed with respect to the starting graph and are not reindexed when track exchanges are applied. This is the reason why neighboring tracks do not necessarily have indices which differ by 1; thus, we call them t_i and t_j with the only constraint $i\neq j$.

All of the above may be summarised as follows. A convexification of G provides all the horizontal track intersections necessary to exchange any two horizontal tracks (that is the gray rhombus in Figure 3.1 for any pair of horizontal tracks). In order to exchange two adjacent horizontal tracks t_i and t_j, the sequence of transformations Σ_{t_i,t_j} starts from bringing the intersection of t_i and t_j next to G (this is done through star-triangle transformations that do not affect G), then slides it through t_i and t_j.

In certain arguments below, it will be more convenient to work with a "double" strip of square lattice $G=G_{\boldsymbol{\alpha},\boldsymbol{\beta}}$ where $\boldsymbol{\alpha}$ and $\boldsymbol{\beta}$ are finite sequences of angles and $\boldsymbol{\beta}=(\beta_n)_{-N\leqslant n\leqslant N}$ for some $N>0$. We will then separately convexify the upper half $G_{\boldsymbol{\alpha},(\beta_0,\dots,\beta_N)}$ and $G_{\boldsymbol{\alpha},(\beta_{-N},\dots,\beta_{-1})}$ (as in Figure 3.4). Track exchanges will only be between tracks above t_0 or strictly below t_0; the base (that is the vertices between t_{-1} and t_0) will never be affected by track exchanges.

Construction of the mixed graph by gluing Consider two isoradial square lattices with same sequence $\boldsymbol{\alpha}$ of transverse angles for the vertical tracks. Write $\mathbb{G}^{(1)}=G_{\boldsymbol{\alpha},\boldsymbol{\beta}^{(1)}}$ and $\mathbb{G}^{(2)}=G_{\boldsymbol{\alpha},\boldsymbol{\beta}^{(2)}}$. Additionally, suppose that they both belong to $\mathcal{G}(\varepsilon)$ for some $\varepsilon>0$.

Fix integers $N_1,N_2,M\in\mathbb{N}$. We create an auxiliary graph G_{mix}, called the *mixed graph*, by superimposing strips of $\mathbb{G}^{(1)}$ and $\mathbb{G}^{(2)}$ of width $2M+1$, then convexifying the result. More precisely, let $\widetilde{\boldsymbol{\beta}}=(\beta_0^{(1)},\dots,\beta_{N_1}^{(1)},\beta_0^{(2)},\dots,\beta_{N_2}^{(2)})$ and $\widetilde{\boldsymbol{\alpha}}=(\alpha_n)_{-M\leqslant n\leqslant M}$. Define G_{mix} to be a convexification of $G_{\widetilde{\boldsymbol{\alpha}},\widetilde{\boldsymbol{\beta}}}$.

Write $G^{(1)}=G_{\widetilde{\boldsymbol{\alpha}},\widetilde{\boldsymbol{\beta}}^{(1)}}$ and $G^{(2)}=G_{\widetilde{\boldsymbol{\alpha}},\widetilde{\boldsymbol{\beta}}^{(2)}}$, where

$$\widetilde{\boldsymbol{\beta}}^{(1)}=(\beta_0^{(1)},\dots,\beta_{N_1}^{(1)})\qquad\text{and}\qquad\widetilde{\boldsymbol{\beta}}^{(2)}=(\beta_0^{(2)},\dots,\beta_{N_2}^{(2)}).$$

These are both subgraphs of G_{mix}; we call them the blocks of $\mathbb{G}^{(1)}$ and $\mathbb{G}^{(2)}$ inside G_{mix}.

Next, we aim to switch these two blocks of G_{mix} using star-triangle transformations. That is, we aim to transform G_{mix} into a graph G'_{mix} obtained as above, with the sequence

$\widetilde{\beta}$ replaced by $(\beta_0^{(2)},\dots,\beta_{N_2}^{(2)},\beta_0^{(1)},\dots,\beta_{N_1}^{(1)})$. There are two ways of doing this, each having its own advantages.

One way is to use track exchanges to send the tracks $t_{N_1+1},\dots,t_{N_1+N_2+1}$ of G_{mix} all the way down, one by one. Using the notation of the previous section, this corresponds to the following sequence of track exchanges

$$\Sigma^{\downarrow} = \Sigma^{\downarrow}_{N_1+N_2+1} \circ \cdots \circ \Sigma^{\downarrow}_{N_1+1},$$

where $\Sigma^{\downarrow}_k = \Sigma_{t_0,t_k} \circ \cdots \circ \Sigma_{t_{N_1},t_k}$ is a sequence of star-triangle transformations sending the track t_k to the bottom of the block $G^{(1)}$ in G_{mix}. This will be useful in the proof of Proposition 3.15, where we need to control the upward drift of an open path.

The other is to push the tracks $t_{N_1},\dots,t_0$ all the way up, one by one. It formally reads

$$\Sigma^{\uparrow} = \Sigma^{\uparrow}_0 \circ \cdots \circ \Sigma^{\uparrow}_{N_1},$$

where $\Sigma^{\uparrow}_k = \Sigma_{t_k,t_{N_1+N_2+1}} \circ \cdots \circ \Sigma_{t_k,t_{N_1+1}}$ is a sequence of star-triangle transformations sending the track t_k to the top of the block $G^{(2)}$ in G_{mix}. This will be used to study the downward drift of an open path in Proposition 3.16.

One may easily check that the sequences $\Sigma^{\downarrow}$ and $\Sigma^{\uparrow}$ may be applied to G_{mix}. That is that whenever a track exchange $\Sigma_{t,t'}$ is applied, the previous track exchanges are such that the tracks t and t' are adjacent. The two sequences of track exchanges are illustrated in Figure 3.3.

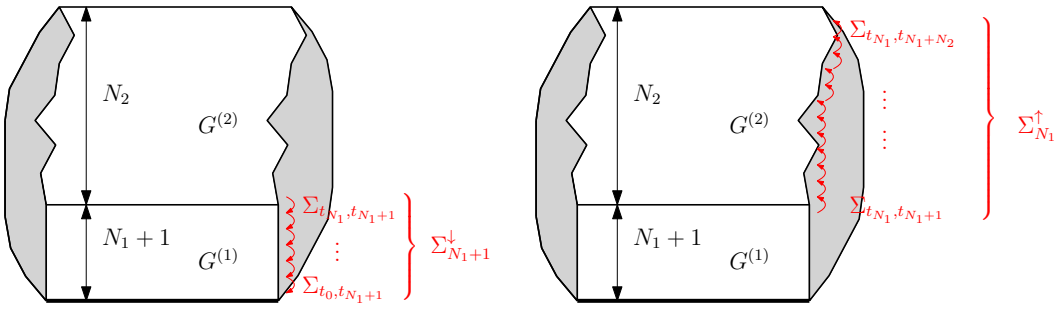

Figure 3.3 – The graph G_{mix} is obtained by superimposing $G^{(1)}$ and $G^{(2)}$ then convexifying the result (in gray). **Left:** The sequence $\Sigma^{\downarrow}_{N_1+1}$ moves the track t_{N_1+1} below the block $G^{(1)}$. **Right:** The sequence $\Sigma^{\uparrow}_{N_1}$ moves the track t_{N_1} above the block $G^{(2)}$.

The resulting graphs $\Sigma^{\uparrow}(G_{\mathrm{mix}})$ and $\Sigma^{\downarrow}(G_{\mathrm{mix}})$ both contain the desired block of isoradial square lattice, but their convexification may differ. However, by Lemma 3.6, we may fix one convexification G'_{mix} of the resulting square lattice block and add star-triangle transformations at the end of both $\Sigma^{\uparrow}$ and $\Sigma^{\downarrow}$ that only affect the convexification and such that $\Sigma^{\uparrow}(G_{\mathrm{mix}}) = \Sigma^{\downarrow}(G_{\mathrm{mix}}) = G'_{\mathrm{mix}}$. Henceforth, we will always assume that both $\Sigma^{\uparrow}$ and $\Sigma^{\downarrow}$ contain these star-triangle transformations.

Since each star-triangle transformation preserves the random-cluster measure, we have

$$\Sigma^{\uparrow}\varphi^{\xi}_{G_{\mathrm{mix}}} = \Sigma^{\downarrow}\varphi^{\xi}_{G_{\mathrm{mix}}} = \varphi^{\xi}_{G'_{\mathrm{mix}}}$$

for all boundary conditions ξ. Above, $\varphi^{\xi}_{G_{\mathrm{mix}}}$ and $\varphi^{\xi}_{G'_{\mathrm{mix}}}$ denote the random-cluster measures with $\beta = 1$ and boundary conditions ξ on G_{mix} and G'_{mix} respectively. The action of $\Sigma^{\uparrow}$ (and

$\Sigma^{\downarrow}$) should be understood as follows. For a configuration ω chosen according to $\varphi^{\xi}_{G_{\text{mix}}}$, the sequence $\Sigma^{\uparrow}$ of star-triangle transformations is applied to ω with the resulting configuration sampled as described in Figure 2.8, independently for each star-triangle transformation. Then the final configuration follows $\varphi^{\xi}_{G'_{\text{mix}}}$. The same holds for $\Sigma^{\downarrow}$.

The reader may note that we do not claim that $\Sigma^{\uparrow}(\omega)$ and $\Sigma^{\downarrow}(\omega)$ have the same law for any *fixed* configuration ω on G_{mix}; this is actually not the case in general.

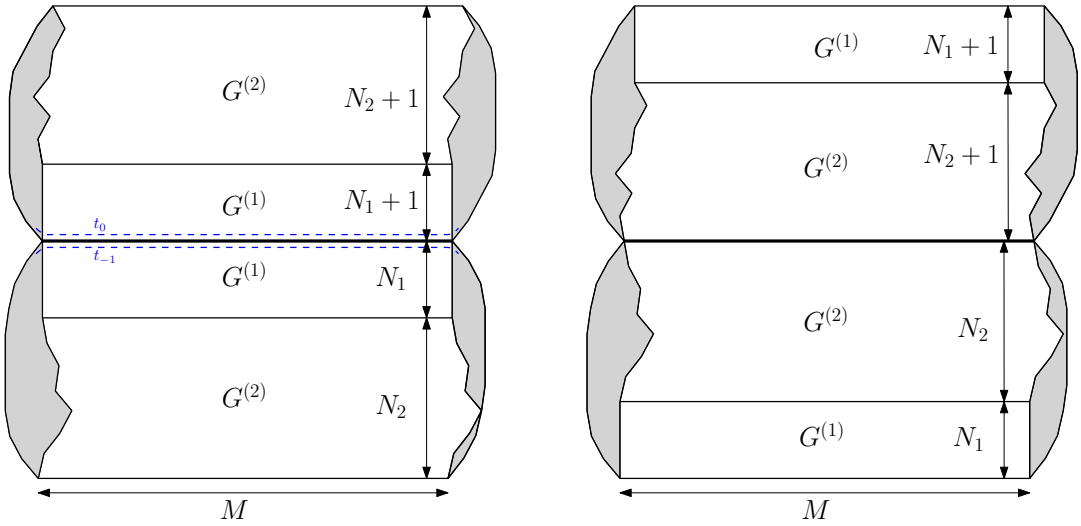

Figure 3.4 – **Left:** The graph G_{mix} constructed in both the upper and lower half plane. The convexification is drawn in gray **Right:** By exchanging tracks, the relative positions of $G^{(1)}$ and $G^{(2)}$ are switched, the resulting graph is $\Sigma^{\uparrow}(G_{\text{mix}}) = \Sigma^{\downarrow}(G_{\text{mix}}) = G'_{\text{mix}}$. Note that there is a slight assymetry in the upper-half and the lower-half planes.

In certain parts of the proofs that follow, we construct a mixture as described above, in both the upper and lower half-plane, as depicted in Figure 3.4. That is, we set

$$\widetilde{\boldsymbol{\beta}} = (\beta^{(2)}_{-N_2}, \dots, \beta^{(2)}_{-1}, \beta^{(1)}_{-N_1}, \dots, \beta^{(1)}_{N_1}, \beta^{(2)}_{0}, \dots, \beta^{(2)}_{N_2})$$

and $\widetilde{\boldsymbol{\alpha}} = (\alpha_n)_{-M \leqslant n \leqslant M}$ and define the base as the vertices of $G^{\diamond}_{\widetilde{\boldsymbol{\alpha}},\widetilde{\boldsymbol{\beta}}}$ between t_{-1} and t_0. Then, set G_{mix} to be the separate convexification of the portions of $G_{\widetilde{\boldsymbol{\alpha}},\widetilde{\boldsymbol{\beta}}}$ above and below the base. We will call G_{mix} the *symmetric* version of the *mixed graph*.

The sequences $\Sigma^{\uparrow}$ and $\Sigma^{\downarrow}$ of track exchanges are defined in this case by performing the procedure described above separately on both sides of the base. For instance, $\Sigma^{\uparrow}$ is the sequence of star-triangle transformations that pushes t_{N_1} all the way to the top and t_{-N_1} all the way to the bottom, then t_{N_1-1} and t_{-N_1+1} all the way to the top and bottom respectively, etc. Observe that the blocks below the base, and therefore the number of line exchanges applied, differ by one from those above due to the track t_0.

Local behaviour of an open path In the proofs of the coming sections we will utilize the line exchanges defined above to transport certain connection estimates from $\mathbb{G}^{(1)}$ to $\mathbb{G}^{(2)}$. To that end, we will need to control the effect that the line exchanges have on open paths. Recall that the coupling of Figure 2.8 is designed to preserve connections. As such, any open path before a star-triangle transformation has a corresponding open path in the resulting configuration.

Let G_{mix} be a mixed graph and t, t' be two adjacent horizontal tracks. Let ω be a configuration on G_{mix} and γ be a simple path, open in ω, and contained in the square lattice block of G_{mix}. Then, the intersection of γ with the tracks t and t' may be split into disjoint segments of two edges (or of one edge if the endpoint of γ is on the line between t and t'). The effect of the transformations on γ may therefore be understood simply by studying how each individual segment is affected. Each segment is actually only affected by at most three consecutive star-triangle transformations of $\Sigma_{t,t'}$, and the effect of these is summarized in Figure 3.5.

A very similar analysis appears in [GM14, Sec. 5.3]. The only difference between Figure 3.5 and [GM14, Fig. 5.5.] is in the probabilities of secondary outcomes, which are adapted to the random-cluster model. The exact values will be relevant in Chapter 4, when studying the quantum model.

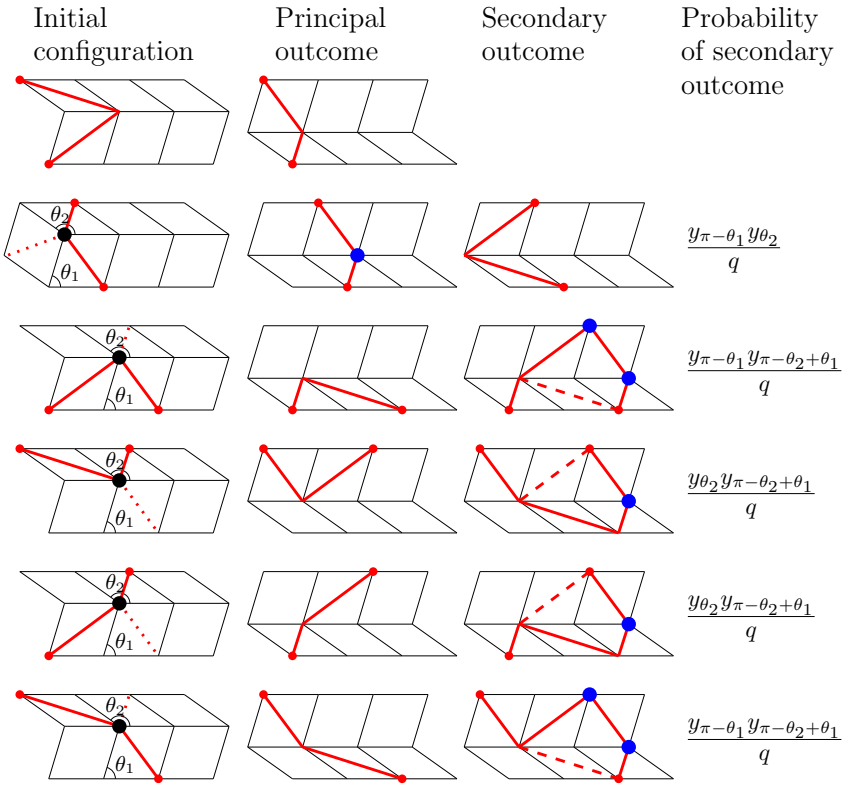

Figure 3.5 – Path transformations. The left column exhausts all the possible intersections of γ (in thick red lines) with t and t'. The second column depicts the "principal" outcome, which arises with probability 1 when there is no secondary outcome or when the dotted red edge in the initial diagram is closed. Otherwise, the resulting configuration is random: either the principal or the secondary outcome (third column) appear, the latter with the probability given in the last column. Dashed edges in the secondary outcome are closed. The randomness comes from a star-triangle transformation, and hence is independent of any other randomness.

Finally, if an endpoint of γ lies between the two adjacent horizontal tracks t and t', a special segment of length 1 appears in the intersection of γ with t and t'. This segment obeys separate rules; in particular it may be contracted to a single point, as shown in Figure 3.6.

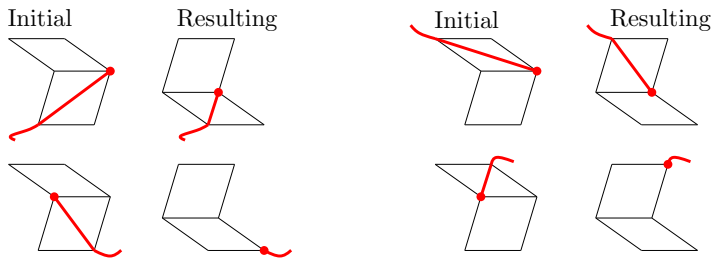

Figure 3.6 – If an endpoint of a path lies between two tracks, the corresponding edge is sometimes contracted to a single point.

3.2.2 From isoradial square lattices to general graphs

Let $\mathbb{G}$ be an isoradial graph. We call a *grid* of $\mathbb{G}$ two bi-infinite families of tracks $(s_n)_{n\in\mathbb{Z}}$ and $(t_n)_{n\in\mathbb{Z}}$ of $\mathbb{G}$ with the following properties.

- The tracks of each family do not intersect each other.
- All tracks of $\mathbb{G}$ not in $(t_n)_{n\in\mathbb{Z}}$ intersect all those of $(t_n)_{n\in\mathbb{Z}}$.
- All tracks of $\mathbb{G}$ not in $(s_n)_{n\in\mathbb{Z}}$ intersect all those of $(s_n)_{n\in\mathbb{Z}}$.
- The intersections of $(s_n)_{n\in\mathbb{Z}}$ with t_0 appear in order along t_0 (according to some arbitrary orientation of t_0) and the same holds for the intersections of $(t_n)_{n\in\mathbb{Z}}$ with s_0.

The tracks $(s_n)_{n\in\mathbb{Z}}$ and $(t_n)_{n\in\mathbb{Z}}$ are called *vertical* and *horizontal* respectively. The vertices of $\mathbb{G}^\diamond$ below and adjacent to t_0 are called the base of $\mathbb{G}$.

In our setting, the existence of a grid is guaranteed by the following lemma.

Lemma 3.8. *Let $\mathbb{G}$ be an isoradial graph. Then,*

- *if $\mathbb{G}$ is doubly-periodic, it contains a grid;*
- *$\mathbb{G}$ is an embedding of the square lattice if and only if any of its grid contains all its tracks.*

It may be worth mentioning that if $\mathbb{G}$ has a grid $(s_n)_{n\in\mathbb{Z}}$ and $(t_n)_{n\in\mathbb{Z}}$ and $\sigma_1,\dots,\sigma_K$ are star-triangle transformations that may be applied to $\mathbb{G}$, then the tracks $(s_n)_{n\in\mathbb{Z}}$ and $(t_n)_{n\in\mathbb{Z}}$ of $(\sigma_K\circ\cdots\circ\sigma_1)(\mathbb{G})$ also form a grid of the transformed graph $(\sigma_K\circ\cdots\circ\sigma_1)(\mathbb{G})$. Observe also that generally, grids are not unique.

Proof. Let $\mathbb{G}$ be a doubly-periodic isoradial graph, invariant under the translation by two linearly independent vectors $\tau_1,\tau_2\in\mathbb{R}^2$. First notice that, by the periodicity of $\mathbb{G}$, each track t of $\mathbb{G}$ is also invariant under some translation $a\tau_1+b\tau_2$ for a certain pair $(a,b)\in\mathbb{Z}^2\backslash\{(0,0)\}$. Thus, t stays within bounded distance of the line of direction $a\tau_1+b\tau_2$, which we now call the *asymptotic direction* of t. Call two tracks *parallel* if they have the same asymptotic direction.

By the periodicity of $\mathbb{G}$, the set of all asymptotic directions of tracks of $\mathbb{G}$ is finite. Thus, the tracks of $\mathbb{G}$ may be split into a finite number of sets of parallel tracks. It is immediate that two tracks which are not parallel intersect. Conversely, if two parallel tracks intersect, they must do so infinitely many times, due to periodicity. This is impossible, since two tracks can intersect at most once. In conclusion, tracks intersect if and only if they are not parallel.

Let t_0 and s_0 be two intersecting tracks of $\mathbb{G}$. Orient each of them in some arbitrary direction. Write $\dots,t_{-1},t_0,t_1,\dots$ for the tracks parallel to t_0, ordered by their intersections with s_0. Similarly, let $\dots,s_{-1},s_0,s_1,\dots$ be the tracks parallel to s_0, in the order of their intersections with t_0.

Then, the two families $(s_n)_{n\in\mathbb{Z}}$ and $(t_n)_{n\in\mathbb{Z}}$ defined above form a grid for $\mathbb{G}$: the tracks of each family do not intersect each other since they are parallel, but intersect all other tracks, since these have distinct asymptotic directions.

The second point of the lemma is straightforward. □

In an isoradial graph $\mathbb{G}$ with grid $(s_n)_{n\in\mathbb{Z}}$ and $(t_n)_{n\in\mathbb{Z}}$, write $\mathsf{R}(i,j;k,\ell)$ for the region enclosed by s_i, s_j, t_k and t_ℓ, including the four boundary tracks. We say that $\mathsf{R}(i,j;k,\ell)$ has a *square lattice structure* if it is the subgraph of some isoradial square lattice. This will be applied to local modifications of bi-periodic graphs, thus inside $\mathsf{R}(i,j;k,\ell)$ there may exist tracks not belonging to $(s_n)_{i\leqslant n\leqslant j}$ which do not intersect any of the tracks $(s_n)_{i\leqslant n\leqslant j}$. Such tracks would be vertical in a square lattice containing $\mathsf{R}(i,j;k,\ell)$, but are not vertical in $\mathbb{G}$. See the right-hand side of Figure 3.7 for an illustration.

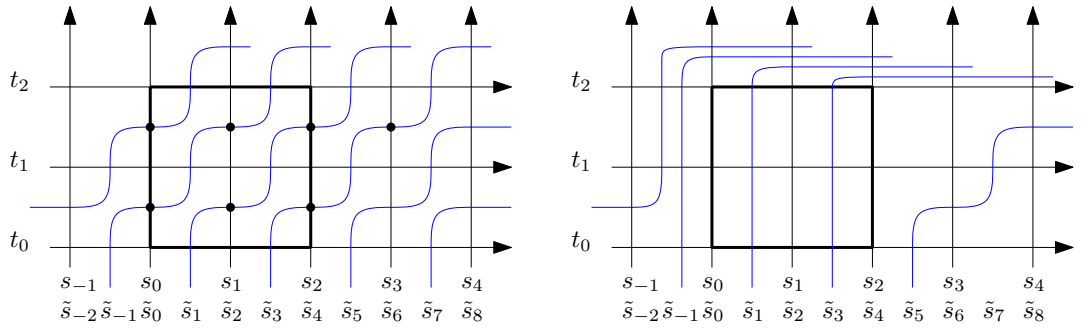

Figure 3.7 – **Left:** The train tracks of a portion of a doubly-periodic isoradial graph $\mathbb{G}$. A grid of $\mathbb{G}$ is given by horizontal tracks (s_n) and vertical tracks (t_n). We denote by $(\widetilde{s_n})$ its non-horizontal tracks. We want to make the region $\mathsf{R}(0,2;0;2)$ have a square lattice structure by removing all the black points using star-triangle transformations. **Right:** The black points are removed (from the top) from the region $\mathsf{R}(0,2;0;2)$, making a square structure appear inside. This region contains tracks $\widetilde{s_1}$ and $\widetilde{s_3}$ which would be vertical in a square lattice containing $\mathsf{R}(0,2;0,2)$ but are not vertical in the original graph $\mathbb{G}$ on the left.

In the second stage of our transformation from the regular square lattice to arbitrary doubly-periodic isoradial graphs, we use star-triangle transformations to transfer crossing estimates from isoradial square lattices to periodic graphs. To that end, given a doubly-periodic isoradial graph, we will use star-triangle transformations to construct a large region with a square lattice structure. The proposition below is the key to these transformations.

A star-triangle transformation is said to act between two tracks t and t' if the three rhombi affected by the transformation are all between t and t', including potentially on t and t'.

Proposition 3.9. *Let $\mathbb{G}$ be a doubly-periodic isoradial graph with grid $(s_n)_{n\in\mathbb{Z}}$, $(t_n)_{n\in\mathbb{Z}}$. There exists $d\geqslant 1$ such that for all $M,N\in\mathbb{N}$, there exists a finite sequence of star-triangle transformations $(\sigma_k)_{1\leqslant k\leqslant K}$, each acting between $s_{-(M+dN)}$ and s_{M+dN} and between t_N and t_0, none of them affecting any rhombus of t_0 and such that in the resulting graph $(\sigma_k\circ\cdots\circ\sigma_1)(\mathbb{G})$, the region $\mathsf{R}(-M,M;0,N)$ has a square lattice structure.*

This is a version of [GM14, Lem. 7.1] with a quantitative control over the horizontal position of the star-triangle transformations involved. Obviously, the lemma may be applied also below the base level t_0 by symmetry.

Proof. We only sketch this proof since it is very similar to the corresponding one in [GM14]. We will only refer below to the track system of $\mathbb{G}$; we call an intersection of two tracks a *point*. Fix $M, N \in \mathbb{N}$.

Index all non-horizontal tracks of $\mathbb{G}$ as $(\widetilde{s}_n)_{n\in\mathbb{Z}}$, in the order of their orientation with t_0, such that $\widetilde{s}_0 = s_0$. Then the vertical tracks $(s_n)_{n\in\mathbb{Z}}$ of $\mathbb{G}$ form a periodically distributed subset of $(\widetilde{s}_n)_{n\in\mathbb{Z}}$. Let M_+ and M_- be such that $\widetilde{s}_{M_+} = s_M$ and $\widetilde{s}_{M_-} = s_{-M}$.

We will work with $\mathbb{G}$ and transformations of $\mathbb{G}$ by a finite number of star-triangle transformations. The tracks of any such transformations are the same as those of $\mathbb{G}$, we therefore use the same indexing for them. Call a *black point* of $\mathbb{G}$, or of any transformation of $\mathbb{G}$, an intersection of a track $\widetilde{s}_k$ with $M_- \leqslant k \leqslant M_+$ with a non-horizontal track, contained between t_0 and t_N. See Figure 3.7 for an example.

Observe that, if in a transformation $(\sigma_k \circ \cdots \circ \sigma_1)(\mathbb{G})$ of $\mathbb{G}$ there are no black points, then $(\sigma_k \circ \cdots \circ \sigma_1)(\mathbb{G})$ has the desired property. The strategy of the proof is therefore to eliminate the black points one by one as follows.

Orient all non-horizontal tracks of $\mathbb{G}$ upwards (that is from their intersection with t_0 to that with t_1). We say that a black point is *maximal* if, along any of the two tracks whose intersection gives this black point, there is no other black point further. One may then check (see the proof of [GM14]) that if black points exist, then at least one maximal one exists. Moreover, a maximal black point may be eliminated by a series of star-triangle transformations involving its two intersecting tracks and the horizontal tracks between it and t_N. Thus, black points may be eliminated one by one, until none of them is left (by the fact that $(s_n)_{n\in\mathbb{Z}}$ and $(t_n)_{n\in\mathbb{Z}}$ form a grid, only finitely many black points exist to begin with). Call $\sigma_1, \dots, \sigma_K$ the successive star-triangle transformations involved in this elimination. Then $(\sigma_K \circ \cdots \circ \sigma_1)(\mathbb{G})$ has a square lattice structure in $\mathsf{R}(-M, M; 0, N)$.

We are left with the matter of controlling the region where star-triangle transformations are applied. Notice that $\sigma_1, \dots, \sigma_K$ each involve exactly one horizontal track t_k with $0 < k \leqslant N$. Thus, they all only involve rhombi between t_0 and t_N, but none of those along t_0.

Also observe that, due to the periodicity of $\mathbb{G}$, between t_0 and t_N, a track $\widetilde{s}_k$ intersects only tracks $\widetilde{s}_j$ with $|j - k| \leqslant cN$ for some constant c depending only on the fundamental domain of $\mathbb{G}$. It follows, by the periodicity of the tracks $(s_n)_{n\in\mathbb{Z}}$ in $(\widetilde{s}_n)_{n\in\mathbb{Z}}$, that all black points are initially in $\mathsf{R}(-M - dN, M + dN; 0, N)$ for some constant $d \geqslant 0$ depending only on the fundamental domain of $\mathbb{G}$. Finally, since all star-triangle transformations $(\sigma_k)_{0\leqslant k\leqslant K}$ involve one horizontal track and two others intersecting at a black point, each σ_k acts in the region of $(\sigma_{k-1} \circ \cdots \circ \sigma_1)(\mathbb{G})$ delimited by s_{-M-dM}, s_{M+dN}, t_0 and t_N. □

3.3 Proofs for $1 \leqslant q \leqslant 4$

Starting from now, fix $q \in [1, 4]$ and let $\mathbb{G}$ be a doubly-periodic graph with grid $(s_n)_{n\in\mathbb{Z}}, (t_n)_{n\in\mathbb{Z}}$. Recall that $\mathbb{G} \in \mathcal{G}(\varepsilon)$ for some $\varepsilon > 0$. All the constants below depend on the value of ε. Write $\varphi^{\xi}_{\mathbb{G}} := \varphi^{\xi}_{\mathbb{G},1,q}$ for the random-cluster measure with parameters q and $\beta = 1$ and boundary conditions $\xi \in \{0, 1\}$ on $\mathbb{G}$.

3.3.1 Notations and properties

For integers $i \leqslant j$ and $k \leqslant \ell$ recall that $\mathsf{R}(i, j; k, \ell)$ is the subgraph of $\mathbb{G}$ contained between tracks s_i and s_j and between t_k and t_ℓ (including the boundary tracks). Write $\mathsf{R}(i; k)$ for the centred rectangle $\mathsf{R}(-i, i; k, k)$ and $\Lambda(n) = \mathsf{R}(n; n)$. The same notation applies to $\mathbb{G}^\diamond$ and $\mathbb{G}^*$. We define R and Λ in the same way using Euclidean distances. Note that R and Λ are domains

with respect to a grid of $\mathbb{G}$ whereas R and Λ are Euclidean ones and they should all be seen as subregions of $\mathbb{R}^2$.

Similarly to the crossings events defined in the introduction, set

- $\mathcal{C}_h(i,j;k,\ell)$: the event that there exists an open path in $\mathsf{R}(i,j;k,\ell)$ with one endpoint left of the track s_i and the other right of the track s_j. This is called a *horizontal crossing* of $\mathsf{R}(i,j;k,\ell)$.
- $\mathcal{C}_v(i,j;k,\ell)$: the event that there exists an open path in $\mathsf{R}(i,j;k,\ell)$ with one endpoint below t_k and the other above t_ℓ. This is called a *vertical crossing* of $\mathsf{R}(i,j;k,\ell)$.

The crossings $\mathcal{C}_h$ and $\mathcal{C}_v$ can also be defined for symmetric rectangular domains $\mathsf{R}(m;n)$, in which case we write $\mathcal{C}_h(m;n)$ and $\mathcal{C}_v(m;n)$. Also write $\mathcal{C}_h^*(i,j;k,\ell)$, $\mathcal{C}_v^*(i,j;k,\ell)$, $\mathcal{C}_h^*(m;n)$ and $\mathcal{C}_v^*(m;n)$ for the corresponding events for the dual model.

To abbreviate the notation, we will henceforth say that $\mathbb{G}$ satisfies the RSW property if the random-cluster model on $\mathbb{G}$ with $\beta = 1$ satisfies this property. It will be easier to work with the crossing events defined above, rather than the one of the introduction, hence the following lemma.

Lemma 3.10. *Fix $\rho > 1$ and $\nu > 0$. Then, $\mathbb{G}$ has the RSW property if and only if there exists $\delta := \delta_1(\rho,\nu) > 0$ such that for all $n \geqslant 1$,*

$$\begin{aligned} &\varphi^0_{\mathsf{R}((\rho+\nu)n,(1+\nu)n)}\big[\mathcal{C}_h(\rho n;n)\big] \geqslant \delta, \qquad \varphi^1_{\mathsf{R}((\rho+\nu)n,(1+\nu)n)}\big[\mathcal{C}_h^*(\rho n;n)\big] \geqslant \delta,\\ &\varphi^0_{\mathsf{R}((1+\nu)n,(\rho+\nu)n)}\big[\mathcal{C}_v(n;\rho n)\big] \geqslant \delta, \qquad \varphi^1_{\mathsf{R}((1+\nu)n,(\rho+\nu)n)}\big[\mathcal{C}_v^*(n;\rho n)\big] \geqslant \delta. \end{aligned} \tag{BXP(ρ, ν))}$$

In other words, crossing estimates for Euclidean rectangles and rectangles in $\mathbb{G}^\diamond$ imply each other. Moreover, the aspect ratio ρ and distance νn to the boundary conditions is irrelevant; indeed it is a by-product of the lemma that the conditions (BXP(ρ, ν)) with different values of $\rho > 1$ and $\nu > 0$ are equivalent (obviously with different values for $\delta > 0$).

In general, one would also require crossing estimates as those of (BXP(ρ, ν)) for translates of the rectangles $\mathsf{R}(n;\rho n)$ and $\mathsf{R}(\rho n;n)$. This is irrelevant here due to periodicity.

The proof of the lemma is elementary. It emploies the quasi-isometry between Euclidean distance and the graph distance of $\mathbb{G}^\diamond$, the FKG inequality and the comparison between boundary conditions. A similar statement was proved in [GM14, Prop. 4.2] for Bernoulli percolation. Since the boundary conditions matter, additional care is needed here, and the proof is slightly more technical. Details are skipped here and are given in Appendix B.

It is straightforward (as will be seen in Section 3.3.4) that the RSW property implies the rest of the points of Theorem 3.1 for $1 \leqslant q \leqslant 4$. The following two sections will thus focus on proving the RSW property for isoradial square lattices (Section 3.3.2), then on general doubly-periodic isoradial graphs (Section 3.3.3), when $1 \leqslant q \leqslant 4$.

3.3.2 Isoradial square lattices

The relevant result for the first stage of the proof (the transfer from regular to arbitrary square lattices) is the following.

Proposition 3.11. *Let $\mathbb{G}^{(1)} = \mathbb{G}_{\alpha,\beta^{(1)}}$ and $\mathbb{G}^{(2)} = \mathbb{G}_{\alpha,\beta^{(2)}}$ be two isoradial square lattices in $\mathcal{G}(\varepsilon)$. If $\mathbb{G}^{(1)}$ satisfies the RSW property, then so does $\mathbb{G}^{(2)}$.*

The proposition is proved in the latter subsections of this section. For now, let us see how it implies the following corollary.

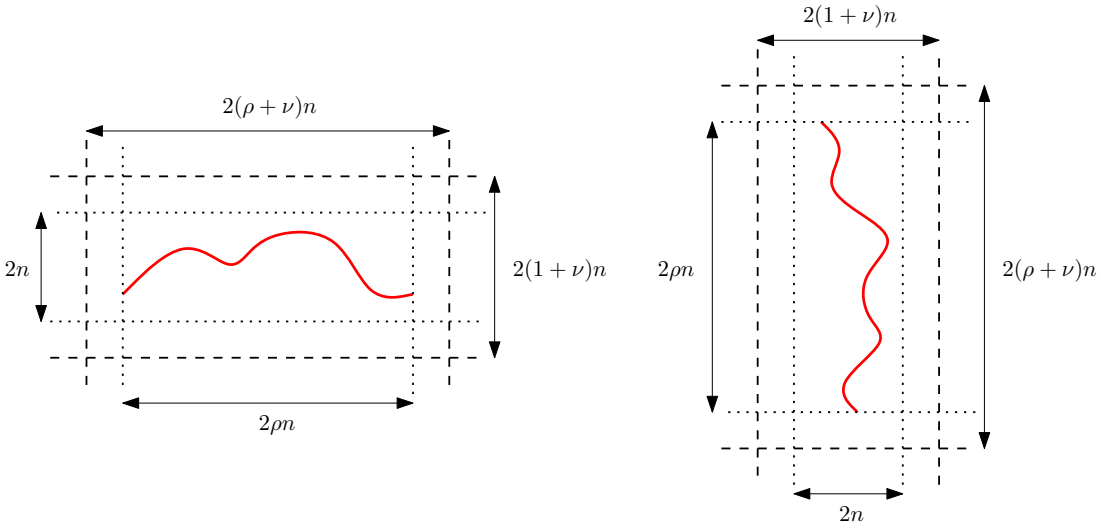

Figure 3.8 – Crossing events in the condition (BXP(ρ, ν)). The dotted lines represent the tracks enclosing the domain in which the event takes place, the dashed lines represent the domain in which the random-cluster measure is defined.

Corollary 3.12. *For any $1 \leqslant q \leqslant 4$ and any isoradial square lattice $\mathbb{G} \in \mathcal{G}(\varepsilon)$, $\mathbb{G}$ satisfies the RSW property.*

Proof of Corollary 3.12. For the regular square lattice $\mathbb{G}_{0,\frac{\pi}{2}}$, the random-cluster measure associated by isoradiality (see (2.2)) is that with edge-parameter $p_e = \frac{\sqrt{q}}{1+\sqrt{q}}$. It is then known by [DCST17] that $\mathbb{G}_{0,\frac{\pi}{2}}$ satisfies the RSW property.

It follows from the application of Proposition 3.11 that for any sequence $\boldsymbol{\beta} \in [\varepsilon, \pi-\varepsilon]^{\mathbb{Z}}$, the graph $\mathbb{G}_{0,\boldsymbol{\beta}}$ also satisfies the RSW property.

Let $\mathbb{G}_{\boldsymbol{\alpha},\boldsymbol{\beta}} \in \mathcal{G}(\varepsilon)$ be an isoradial square lattice. Below β_0 stands for the constant sequence equal to β_0. Then, $\mathbb{G}_{\boldsymbol{\alpha},\beta_0}$ is the rotation by β_0 of the graph $\mathbb{G}_{0,\widetilde{\boldsymbol{\alpha}}-\beta_0+\pi}$, where $\widetilde{\boldsymbol{\alpha}}$ is the sequence $\boldsymbol{\alpha}$ with reversed order. By the previous point, $\mathbb{G}_{0,\widetilde{\boldsymbol{\alpha}}-\beta_0+\pi}$ satisfies the RSW property, and hence so does $\mathbb{G}_{\boldsymbol{\alpha},\beta_0}$. Finally, apply again Proposition 3.11 to conclude that $\mathbb{G}_{\boldsymbol{\alpha},\boldsymbol{\beta}}$ also satisfies the RSW property. □

The rest of the section is dedicated to proving Proposition 3.11.

3.3.2.1 RSW: an alternative definition

Fix an isoradial square lattice $\mathbb{G} = \mathbb{G}_{\boldsymbol{\alpha},\boldsymbol{\beta}} \in \mathcal{G}(\varepsilon)$ for some $\varepsilon > 0$. Recall that $q \in [1,4]$ is fixed; the estimates below depend only on q and ε. Let $x_{i,j}$ be the vertex of $\mathbb{G}^\diamond$ between tracks s_{i-1}, s_i and t_{j-1}, t_j. Suppose that $\mathbb{G}$ is such that its vertices are those $x_{i,j}$ with $i+j$ even. The base of $\mathbb{G}$ is then the set $\{(x_{i,0} : i \in \mathbb{Z}\}$. Moreover, $\mathbb{G}$ is translated so that $x_{0,0}$ is the origin 0 of the plane.

Define $\mathcal{C}(m_1, m_2; n)$ to be the event that there exists an open (primal) circuit contained in $\mathsf{R}(m_2; n)$ that surrounds the segment of the base between vertices $x_{-m_1,0}$ and $x_{m_1,0}$ [1]. Write $\mathcal{C}^*(.,.;.)$ for the same event for the dual model. See figure 3.9 for an illustration.

[1] Formally, we allow the circuit to visit vertices of the base, but it is not allowed to cross the base between $x_{-m_1,0}$ and $x_{m_1,0}$.

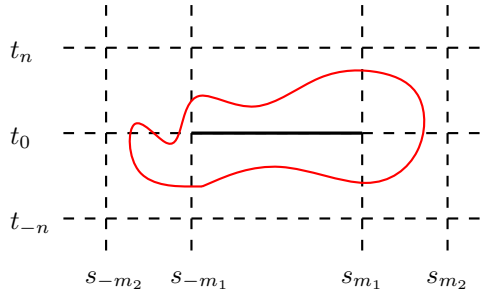

Figure 3.9 – The event $\mathcal{C}(m_1, m_2; n)$. Such a circuit should not cross the bold segment.

The following two results offer a convenient criterion for the RSW property. The advantage of the conditions of (3.2) is that they are easily transported between different isoradial square lattices, unlike those of (BXP(ρ, ν)). The main reason is that, due to the last case of Figure 2.10, paths may shrink at their endpoints during star-triangle transformations. Circuits avoid this problem.

Lemma 3.13. *Suppose $\mathbb{G}$ is as above and suppose that the following conditions hold. There exists $\delta_v > 0$ such that for any $\delta_h > 0$, there exist constants $a \geqslant 3$ and $b > 3a$ such that for all n large enough, there exist boundary conditions ξ on $\Lambda(bn)$ such that*

$$\begin{aligned} \varphi^{\xi}_{\Lambda(bn)}\big[\mathcal{C}(3an, bn; bn)\big] \geqslant 1-\delta_h \quad \text{and} \quad \varphi^{\xi}_{\Lambda(bn)}\big[\mathcal{C}^*(3an, bn; bn)\big] \geqslant 1-\delta_h, \\ \varphi^{\xi}_{\Lambda(bn)}\big[\mathcal{C}_v(an; 2n)\big] \geqslant \delta_v \quad \text{and} \quad \varphi^{\xi}_{\Lambda(bn)}\big[\mathcal{C}^*_v(an; 2n)\big] \geqslant \delta_v, \\ \varphi^{\xi}_{\Lambda(bn)}\big[\mathcal{C}(an, 3an; n)\big] \geqslant \delta_v \quad \text{and} \quad \varphi^{\xi}_{\Lambda(bn)}\big[\mathcal{C}^*(an, 3an; n)\big] \geqslant \delta_v. \end{aligned} \tag{3.2}$$

Then $\mathbb{G}$ has the RSW property.

Let us mention that the boundary conditions ξ above may be random, in which case $\varphi^{\xi}_{\Lambda(bn)}$ is simply an average of random-cluster measures with different fixed boundary conditions. The only important requirement is that they are the same for all the bounds.

Again, if we were to consider also non-periodic graphs $\mathbb{G}$, we would require (3.2) also for all translates of the events above.

The conditions of the lemma above should be understood as follows. The last two lines effectively offer lower bounds for the probabilities of vertical and horizontal crossings of certain rectangles. For Bernoulli percolation, these estimates alone would suffice to prove the RSW property; for the random-cluster model however, boundary conditions come into play. The first line is then used to shield the crossing events from any potentially favorable boundary conditions. Notice that the fact that $\delta_v > 0$ is fixed and δ_h may be taken arbitrarily small ensures that events such as those estimated in the first and second (or third) lines must occur simultaneously with positive probability. This is the key to the proof.

Even though the proof is standard (and may be skipped by those familiar with the RSW techniques for the random-cluster measure), we present it below.

Proof. Suppose to start that the condition (3.2) is satisfied. Let $\delta_v > 0$ be fixed. Choose $\delta_h \leqslant \delta_v/2$. Fix a, b as given by the condition. Then, for n large enough, by assumption and the inclusion-exclusion formula, there exists ξ such that

$$\varphi^{\xi}_{\Lambda(bn)}\big[\mathcal{C}^*(3an, bn; bn) \cap \mathcal{C}_v(an; 2n)\big] \geqslant \delta_v - \delta_h \geqslant \delta_h.$$

Notice that the vertical path defining $\mathcal{C}_v(an;2n)$ is necessarily inside the dual circuit defining $C^*(3an,bn;bn)$, since the two may not intersect. Also, notice that $\mathcal{C}_v(an;2n)$ induces a vertical crossing of $\mathsf{R}(an;2n)$. Thus, we can use the following exploration argument to compare boundary conditions.

For a configuration ω, define $\Gamma^*(\omega)$ to be the outmost dually-open circuit as in the definition of $C^*(3an,bn;bn)$ if such a circuit exists. Let $\mathrm{Int}(\Gamma^*)$ be the region surrounded by Γ^*, seen as a subgraph of $\mathbb{G}$. We note that Γ^* can be explored from the outside and as a consequence, the random-cluster measure in $\mathrm{Int}(\Gamma^*)$, conditionally on Γ^*, is given by $\varphi^0_{\mathrm{Int}(\Gamma^*)}$. Thus,

$$\begin{aligned}
\varphi^{\xi}_{\Lambda(bn)}\big[C^*(3an,bn;bn)\cap\mathcal{C}_v(an;2n)\big] &= \sum_{\gamma^*}\varphi^{\xi}_{\Lambda(bn)}\big[\mathcal{C}_v(an;2n)\,\big|\,\Gamma^*=\gamma^*\big]\varphi^{\xi}_{\Lambda(bn)}\big[\Gamma^*=\gamma^*\big]\\
&= \sum_{\gamma^*}\varphi^{0}_{\mathrm{Int}(\Gamma^*)}\big[\mathcal{C}_v(an;2n)\big]\varphi^{\xi}_{\Lambda(bn)}\big[\Gamma^*=\gamma^*\big]\\
&\leqslant \sum_{\gamma^*}\varphi^{0}_{\Lambda(bn)}\big[\mathcal{C}_v(an;2n)\big]\varphi^{\xi}_{\Lambda(bn)}\big[\Gamma^*=\gamma^*\big]\\
&\leqslant \varphi^{0}_{\Lambda(bn)}\big[\mathcal{C}_v(an;2n)\big],
\end{aligned}$$

where the summations are over all possible realisations γ^* of Γ^*. The first inequality is based on the comparison between boundary conditions and on the fact that $\mathrm{Int}(\gamma^*)\subset\Lambda(bn)$ for all γ^*. Hence, we deduce that,

$$\varphi^{0}_{\Lambda(bn)}\big[\mathcal{C}_v(an;2n)\big]\geqslant\delta_h.$$

Similarly, observe that

$$\varphi^{\xi}_{\Lambda(bn)}\big[C^*(3an,bn;bn)\cap\mathcal{C}(an,3an;n)\big]\geqslant\delta_h.$$

Again, the circuit defining $\mathcal{C}(an,3an;n)$ is necessarily inside the dual circuit defining $C^*(3an,bn;bn)$ and it therefore induces a horizontal crossing of $\mathsf{R}(an;n)$. Using the same exploration argument as above, we deduce that

$$\varphi^{0}_{\Lambda(bn)}\big[\mathcal{C}_h(an;n)\big]\geqslant\delta_h. \tag{3.3}$$

The same may be performed for the dual model. Since these computations hold for arbitrary n large enough, we obtain for all $n\geqslant 1$

$$\begin{aligned}
&\varphi^{0}_{\Lambda(bn)}\big[\mathcal{C}_v(an;2n)\big]\geqslant\delta_h, \qquad \varphi^{0}_{\Lambda(bn)}\big[\mathcal{C}_h(an;n)\big]\geqslant\delta_h \qquad \text{and}\\
&\varphi^{1}_{\Lambda(bn)}\big[\mathcal{C}^*_v(an;2n)\big]\geqslant\delta_h, \qquad \varphi^{1}_{\Lambda(bn)}\big[\mathcal{C}^*_h(an;n)\big]\geqslant\delta_h.
\end{aligned}$$

We claim that (BXP(ρ, ν)) follows from the above. Indeed, the inequalities above for horizontal crossing are of the desired form. However, vertical crossings are only bounded for short and potentially wide rectangles. Notice however that, by combining crossings as in Figure 3.10 and using the FKG inequality,

$$\varphi^{0}_{\Lambda(abn)}\big[\mathcal{C}_v(an;a^2n)\big]\geqslant\varphi^{0}_{\Lambda(bn)}\big[\mathcal{C}_v(an;2n)\big]^{a^2-1}\varphi^{0}_{\Lambda(bn)}\big[\mathcal{C}_h(an;n)\big]^{a^2-1}\geqslant\delta_h^{2a^2-2} \tag{3.4}$$

Equations (3.3) and (3.4) imply (BXP(ρ, ν)) with $\rho=a$ and $\nu=a(b-a)$, and Lemma 3.10 may be used to conclude. □

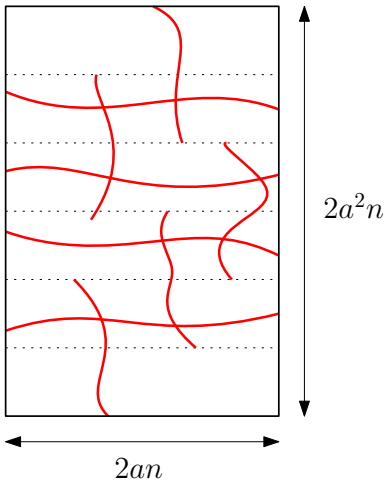

Figure 3.10 – A vertical crossing in $\mathsf{R}(an; a^2n)$ created by superimposing shorter vertical and horizontal crossings. The distance between two consecutive horizontal dotted lines is $2n$.

As the next lemma suggests, condition (3.2) is actually equivalent to the RSW property. The following statement may be viewed as a converse to Lemma 3.13.

Lemma 3.14. *Assume that $\mathbb{G}$ has the RSW property. Fix $a > 1$. Then, there exists $\delta_v > 0$ such that for any $\delta_h > 0$, there exist $b > 3a$ such that for all n large enough, the following condition holds,*

$$\begin{aligned} \varphi^0_{\Lambda(bn)}\Big[\mathcal{C}(3an, bn; bn)\Big] &\geqslant 1 - \delta_h/2 \quad \text{and} \quad \varphi^1_{\Lambda(bn)}\Big[\mathcal{C}^*(3an, bn; bn)\Big] \geqslant 1 - \delta_h/2, \\ \varphi^0_{\Lambda(bn)}\Big[\mathcal{C}_v(\tfrac{an}{2}; \tfrac{an}{2})\Big] &\geqslant 2\delta_v \quad \text{and} \quad \varphi^1_{\Lambda(bn)}\Big[\mathcal{C}^*_v(\tfrac{an}{2}; \tfrac{an}{2})\Big] \geqslant 2\delta_v, \\ \varphi^0_{\Lambda(bn)}\Big[\mathcal{C}(an, 2an; \tfrac{n}{a})\Big] &\geqslant 2\delta_v \quad \text{and} \quad \varphi^1_{\Lambda(bn)}\Big[\mathcal{C}^*(an, 2an; \tfrac{n}{a})\Big] \geqslant 2\delta_v. \end{aligned} \tag{3.5}$$

The proof is a standard application of the RSW theory and is deferred to Appendix B. Let us only mention that it uses the fact that

$$\varphi^0_{\Lambda(bn)}\Big[\mathcal{C}(3an, bn; bn)\Big] \xrightarrow[b\to\infty]{} 1, \qquad \text{uniformly in } n.$$

This is a typical consequence of the *strong* RSW property; it appears in other forms in various applications.

3.3.2.2 Transporting RSW: proof of Proposition 3.11

Fix $\mathbb{G}^{(1)} = \mathbb{G}_{\alpha,\beta^{(1)}}$ and $\mathbb{G}^{(2)} = \mathbb{G}_{\alpha,\beta^{(2)}}$ two isoradial square lattices in $\mathcal{G}(\varepsilon)$. Suppose $\mathbb{G}^{(1)}$ satisfies the RSW property.

Let G_{mix} be the symmetric mixed graph of $\mathbb{G}^{(1)}$ and $\mathbb{G}^{(2)}$ constructed in Section 3.2.1, where the width of each strip is $2M + 1$ and the height is $N = N_1 = N_2$ (for M and N to be mentioned below). We use here the construction both above and below the base, where each side is convexified separately. Let $\widetilde{G}_{\text{mix}} = \Sigma^{\uparrow}(G_{\text{mix}}) = \Sigma^{\downarrow}(G_{\text{mix}})$ be the graph obtained after exchanging the tracks $t_0, \dots, t_N$ of G_{mix} with $t_{N+1}, \dots, t_{2N+1}$ and $t_{-1}, \dots, t_{-N}$ with $t_{-(N+1)}, \dots, t_{-2N}$. Write $\varphi_{G_{\text{mix}}}$ and $\varphi_{\widetilde{G}_{\text{mix}}}$ for the random-cluster measures on G_{mix} and $\widetilde{G}_{\text{mix}}$, respectively, with parameters $q \in [1, 4]$, $\beta = 1$ and free boundary conditions.

The estimates below are the key to the proof of Proposition 3.11. They correspond to similar statements in [GM14] for Bernoulli percolation.

Proposition 3.15 (Prop. 6.4 of [GM14]). *There exist $\lambda, n_0 > 1$, depending on ε only, such that, for all $\rho_{out} > \rho_{in} > 0$, $n \geqslant n_0$ and sizes $M \geqslant (\rho_{out} + \lambda)n$ and $N \geqslant \lambda n$,*

$$\varphi_{\widetilde{G}_{mix}}\Big[\mathcal{C}(\rho_{in}n, (\rho_{out}+\lambda)n; \lambda n)\Big] \geqslant (1 - \rho_{out}e^{-n})\varphi_{G_{mix}}\Big[\mathcal{C}(\rho_{in}n, \rho_{out}n; n)\Big].$$

Proposition 3.16 (Prop. 6.8 of [GM14]). *There exist $\delta \in (0, \frac{1}{2})$ and $c_n > 0$ satisfying $c_n \to 1$ as $n \to \infty$ such that, for all n and sizes $M \geqslant 4n$ and $N \geqslant n$,*

$$\varphi_{\widetilde{G}_{mix}}\Big[\mathcal{C}_v(4n; \delta n)\Big] \geqslant c_n \varphi_{G_{mix}}\Big[\mathcal{C}_v(n; n)\Big].$$

The proofs of the two statements are similar to those of [GM14]. They do not rely on the independence of the percolation measure, they do however use crucially the independence of the randomness appearing in the star-triangle transformations. More details about this step are given in Section 4.3 when we will treat the quantum case, since more explicit estimates will be needed. However, we will not provide full proofs since they are very similar to the corresponding statements in [GM14].

Let us admit the two propositions above for now and finish the proof of Proposition 3.11.

Proof of Proposition 3.11. Fix parameters $n_0, \lambda > 1$ and $\delta > 0$ as in Propositions 3.15 and 3.16. Since $\mathbb{G}^{(1)}$ satisfies the RSW property, Lemma 3.14 applies to it. Choose $a = \max\{\lambda, \frac{2}{\delta}, 1\}$ and an arbitrary $\delta_h > 0$. By Lemma 3.14, there exist $b > 3a$ and $\delta_v > 0$ such that, for all n large enough,

$$\begin{aligned}
&\varphi^0_{\Lambda(bn)}\Big[\mathcal{C}(3an, bn; bn)\Big] \geqslant 1 - \delta_h/2,\\
&\varphi^0_{\Lambda(bn)}\Big[\mathcal{C}_v(\tfrac{an}{2}; \tfrac{an}{2})\Big] \geqslant 2\delta_v,\\
&\varphi^0_{\Lambda(bn)}\Big[\mathcal{C}(an, 2an; \tfrac{n}{a})\Big] \geqslant 2\delta_v.
\end{aligned} \tag{3.6}$$

We will prove that $\mathbb{G}^{(2)}$ satisfies (3.2) for these values of a, δ_v and δ_h, with b replaced by $\widetilde{b} = (1+\lambda)b$. The boundary conditions ξ will be fixed below. We start by proving (3.2) for the primal events.

Take $M = N \geqslant (\lambda+1)bn$ for constructing G_{mix}. Then, since the balls of radius bn in G_{mix} and in $\mathbb{G}^{(1)}$ are identical, we deduce from the above that

$$\begin{aligned}
&\varphi_{G_{\text{mix}}}\Big[\mathcal{C}(3an, bn; bn)\Big] \geqslant 1 - \delta_h/2,\\
&\varphi_{G_{\text{mix}}}\Big[\mathcal{C}_v(\tfrac{an}{2}; \tfrac{an}{2})\Big] \geqslant 2\delta_v,\\
&\varphi_{G_{\text{mix}}}\Big[\mathcal{C}(an, 2an; \tfrac{n}{a})\Big] \geqslant 2\delta_v.
\end{aligned}$$

We used here that the boundary conditions on $\Lambda(bn)$ in (3.6) are the least favorable for the existence of open paths.

For $n \geqslant an_0$, Propositions 3.15 and 3.16 then imply

$$\begin{aligned}
&\varphi_{\widetilde{G}_{\text{mix}}}\Big[\mathcal{C}(3an, (\lambda+1)bn; \lambda bn)\Big] \geqslant (1 - e^{-bn})(1 - \delta_h/2),\\
&\varphi_{\widetilde{G}_{\text{mix}}}\Big[\mathcal{C}_v(an; \tfrac{\delta}{2}an)\Big] \geqslant 2c_n\delta_v,\\
&\varphi_{\widetilde{G}_{\text{mix}}}\Big[\mathcal{C}(an, (2a + \tfrac{\lambda}{a})n; \tfrac{\lambda}{a}n)\Big] \geqslant 2(1 - 2a^2e^{-n/a})\delta_v.
\end{aligned}$$

Now, take n large enough so that $2e^{-bn} < \delta_h$, $2c_n > 1$ and $a^2e^{-n/a} < 1/4$. These bounds ultimately depend on ε only. Observe that this implies (3.2) for the primal model. Indeed, set

$\widetilde{b} = (\lambda+1)b$, then, due to the choice of a,

$$\varphi_{\widetilde{G}_{\mathrm{mix}}}\Big[\mathcal{C}(3an, \widetilde{b}n; \widetilde{b}n)\Big] \geqslant (1-\delta_h/2)^2 \geqslant 1-\delta_h,$$
$$\varphi_{\widetilde{G}_{\mathrm{mix}}}\Big[\mathcal{C}_v(an; n)\Big] \geqslant \delta_v,$$
$$\varphi_{\widetilde{G}_{\mathrm{mix}}}\Big[\mathcal{C}(an, 3an; n)\Big] \geqslant \delta_v.$$

The same procedure may be applied for the dual model to obtain the identical bounds for $\mathcal{C}^*(.,.;,)$ and $\mathcal{C}^*_v(.;.)$.

By choice of M and N, the region $\Lambda(\widetilde{b}n)$ of $\widetilde{G}_{\mathrm{mix}}$ is also a subgraph of $\mathbb{G}^{(2)}$. This implies (3.2) for $\mathbb{G}^{(2)}$. The boundary conditions ξ appearing in (3.2) are those induced on $\Lambda(\widetilde{b}n)$ by the free boundary conditions on $\widetilde{G}_{\mathrm{mix}}$. These are random boundary conditions, but do not depend on the events under study. In particular, they are the same for all the six bounds of (3.2). □

3.3.2.3 Sketch of proof for Propositions 3.15 and 3.16

The proofs of Propositions 3.15 and 3.16 are very similar to those of Propositions 6.4 and 6.8 in [GM14], with only minor differences. Nevertheless, we sketch them below for completeness. The estimates in the proofs are specific to the random-cluster model and will be important in Chapter 4.

We keep the notations G_{mix} and $\widetilde{G}_{\mathrm{mix}}$ introduced in the previous section.

Proof of Proposition 3.15. We adapt the proof from Proposition 6.4 (more precisely, Lemma 6.7) of [GM14] to our case.

Recall the definition of $\Sigma^{\downarrow}$, the sequence of star-triangle transformations to consider here: above the base level, we push down tracks of $\mathbb{G}^{(2)}$ below those of $\mathbb{G}^{(1)}$ one by one, from the bottom-most to the top-most; below the base level, we proceed symmetrically. Let $\mathbb{P}$ be a probability measure defined as follows. Pick a configuration ω on G_{mix} according to $\varphi_{G_{\mathrm{mix}}}$; apply the sequence of star-triangle transformations $\Sigma^{\downarrow}$ to it using the coupling described in Figure 2.8, where the randomness potentially appearing in each transformation is independent of ω and of all other transformations. Thus, under $\mathbb{P}$ we dispose of configurations on all intermediate graphs in the transformation from G_{mix} to $\widetilde{G}_{\mathrm{mix}}$. Moreover, in light of Proposition 2.12, $\Sigma^{\downarrow}(\omega)$ has law $\varphi_{\widetilde{G}_{\mathrm{mix}}}$.

We will prove the following statement

$$\mathbb{P}\Big[\Sigma^{\downarrow}(\omega) \in \mathcal{C}(\rho_{\mathrm{in}}n, (\rho_{\mathrm{out}}+\lambda)n; \lambda n) \,\Big|\, \omega \in \mathcal{C}(\rho_{\mathrm{in}}n, \rho_{\mathrm{out}}n; n)\Big] \geqslant 1-\rho_{\mathrm{out}}e^{-n}, \tag{3.7}$$

for any values $\rho_{\mathrm{out}} > \rho_{\mathrm{in}} > 0$, $n \geqslant n_0$, $M \geqslant (\rho_{\mathrm{out}}+\lambda)n$ and $N \geqslant \lambda n$, where $\lambda, n_0 > 1$ will be chosen below. This readily implies Proposition 3.15.

Fix $\rho_{\mathrm{out}}, \rho_{\mathrm{in}}, n, M$ and N as above. Choose $\omega_0 \in \mathcal{C}(\rho_{\mathrm{in}}n, \rho_{\mathrm{out}}n; n)$ and let γ be an ω_0-open circuit as in the definition of $\mathcal{C}(\rho_{\mathrm{in}}n, \rho_{\mathrm{out}}n; n)$. As the transformations of $\Sigma^{\downarrow} = \sigma_K \circ \cdots \circ \sigma_1$ are applied to ω_0, the circuit γ is transformed along with ω_0. Thus, for each $0 \leqslant k \leqslant K$, $(\sigma_k \circ \cdots \circ \sigma_1)(\gamma)$ is an open path in $(\sigma_k \circ \cdots \circ \sigma_1)(\omega_0)$ on the graph $(\sigma_k \circ \cdots \circ \sigma_1)(G_{\mathrm{mix}})$.

Since no star-triangle transformation of $\Sigma^{\downarrow}$ affects the base, $\Sigma^{\downarrow}(\gamma)$ remains a circuit surrounding the segment of the base between $x_{-\rho_{\mathrm{in}}n,0}$ and $x_{\rho_{\mathrm{in}}n,0}$. Therefore, the only thing that is left to prove is that

$$\mathbb{P}\Big[\Sigma^{\downarrow}(\gamma) \in R\Big((\rho_{\mathrm{out}}+\lambda)n; \lambda n\Big) \,\Big|\, \omega = \omega_0\Big] \geqslant 1-\rho_{\mathrm{out}}e^{-n}. \tag{3.8}$$

Set

$$\gamma^{(k)} = (\Sigma^{\downarrow}_{N_1+k} \circ \Sigma^{\downarrow}_{-(N_1+k)}) \circ \cdots \circ (\Sigma^{\downarrow}_{N_1+1} \circ \Sigma^{\downarrow}_{-(N_1+1)}),$$

where $\Sigma^{\downarrow}_i = \Sigma_{t_0,t_i} \circ \cdots \circ \Sigma_{t_{N_1},t_i}$ for $i \geqslant 0$ and $\Sigma^{\downarrow}_i = \Sigma_{t_{-1},t_i} \circ \cdots \circ \Sigma_{t_{-N_1},t_i}$ for $i < 0$. The path $\gamma^{(k)}$ thus defined is the transformation of γ after the first k tracks of $\mathbb{G}^{(2)}$ above the base were sent down, and the symmetric procedure was applied below the base.

In [GM14], the vertices of G_{mix} visited by $\gamma^{(k)}$ were shown to be contained in a region whose evolution with $k = 0, \dots, N_2 + 1$ is explicit. This is done separately above and below the base level, and we focus next on the upper half-space.

Let $H^0 = \{(i,j) \in \mathbb{Z} \times \mathbb{N} : -(\rho_{\text{out}} + 1)n \leqslant i - j \text{ and } i + j \leqslant (\rho_{\text{out}} + 1)n \text{ and } j \leqslant n\}$. Then, H^{k+1} is defined from H^k as follows. If $(i,j) \in \mathbb{Z} \times \mathbb{N}$ is such that $(i,j), (i-1,j)$ or $(i+1,j)$ are in H^k, then $(i,j) \in H^{k+1}$. Otherwise, if $(i,j-1) \in H^k$, then (i,j) is included in H^k with probability $\eta \in (0,1)$, independently of all previous choices. We will see later how the value of η is chosen using the bounded-angles property.

In consequence, the sets $(H^k)_{0 \leqslant k \leqslant N}$ are interpreted as a growing pile of sand, with a number of particles above every $i \in \mathbb{Z}$. At each stage of the evolution, the pile grows laterally by one unit in each direction; additionally, each column of the pile may increase vertically by one unit with probability η (see Figure 3.11).

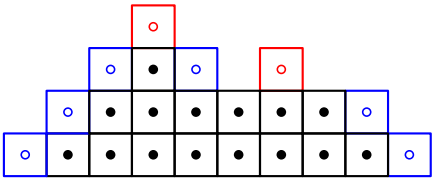

Figure 3.11 – One step of the evolution of H: H^k is drawn in black, H^{k+1} contains the additional blue points (since they are to the left or right of vertices in H^k) and the red points (these are added due to the random increases in height).

Loosely speaking, [GM14, Lem. 6.6] shows that, if η is chosen well, then all vertices $x_{i,j}$ visited by $\gamma^{(k)}$ have $(i,j) \in H^k$ [2]. More precisely, the process $(H^k)_{0 \leqslant k \leqslant N}$ may be coupled with the evolution of $(\gamma^{(k)})_{0 \leqslant k \leqslant N}$ so that the above is true. This step is proved by induction on k, and relies solely on the independence of the star-triangle transformations and on the estimates of Figure 3.5. Then, (3.8) is implied by the following bound on the maximal height of H^N:

$$\mathbb{P}\Big[\max\{j : (i,j) \in H^{\lambda n}\} \geqslant \lambda n\Big] < \rho_{\text{out}} e^{-n} \tag{3.9}$$

for some $\lambda > 0$ and all n large enough. The existence of such a (finite) constant λ is guaranteed by [GM13a, Lem. 3.11]. It depends on η, and precisely on the fact that $\eta < 1$ [GM14, Lem. 6.7]. The choice of $\eta < 1$ that allows the domination of $(\gamma^{(k)})_{0 \leqslant k \leqslant N}$ by $(H^k)_{0 \leqslant k \leqslant N}$ is done as follows.

We proceed in the same way as in the proofs of Lemmas 6.6 and 6.7 of [GM14]. We shall analyze the increase in height of portions of $\gamma^{(k)}$ as given by Figure 3.5. Essentially, the only cases in which $\gamma^{(k)}$ increases significantly in height are depicted in the third and the last line of Figure 3.5.

[2] This is not actually true, since there is a horizontal shift to be taken into account; let us ignore this technical detail here.

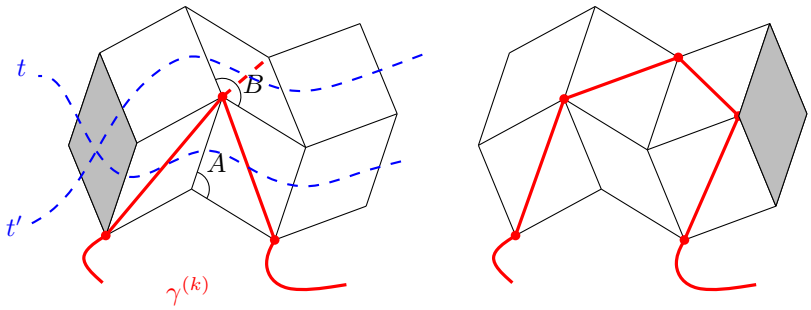

Figure 3.12 – Star-triangle transformations between tracks t and t' corresponding to the third line of Figure 3.5. The tracks t and t' have transverse angles A and B respectively. We assume that a portion of the path $\gamma^{(k)}$ reaches between the tracks t and t' as shown in the figure. Moreover, if the dashed edge is open on the left, with probability $\eta_{A,B} = y_{\pi-A}y_{\pi-(B-A)}/q$, the path $\gamma^{(k)}$ drifts upwards by 1 after the track exchange.

Let us examine the situation which appears in the third line of Figure 3.5 and consider the notations as in Figure 3.12. Using the notation of Figure 3.12 for the angles A and B, the probability that the height of such a $\gamma^{(k)}$ increases by 1 is given by

$$\begin{aligned}\eta_{A,B} &= \frac{y_{\pi-A}y_{\pi-(B-A)}}{q} = \frac{\sin(rA)\sin(r(B-A))}{\sin(r(\pi-A))\sin(r(\pi-(B-A)))} \\ &= \frac{\cos(r(2A-B))-\cos(rB)}{\cos(r(2A-B))-\cos(r(2\pi-B))},\end{aligned}$$

where we recall that $r = \cos^{-1}(\frac{\sqrt{q}}{2}) \leqslant \frac{1}{3}$ and that, due to the $BAP(\varepsilon)$, $A, B \in [\varepsilon, \pi-\varepsilon]$.

The same computation also applies to the last line of Figure 3.5. Then, η may be chosen as

$$\eta := \sup_{A,B\in[\varepsilon,\pi-\varepsilon]} \eta_{A,B} < 1. \tag{3.10}$$

The domination of the set of vertices of $\gamma^{(k)}$ by H^k is therefore valid for this value of η, and (3.8) is proved for the resulting constant λ.

□

Remark 3.17. When we deal with the quantum model in Chapter 4, it will be important to have a more precise estimate on $\eta(\varepsilon)$. In particular, we will show that, in this special case, $1-\eta(\varepsilon) \sim \tau(q)\varepsilon$ as $\varepsilon \to 0$ for some constant $\tau := \tau(q)$ depending only on $q \in [1,4]$.

Proof of Proposition 3.16. We adapt Proposition 6.8 of [GM14] to our case. Fix n and $N, M \geqslant 2n$, and consider the graph G_{mix} as described in the previous section. We recall the definition of $\Sigma^{\uparrow}$, the sequence of star-triangle transformations we consider here: above the base level, we pull up tracks of $\mathbb{G}^{(1)}$ above those of $\mathbb{G}^{(2)}$ one by one, from the top-most to the bottom-most; below the base level, we proceed symmetrically.

As in the previous proof, write $\mathbb{P}$ for the measure taking into account the choice of a configuration ω_0 according to the random-cluster measure $\varphi_{G_{\text{mix}}}$ as well as the results of the star-triangle transformations in $\Sigma^{\uparrow}$ applied to the configuration ω_0.

The events we are interested in only depend on the graph above the base level, hence we are not concerned with what happens below. For $0 \leqslant i \leqslant N$, recall from Section 3.2.1 the

notation

$$\Sigma_i^{\uparrow} = \Sigma_{t_i,t_{2N+1}} \circ \cdots \circ \Sigma_{t_i,t_{N+1}},$$

for the sequence of star-triangle transformations moving the track t_i of $\mathbb{G}^{(1)}$ above $\mathbb{G}^{(2)}$. Then $\Sigma^{\uparrow} = \Sigma_0^{\uparrow} \circ \cdots \circ \Sigma_N^{\uparrow}$.

First, note that if $\omega \in \mathcal{C}_v(n;n)$, we also have $\Sigma_{n+1}^{\uparrow} \circ \cdots \circ \Sigma_N^{\uparrow}(\omega) \in \mathcal{C}_v(n;n)$, since the two configurations are identical between the base and t_n. We will now write, for $0 \leqslant k \leqslant n+1$,

$$\begin{aligned}
G^k &= \Sigma_{n-k+1}^{\uparrow} \circ \cdots \circ \Sigma_N^{\uparrow}(G_{\mathrm{mix}}),\\
\omega^k &= \Sigma_{n-k+1}^{\uparrow} \circ \cdots \circ \Sigma_N^{\uparrow}(\omega),\\
D^k &= \{x_{u,v} \in G^k : |u| \leqslant n+2k+v, 0 \leqslant v \leqslant N+n\},\\
h^k &= \sup\{h \leqslant N : \exists u, v \in \mathbb{Z} \text{ with } x_{u,0} \xleftrightarrow{D^k,\omega^k} x_{v,h}\}.
\end{aligned}$$

That is, h^k is the highest level that may be reached by an ω^k-open path lying in the trapezoid D^k. We note that $G^{n+1} = \widetilde{G}_{\mathrm{mix}}$ and ω^{n+1} follows the law of $\varphi_{\widetilde{G}_{\mathrm{mix}}}$.

With these notations, in order to prove Proposition 3.16, it suffices to show the equivalent of [GM14, (6.23)], that is

$$\mathbb{P}\Big[h^{n+1} \geqslant \delta n\Big] \geqslant c_n \mathbb{P}\Big[h^0 \geqslant n\Big], \tag{3.11}$$

for some $\delta \in (0, \frac{1}{2})$ to be specified below and explicit constants c_n with $c_n \to 1$ as $n \to \infty$. Indeed,

$$\mathbb{P}[h^0 \geqslant n] \geqslant \mathbb{P}[\omega^0 \in \mathcal{C}_v(n;n)] = \varphi_{G_{\mathrm{mix}}}[\mathcal{C}_v(n;n)].$$

Moreover, if $h^{n+1} \geqslant \delta n$, then $\omega^{n+1} \in \mathcal{C}_v(4n;\delta n)$, and therefore we have $\varphi_{\widetilde{G}_{\mathrm{mix}}}[\mathcal{C}_v(4n;\delta n)] \geqslant \mathbb{P}(h^{n+1} \geqslant \delta n)$.

We may now focus on proving (3.11). To do that, we adapt the corresponding step of [GM14] (namely Lemma 6.9). It shows that $(h^k)_{0\leqslant k\leqslant n}$ can be bounded stochastically from below by the Markov process $(H^k)_{0\leqslant k\leqslant n}$ [3] given by

$$H^k = H^0 + \sum_{i=1}^{k} \Delta_i, \tag{3.12}$$

where $H^0 = n$ and the Δ_i are independent random variables with common distribution

$$\mathbb{P}(\Delta = 0) = 2\delta, \quad \mathbb{P}(\Delta = -1) = 1 - 2\delta, \tag{3.13}$$

for some parameter δ to be specified later. Once the above domination is proved, the inequality (3.11) follows by the law of large numbers.

The proof of (3.13) in [GM14] (see Equation (6.24) there) uses only the independence between different star-triangle transformations and the finite-energy property of the model. Both are valid in our setting. We sketch this below.

Fix $0 \leqslant k \leqslant n$ and let us analyse the $(N-(n-k)+1)^{th}$ step of $\Sigma^{\uparrow}$, that is $\Sigma_{n-k}^{\uparrow}$. Write $\Psi_j := \Sigma_{t_{n-k},t_{N+j}} \circ \cdots \circ \Sigma_{t_{n-k},t_{N+1}}$ for $0 \leqslant j \leqslant N$. In other words, Ψ_j is the sequence of star-triangle transformations that applies to G^k and moves the track t_{n-k} above j tracks of $\mathbb{G}^{(2)}$, namely $t_{N+1}, \ldots, t_{N+j}$. Moreover, $\Psi_N = \Sigma_{n-k}^{\uparrow}$; hence, $\Psi_N(G^k) = G^{k+1}$.

[3] To be precise, it is shown that for any k, the law of h_k dominates that of H^k. It is not true that the law of the whole process $(h^k)_{0\leqslant k\leqslant n}$ dominates that of $(H^k)_{0\leqslant k\leqslant n}$. This step uses [GM13a, Lem. 3.7].

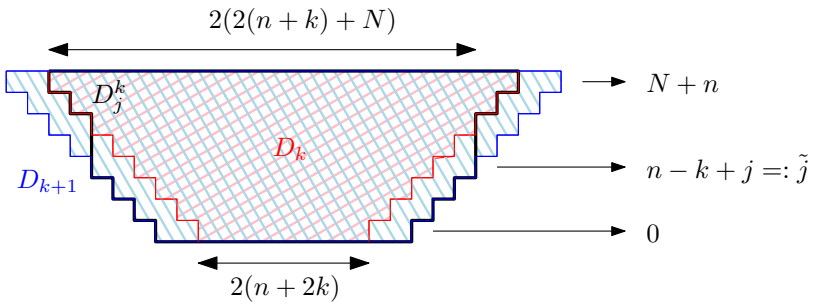

Figure 3.13 – The evolution of D^k (red) to D^{k+1} (blue) via intermediate steps D_j^k (black).

Let D_j^k be the subgraph of $\Psi_j(G^k)$ induced by vertices $x_{u,v}$ with $0 \leqslant v \leqslant N+n$ and

$$|u| \leqslant \begin{cases} n+2k+v+2 & \text{if } v \leqslant \widetilde{j}, \\ n+2k+v+1 & \text{if } v = \widetilde{j}+1, \\ n+2k+v & \text{if } v \geqslant \widetilde{j}+2. \end{cases},$$

where we let $\widetilde{j} = n-k+j$. Note that $D^k \subseteq D_0^k \subseteq \cdots \subseteq D_N^k \subseteq D^{k+1}$, see Figure 3.13 for an illustration. Let $\omega_j^k = \Psi_j(\omega^k)$. If γ is a ω_j^k-open path living in D_j^k, then $\Sigma_{t_{n-k},t_{N+j+1}}(\gamma)$ is a ω_{j+1}^k-open path living in D_{j+1}^k. This is a consequence after a careful inspection of Figure 3.5, where blue points indicate possible horizontal drifts. Define also

$$h_j^k = \sup\{h \leqslant N : \exists u, v \in \mathbb{Z} \text{ with } x_{u,0} \xleftrightarrow{D_j^k, \omega_j^k} x_{v,h}\}.$$

Then, $h^k \leqslant h_0^k$ and $h_n^k \leqslant h^{k+1}$. As in [GM14], we need to prove that for $0 \leqslant j \leqslant N-1$,

$$h_{j+1}^k = h_j^k \qquad \text{if } h_j^k \neq \widetilde{j}, \widetilde{j}+1, \tag{3.14}$$

$$h_{j+1}^k - h_j^k = 0 \text{ or } 1 \qquad \text{if } h_j^k = \widetilde{j}, \tag{3.15}$$

$$h_{j+1}^k - h_j^k = -1 \text{ or } 0 \qquad \text{if } h_j^k = \widetilde{j}+1, \tag{3.16}$$

$$\mathbb{P}(h_{j+1}^k \geqslant h \,|\, h_j^k = h) \geqslant 2\delta \qquad \text{if } h = \widetilde{j}+1. \tag{3.17}$$

The four equations above imply the existence of a process H^k as in (3.13).

As explained in [GM14], (3.14), (3.15) and (3.16) are clear because the upper endpoint of a path is affected by $\Sigma := \Sigma_{t_{n-k},t_{N+j+1}}$ only if it is at height $\widetilde{j}$ or $\widetilde{j}+1$. And the behavior of the upper endpoint can be analyzed using Figure 3.6. More precisely,

- when it is at height $\widetilde{j}+1$, the upper endpoint either stays at the same level or drifts downwards by 1;
- when it is at height $\widetilde{j}$, it either stays at the same level or drifts upwards by 1.

Hence, the rest of the proof is dedicated to showing (3.17).

We start with a preliminary computation. Fix j and let $\mathcal{P}_j$ be the set of paths γ of $\Psi_j(G^k)$, contained in D_j^k, with one endpoint at height 0, the other at height $h(\gamma)$, and all other vertices with heights between 1 and $h(\gamma)-1$.

Assume that in Σ, the additional rhombus is slid from left to right and define Γ to be the left-most path of $\mathcal{P}_j$ reaching height h_j^k [4]. (Such a path exists due to the definition of h_j^k.) This

[4] Otherwise Γ should be taken right-most.

choice is relevant since later on, we will need to use negative information in the region on the left of the path γ. Moreover, for $\gamma, \gamma' \in \mathcal{P}_j$, we write $\gamma' < \gamma$ if $\gamma' \neq \gamma$, $h(\gamma') = h(\gamma)$ and γ' does not contain any edge strictly to the right of γ.

Denote by $\Gamma = \Gamma(\omega_j^k)$ the ω_j^k-open path of $\mathcal{P}_j$ that is the minimal element of $\{\gamma \in \mathcal{P}_j : h(\gamma) = h_j^k, \gamma \text{ is } \omega_j^k\text{-open}\}$. Given a path $\gamma \in \mathcal{P}_j$, we can write $\{\Gamma = \gamma\} = \{\gamma \text{ is } \omega_j^k\text{-open}\} \cap N_\gamma$ where N_γ is the decreasing event that

(a) there is no $\gamma' \in \mathcal{P}_j$ with $h(\gamma') > h(\gamma)$, all of whose edges not belonging to γ are ω_j^k-open;

(b) there is no $\gamma' < \gamma$ with $h(\gamma') = h(\gamma)$, all of whose edges not belonging to γ are ω_j^k-open.

Let F be a set of edges disjoint from γ, write C_F for the event that all the edges in F are closed. We find,

$$\begin{aligned}\mathbb{P}[C_F \,|\, \Gamma = \gamma] &= \frac{\mathbb{P}[N_\gamma \cap C_F \,|\, \gamma \text{ is open}]}{\mathbb{P}[N_\gamma \,|\, \gamma \text{ is open}]} \\ &\geqslant \mathbb{P}[C_F \,|\, \gamma \text{ is open}] \\ &\geqslant \varphi_K^1[C_F], \end{aligned} \tag{3.18}$$

where the second line is given by the FKG inequality due to the fact that $\mathbb{P}[\cdot \,|\, \gamma \text{ is open}]$ is still a random-cluster measure and both N_γ and C_F are decreasing events. And in the last line, we compare the boundary conditions, where K is the subgraph consisting of rhombi containing the edges of F.

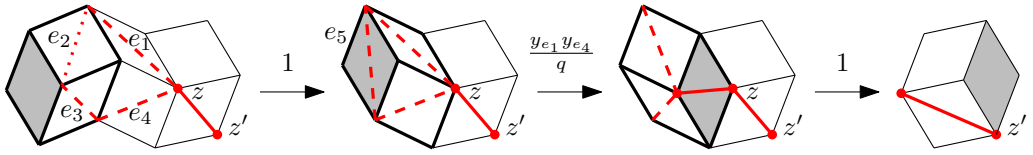

Figure 3.14 – Three star-triangle transformations contributing to Σ slid the gray rhombus from left to right. The dashed edges are closed, the bold edges are open and the state of dotted edge e_2 does not really matter. The first and last passages occur with probability 1, and the second with probability $y_{e_1} y_{e_4}/q$.

Now, we are ready to show (3.17). Let $\gamma \in \mathcal{P}_j$ with $h(\gamma) = \widetilde{j} + 1$ and assume $\Gamma(\omega_j^k) = \gamma$. Now, it is enough to show that

$$\mathbb{P}\Big[h(\Sigma(\gamma)) \geqslant \widetilde{j} + 1 \,\Big|\, \Gamma = \gamma\Big] \geqslant 2\delta. \tag{3.19}$$

Let $z = x_{u,\widetilde{j}+1}$ denote the upper endpoint of γ and let z' denote the other endpoint of the unique edge of γ leading to z. Either $z' = x_{u+1,\widetilde{j}}$ or $z' = x_{u-1,\widetilde{j}}$. In the second case, it is always the case that $h(\Sigma(\gamma)) \geqslant \widetilde{j} + 1$.

Assume that $z' = x_{u+1,\widetilde{j}}$ as in Figure 3.14 and consider edges e_i for $i = 1, \dots, 4$ as follow,

$$\begin{aligned} e_1 &= \langle x_{u,\widetilde{j}+1}, x_{u-1,\widetilde{j}+2} \rangle, \quad & e_2 &= \langle x_{u-1,\widetilde{j}+2}, x_{u-2,\widetilde{j}+1} \rangle, \\ e_3 &= \langle x_{u-2,\widetilde{j}+1}, x_{u-1,\widetilde{j}} \rangle, \quad & e_4 &= \langle x_{u-1,\widetilde{j}}, x_{u,\widetilde{j}+1} \rangle. \end{aligned}$$

Let us now analyse the star-triangle transformations that affect $e_1, \dots, e_4$; these are depicted in Figure 3.14. We note that conditioning on the event $C_F \cap \{\Gamma = \gamma\}$, where $F = \{e_3, e_4\}$, we have:

(a) The edge e_1 must be closed due to the conditioning $\{\Gamma = \gamma\}$.

(b) Whichever the state of e_2 is, the edge e_5 is always closed.

(c) The second passage occurs with probability $y_{e_1} y_{e_4}/q$.

(d) The third passage is deterministic.

Thus,

$$\mathbb{P}\Big[h(\Sigma) \geqslant \widetilde{j} + 1 \,\Big|\, \Gamma = \gamma\Big] \geqslant \frac{y_{e_1} y_{e_4}}{q} \cdot \mathbb{P}[C_F \,|\, \Gamma = \gamma].$$

Moreover, the preliminary computation (3.18) gives that

$$\mathbb{P}[C_F \,|\, \Gamma = \gamma] \geqslant \varphi^1_K[C_F] = (1 - p_{e_3})(1 - p_{e_4}),$$

where K consists only of the two rhombi containing e_3 and e_4 and we use the fact that in the random-cluster measure φ^1_K, these edges are independent (the number of clusters is always equal to 1). Finally,

$$\mathbb{P}\Big[h(\Sigma) \geqslant \widetilde{j} + 1 \,\Big|\, \Gamma = \gamma\Big] \geqslant \frac{y_{e_1} p_{e_4}(1 - p_{e_3})}{q} \geqslant \frac{y_{\pi-\varepsilon} p_{\pi-\varepsilon}(1 - p_\varepsilon)}{q} \geqslant 2\delta, \tag{3.20}$$

where

$$\delta = \frac{1}{2} \min\left\{ \frac{y_{\pi-\varepsilon} p_{\pi-\varepsilon}(1 - p_\varepsilon)}{q}, 1 \right\} > 0. \tag{3.21}$$

To conclude, we have

$$\frac{\mathbb{P}[h^n \geqslant \delta n]}{\mathbb{P}[h^0 \geqslant n]} \geqslant \frac{\mathbb{P}[H^n \geqslant \delta n]}{\mathbb{P}[H^0 \geqslant n]} \geqslant \mathbb{P}[H^n \geqslant \delta n \,|\, H^0 \geqslant n] =: c_n(\delta),$$

and since $H^n/n \to 2\delta$ as $n \to \infty$ due to the law of large numbers, we know that $c_n \to 1$ as $n \to \infty$. □

3.3.3 Doubly-periodic isoradial graphs

Now that the RSW property is proved for isoradial square lattices, we transfer it to arbitrary doubly-periodic isoradial graphs $\mathbb{G}$. We do this by transforming a finite part of $\mathbb{G}$ (as large as we want) into a local isoradial square lattice using star-triangle transformations. The approach is based on the combinatorial result Proposition 3.9.

Proposition 3.18. *Any doubly-periodic isoradial graph $\mathbb{G}$ satisfies the RSW property.*

Proof. Let $\mathbb{G}$ be a doubly-periodic isoradial graph with grid $(s_n)_{n\in\mathbb{Z}}$ and $(t_n)_{n\in\mathbb{Z}}$. Fix a constant $d > 1$ as given by Proposition 3.9 applied to $\mathbb{G}$. In the below formula, $\mathcal{C}_h^{\mathrm{hp}}(n; n)$ denotes the horizontal crossing event in the half-plane rectangular domain $\mathsf{R}^{\mathrm{hp}}(n; n) := \mathsf{R}(-n, n; 0, n)$. We will show that

$$\varphi^0_{\Lambda(6dn)}\Big[\mathcal{C}_h^{\mathrm{hp}}(n; n)\Big] = \varphi^0_{\Lambda(6dn)}\Big[\mathcal{C}_h(-n, n; 0, n)\Big] \geqslant \delta, \tag{3.22}$$

for some constant $\delta > 0$ which does not depend on n. Moreover, a careful inspection of the forthcoming proof shows that δ only depends the bounded angles parameter $\varepsilon > 0$ and on

the size of the fundamental domain of $\mathbb{G}$. The same estimate is valid for the dual model, since it is also a random-cluster model on an isoradial graph with $\beta = 1$.

The two families of tracks $(s_n)_{n\in\mathbb{Z}}$ and $(t_n)_{n\in\mathbb{Z}}$ play symmetric roles, therefore (3.22) may also be written

$$\varphi^0_{\Lambda(6dn)}\Big[\mathcal{C}_v(0,n;-n,n)\Big] \geqslant \delta. \tag{3.23}$$

The two inequalities (3.22) and (3.23) together with their dual counterparts imply the RSW property by Lemma 3.10 [5].

The rest of the proof is dedicated to (3.22). In proving (3.22), we will assume n to be larger than some threshold depending on $\mathbb{G}$ only; this is not a restrictive hypothesis.

Let $(\sigma_k)_{1\leqslant k\leqslant K}$ be a sequence of star-triangle transformations as in Proposition 3.9 such that in $\widetilde{\mathbb{G}} := (\sigma_K \circ \cdots \circ \sigma_1)(\mathbb{G})$, the region enclosed by s_{-4n}, s_{4n}, t_{-2n} and t_{2n} has a square lattice structure. Recall that all the transformations σ_k act horizontally between s_{-6dn} and s_{6dn} and vertically between t_n and t_{-n}.

Consider the following events for $\widetilde{\mathbb{G}}$. Let $\widetilde{\mathcal{C}}$ be the event that there exists an open circuit contained in the region between s_{-2n} and s_{2n} and between $t_{-n/2}$ and $t_{n/2}$ surrounding the segment of the base between s_{-n} and s_n. Let $\widetilde{\mathcal{C}}^*$ be the event that there exists an open circuit contained in the region between s_{-3n} and s_{3n} and between $t_{-3n/2}$ and $t_{3n/2}$ surrounding the segment of the base between s_{-2n} and s_{2n}.

Let $\widetilde{G}$ be the subgraph of $\widetilde{\mathbb{G}}$ contained between s_{-4n}, s_{4n}, t_{-2n} and t_{2n}. Then $\widetilde{G}$ is a finite section of a square lattice with $4n+1$ horizontal tracks, but potentially more than $8n+1$ vertical ones. Indeed, any track of $\mathbb{G}$ that intersects the base between s_{-4n}, s_{4n} is transformed into a vertical track of $\widetilde{G}$.

Write $(\widetilde{s}_n)_{n\in\mathbb{Z}}$ for the vertical tracks of $\widetilde{G}$, with $\widetilde{s}_0$ coinciding with s_0 (this is coherent with the notation in the proof of Proposition 3.9). Then, the tracks $(s_n)_{n\in\mathbb{Z}}$ are a periodic subset of $(\widetilde{s}_n)_{n\in\mathbb{Z}}$, with period bounded by the number of tracks intersecting a fundamental domain of $\mathbb{G}$. It follows that there exist constants a, b depending only on $\mathbb{G}$, not on n, such that the number of tracks $(\widetilde{s}_n)_{n\in\mathbb{Z}}$ between any two tracks s_i and s_j (with $i \leqslant j$) is between $(j-i)a-b$ and $(j-i)a+b$.

By the above discussion, for some constant $c > 1$ and n large enough (larger than some n_0 depending only on a and b, therefore only on the size of the fundamental domain of $\mathbb{G}$), the events $\widetilde{\mathcal{C}}$ and $\widetilde{\mathcal{C}}^*$ may be created using crossing events as follow:

$$\widetilde{\mathcal{H}}_1 \cap \widetilde{\mathcal{H}}_2 \cap \widetilde{\mathcal{V}}_1 \cap \widetilde{\mathcal{V}}_2 \subseteq \widetilde{\mathcal{C}} \qquad \text{and} \qquad \widetilde{\mathcal{H}}^*_1 \cap \widetilde{\mathcal{H}}^*_2 \cap \widetilde{\mathcal{V}}^*_1 \cap \widetilde{\mathcal{V}}^*_2 \subseteq \widetilde{\mathcal{C}}^*,$$

where

$$\begin{aligned}
\widetilde{\mathcal{H}}_1 &= \mathcal{C}_h(-(c+1)n, (c+1)n; 0, \tfrac{n}{2}), & \widetilde{\mathcal{H}}^*_1 &= \mathcal{C}^*_h(-(2c+1)n, (2c+1)n; n, \tfrac{3n}{2}),\\
\widetilde{\mathcal{H}}_2 &= \mathcal{C}_h(-(c+1)n, (c+1)n; -\tfrac{n}{2}, 0), & \widetilde{\mathcal{H}}^*_2 &= \mathcal{C}^*_h(-(2c+1)n, (2c+1)n; -\tfrac{3n}{2}, -n),\\
\widetilde{\mathcal{V}}_1 &= \mathcal{C}_v(-(c+1)n, -cn; -\tfrac{n}{2}, \tfrac{n}{2}), & \widetilde{\mathcal{V}}^*_1 &= \mathcal{C}^*_v(-(2c+1)n, -2cn; -\tfrac{3n}{2}, \tfrac{3n}{2}),\\
\widetilde{\mathcal{V}}_2 &= \mathcal{C}_v(cn, (c+1)n; -\tfrac{n}{2}, \tfrac{n}{2}), & \widetilde{\mathcal{V}}^*_2 &= \mathcal{C}^*_v(2cn, (2c+1)n; -\tfrac{3n}{2}, \tfrac{3n}{2}),
\end{aligned}$$

are defined in terms of the tracks $(\widetilde{s}_n)_{n\in\mathbb{Z}}$ and $(t_n)_{n\in\mathbb{Z}}$. These horizontal and vertical crossing events are shown in Figure 3.15.

[5] The conditions of Lemma 3.10 differ slightly from (3.22) and (3.23) in the position of the rectangle and the domain where the measure is defined. Getting from one to the other is a standard application of the comparison between boundary conditions.

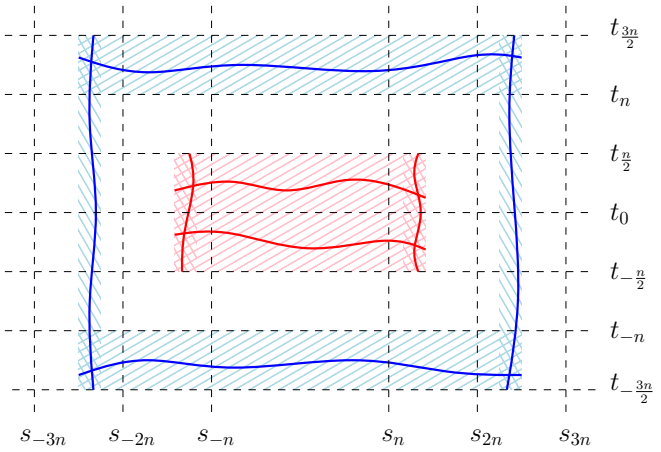

Figure 3.15 – The crossing events $\widetilde{\mathcal{H}}_1$, $\widetilde{\mathcal{H}}_2$, $\widetilde{\mathcal{V}}_1$ and $\widetilde{\mathcal{V}}_2$ are depicted in red; they induce a circuit around the segment of the base between s_{-n} and s_n. The events $\widetilde{\mathcal{H}}_1^*$, $\widetilde{\mathcal{H}}_2^*$, $\widetilde{\mathcal{V}}_1^*$ and $\widetilde{\mathcal{V}}_2^*$ are represented in blue.

Notice that all events above depend only on the configuration in $\widetilde{G}$. Let $\varphi_{\widetilde{\mathbb{G}}}$ denote some infinite-volume measure on $\widetilde{\mathbb{G}}$. By the RSW property for the square lattice $\widetilde{G}$ (that is, by Corollary 3.12), the comparison between boundary conditions and the FKG inequality,

$$\varphi_{\widetilde{\mathbb{G}}}\big[\widetilde{\mathcal{C}}^*\big] \geqslant \varphi^1_{\widetilde{G}}\big[\widetilde{\mathcal{H}}_1^*\big]\varphi^1_{\widetilde{G}}\big[\widetilde{\mathcal{H}}_2^*\big]\varphi^1_{\widetilde{G}}\big[\widetilde{\mathcal{V}}_1^*\big]\varphi^1_{\widetilde{G}}\big[\widetilde{\mathcal{V}}_2^*\big] \geqslant \delta_1,$$

for some $\delta_1 > 0$ independent of n. Moreover, by the same reasoning,

$$\varphi_{\widetilde{\mathbb{G}}}\big[\widetilde{\mathcal{C}}\,\big|\,\widetilde{\mathcal{C}}^*\big] \geqslant \varphi^0_{\widetilde{\mathsf{R}}}\big[\widetilde{\mathcal{H}}_1\big]\varphi^0_{\widetilde{\mathsf{R}}}\big[\widetilde{\mathcal{H}}_2\big]\varphi^0_{\widetilde{\mathsf{R}}}\big[\widetilde{\mathcal{V}}_1\big]\varphi^0_{\widetilde{\mathsf{R}}}\big[\widetilde{\mathcal{V}}_2\big] \geqslant \delta_2,$$

for some $\delta_2 > 0$ independent of n, where $\widetilde{\mathsf{R}} = \widetilde{\mathsf{R}}(2cn; n)$ is defined with respect to the tracks $(\widetilde{s}_n)_{n\in\mathbb{Z}}$ and $(t_n)_{n\in\mathbb{Z}}$. We conclude that

$$\varphi_{\widetilde{\mathbb{G}}}\big[\widetilde{\mathcal{C}} \cap \widetilde{\mathcal{C}}^*\big] \geqslant \delta_1\delta_2 > 0.$$

Let $\mathbb{P}$ be the probability that consists of choosing a configuration $\widetilde{\omega}$ on $\widetilde{\mathbb{G}}$ according to $\varphi_{\widetilde{\mathbb{G}}}$, then applying the inverse transformations $\sigma_K^{-1}, \dots, \sigma_1^{-1}$ to it. Thus, $\omega := (\sigma_1^{-1} \circ \cdots \circ \sigma_K^{-1})(\widetilde{\omega})$ is a configuration on $\mathbb{G}$ chosen according to some infinite-volume measure $\varphi_{\mathbb{G}}$.

Let $\widetilde{\omega} \in \widetilde{\mathcal{C}} \cap \widetilde{\mathcal{C}}^*$, and write $\widetilde{\gamma}$ and $\widetilde{\gamma}^*$ for two circuits as in the definitions of $\widetilde{\mathcal{C}}$ and $\widetilde{\mathcal{C}}^*$ respectively. The two circuits $\widetilde{\gamma}$ and $\widetilde{\gamma}^*$ are transformed by $(\sigma_1^{-1} \circ \cdots \circ \sigma_K^{-1})$ into circuits on $\mathbb{G}$; call $\gamma = (\sigma_1^{-1} \circ \cdots \circ \sigma_K^{-1})(\widetilde{\gamma})$ and $\gamma^* = (\sigma_1^{-1} \circ \cdots \circ \sigma_K^{-1})(\widetilde{\gamma}^*)$ their respective images. Then, γ is ω-open and γ^* is ω^*-open.

Since the transformations $\sigma_1^{-1}, \dots, \sigma_K^{-1}$ only affect the region between s_{-6dn}, s_{6dn}, t_{-2n} and t_{2n}, both γ and γ^* are contained in this region of $\mathbb{G}$, that is in $\mathsf{R}(6dn; 2n)$. Additionally, since the transformations do not affect the base, γ^* surrounds the segment of the base between s_{-2n} and s_{2n} while γ surrounds the segment of the base between s_{-n} and s_n but only traverses the base between s_{-2n} and s_{2n}.

Write $\mathcal{C}$ for the event that a configuration on $\mathbb{G}$ has an open circuit contained in $\mathsf{R}(6dn; 2n)$, surrounding the segment of the base between s_{-n} and s_n and traversing the base only between s_{-2n} and s_{2n}. Also, set $\mathcal{C}^*$ to be the event that a configuration on $\mathbb{G}$ has a dually-open circuit contained in $\mathsf{R}(6dn; 2n)$, surrounding the segment of the base between s_{-2n} and s_{2n}.

Both $\mathcal{C}$ and $\mathcal{C}^*$ are reminiscent of the events $\widetilde{\mathcal{C}}$ and $\widetilde{\mathcal{C}}^*$, in spite of small differences. Indeed, the discussion above shows that if $\widetilde{\omega} \in \widetilde{\mathcal{C}} \cap \widetilde{\mathcal{C}}^*$, then $\omega \in \mathcal{C} \cap \mathcal{C}^*$. Thus,

$$\varphi_{\mathbb{G}}\big[\mathcal{C} \cap \mathcal{C}^*\big] = \mathbb{P}\big[\omega \in \mathcal{C} \cap \mathcal{C}^*\big] \geqslant \mathbb{P}\big[\widetilde{\omega} \in \widetilde{\mathcal{C}} \cap \widetilde{\mathcal{C}}^*\big] = \varphi_{\widetilde{\mathbb{G}}}\big[\widetilde{\mathcal{C}} \cap \widetilde{\mathcal{C}}^*\big] \geqslant \delta_1 \delta_2.$$

For a configuration ω on $\mathbb{G}$, write $\Gamma^*(\omega)$ for the exterior-most dually-open circuit as in the definition of $\mathcal{C}^*$ (that is contained in $\mathsf{R}(6dn; 2n)$ and surrounding the segment of the base between s_{-2n} and s_{2n}), if such a circuit exists. Let $\mathrm{Int}(\Gamma^*)$ be the region surrounded by Γ^*, seen as a subgraph of $\mathbb{G}$.

It is standard that Γ^* may be explored from the outside and therefore that, conditionally on Γ^*, the random-cluster measure in $\mathrm{Int}(\Gamma^*)$ is $\varphi^0_{\mathrm{Int}(\Gamma^*)}$.

Observe that for $\omega \in \mathcal{C} \cap \mathcal{C}^*$, due to the restrictions over the intersections with the base, any circuit in the definition of $\mathcal{C}$ is surrounded by any in the definition of $\mathcal{C}^*$. Thus, if for $\omega \in \mathcal{C}^*$, the occurence of $\mathcal{C}$ only depends on the configuration inside $\mathrm{Int}(\Gamma^*)$. Therefore,

$$\begin{aligned}
\varphi_{\mathbb{G}}\big[\mathcal{C} \cap \mathcal{C}^*\big] &= \varphi_{\mathbb{G}}\big[\mathcal{C} \,\big|\, \mathcal{C}^*\big]\varphi_{\mathbb{G}}\big[\mathcal{C}^*\big] \\
&= \sum_{\gamma^*} \varphi_{\mathbb{G}}\big[\mathcal{C} \,\big|\, \Gamma^* = \gamma^*\big]\varphi_{\mathbb{G}}\big[\Gamma^* = \gamma^*\big] \\
&= \sum_{\gamma^*} \varphi^0_{\mathrm{Int}(\gamma^*)}\big[\mathcal{C}\big]\varphi_{\mathbb{G}}\big[\Gamma^* = \gamma^*\big] \\
&\leqslant \sum_{\gamma^*} \varphi^0_{\mathsf{R}(6dn;2n)}\big[\mathcal{C}\big]\varphi_{\mathbb{G}}\big[\Gamma^* = \gamma^*\big] \\
&= \varphi^0_{\mathsf{R}(6dn;2n)}\big[\mathcal{C}\big]\varphi_{\mathbb{G}}\big[\mathcal{C}^*\big],
\end{aligned}$$

where the sum above is over all deterministic circuits γ^* on $\mathbb{G}^*$, as in the definition of $\mathcal{C}^*$. In the before last line, we used the fact that $\mathrm{Int}(\gamma^*) \subseteq \mathsf{R}(6dn; 2n)$, where $\mathsf{R}(6dn; 2n)$ is defined using tracks in $\mathbb{G}$, and the comparison between boundary conditions to say that the free boundary conditions on $\partial\mathrm{Int}(\gamma^*)$ are less favorable to the increasing event $\mathcal{C}$ than those on the more distant boundary $\partial\mathsf{R}(6dn; 2n)$.

Due to the previous bound on $\varphi_{\mathbb{G}}\big[\mathcal{C} \cap \mathcal{C}^*\big]$, we deduce that

$$\varphi^0_{\mathsf{R}(6dn;2n)}\big[\mathcal{C}\big] \geqslant \delta_1 \delta_2.$$

Finally, notice that any circuit as in the definition of $\mathcal{C}$ contains a horizontal crossing of $\mathsf{R}^{\mathrm{hp}}(n; n)$. We conclude from the above that

$$\varphi^0_{\mathsf{R}(6dn;2n)}\big[\mathsf{R}^{\mathrm{hp}}(n; n)\big] \geqslant \delta_1 \delta_2.$$

This implies (3.22) by further pushing away the unfavorable boundary conditions. □

3.3.4 Tying up loose ends

As mentioned already, Theorem 3.1 and Corollary 3.3 for $1 \leqslant q \leqslant 4$ follow directly from the RSW property (i.e., from Proposition 3.18). We mention here the necessary steps. They are all standard for those familiar with the random-cluster model; detail are provided in Appendix C.

Fix $\mathbb{G}$ a doubly-periodic isoradial graph and $q \in [1, 4]$. We start with the following lemma which is the key to all the proofs.

Lemma 3.19. *For $j \geqslant 1$, define the annuli $A_j = [-2^{j+1}, 2^{j+1}]^2 \setminus [-2^j, 2^j]^2$. Then, there exists $c > 0$ such that for all $j \geqslant 1$ and $\xi = 0, 1$, we have*

$$\varphi^{\xi}_{A_j}\Big[\text{there exists an open circuit surrounding 0 in } A_j\Big] \geqslant c. \tag{3.24}$$

By duality, the same also holds for a dually-open circuit.

Proof. This is proved by combining crossings of rectangles via the FKG inequality, as in Figure 3.15. □

The estimates of the Lemma 3.19 for the dual model imply an upper bound on the one-arm probability under $\varphi^1_{\mathbb{G}}$, as that in the second point of Theorem 3.1. Indeed, if a dually-open circuit occurs in A_j for some $j \leqslant \log_2 n - 2$, then the event $\{0 \leftrightarrow \partial B_n\}$ fails. The fact (3.24) is uniform in the boundary conditions on A_j allows us to "decouple" the events of (3.24), and proves that the probability of no circuit occurring in any of $A_1, \dots, A_{\log_2 n - 2}$ is bounded above by $(1-c)^{\log_2 n - 2}$.

The converse bound is obtained by a straightforward construction of a large cluster using crossings of rectangles of the form $[0, 2^j] \times [0, 2^{j+1}]$ and their rotation by $\frac{\pi}{2}$, combined using the FKG inequality.

From the above, we deduce that $\varphi^1_{\mathbb{G}}(0 \leftrightarrow \infty) = 0$. The uniqueness of the critical infinite volume measure (the first point of Theorem 3.1) follows using a standard coupling argument.

Finally, to prove Corollary 3.3, we use the differential inequality of [GG11], as done in [DCM16].

3.3.5 Universality of arm exponents: Theorem 3.4

The proof of universality of arm exponents (Theorem 3.4) follows exactly the steps of [GM14, Sec. 8]. Arm events will be transferred between isoradial graphs using the same transformations as in the previous sections. As already discussed in Section 2.6, these transformations alter primal and dual paths, especially at their endpoints. When applied to arm events, this could considerably reduce the length of the arms. To circumvent such problems and shield the endpoints of the arms from the effect of the star-triangle transformations, we define a variation of the arm events. It roughly consists in "attaching" the endpoints of the arms to a track which is not affected by the transformations. Some notation is necessary.

Fix $\varepsilon > 0$ and a doubly-periodic isoradial graph $\mathbb{G} \in \mathcal{G}(\varepsilon)$ with grid $(s_n)_{n\in\mathbb{Z}}$ and $(t_n)_{n\in\mathbb{Z}}$. Recall that the vertices of $\mathbb{G}^\diamond$ that are below and adjacent to t_0 form the base of $\mathbb{G}$. Also, recall the notation $x \leftrightarrow y$ and write $x \overset{*}{\leftrightarrow} y$ for connections in the dual configuration.

For $n < N$ and $k \in \{1\} \cup 2\mathbb{N}$, define the event $\widetilde{A}_k(n, N)$ as

1. for $k = 1$: there exist primal vertices $x_1 \in \Lambda(n)$ and $y_1 \notin \Lambda(N)$, both on the base, such that $x_1 \leftrightarrow y_1$;
2. for $k = 2$: there exist $x_1, x_1^* \in \Lambda(n)$ and $y_1, y_1^* \notin \Lambda(N)$, all on the base, such that $x_1 \leftrightarrow y_1$ and $x_1^* \overset{*}{\leftrightarrow} y_1^*$;
3. for $k = 2j \geqslant 4$: $\widetilde{A}_k(n, N)$ is the event that there exist $x_1, \dots, x_j \in \Lambda(n)$ and $y_1, \dots, y_j \notin \Lambda(N)$, all on the base, such that $x_i \leftrightarrow y_i$ for all i and $x_i \nleftrightarrow x_j$ for all $i \neq j$.

Notice the resemblance between $\widetilde{A}_k(n, N)$ and $A_k(n, N)$, where the latter is defined just before the statement of Theorem 3.4. In particular, observe that in the third point, the existence of j disjoint clusters uniting $\partial\Lambda(n)$ to $\partial\Lambda(N)$ indeed induces $2j$ arms of alternating colours in counterclockwise order. Two differences between $\widetilde{A}_k(n, N)$ and $A_k(n, N)$ should

be noted: the fact that in the former arms are forced to have extremities on the base and that the former is defined in terms or graph distance while the latter in terms of Euclidean distance. As readers probably expect, this has only a limited impact on the probability of such events.

For the rest of the section, fix $q \in [1,4]$ and write $\varphi_{\mathbb{G}}$ for the unique infinite-volume random-cluster measure on $\mathbb{G}$ with parameters $\beta = 1$ and q.

Lemma 3.20. *Fix $k \in \{1\} \cup 2\mathbb{N}$. There exists $c > 0$ depending only on ε, q, k and the fundamental domain of $\mathbb{G}$ such that*

$$c\,\varphi_{\mathbb{G}}[A_k(n,N)] \leqslant \varphi_{\mathbb{G}}[\widetilde{A}_k(n,N)] \leqslant c^{-1}\varphi_{\mathbb{G}}[A_k(n,N)] \tag{3.25}$$

for all $N > n$ large enough.

The above is a standard consequence of what is known in the field as the arm separation lemma (Lemma D.1). The proofs of the separation lemma and Lemma 3.20 are both fairly standard but lengthy applications of the RSW theory of Theorem 3.1; they are discussed in Appendix D (see also [Man12, Prop. 5.4.2] for a version of these for Bernoulli percolation).

We obtain Theorem 3.4 in two steps, first for isoradial square lattices, then for doubly-periodic isoradial graphs. The key to the first step is the following proposition.

Proposition 3.21. *Let $\mathbb{G}^{(1)} = \mathbb{G}_{\alpha,\beta^{(1)}}$ and $\mathbb{G}^{(2)} = \mathbb{G}_{\alpha,\beta^{(2)}}$ be two isoradial square lattices in $\mathcal{G}(\varepsilon)$. Fix $k \in \{1\} \cup 2\mathbb{N}$. Then*

$$\varphi^{\xi}_{\mathbb{G}^{(1)}}[\widetilde{A}_k(n,N)] = \varphi^{\xi}_{\mathbb{G}^{(2)}}[\widetilde{A}_k(n,N)],$$

for all $n < N$.

Proof. Fix $k \in \{1\} \cup 2\mathbb{N}$ and take $N > n > 0$ and $M \geqslant N$ (one should imagine M much larger than N). Let G_{mix} be the symmetric mixed graph of Section 3.2.1 formed above the base of a block of M rows and $2M+1$ columns of $\mathbb{G}^{(2)}$ superposed on an equal block of $\mathbb{G}^{(1)}$, then convexified, and symmetrically in below the base. Construct $\widetilde{G}_{\text{mix}}$ in the same way, with the role of $\mathbb{G}^{(1)}$ and $\mathbb{G}^{(2)}$ inversed. Recall, from Section 3.2.1, the series of star-triangle transformations $\Sigma^{\downarrow}$ that transforms G_{mix} into $\widetilde{G}_{\text{mix}}$.

Write $\varphi_{G_{\text{mix}}}$ and $\varphi_{\widetilde{G}_{\text{mix}}}$ for the random-cluster measures on G_{mix} and $\widetilde{G}_{\text{mix}}$, respectively, with $\beta = 1$ and free boundary conditions. The events $\widetilde{A}_k(n,N)$ are also defined on G_{mix} and $\widetilde{G}_{\text{mix}}$.

Let ω be a configuration on G_{mix} such that $\widetilde{A}_k(n,N)$ occurs. Then, under the configuration $\Sigma^{\downarrow}(\omega)$ on $\widetilde{G}_{\text{mix}}$, $\widetilde{A}_k(n,N)$ also occurs. Indeed, the vertices x_i and y_i (and x_1^* and y_1^* when $k = 2$) are not affected by the star-triangle transformations in $\Sigma^{\downarrow}$ and connections between them are not broken nor created by any star-triangle transformation. Thus, $\varphi_{G_{\text{mix}}}[\widetilde{A}_k(n,N)] \leqslant \varphi_{\widetilde{G}_{\text{mix}}}[\widetilde{A}_k(n,N)]$. Since the roles of G_{mix} and $\widetilde{G}_{\text{mix}}$ are symmetric, we find

$$\varphi_{G_{\text{mix}}}[\widetilde{A}_k(n,N)] = \varphi_{\widetilde{G}_{\text{mix}}}[\widetilde{A}_k(n,N)] \tag{3.26}$$

Observe that the quantities in (3.26) depend implicitly on M. When taking $M \to \infty$, due to the uniqueness of the infinite-volume random-cluster measures in $\mathbb{G}^{(1)}$ and $\mathbb{G}^{(2)}$, we obtain

$$\varphi_{G_{\text{mix}}}[\widetilde{A}_k(n,N)] \xrightarrow[M\to\infty]{} \varphi_{\mathbb{G}^{(1)}}[\widetilde{A}_k(n,N)] \qquad \text{and}$$
$$\varphi_{\widetilde{G}_{\text{mix}}}[\widetilde{A}_k(n,N)] \xrightarrow[M\to\infty]{} \varphi_{\mathbb{G}^{(2)}}[\widetilde{A}_k(n,N)].$$

Thus, (3.26) implies the desired conclusion. □

Corollary 3.22. *Let $\mathbb{G} = \mathbb{G}_{\boldsymbol{\alpha},\boldsymbol{\beta}}$ be an isoradial square lattice in $\mathcal{G}(\varepsilon)$ and fix $k \in \{1\} \cup 2\mathbb{N}$. Then, there exists $c > 0$ depending only on ε, q and k such that,*

$$c\,\varphi_{\mathbb{G}}[A_k(n,N)] \leqslant \varphi_{\mathbb{Z}^2}[A_k(n,N)] \leqslant c^{-1}\varphi_{\mathbb{G}}[A_k(n,N)],$$

for any $n < N$.

Proof. Fix $\mathbb{G}_{\boldsymbol{\alpha},\boldsymbol{\beta}}$ and k as in the statement. The constants c_i below depend on ε, q and k only.

Let $\widetilde{\beta}_k = \alpha_{-k} - \beta_0 + \pi$ and write $\widetilde{\boldsymbol{\beta}}$ for the sequence $(\widetilde{\beta}_k)_{k\in\mathbb{Z}}$. Due to the choice of $\mathbb{G}_{\boldsymbol{\alpha},\boldsymbol{\beta}}$, we have $\widetilde{\boldsymbol{\beta}} \in [\varepsilon, \pi-\varepsilon]^{\mathbb{Z}}$. Proposition 3.21 and Lemma 3.20 applied to $\mathbb{Z}^2 = \mathbb{G}_{0,\frac{\pi}{2}}$ and $\mathbb{G}_{0,\widetilde{\boldsymbol{\beta}}}$ yield a constant $c_1 > 0$ such that

$$c_1\,\varphi_{\mathbb{G}_{0,\widetilde{\boldsymbol{\beta}}}}[A_k(n,N)] \leqslant \varphi_{\mathbb{Z}^2}[A_k(n,N)] \leqslant c_1^{-1}\varphi_{\mathbb{G}_{0,\widetilde{\boldsymbol{\beta}}}}[A_k(n,N)]. \tag{3.27}$$

As in the proof of Corollary 3.12, $\mathbb{G}_{\boldsymbol{\alpha},\beta_0}$ is the rotation by β_0 of the graph $\mathbb{G}_{0,\widetilde{\boldsymbol{\beta}}}$. This does not imply that the arm events have the same probability in both graphs (since they are defined in terms of square annuli). However, Proposition D.2] about arms extension provides a constant $c_2 > 0$ such that

$$c_2\,\varphi_{\mathbb{G}_{\boldsymbol{\alpha},\beta_0}}[A_k(n,N)] \leqslant \varphi_{\mathbb{G}_{0,\widetilde{\boldsymbol{\beta}}}}[A_k(n,N)] \leqslant c_2^{-1}\varphi_{\mathbb{G}_{\boldsymbol{\alpha},\beta_0}}[A_k(n,N)]. \tag{3.28}$$

Finally apply Proposition 3.21 and Lemma 3.20 to $\mathbb{G}_{\boldsymbol{\alpha},\beta_0}$ and $\mathbb{G}_{\boldsymbol{\alpha},\boldsymbol{\beta}}$ to obtain a constant $c_3 > 0$ such that

$$c_3\,\varphi_{\mathbb{G}_{\boldsymbol{\alpha},\beta_0}}[A_k(n,N)] \leqslant \varphi_{\mathbb{G}_{\boldsymbol{\alpha},\boldsymbol{\beta}}}[A_k(n,N)] \leqslant c_3^{-1}\varphi_{\mathbb{G}_{\boldsymbol{\alpha},\beta_0}}[A_k(n,N)]. \tag{3.29}$$

Writing (3.27), (3.28) and (3.29) together yields the conclusion with $c = c_1c_2c_3$. □

Theorem 3.4 is now proved for isoradial square lattices. To conclude, we extend the result to all doubly-periodic isoradial graphs.

Proof of Theorem 3.4. Consider a doubly-periodic graph $\mathbb{G} \in \mathcal{G}(\varepsilon)$ for some $\varepsilon > 0$, with grid $(s_n)_{n\in\mathbb{Z}}$ and $(t_n)_{n\in\mathbb{Z}}$. Fix $k \in \{1\} \cup 2\mathbb{N}$. The constants c_i below depend on ε, q, k and the size of the period of $\mathbb{G}$.

Choose $n < N$ and $M \geqslant N$ (one should think of M as much larger than N). Proposition 3.9 (the symmetrized version) provides star-triangle transformations $(\sigma_k)_{1\leqslant k\leqslant K}$ such that, in $\widetilde{\mathbb{G}} = (\sigma_K \circ \cdots \circ \sigma_1)(\mathbb{G})$, the region $\Lambda(M)$ has a square lattice structure. Moreover, each σ_k acts between s_{-dM} and s_{dM} (for some fixed $d \geqslant 1$) and between t_M and t_{-M}, none of them affecting any rhombus of t_0.

In a slight abuse of notation (since $(s_n)_{n\in\mathbb{Z}}, (t_n)_{n\in\mathbb{Z}}$ is not formally a grid in $\widetilde{\mathbb{G}}$) we define $\widetilde{A}_k(n,N)$ for $\widetilde{\mathbb{G}}$ as for $\mathbb{G}$.

Let ω be a configuration on $\mathbb{G}$ such that $\widetilde{A}_k(n,N)$ occurs. Then, the image configuration $(\sigma_K \circ \cdots \circ \sigma_1)(\omega)$ on $\widetilde{\mathbb{G}}$ is such that $\widetilde{A}_k(n,N)$ occurs. Indeed, the transformations do not affect the endpoints of any of the paths defining $\widetilde{A}_k(n,N)$. Thus,

$$\varphi_{\mathbb{G}}[\widetilde{A}_k(n,N)] \leqslant \varphi_{\widetilde{\mathbb{G}}}[\widetilde{A}_k(n,N)].$$

The transformations may be applied in reverse order to obtain the converse inequality. In conclusion,

$$\varphi_{\mathbb{G}}[\widetilde{A}_k(n,N)] = \varphi_{\widetilde{\mathbb{G}}}[\widetilde{A}_k(n,N)]. \tag{3.30}$$

The right-hand side of the above depends implicitly on M. Write $\mathbb{G}^{\mathrm{sq}}$ for the isoradial square lattice such that the region $\Lambda(M)$ of $\widetilde{\mathbb{G}}$ is a centered rectangle of $\mathbb{G}^{\mathrm{sq}}$. (It is easy to see that there exists a lattice that satisfies this condition for all M simultaneously). The vertical tracks s_k of $\widetilde{\mathbb{G}}$ correspond to vertical tracks in $\mathbb{G}^{\mathrm{sq}}$ with an index between k and dk, where d is the maximal number of track intersection on t_0 between two consecutive tracks s_j, s_{j+1} in $\mathbb{G}$.

In conclusion, taking $M \to \infty$ and using the uniqueness of the infinite-volume measure on $\mathbb{G}^{\mathrm{sq}}$, we find

$$\varphi_{\mathbb{G}^{\mathrm{sq}}}[\widetilde{A}_k(n, dN)] \leqslant \lim_{M\to\infty} \varphi_{\widetilde{\mathbb{G}}}[\widetilde{A}_k(n, N)] \leqslant \varphi_{\mathbb{G}^{\mathrm{sq}}}[\widetilde{A}_k(dn, N)]. \tag{3.31}$$

Due to Lemma 3.20 and to the extension of arms (Proposition D.2),

$$c_1 \varphi_{\mathbb{G}^{\mathrm{sq}}}[A_k(n, N)] \leqslant \varphi_{\mathbb{G}^{\mathrm{sq}}}[\widetilde{A}_k(n, dN)] \leqslant \varphi_{\mathbb{G}^{\mathrm{sq}}}[\widetilde{A}_k(dn, N)] \leqslant c_1^{-1} \varphi_{\mathbb{G}^{\mathrm{sq}}}[A_k(n, N)],$$

for some constant $c_1 > 0$. Using this, (3.31) and Lemma 3.20, we find

$$c_2 \varphi_{\mathbb{G}^{\mathrm{sq}}}[A_k(n, N)] \leqslant \varphi_{\mathbb{G}}[A_k(n, N)] \leqslant c_2^{-1} \varphi_{\mathbb{G}^{\mathrm{sq}}}[A_k(n, N)],$$

for some $c_2 > 0$. Using Corollary (3.22), we obtain the desired result. □

3.4 Proofs for $q > 4$

Fix $q > 4$ and $\mathbb{G}$ a doubly-periodic isoradial graph with grid $(s_n)_{n\in\mathbb{Z}}$, $(t_n)_{n\in\mathbb{Z}}$. Unless otherwise stated, write $\varphi^{\xi}_{\mathbb{G}}$ for the isoradial random-cluster measure on $\mathbb{G}$ with parameters q, $\beta = 1$ and free ($\xi = 0$) or wired ($\xi = 1$) boundary conditions. We will use the same notation as in Sections 3.3.1 and 3.3.2.1.

The main goal of this section is to prove that there exist constants $C, c > 0$ such that

$$\varphi^0_{\mathbb{G}}\Big[0 \leftrightarrow \partial\Lambda(n)\Big] \leqslant C \exp(-cn), \qquad \forall n \geqslant 1. \tag{3.32}$$

As we will see in Section 3.4.3, Theorem 3.2 and Corollary 3.3 follow from (3.32) through standard arguments [6].

The strategy used to transfer (3.32) from the regular square lattice to arbitrary isoradial graphs is similar to that used in the previous section. However, note that the hallmark of the regime $q > 4$ is that boundary conditions influence the model at infinite distance. The arguments in the previous section were based on local modifications of graphs; in the present context, the random-cluster measure in the modified regions is influenced by the structure of the graph outside. This generates additional difficulties that require more careful constructions.

We start with a technical result that will be useful throughout the proofs. For $N, M \geqslant 1$, write $\mathsf{R}^{\mathrm{hp}}(N; M) = \mathsf{R}(-N, N; 0, M)$ for the half-plane rectangle which is the subgraph of $\mathbb{G}$ contained between t_{-N}, t_N, s_0 and s_M.

Proposition 3.23. *Suppose that there exist constants $C_0, c_0 > 0$ such that for all $N > n$,*

$$\varphi^0_{\mathsf{R}^{hp}(N;N)}\Big[0 \leftrightarrow \partial\Lambda(n)\Big] \leqslant C_0 \exp(-c_0 n). \tag{3.33}$$

[6] When the graph is not periodic, a condition similar to (3.32) should be shown for all vertices of $\mathbb{G}$, not just 0. It will be apparent from the proof that the values of c and C only depend on the parameter in the bounded angles property and on the distance between the tracks of the grid. It is then straightforward to adapt the proof to graphs with the conditions of [GM14].

Then, there exist constants $C, c > 0$ such that (3.32) is satisfied. The constants C, c depend only on C_0, c_0, on the parameter ε such that $\mathbb{G} \in \mathcal{G}(\varepsilon)$ and on the size of the fundamental domain of $\mathbb{G}$.

Observe that (3.33) may seem weaker than (3.32). Indeed, while $\varphi^0_{\mathbb{G}}$ is the limit of $\varphi^0_{\Lambda(N)}$ as $N \to \infty$, the limit of the measures $\varphi^0_{\mathsf{R}^{\mathrm{hp}}(N;N)}$ is what would naturally be called the half-plane infinite-volume measure with free boundary conditions. Connections departing from 0 in the latter measure are (potentially) considerably less likely than in $\varphi^0_{\mathbb{G}}$ due to their proximity to a boundary with the free boundary conditions.

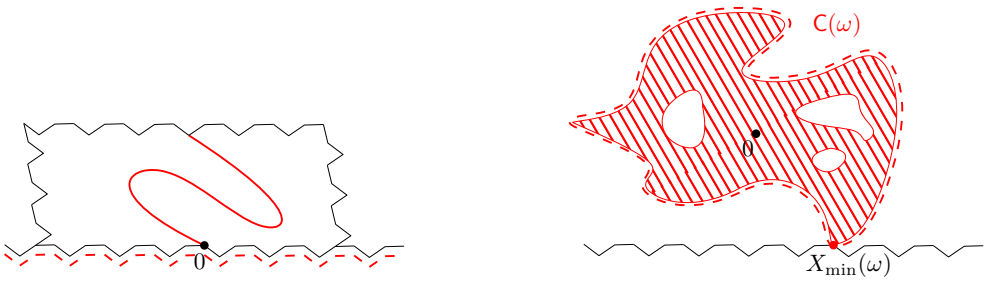

Figure 3.16 – **Left:** The event of (3.33). **Right:** If $X_{\min}$ is the lowest point of the cluster of 0 in $\Lambda(N)$, then the environment around $X_{\min}$ is less favourable to connections than that of the left image.

Proof. Fix $N \geqslant 1$. We will prove (3.32) for the measure $\varphi^0_{\Lambda(N)}$ instead of $\varphi^0_{\mathbb{G}}$. It will be apparent from the proof that the constants c, C do not depend on N. Thus N may be taken to infinity, and this will provide the desired conclusion.

For simplicity of notation, let us assume that the grid $(s_n), (t_n)$ of $\mathbb{G}$ is such that $\mathsf{R}(0,1;0,1)$ is a fundamental domain of $\mathbb{G}$. Recall that $x_{i,j}$ denotes the vertex of $\mathbb{G}$ just to the left of s_i and just below t_j. Then, all vertices $x_{i,j}$ are translates of 0 by vectors that leave $\mathbb{G}$ invariant. Write $\|x_{i,j}\| = \max\{|i|,|j|\}$, in accordance with the notation $\Lambda(\cdot)$.

For a random-cluster configuration ω on $\Lambda(N)$, let $\mathsf{C}(0)$ denote the connected component of the origin. Let $X_{\min} = X_{\min}(\omega)$ be a point $x_{i,j}$ of minimal index j such that $\mathsf{C}(0)$ intersects $x_{i,j} + \mathsf{R}(0,1;0,1)$. If several such points exist, choose one according to some rule (e.g., that of minimal i). We will estimate the connection probability $\varphi^0_{\Lambda(N)}\big[0 \leftrightarrow \partial\Lambda(n)\big]$ by studying the possible values of $X_{\min}(\omega)$:

$$\varphi^0_{\Lambda(N)}\big[0 \leftrightarrow \partial\Lambda(n)\big] = \sum_{\substack{-N\leqslant i\leqslant N\\ -N\leqslant j\leqslant 0}} \varphi^0_{\Lambda(N)}\big[0 \leftrightarrow \partial\Lambda(n) \text{ and } X_{\min} = x_{i,j}\big]. \tag{3.34}$$

Fix i, j as in the sum and write $\mathsf{C}(x_{i,j})$ for the connected component of $x_{i,j}$. By the finite energy property, there exists η depending only on the bounded angles property and the size of the fundamental domain of $\mathbb{G}$ such that

$$\varphi^0_{\Lambda(N)}\big[0 \leftrightarrow \partial\Lambda(n) \text{ and } X_{\min} = x_{i,j}\big] \leqslant \eta\, \varphi^0_{\Lambda(N)}\big[0 \leftrightarrow x_{i,j} \leftrightarrow \partial\Lambda(n) \text{ and } X_{\min} = x_{i,j}\big].$$

Notice that if the event on the right-hand side above occurs, then $x_{i,j}$ is connected to "distance" $r := \max\{\|x_{i,j}\|, \frac{n}{2}\}$; that is $x_{i,j} \leftrightarrow x_{i,j} + \partial\Lambda(r)$. Moreover, the connected component of

$x_{i,j}$ is contained above track t_j. By the translation invariance and the comparison between boundary conditions,

$$\begin{aligned}&\varphi^0_{\Lambda(N)}\Big[x_{i,j} \leftrightarrow x_{i,j} + \partial\Lambda(r) \text{ and } \mathrm{C}(x_{i,j}) \text{ contained above } t_j\Big]\\ &\leqslant \varphi^0_{\Lambda(2N)}\Big[0 \leftrightarrow \partial\Lambda(r) \text{ and } \mathrm{C}(0) \text{ contained above } t_0\Big]\end{aligned}$$

Let Γ^* be the lowest dual left-right crossing of $\Lambda(2N)$ contained above t_0 (actually we allow Γ^* to use the faces of $\mathbb{G}^\diamond$ below t_0 but adjacent to it). If $\mathrm{C}(0)$ is contained above t_0, then Γ^* passes under $\mathrm{C}(0)$. By conditioning on the values γ^* that Γ^* may take and using the comparison between boundary conditions we find

$$\begin{aligned}&\varphi^0_{\Lambda(2N)}\Big[0 \leftrightarrow \partial\Lambda(r) \text{ and } \mathrm{C}(0) \text{ contained above } t_0\Big]\\ &\quad\leqslant \sum_{\gamma^*} \varphi^0_{\Lambda(2N)}\Big[0 \leftrightarrow \partial\Lambda(r) \text{ and } \mathrm{C}(0) \text{ contained above } \gamma^* \,|\, \Gamma^* = \gamma^*\Big]\varphi^0_{\Lambda(2N)}\Big[\Gamma^* = \gamma^*\Big]\\ &\quad\leqslant \sum_{\gamma^*} \varphi^0_{\mathsf{R}^{\mathrm{hp}}(2N;2N)}\Big[0 \leftrightarrow \partial\Lambda(r)\Big]\varphi^0_{\Lambda(2N)}\Big[\Gamma^* = \gamma^*\Big] \leqslant C\exp(-cr).\end{aligned}$$

The last inequality is due to (3.33). Inserting this into (3.34) (recall that $r = \max\{\|x_{i,j}\|, \frac{n}{2}\}$) we find

$$\begin{aligned}\varphi^0_{\Lambda(N)}\Big(0 \leftrightarrow \partial\Lambda(n)\Big) &= \sum_{\substack{-N\leqslant i\leqslant N\\ -N\leqslant j\leqslant 0}} \eta C\exp(-c\max\{\|x_{i,j}\|; n/2\})\\ &\leqslant \tfrac{n^2}{2}\eta C\exp(-\tfrac{c}{2}n) + \sum_{k>n} 2k\eta C\exp(-ck)\\ &\leqslant C'\exp(-c'n),\end{aligned}$$

for some adjusted constants $c', C' > 0$ that do not depend on n or N. Taking $N \to \infty$, we obtain the desired conclusion.

□

The following result will serve as the input to our procedure. It concerns only the regularly embedded square lattice and is a consequence of [DCST17] and [DGH+16]. For coherence with the notation above, we consider the square lattice as having edge-length $\sqrt{2}$ and rotated by $\frac{\pi}{4}$ with respect to its usual embedding. This is such that the diamond graph has vertices $\{(a,b) : a,b \in \mathbb{Z}\}$, with those with $a+b$ even being primal vertices. In a slight abuse of notation, write $\mathbb{Z}^2$ for the lattice thus embedded.

Write $\varphi^{1/0}_{\mathsf{R}^{\mathrm{hp}}(N;N)}$ for the random-cluster measure on the domain $\mathsf{R}^{\mathrm{hp}}(N;N)$ of $\mathbb{Z}^2$ with $\beta = 1$, free boundary conditions on $[-N,N]\times\{0\}$ and wired boundary conditions for the rest of the boundary. Also define $\mathbb{H} = \mathbb{Z}\times\mathbb{N}$ to be the upper-half plane of $\mathbb{Z}^2$. Write $\varphi^{1/0}_{\mathbb{H}}$ for the half-plane random-cluster measure which is the weak (decreasing) limit of $\varphi^{1/0}_{\mathsf{R}^{\mathrm{hp}}(N;N)}$ for $N \to \infty$.

Proposition 3.24. *For the regular square lattice and $q > 4$, there exist constants $C_0, c_0 > 0$ such that, for all $n \geqslant 1$,*

$$\varphi^{1/0}_{\mathbb{H}}\Big[0 \leftrightarrow \partial\Lambda(n)\Big] \leqslant C_0\exp(-c_0 n). \tag{3.35}$$

Proof. Fix $q > 4$. It is shown in [DGH+16] that the phase transition of the random-cluster measure on $\mathbb{Z}^2$ is discontinuous and that the critical measure with free boundary conditions exhibits exponential decay. That is, $\varphi^0_{\mathbb{Z}^2}$ satisfies (3.32) for some constants $C, c > 0$. To prove (3.35), it suffices to show that the weak limit $\varphi^{1/0}_{\mathbb{H}}$ of the measures $\varphi^{1/0}_{\mathsf{R}^{\mathrm{hp}}(N;N)}$ has no infinite cluster almost surely. Indeed, then $\varphi^{1/0}_{\mathbb{H}}$ is stochastically dominated by $\varphi^0_{\mathbb{Z}^2}$.

The rest of the proof is dedicated to showing that $\varphi^{1/0}_{\mathbb{H}}\big[0 \leftrightarrow \infty\big] = 0$, and we do so by contradiction. Assume the opposite. By ergodicity of $\varphi^{1/0}_{\mathbb{H}}$, for any $\varepsilon > 0$, there exists $N > 0$ such that

$$\varphi^{1/0}_{\mathbb{H}}\big[\Lambda(N) \leftrightarrow \infty\big] \geqslant 1 - \varepsilon. \tag{3.36}$$

Furthermore, $\varphi^{1/0}_{\mathbb{H}}$ is also the decreasing limit of the measures $\varphi^{1/0}_{\mathbb{S}_\ell}$, where $\mathbb{S}_\ell = \mathbb{Z} \times [0, \ell]$ and $1/0$ refers to the boundary conditions which are wired on the top and free on the bottom of the strip $\mathbb{S}_\ell$ (boundary conditions at infinity on the left and right are irrelevant since the strip is essentially one dimensional). Therefore,

$$\varphi^{1/0}_{\mathbb{S}_{4N}}\big[\Lambda(N) \leftrightarrow \text{ top of } \mathbb{S}_{4N}\big] \geqslant 1 - \varepsilon. \tag{3.37}$$

In [DCST17], Lemma 2 [7] shows that

$$\varphi^{1/0}_{\mathbb{S}_{4N}}\big[\mathcal{C}^*_h(-4N, 4N; N, 3N)\big] \geqslant c_1,$$

for some constant $c_1 > 0$ not depending on N. If $\mathcal{C}^*_h(-4N, 4N; N, 3N)$ occurs, denote by Γ^* the top-most dual crossing in its definition. Moreover, let A be the event that Γ^* is connected to the line $\mathbb{Z} \times \{0\}$ by two dually-open paths contained in $\mathsf{R}(-4N, -N; 0, 3N)$ and $\mathsf{R}(N, 4N; 0, 3N)$, respectively (see Figure 3.17). Then, using the comparison between boundary conditions and the self-duality of the model, we deduce the existence of $c_2 > 0$ such that

$$\varphi^{1/0}_{\mathbb{S}_{4N}}\big[A \,\big|\, \mathcal{C}^*_h(-4N, 4N; N, 3N)\big] \geqslant c_2. \tag{3.38}$$

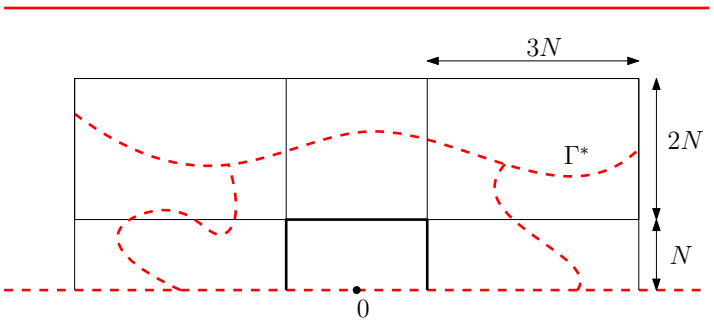

Figure 3.17 – The strip $\mathbb{S}_{4N}$ with wired boundary conditions on the top and free on the bottom. If $\mathcal{C}^*_h(-4N, 4N; N, 3N) \cap A$ occurs, then $\Lambda(N)$ is disconnected from the top of the strip. Due to the self-duality, both $\mathcal{C}^*_h(-4N, 4N; N, 3N)$ and A conditionally on $\mathcal{C}^*_h(-4N, 4N; N, 3N)$ occur with positive probability.

[7] Actually a slight adaptation of [DCST17, Lem. 2] is necessary to account for the rotation by $\frac{\pi}{4}$ of the lattice.

Notice that, if $\mathcal{C}_h^*(-4N, 4N; N, 3N)$ and A both occur, then $\Lambda(N)$ may not be connected to the top of $\mathbb{S}_{4N}$ by an open path. Thus

$$\varphi^{1/0}_{\mathbb{S}_{4N}}\Big[\Lambda(N) \leftrightarrow \text{ top of } \mathbb{S}_{4N}\Big] \leqslant 1 - c_1 c_2.$$

This contradicts (3.37) for $\varepsilon < c_1 c_2$, and the proof is complete. □

The proof of (3.32) is done in two stages, first it is proved for isoradial square lattices, then for arbitrary doubly-periodic isoradial graphs.

3.4.1 Isoradial square lattices

The proof of (3.33) for isoradial embeddings of square lattices follows the procedure of Section 3.3.2. That is, two lattices with same transverse angles for the vertical tracks are glued along a horizontal track. Track exchanges are performed, and estimates as those of (3.33) are transported from one lattice to the other.

Transforming the regular lattice $\mathbb{Z}^2$ into an arbitrary isoradial one is done in two steps: first $\mathbb{Z}^2$ is transformed into a lattice with constant transverse angles for vertical tracks; then the latter (or rather its rotation) is transformed into a general isoradial square lattice. For technical reasons, we will perform the two parts separately.

We should mention that some significant difficulties arise in this step due to the long-range effect of boundary conditions. Indeed, recall that in order to perform track exchanges, the graph needs to be convexified. This completion affects boundary conditions in an uncontrolled manner, which in this case is crucial. Two special arguments are used to circumvent these difficulties; hence the two separate stages in the proof below.

Recall the notation $\mathbb{G}_{\boldsymbol{\alpha},\boldsymbol{\beta}}$ for the isoradial square lattice with transverse angles $\boldsymbol{\alpha} = (\alpha_n)_{n\in\mathbb{Z}}$ for the vertical train tracks $(s_n)_{n\in\mathbb{Z}}$ and $\boldsymbol{\beta} = (\beta_n)_{n\in\mathbb{Z}}$ for the horizontal train tracks $(t_n)_{n\in\mathbb{Z}}$. Write 0 (also written $x_{0,0}$) for the vertex of $\mathbb{G}_{\boldsymbol{\alpha},\boldsymbol{\beta}}$ just below track t_0 and just to the left of s_0. We will always assume that $\mathbb{G}_{\boldsymbol{\alpha},\boldsymbol{\beta}}$ is indexed such that 0 is a primal vertex.

The result of the first part is the following.

Proposition 3.25. *Let $\mathbb{G}_{0,\boldsymbol{\beta}}$ be an isoradial square lattice in $\mathcal{G}(\varepsilon)$ for some $\varepsilon > 0$, with transverse angles 0 for all vertical tracks. Then, there exist constants $C, c > 0$ depending on ε only such that*

$$\varphi^0_{\mathsf{R}^{hp}(N;N)}\Big[0 \leftrightarrow \partial\Lambda(n)\Big] \leqslant C\exp(-cn), \qquad \forall n < N. \tag{3.39}$$

Proof. Fix a lattice $\mathbb{G}_{0,\boldsymbol{\beta}}$ as in the statement. For integers $2n < N$, let G_{mix} be the mixture of $\mathbb{G}_{0,\boldsymbol{\beta}}$ and $\mathbb{Z}^2$, as described in Section 3.2. Notice that here the order of the regular block (that of $\mathbb{Z}^2$) and the irregular one (that of $G_{0,\boldsymbol{\beta}}$) is opposite to that in the previous section.

In this proof, the mixed graph is only constructed above the base level; it has $2N+1$ vertical tracks $(s_i)_{-N\leqslant i\leqslant N}$ of transverse angle 0 and $2N+2$ horizontal tracks $(t_j)_{0\leqslant j\leqslant 2N+1}$, the first $N+1$ having transverse angles $\beta_0, \beta_1, \dots, \beta_N$, respectively and the following $N+1$ having transverse angles $\frac{\pi}{2}$. Finally, G_{mix} is a convexification of the piece of square lattice described above.

Set $\widetilde{G}_{\text{mix}}$ to be the result of the inversion of the regular and irregular blocks of G_{mix} using the sequence of transformations $\Sigma^{\uparrow}$. Let $\varphi_{G_{\text{mix}}}$ and $\varphi_{\widetilde{G}_{\text{mix}}}$ be the random-cluster measures with the free boundary conditions on G_{mix} and $\widetilde{G}_{\text{mix}}$ respectively. The latter is then the push-forward of the former by the sequence of transformations $\Sigma^{\uparrow}$.

Let $\delta_0 \in (0,1)$ be a constant that will be set below; it will be chosen only depending on ε and q. Write ∂_L, ∂_R and ∂_T for the left, right and top boundaries, respectively, of a rectangular domain $\mathsf{R}^{\mathrm{hp}}(.;.)$.

Consider a configuration ω on G_{mix} such that the event $\{0 \leftrightarrow \partial\Lambda(n)\}$ occurs. Then, 0 is connected in ω to either $\partial_L\mathsf{R}^{\mathrm{hp}}(n;\delta_0 n)$, $\partial_R\mathsf{R}^{\mathrm{hp}}(n;\delta_0 n)$ or $\partial_T\mathsf{R}^{\mathrm{hp}}(n;\delta_0 n)$. Thus,

$$\begin{aligned}\varphi_{G_{\mathrm{mix}}}\Big[0 \leftrightarrow \partial\Lambda(n)\Big] \leqslant{}& \varphi_{G_{\mathrm{mix}}}\Big[0 \xleftrightarrow{\mathsf{R}^{\mathrm{hp}}(n;\delta_0 n)} \partial_L\mathsf{R}^{\mathrm{hp}}(n;\delta_0 n)\Big]\\ &+\varphi_{G_{\mathrm{mix}}}\Big[0 \xleftrightarrow{\mathsf{R}^{\mathrm{hp}}(n;\delta_0 n)} \partial_R\mathsf{R}^{\mathrm{hp}}(n;\delta_0 n)\Big]\\ &+\varphi_{G_{\mathrm{mix}}}\Big[0 \xleftrightarrow{\mathsf{R}^{\mathrm{hp}}(n;\delta_0 n)} \partial_T\mathsf{R}^{\mathrm{hp}}(n;\delta_0 n)\Big]. \qquad (3.40)\end{aligned}$$

Moreover, since the graph G_{mix} and $G_{0,\beta}$ are identical in the ball of radius N around 0 for the graph-distance,

$$\varphi^0_{\mathsf{R}^{\mathrm{hp}}(N;N)}\Big[0 \leftrightarrow \partial\Lambda(n)\Big] \leqslant \varphi_{G_{\mathrm{mix}}}\Big[0 \leftrightarrow \partial\Lambda(n)\Big], \qquad (3.41)$$

where in the left-hand side $\mathsf{R}^{\mathrm{hp}}(N;N)$ denotes the rectangular domain of $G_{0,\beta}$. We used above the comparison between boundary conditions.

In conclusion, in order to obtain (3.39), it suffices to prove that the three probabilities of the right-hand side of (3.40) are bounded by an expression of the form Ce^{-cn}, uniformly in N. We concentrate on this from now on.

Let us start with the last line of (3.40). Recall Proposition 3.16; a straightforward adaptation reads:

Adaptation of Proposition 3.16. *There exist $\delta > 0$ and $c_n > 0$ satisfying $c_n \to 1$ as $n \to \infty$ such that, for all n and sizes $N \geqslant 4n$,*

$$\varphi_{\widetilde{G}_{mix}}\Big[0 \xleftrightarrow{\mathsf{R}^{hp}(4n;\delta\delta_0 n)} \partial_T\mathsf{R}^{hp}(4n;\delta\delta_0 n)\Big] \geqslant c_n\varphi_{G_{mix}}\Big[0 \xleftrightarrow{\mathsf{R}^{hp}(n;\delta_0 n)} \partial_T\mathsf{R}^{hp}(n;\delta_0 n)\Big]. \qquad (3.42)$$

The proof of the above is identical to that of Proposition 3.16. The constant δ and the sequence $(c_n)_n$ only depend on ε and q.

By the comparison between boundary conditions,

$$\begin{aligned}\varphi_{\widetilde{G}_{\mathrm{mix}}}\Big[0 \xleftrightarrow{\mathsf{R}^{\mathrm{hp}}(4n;\delta\delta_0 n)} \partial_T\mathsf{R}^{\mathrm{hp}}(4n;\delta\delta_0 n)\Big] &\leqslant \varphi^{1/0}_{\mathsf{R}^{\mathrm{hp}}(N;N)}\Big[0 \leftrightarrow \partial\Lambda(\delta\delta_0 n)\Big]\\ &\leqslant C_0\exp(-c_0\delta\delta_0 n).\end{aligned}$$

The second inequality is due to Proposition 3.24 and to the fact that the rectangle $\mathsf{R}^{\mathrm{hp}}(N;N)$ of $\widetilde{G}_{\mathrm{mix}}$ is fully contained in the regular block. Thus, from (3.42) and the above, we obtain,

$$\varphi_{G_{\mathrm{mix}}}\Big[0 \xleftrightarrow{\mathsf{R}^{\mathrm{hp}}(4n;\delta_0 n)} \partial_T\mathsf{R}^{\mathrm{hp}}(4n;\delta_0 n)\Big] \leqslant \frac{C_0}{c_n}\exp(-c_0\delta\delta_0 n). \qquad (3.43)$$

For n large enough, we have $c_n > 1/2$, and the left-hand side of (3.43) is smaller than $2C_0\exp(-c_0\delta\delta_0 n)$. Since the threshold for n and the constants c_0, δ and δ_0 only depend on ε and q, the bound is of the required form.

We now focus on bounding the probabilities of connection to the left and right boundaries of $\mathsf{R}^{\mathrm{hp}}(n;\delta_0 n)$. Observe that, for a configuration in the event $\{0 \xleftrightarrow{\mathsf{R}^{\mathrm{hp}}(n;\delta_0 n)} \partial_R \mathsf{R}^{\mathrm{hp}}(n;\delta_0 n)\}$, it suffices to change the state of at most $\delta_0 n$ edges to connect 0 to the vertex $x_{0,n}$ (we will assume here n to be even, otherwise $x_{0,n}$ should be replaced by $x_{0,n+1}$). By the finite-energy property, there exists a constant $\eta = \eta(\varepsilon, q) > 0$ such that

$$\varphi_{G_{\mathrm{mix}}}\Big[0 \xleftrightarrow{\mathsf{R}^{\mathrm{hp}}(n;\delta_0 n)} \partial_R \mathsf{R}^{\mathrm{hp}}(n;\delta_0 n)\Big] \leqslant \exp(\eta\delta_0 n)\, \varphi_{G_{\mathrm{mix}}}\Big[0 \leftrightarrow x_{0,n}\Big].$$

The points 0 and $x_{0,n}$ are not affected by the transformations in $\Sigma^{\uparrow}$, therefore

$$\begin{aligned}\varphi_{G_{\mathrm{mix}}}\Big[0 \leftrightarrow x_{0,n}\Big] &= \varphi_{\widetilde{G}_{\mathrm{mix}}}\Big[0 \leftrightarrow x_{0,n}\Big] \\ &\leqslant \varphi_{\widetilde{G}_{\mathrm{mix}}}\Big[0 \leftrightarrow \partial\Lambda(n)\Big] \\ &\leqslant \varphi^{1/0}_{\mathsf{R}^{\mathrm{hp}}(N;N)}\Big[0 \leftrightarrow \partial\Lambda(n)\Big] \leqslant C_0 \exp(-c_0 n),\end{aligned}$$

where in the last line, $\mathsf{R}^{\mathrm{hp}}(N;N)$ is a subgraph of $\widetilde{G}_{\mathrm{mix}}$, or equivalently of $\mathbb{Z}^2$ since these two are identical. The last inequality is given by Proposition 3.24. We conclude that,

$$\varphi_{G_{\mathrm{mix}}}\Big[0 \xleftrightarrow{\mathsf{R}^{\mathrm{hp}}(n;\delta_0 n)} \partial_R \mathsf{R}^{\mathrm{hp}}(n;\delta_0 n)\Big] \leqslant C_0 \exp\Big[-(c_0 - \delta_0\eta)n\Big]. \tag{3.44}$$

The same procedure also applies to $\{0 \xleftrightarrow{\mathsf{R}^{\mathrm{hp}}(n;\delta_0 n)} \partial_L \mathsf{R}^{\mathrm{hp}}(n;\delta_0 n)\}$.

Suppose now that $\delta_0 = \frac{c_0}{c_0\delta+\eta}$ is chosen such that

$$c := c_0 - \delta_0\eta = c_0\delta\delta_0 > 0.$$

Note that $\delta_0 \in (0,1)$ since $\eta \geqslant c_0$ and that c depends only on ε and q. Then, (3.40), (3.43) and (3.44) imply that for n larger than some threshold depending only on ε,

$$\varphi_{G_{\mathrm{mix}}}\Big[0 \leftrightarrow \partial\Lambda(n)\Big] \leqslant 4C_0 \exp(-cn).$$

Finally, by (3.41), we deduce (3.39) for all $N \geqslant 2n$ and n large enough. The condition on n may be removed by adjusting the constant C; the bound on N is irrelevant, since the left-hand side of (3.39) is increasing in N. □

The same argument may not be applied again to obtain (3.39) for general isoradial square lattices since it uses the bound (3.35), which we have not proved for lattices of the form $\mathbb{G}_{0,\beta}$. Indeed, (3.35) is not implied by (3.39) when no rotational symmetry is available. A different argument is necessary for this step.

We draw the attention of the reader to the fact that the lattice of Proposition 3.25 was not assumed to be doubly-periodic, neither will be the following one.

Proposition 3.26. *Let $\mathbb{G}_{\alpha,\beta}$ be an isoradial square lattice in $\mathcal{G}(\varepsilon)$ for some $\varepsilon > 0$. Then, there exist constants $C, c > 0$ depending only on ε, such that*

$$\varphi^{0}_{\mathsf{R}^{hp}(N;N)}\Big[0 \leftrightarrow \partial\Lambda(n)\Big] \leqslant C\exp(-cn), \qquad \forall n < N. \tag{3.45}$$

Proof. Fix a lattice $\mathbb{G}_{\alpha,\beta}$ as in the statement. The proof follows the same lines as that of Proposition 3.25, with certain small alterations.

Set $\theta = \frac{1}{2}(\inf\{\beta_n : n \in \mathbb{Z}\} + \sup\{\alpha_n : n \in \mathbb{Z}\})$ and write $\mathbb{G}_{\boldsymbol{\alpha},\theta}$ for the lattice with transverse angles $\boldsymbol{\alpha}$ for vertical tracks and constant angle θ for all horizontal tracks. We will refer to this lattice as *regular*.

For integers $2n \leqslant N < M$, define G_{mix} to be the mixture of $\mathbb{G}_{\boldsymbol{\alpha},\boldsymbol{\beta}}$ and $\mathbb{G}_{\boldsymbol{\alpha},\theta}$ as in the previous proof, with the exception that, while both blocks have width $2N+1$ and the irregular block (that is that of $\mathbb{G}_{\boldsymbol{\alpha},\boldsymbol{\beta}}$) has height $N+1$, the regular block (that of $\mathbb{G}_{\boldsymbol{\alpha},\theta}$) has height $M+1$. Precisely, G_{mix} is the convexification of the lattice with $2N+1$ vertical tracks $(s_i)_{-N\leqslant i\leqslant N}$ of transverse angles $(\alpha_{-N},\dots,\alpha_N)$ and $M+N+2$ horizontal tracks $(t_j)_{0\leqslant j\leqslant M+N+1}$, the first $N+1$ having transverse angles $\beta_0,\dots,\beta_N$ and the following $M+1$ having transverse angle θ.

Recall that $\widetilde{G}_{\mathrm{mix}}$, which is the result of the inversion of the regular and irregular blocks of G_{mix} by $\Sigma^{\uparrow}$, may be chosen to be an arbitrary convexification of the lattice $G_{(\alpha_{-N},\dots,\alpha_N),(\theta,\dots,\theta,\beta_0,\dots,\beta_N)}$. More precisely, once such a convexification $\widetilde{G}_{\mathrm{mix}}$ is chosen, a series of star-triangle transformations $\Sigma^{\uparrow}$ may be exhibited. This fact will be useful later.

Write as before $\varphi_{G_{\mathrm{mix}}}$ and $\varphi_{\widetilde{G}_{\mathrm{mix}}}$ for the random-cluster measures with free boundary conditions on G_{mix} and $\widetilde{G}_{\mathrm{mix}}$, respectively. Then, by the comparison between boundary conditions,

$$\varphi^0_{\mathsf{R}^{\mathrm{hp}}(N;N)}\Big[0 \leftrightarrow \partial\Lambda(n)\Big] \leqslant \varphi_{G_{\mathrm{mix}}}\Big[0 \leftrightarrow \partial\Lambda(n)\Big],$$

where $\mathsf{R}^{\mathrm{hp}}(N;N)$ refers to the domain in $\mathbb{G}_{\boldsymbol{\alpha},\boldsymbol{\beta}}$, or equivalently in G_{mix} since the two are equal. Notice that the above inequality is valid for all M.

Let $\delta_0 \in (0,1)$ be a constant that will be set below. Using the same notation and reasoning as in the previous proof, we find

$$\begin{aligned}\varphi_{G_{\mathrm{mix}}}\Big[0 \leftrightarrow \partial\Lambda(n)\Big] &\leqslant \tfrac{1}{c_n}\varphi_{\widetilde{G}_{\mathrm{mix}}}\Big[0 \xleftrightarrow{\mathsf{R}^{\mathrm{hp}}(2n;\delta\delta_0 n)} \partial_T\mathsf{R}(2n;\delta\delta_0 n)\Big] + 2\exp(\eta\delta_0 n)\,\varphi_{\widetilde{G}_{\mathrm{mix}}}\Big[0 \leftrightarrow x_{0,n}\Big] \\ &\leqslant 2\varphi_{\widetilde{G}_{\mathrm{mix}}}\Big[0 \leftrightarrow \partial\Lambda(\delta\delta_0 n)\Big] + 2\exp(\eta\delta_0 n)\,\varphi_{\widetilde{G}_{\mathrm{mix}}}\Big[0 \leftrightarrow \partial\Lambda(n)\Big], \qquad (3.46)\end{aligned}$$

where $\delta > 0$ and $\eta > 0$ are constants depending only on ε and q. The latter inequality is only valid for n above a threshold also only depending on ε and q.

At this point, the previous proof used (3.35) to bound the right-hand side. Since this is no longer available, we will proceed differently.

As previously stated, we may choose the convexification for $\widetilde{G}_{\mathrm{mix}}$. Let it be such that the tracks with transverse angle θ are as low as possible. That is, $\widetilde{G}_{\mathrm{mix}}$ is such that, for any track t with transverse angle θ, any intersection below t involves one track with transverse angle θ. The existence of such a convexification is easily proved; rather than writing a formal proof, we prefer to direct the reader to the example of Figure 3.18.

Write $\widetilde{t}_0,\dots,\widetilde{t}_M$ for the tracks of transverse angle θ of $\widetilde{G}_{\mathrm{mix}}$, indexed in increasing order. Call $\widetilde{s}_{-2N-1},\dots,\widetilde{s}_N$ the tracks intersecting $\widetilde{t}_0$, ordered by their intersection points from left to right. Denote by $\widetilde{\alpha}_{-2N-1},\dots,\widetilde{\alpha}_N$ their transverse angles.

The family $\widetilde{s}_{-2N-1},\dots,\widetilde{s}_N$ contains all vertical tracks of the original graph $\mathbb{G}_{\boldsymbol{\alpha},\boldsymbol{\beta}}$ (that is those denoted by $s_{-N},\dots,s_N$) but also the horizontal tracks of $\mathbb{G}_{\boldsymbol{\alpha},\boldsymbol{\beta}}$ with transverse angles different from θ. Since $\theta < \beta_j$ for all $0 \leqslant j \leqslant N$, the latter intersect t_0 left of the former. Thus, $\widetilde{s}_i = s_i$ for $-N \leqslant i \leqslant N$, hence the indexing.

The region of $\widetilde{G}_{\mathrm{mix}}$ contained below $\widetilde{t}_M$ is a (finite part of a) square lattice. Precisely, it is the square lattice $G_{(\widetilde{\alpha}_i)_{-2N-1\leqslant i\leqslant N},(\theta)_{0\leqslant j\leqslant M}}$. Complete the sequence $(\widetilde{\alpha}_i)_{-2N-1\leqslant i\leqslant N}$ into a bi-infinite sequence $\widetilde{\boldsymbol{\alpha}} = (\widetilde{\alpha}_i)_{i\in\mathbb{Z}}$ by declaring all additional terms equal to $\widetilde{\alpha}_0$. Write $\widetilde{\mathsf{R}}(.,.;.,.)$

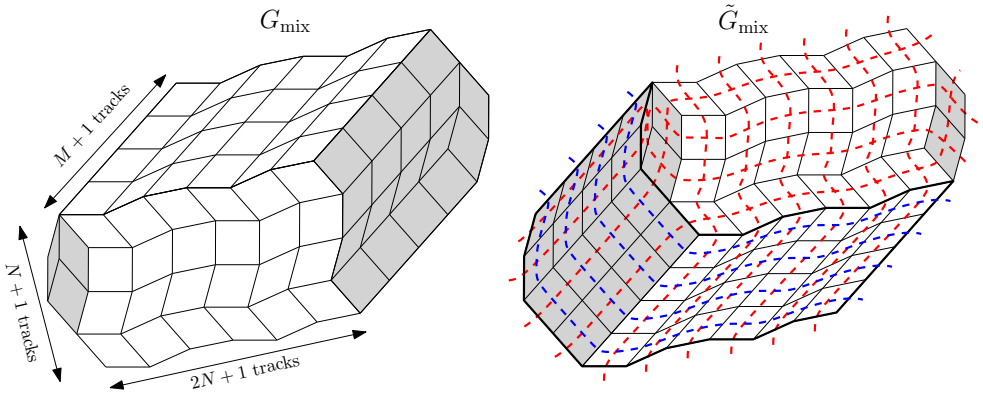

Figure 3.18 – **Left:** The diamond graph $G^{\diamond}_{\text{mix}}$ obtained by superposing a block of $\mathbb{G}^{\diamond}_{\alpha,\theta}$ to one of $\mathbb{G}^{\diamond}_{\alpha,\beta}$. The convexification is drawn in gray. **Right:** The diamond graph $\widetilde{G}^{\diamond}_{\text{mix}}$ with convexification (gray) chosen such that the tracks $\widetilde{t}_0,\dots,\widetilde{t}_M$ (blue) are as low as possible. This ensures that the region below $\widetilde{t}_M$ (delimited in bold) has a square lattice structure.

for the domains of $\mathbb{G}_{\widetilde{\alpha},\theta}$ defined in terms of the tracks $(\widetilde{s}_i)_{i\in\mathbb{Z}}$ and $(\widetilde{t}_j)_{j\in\mathbb{Z}}$. Also write $\mathsf{R}(.,.;.,.)$ for the domains of the original lattice $\mathbb{G}_{\alpha,\beta}$.

By the comparison between boundary conditions, for any increasing event A depending only on the region of $\widetilde{G}_{\text{mix}}$ below $\widetilde{t}_M$,

$$\varphi_{\widetilde{G}_{\text{mix}}}[A] \leqslant \varphi^{\xi}_{\widetilde{\mathsf{R}}(-2N-1,N;0,M)}[A],$$

where ξ are the boundary conditions which are wired on the top of $\widetilde{\mathsf{R}}(-2N-1,N;0,M)$ and free on the rest of the boundary. Thus, (3.46) implies that

$$\begin{aligned}&\varphi^{0}_{\mathsf{R}^{\text{hp}}(N;N)}\Big[0\leftrightarrow\partial\Lambda(n)\Big]\\ &\qquad\leqslant 2\varphi^{\xi}_{\widetilde{\mathsf{R}}(-2N-1,N;0,M)}\Big[0\leftrightarrow\partial\Lambda(\delta\delta_0 n)\Big]+2\exp(\eta\delta_0 n)\,\varphi^{\xi}_{\widetilde{\mathsf{R}}(-2N-1,N;0,M)}\Big[0\leftrightarrow\partial\Lambda(n)\Big].\end{aligned}$$

Since the above is true for all M, we may take M to infinity. Then, the measures $\varphi^{\xi}_{\widetilde{\mathsf{R}}(-2N-1,N;0,M)}$ tend decreasingly to the measure $\varphi^{0}_{\widetilde{\mathsf{R}}(-2N-1,N;0,\infty)}$ with free boundary conditions in the half-infinite strip. [8]. We conclude that

$$\begin{aligned}&\varphi^{0}_{\mathsf{R}^{\text{hp}}(N;N)}\Big[0\leftrightarrow\partial\Lambda(n)\Big]\\ &\qquad\leqslant 2\varphi^{0}_{\widetilde{\mathsf{R}}(-2N-1,N;0,\infty)}\Big[0\leftrightarrow\partial\Lambda(\delta\delta_0 n)\Big]+2\exp(\eta\delta_0 n)\,\varphi^{0}_{\widetilde{\mathsf{R}}(-2N-1,N;0,\infty)}\Big[0\leftrightarrow\partial\Lambda(n)\Big]\\ &\qquad\leqslant 2\varphi^{0}_{\mathbb{G}_{\widetilde{\alpha},\theta}}\Big[0\leftrightarrow\partial\Lambda(\delta\delta_0 n)\Big]+2\exp(\eta\delta_0 n)\,\varphi^{0}_{\mathbb{G}_{\widetilde{\alpha},\theta}}\Big[0\leftrightarrow\partial\Lambda(n)\Big].\end{aligned}\tag{3.47}$$

[8] This step is standard. Let A be an increasing event depending only on the state of edges in $\widetilde{\mathsf{R}}(-2N-1,N;0,M_0)$ for some M_0. Then, for any $M > M_0$, denote by Γ^* the highest dually-open horizontal crossing of $\widetilde{\mathsf{R}}(-2N-1,N;0,M)$ and set H to be the event that Γ^* does not intersect $\widetilde{\mathsf{R}}(-2N-1,N;0,M_0)$. Then, Γ^* may be explored from above, and standard arguments of comparison between boundary conditions imply that

$$\varphi^{\xi}_{\widetilde{\mathsf{R}}(-2N-1,N;0,M)}[A] \leqslant \varphi^{0}_{\widetilde{\mathsf{R}}(-2N-1,N;0,\infty)}[A]\,\varphi^{\xi}_{\widetilde{\mathsf{R}}(-2N-1,N;0,M)}[H]+\varphi^{\xi}_{\widetilde{\mathsf{R}}(-2N-1,N;0,M)}[H^c].$$

By the finite energy property and the fact that $\widetilde{\mathsf{R}}(-2N-1,N;0,\infty)$ has constant width, $\varphi^{\xi}_{\widetilde{\mathsf{R}}(-2N-1,N;0,M)}[H]\to 1$ as $M\to\infty$. This suffices to conclude.

Finally, the square lattice $\mathbb{G}_{\widetilde{\alpha},\theta}$ has constant transverse angle θ for all its horizontal tracks and, by choice of θ, is in $\mathcal{G}(\varepsilon/2)$. Thus, Proposition 3.25 applies to it (or rather to its rotation $\mathbb{G}_{0,(\widetilde{\alpha}_{-j}-\theta+\pi)_j}$). We conclude the existence of constants $C_0, c_0 > 0$ depending on ε only, such that

$$\varphi^0_{\mathbb{G}_{\widetilde{\alpha},\theta}}\Big[0 \leftrightarrow \partial\Lambda(k)\Big] \leqslant C_0 \exp(-c_0 k), \qquad \forall k \geqslant 1.$$

Set $\delta_0 = \frac{c_0}{c_0\delta+\eta}$ and

$$c = c_0 - \delta_0\eta = c_0\delta\delta_0 > 0.$$

Then c only depends on ε and q and the right hand side of (3.47) is bounded by $4C\exp(-cn)$, which provides the desired conclusion. □

The second proposition (Proposition 3.26) appears to use a weaker input than the first. One may therefore attempt to use the same argument for Proposition 3.25, so as to avoid using the more involved bound (3.35). Unfortunately, this is not possible, as the sequence of angles $\widetilde{\alpha}$ in the second proof may never be rendered constant, since it contains all the horizontal and vertical tracks of $\mathbb{G}_{\alpha,\beta}$.

3.4.2 Doubly-periodic isoradial graphs

Let $\mathbb{G}$ be an arbitrary doubly-periodic isoradial graph in some $\mathcal{G}(\varepsilon)$, with grid $(s_n)_{n\in\mathbb{Z}}, (t_n)_{n\in\mathbb{Z}}$. Denote by 0 the vertex just below and to the left of the intersection of t_0 and s_0. We will assume that it is a primal vertex. The goal of this section is the following.

Proposition 3.27. *There exist constants $c, C > 0$ depending only on ε and on the size of the fundamental domain of $\mathbb{G}$, such that*

$$\varphi^0_{\mathsf{R}^{hp}(N;N)}\Big[0 \leftrightarrow \partial\Lambda(n)\Big] \leqslant C\exp(-cn), \qquad \forall n < N. \tag{3.48}$$

Again, some care is needed when handling boundary conditions. Rather than working with $\mathbb{G}$ and modifications of it, we will construct a graph that locally resembles $\mathbb{G}$, but that allows us to control boundary conditions.

Proof. For $\rho \in [0,\pi)$, write $\mathcal{T}^{(\rho)}_{\mathbb{G}}$ for the set of tracks of $\mathbb{G}$ with asymptotic direction ρ (recall the existence of an asymptotic direction from the proof of Lemma 3.8). By periodicity, there exists a finite family $0 \leqslant \rho_0 < \cdots < \rho_T < \pi$ such that

$$\mathcal{T}_{\mathbb{G}} = \bigsqcup_{\ell=0}^{T} \mathcal{T}^{(\rho_\ell)}_{\mathbb{G}}.$$

Assume that the lattice is rotated such that the horizontal tracks $(t_n)_{n\in\mathbb{Z}}$ have asymptotic direction $\rho_0 = 0$. Fix constants $n < N$.

Let τ_L be the right-most track in $\mathcal{T}^{(\rho_T)}_{\mathbb{G}}$ that intersects t_0 left of 0 and does not intersect $\mathsf{R}^{\mathrm{hp}}(N;N)$. Similarly, define τ_R as the left-most track in $\mathcal{T}^{(\rho_1)}_{\mathbb{G}}$ that intersects t_0 right of 0 and does not intersect $\mathsf{R}^{\mathrm{hp}}(N;N)$. Denote by $\mathcal{D}_0$ the domain of $\mathbb{G}$ bounded by t_0 below, above by t_N, to the left by τ_L and to the right by τ_R. One may imagine $\mathcal{D}_0$ as a trapezoid with base t_0 and top t_N. By definition of τ_L and τ_R,

$$\mathsf{R}^{\mathrm{hp}}(N;N) \subset \mathcal{D}_0. \tag{3.49}$$

Complete $\mathcal{D}_0$ to form a bigger, finite graph $\mathcal{D}$ as follows. Let $\widetilde{s}_{K_-}, \dots, \widetilde{s}_{K_+}$ be the tracks of $\mathcal{D}_0$ that intersect t_0, ordered from left to right, with $\widetilde{s}_0 = s_0$. Orient these tracks upwards. Orient the remaining tracks $t_0, \dots, t_N$ from left to right.

In $\mathcal{D}$, we will make sure that $t_1, \dots, t_N$ intersect all tracks $(\widetilde{s}_i)_{K_- \leqslant i \leqslant K_+}$, but that no additional intersections between tracks $(\widetilde{s}_i)_{K_- \leqslant i \leqslant K_+}$ are introduced. One should imagine that the track t_1, after exiting $\mathcal{D}_0$, "slides down" on the side of $\mathcal{D}_0$; t_2 does the same: it slides down along the side of $\mathcal{D}_0$ until reaching t_1, then continues parallel to t_1, etc. The same happens on the left side. Finally, on top of the graph obtained above add a number of parallel tracks $t_{N+1}, \dots, t_M$ adjacent to each other, with constant transverse angle, for instance, that of t_N, for some $M > N$. Call the resulting graph $\mathcal{D}$. In $\mathcal{D}$, each track t_j with $0 \leqslant j \leqslant M$ intersects all tracks $(\widetilde{s}_i)_{K_- \leqslant i \leqslant K_+}$. We do not give a more formal description of the construction of $\mathcal{D}$; we rather direct the readers attention to Figure 3.19 for an illustration.

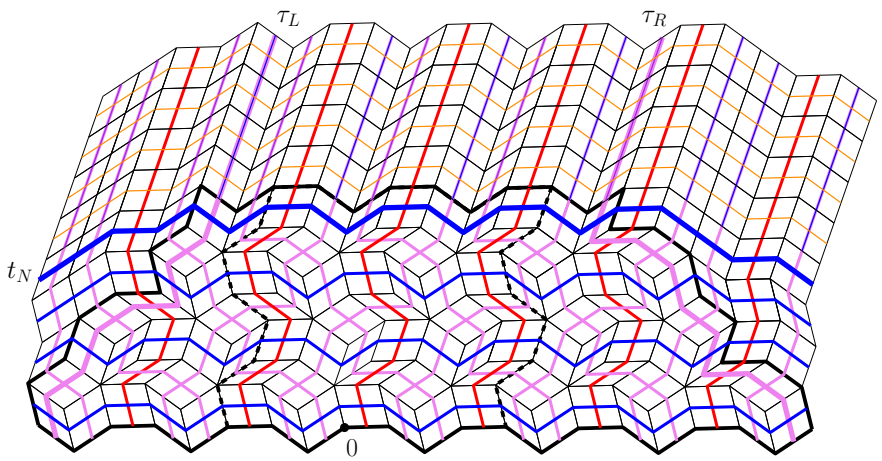

Figure 3.19 – A graph $\mathcal{D}_0$ (the delimited region) and the completion $\mathcal{D}$ – only the diamond graph is depicted. The vertical tracks (s_i) are red, horizontal tracks (t_j) blue, and the others purple. The rectangle $\mathsf{R}^{\mathrm{hp}}(N;N)$ (in reality it should be wider) is delimited by dotted lines. The tracks delimiting $\mathcal{D}_0$ are τ_L, τ_R and t_N; they are marked in bold.

In light of (3.49),

$$\varphi^0_{\mathsf{R}^{\mathrm{hp}}(N;N)}\big[0 \leftrightarrow \partial\Lambda(n)\big] \leqslant \varphi^0_{\mathcal{D}}\big[0 \leftrightarrow \partial\Lambda(n)\big], \tag{3.50}$$

where $\mathsf{R}^{\mathrm{hp}}(N;N)$ refers to the region of the graph $\mathbb{G}$.

Next, we transform $\mathcal{D}$ to create a square lattice. Call a *black point* of $\mathcal{D}$ any intersection of two tracks $\widetilde{s}_i$ and $\widetilde{s}_j$. Then, by a straightforward modification of Proposition 3.9, there exist star-triangle transformations $\sigma_1, \dots, \sigma_K$ applied to $\mathcal{D}$ such that, in $(\sigma_K \circ \cdots \circ \sigma_1)(\mathcal{D})$, there is no black point between t_0 and t_1. Moreover, all transformations $\sigma_1, \dots, \sigma_K$ act between t_0 and t_1.

The existence of $\sigma_1, \dots, \sigma_K$ is proved by eliminating one by one the back points of $\mathcal{D}$ between t_0 and t_1, starting with the top most. The main thing to observe is that, by the construction of $\mathcal{D}$, any black point between t_0 and t_1 is the intersection of two tracks $\widetilde{s}_i$ and $\widetilde{s}_j$, both of which intersect t_1 above.

Set $\Sigma_1 = \sigma_K \circ \cdots \circ \sigma_1$. Then, one may define recurrently sequences of transformations $(\Sigma_j)_{1 \leqslant j \leqslant M}$ such that

- each Σ_j acts on $(\Sigma_{j-1} \circ \cdots \circ \Sigma_1)(\mathbb{G})$ between t_{j-1} and t_j;

- in $(\Sigma_j \circ \cdots \circ \Sigma_1)(\mathbb{G})$, there are no black points below t_j.

Let $\overline{\mathcal{D}} = (\Sigma_M \circ \cdots \circ \Sigma_1)(\mathbb{G})$. Below t_M, $\overline{\mathcal{D}}$ is a rectangular part of a square lattice with width $K_+ - K_- + 1$ and height M.

Let $\widetilde{\boldsymbol{\alpha}} = (\widetilde{\alpha}_i)_{K_- \leqslant i \leqslant K_+}$ be the transverse angles of the tracks $(\widetilde{s}_i)_{K_- \leqslant i \leqslant K_+}$. Also, denote by $\widetilde{\boldsymbol{\beta}} = (\widetilde{\beta}_j)_{j \geqslant 0}$ the sequence of angles constructed as follows: for $0 \leqslant j \leqslant N$, $\widetilde{\beta}_j = \beta_j$ which is the transverse angles of t_j; for $j > N$, set $\widetilde{\beta}_j = \beta_N$. Then, the part of $\overline{\mathcal{D}}$ below t_M is a rectangular domain of the vertical strip of square lattice $G_{\widetilde{\boldsymbol{\alpha}},\widetilde{\boldsymbol{\beta}}}$. Moreover, also let us denote by $\mathbb{G}_{\widetilde{\boldsymbol{\alpha}},\widetilde{\boldsymbol{\beta}}}$ any completion of $G_{\widetilde{\boldsymbol{\alpha}},\widetilde{\boldsymbol{\beta}}}$ into a full plane square lattice. We note that the angles $\widetilde{\boldsymbol{\alpha}}$ and $\widetilde{\boldsymbol{\beta}}$ also are transverse angles of tracks in $\mathbb{G}$, therefore $\mathbb{G}_{\widetilde{\boldsymbol{\alpha}},\widetilde{\boldsymbol{\beta}}} \in \mathcal{G}(\varepsilon)$ as does $\mathbb{G}$.

By the same argument as for (3.47), for any fixed $j \leqslant N$,

$$\limsup_{M\to\infty} \varphi^0_{\overline{\mathcal{D}}}\big[0 \leftrightarrow \partial\Lambda(j)\big] \leqslant \varphi^0_{\mathbb{G}_{\widetilde{\boldsymbol{\alpha}},\widetilde{\boldsymbol{\beta}}}}\big[0 \leftrightarrow \partial\widetilde{\Lambda}(j)\big]. \tag{3.51}$$

In the above inequality, Λ denotes a square domain defined in terms of tracks (s_i) and (t_j) whereas $\widetilde{\Lambda}$ is defined in terms of tracks $(\widetilde{s}_i)$ and (t_j). We also notice that the box defined in terms of (s_i) is larger than that of $(\widetilde{s}_i)$. Proposition 3.26 applies to $\mathbb{G}_{\widetilde{\boldsymbol{\alpha}},\widetilde{\boldsymbol{\beta}}}$ and we deduce the existence of constants $c, C > 0$, depending only on ε, such that, for all $j \leqslant N$,

$$\limsup_{M\to\infty} \varphi^0_{\overline{\mathcal{D}}}\big[0 \leftrightarrow \partial\Lambda(j)\big] \leqslant \varphi^0_{\mathbb{G}_{\widetilde{\boldsymbol{\alpha}},\widetilde{\boldsymbol{\beta}}}}\big[0 \leftrightarrow \partial\Lambda(j)\big] \leqslant C\exp(-cj). \tag{3.52}$$

Let us now come back to connections in $\mathcal{D}$. These can be transformed into connections in $\overline{\mathcal{D}}$ via the sequence of star-triangle transformations $(\Sigma_j)_{1\leqslant j\leqslant M}$. We use the same decomposition as in the proofs of Section 3.4.1 to transfer the exponential decay in $\overline{\mathcal{D}}$ to that in $\mathcal{D}$.

Let ω be a configuration on $\mathcal{D}$ such that $0 \leftrightarrow \partial\Lambda(n)$. Then, either 0 is connected to the left or right sides of $\mathsf{R}^{\mathrm{hp}}(n;\delta_0 n)$ or it is connected to the top of $\mathsf{R}^{\mathrm{hp}}(n;\delta_0 n)$ inside $\mathsf{R}^{\mathrm{hp}}(n;\delta_0 n)$. The constant δ_0 used in this decomposition will be chosen below and will only depend on ε and q. Thus, we find,

$$\begin{aligned}\varphi^0_{\mathcal{D}}\big[0 \leftrightarrow \partial\Lambda(n)\big] \leqslant{}& \varphi^0_{\mathcal{D}}\big[0 \xleftrightarrow{\mathsf{R}^{\mathrm{hp}}(n;\delta_0 n)} \partial_L\mathsf{R}^{\mathrm{hp}}(n;\delta_0 n)\big]\\ &+ \varphi^0_{\mathcal{D}}\big[0 \xleftrightarrow{\mathsf{R}^{\mathrm{hp}}(n;\delta_0 n)} \partial_R\mathsf{R}^{\mathrm{hp}}(n;\delta_0 n)\big]\\ &+ \varphi^0_{\mathcal{D}}\big[0 \xleftrightarrow{\mathsf{R}^{\mathrm{hp}}(n;\delta_0 n)} \partial_T\mathsf{R}^{\mathrm{hp}}(n;\delta_0 n)\big].\end{aligned} \tag{3.53}$$

Let us now bound the three terms above separately. We start with the first two. By the finite-energy property, there exist a constant $\eta > 0$ depending only on ε and the fundamental domain of $\mathbb{G}$ and primal vertices x_- and x_+ just below t_0 (thus on the boundary of $\mathcal{D}$) left of s_{-n} and right of s_n, respectively, such that

$$\begin{aligned}&\varphi^0_{\mathcal{D}}\big[0 \xleftrightarrow{\mathsf{R}^{\mathrm{hp}}(n;\delta_0 n)} \partial_L\mathsf{R}^{\mathrm{hp}}(n;\delta_0 n)\big] \leqslant \exp(\eta\delta_0 n)\,\varphi^0_{\mathcal{D}}(0 \leftrightarrow x_-) \qquad \text{and}\\ &\varphi^0_{\mathcal{D}}\big[0 \xleftrightarrow{\mathsf{R}^{\mathrm{hp}}(n;\delta_0 n)} \partial_R\mathsf{R}^{\mathrm{hp}}(n;\delta_0 n)\big] \leqslant \exp(\eta\delta_0 n)\,\varphi^0_{\mathcal{D}}(0 \leftrightarrow x_+).\end{aligned} \tag{3.54}$$

Since the transformations $\Sigma_1, \ldots, \Sigma_M$ preserve connections between points on the boundary of $\mathcal{D}$,

$$\varphi^0_{\mathcal{D}}\big[0 \leftrightarrow x_-\big] = \varphi^0_{\overline{\mathcal{D}}}\big[0 \leftrightarrow x_-\big] \leqslant \varphi^0_{\overline{\mathcal{D}}}\big[0 \leftrightarrow \partial\Lambda(n)\big]. \tag{3.55}$$

The same holds for $\varphi^0_{\mathcal{D}}\big[0 \longleftrightarrow x_+\big]$.

Since each sequence of transformations Σ_k only acts below t_k, an open path connecting 0 to $\partial_T \mathsf{R}^{\mathrm{hp}}(n;\delta_0 n)$ in $\mathcal{D}$ is transformed into an open path connecting 0 to $t_{\delta_0 n-1}$ (Figure 3.5).

$$\begin{aligned}\varphi^0_{\mathcal{D}}\Big[0 \xleftrightarrow{\mathsf{R}^{\mathrm{hp}}(n;\delta_0 n)} \partial_T \mathsf{R}^{\mathrm{hp}}(n;\delta_0 n)\Big] &\leqslant \varphi^0_{\mathcal{D}}\big[0 \longleftrightarrow t_{\delta_0 n-1}\big] \\ &\leqslant \varphi^0_{\mathcal{D}}\big[0 \longleftrightarrow \partial\Lambda(\delta_0 n-1)\big] \\ &\leqslant C\exp(-c(\delta_0 n-1)). \end{aligned} \tag{3.56}$$

By injecting (3.54), (3.55) and (3.56) into (3.53), then further into (3.50), we find

$$\varphi^0_{\mathsf{R}^{\mathrm{hp}}(N;N)}\big[0 \leftrightarrow \partial\Lambda(n)\big] \leqslant 2\exp(\eta\delta_0 n)\,\varphi^0_{\mathcal{D}}\big[0 \leftrightarrow \partial\Lambda(n)\big] + \varphi^0_{\mathcal{D}}\big[0 \longleftrightarrow \partial\Lambda(\delta_0 n-1)\big].$$

The above is true for all M, and we may take $M \to \infty$. Using (3.52), we find

$$\varphi^0_{\mathsf{R}^{\mathrm{hp}}(N;N)}\big[0 \leftrightarrow \partial\Lambda(n)\big] \leqslant 2C\exp\big[-(c-\eta\delta_0)n\big] + C\exp\big[-c(\delta_0 n-1)\big].$$

Set $\delta_0 = \frac{c}{c+\eta}$ so that $c' := c - \delta_0\eta = c\delta_0 > 0$. Then, we deduce that

$$\varphi^0_{\mathsf{R}^{\mathrm{hp}}(N;N)}\big[0 \leftrightarrow \partial\Lambda(n)\big] \leqslant 3C\,e^c\,\exp(-c'n).$$

Since c and η only depend on ε, q and the size of the fundamental domain of $\mathbb{G}$, we obtain the desired result. □

3.4.3 Conclusion

Below, we show how the previous two parts imply Theorem 3.2 and Corollary 3.3 for $q > 4$. Fix a doubly-periodic isoradial graph $\mathbb{G}$ and one of its grids.

Proof of Theorem 3.2. Due to (3.48) and Proposition 3.23, $\mathbb{G}$ satisfies (3.32). Since $\mathbb{G}$ satisfies the bounded angles property for some $\varepsilon > 0$ and due to its periodicity, there exists a constant $\alpha > 0$ such that $\Lambda(n) \subseteq B_{\alpha n}$ for all $n \geqslant 1$. Then, (3.32) implies

$$\varphi^0_{\mathbb{G}}[0 \leftrightarrow \partial B_n] \leqslant \varphi^0_{\mathbb{G}}[0 \leftrightarrow \partial\Lambda(\tfrac{n}{\alpha})] \leqslant C\exp\Big(-\tfrac{c}{\alpha}n\Big). \tag{3.57}$$

This implies the second point of Theorem 3.2 with an adjusted value for c.

Let us now consider the model with wired boundary conditions. Recall that if ω is sampled according to $\varphi^1_{\mathbb{G}}$, then its dual configuration follows $\varphi^0_{\mathbb{G}^*}$. Since $\mathbb{G}^*$ is also a doubly-periodic isoradial graph, (3.57) applies to it.

For a dual vertex $y \in \mathbb{G}^*$, let $C(y)$ be the event that there exists a dually-open circuit going through y and surrounding the origin. The existence of such a circuit implies that the dual-cluster of y has radius at least $|y|$. Thus,

$$\varphi^1_{\mathbb{G}}\big[C(y)\big] \leqslant \varphi^0_{\mathbb{G}^*}\big[y \leftrightarrow y + \partial B_{|y|}\big] \leqslant C\exp(-c|y|),$$

for some $c, C > 0$ not depending on y [9]. Since the number of vertices in $\mathbb{G}^* \cap B_n$ is bounded by a constant times n^2, the Borel-Cantelli lemma applies and we obtain

$$\varphi^1_{\mathbb{G}}\big[C(y) \text{ for infinitely many } y \in \mathbb{G}^*\big] = 0.$$

The finite-energy property of $\varphi^1_{\mathbb{G}}$ then implies $\varphi^1_{\mathbb{G}}\big[0 \leftrightarrow \infty\big] > 0$. □

[9] We implicitly used here that (3.57) applies to $\varphi^0_{\mathbb{G}^*}$ and to any translate of it. This is true due to the periodicity of $\mathbb{G}^*$. A multiplicative constant depending on the size of the fundamental domain is incorporated in C.

Proof of Corollary 3.3 for $q > 4$. It is a well known fact that $\varphi^0_{\mathbb{G},\beta,q} = \varphi^1_{\mathbb{G},\beta,q}$ for all but countably many values of β (see for instance [Dum17, Thm 1.12] for a recent short proof that can be adapted readily to isoradial graphs). Thus, by the monotonicity of the measures $\varphi^0_{\mathbb{G},\beta,q}$, for any $\beta < 1$, $\varphi^0_{\mathbb{G},1,q}$ dominates $\varphi^1_{\mathbb{G},\beta,q}$. Theorem 3.2 then implies $\varphi^1_{\mathbb{G},\beta,q}(0 \leftrightarrow \infty) = 0$ and [Gri06, Thm. 5.33] yields $\varphi^1_{\mathbb{G},\beta,q} = \varphi^0_{\mathbb{G},\beta,q}$. This proves the uniqueness of the infinite volume measure for all $\beta < 1$. The first point of the corollary follows directly from Theorem 3.2 by the monotonicity mentioned above.

Since measures with $\beta > 1$ are dual to those with $\beta < 1$, the uniqueness of the infinite volume measure also applies when $\beta > 1$. The second point of the corollary follows from Theorem 3.2 by monotonicity. □

Chapter 4

Behavior of the quantum random-cluster model

4.1 Results

The random-cluster model admits a quantum version, as described in [Gri10, Sec. 9.3] for $q = 2$. Consider the set $\mathbb{Z} \times \mathbb{R}$ as a system of vertical axis. Let $\mathcal{C}$ and $\mathcal{B}$ be two independent Poisson point processes with parameters λ and μ respectively, the first on $\mathbb{Z} \times \mathbb{R}$, the second on $(\frac{1}{2} + \mathbb{Z}) \times \mathbb{R}$. Call the points of the former *cuts* and those of the latter *bridges*. For any realisation of the two processes, let ω be the subset of $\mathbb{R}^2$ formed of:

- the set $\mathbb{Z} \times \mathbb{R}$ with the exception of the points in $\mathcal{B}$;
- a horizontal segment of length 1 centered at every point of $\mathcal{C}$.

For a rectangle $R = [a, b] \times [c, b] \subset \mathbb{R}^2$ with $a, b \in \mathbb{Z}$, define the quantum random-cluster measure on R by weighing each configuration ω with respect to the number of clusters in ω. More precisely, we define $\varphi_{\mathcal{Q},R,\lambda,\mu}$ to be the quantum random-cluster measure with parameters λ, μ and $q > 0$ by

$$\mathrm{d}\varphi^0_{\mathcal{Q},R,\lambda,\mu}(\omega) \propto q^{k(\omega)} \mathrm{d}\mathbb{P}_{\lambda,\mu}(\omega)$$

where $\mathbb{P}_{\lambda,\mu}$ is the joint law of the Poisson point processes $\mathcal{B}$ and $\mathcal{C}$, and $k(\omega)$ is the number of connected components of $\omega \cap R$ (notice that this number is a.s. finite).

Similarly, one may define measures with wired boundary conditions $\varphi^1_{\mathcal{Q},R,\lambda,\mu}$ by altering the definition of k. Infinite-volume measures may be defined by taking limits over increasing rectangular regions R, as in the classical case.

As will be discussed in Chapter 4, the quantum model may be seen as a limit of isoradial models on increasingly distorted embeddings of the square lattice. As a result, statements similar to Theorems 3.1, 3.2 and Corollary 3.3 apply to the quantum setting. In particular, we identify the critical parameters as those with $\frac{\mu}{\lambda} = q$. This critical value has already been computed earlier in [Pfe70, BG09] for the case of the quantum Ising model ($q = 2$).

Theorem 4.1. *If $q \in [1, 4]$ and $\mu/\lambda = q$, then*

- $\varphi^1_{\mathcal{Q},\lambda,\mu}[0 \leftrightarrow \infty] = 0$ *and* $\varphi^0_{\mathcal{Q},\lambda,\mu} = \varphi^1_{\mathcal{Q},\lambda,\mu}$;
- *there exist $a, b > 0$ such that for all $n \geqslant 1$,*

$$n^{-a} \leqslant \varphi^0_{\mathcal{Q},\lambda,\mu}\Big[0 \leftrightarrow \partial B_n\Big] \leqslant n^{-b};$$

- *for any $\rho > 0$, there exists $c = c(\rho) > 0$ such that for all $n \geqslant 1$,*

$$\varphi^0_{\mathcal{Q},R,\lambda,\mu}\Big[\mathcal{C}_h(\rho n, n)\Big] \geqslant c,$$

where $R = [-(\rho+1)n, (\rho+1)n] \times [-2n, 2n]$ and $\mathcal{C}_h(\rho n, n)$ is the event that there exists a path in $\omega \cap [-\rho n, \rho n] \times [-n, n]$ from $\{-\rho n\} \times [-n, n]$ to $\{\rho n\} \times [-n, n]$.

If $q > 4$ and $\mu/\lambda = q$, then

- $\varphi^1_{\mathcal{Q},\lambda,\mu}[0 \leftrightarrow \infty] > 0$;
- *there exists $c > 0$ such that for all $n \geqslant 1$, $\varphi^0_{\mathcal{Q},\lambda,\mu}[0 \leftrightarrow \partial B_n] \leqslant \exp(-cn)$.*

Finally, if $\mu/\lambda \neq q$, then $\varphi^0_{\mathcal{Q},\lambda,\mu} = \varphi^1_{\mathcal{Q},\lambda,\mu}$ and

- *when $\mu/\lambda < q$, there exists $c_{\mu/\lambda} > 0$ such that for any $x, y \in \mathbb{Z} \times \mathbb{R}$,*

$$\varphi^0_{\mathcal{Q},\lambda,\mu}[x \leftrightarrow y] \leqslant \exp(-c_{\mu/\lambda}\|x - y\|).$$

- *when $\mu/\lambda > q$, $\varphi^0_{\mathcal{Q},\lambda,\mu}[0 \leftrightarrow \infty] > 0$.*

Notice that multiplying both λ and μ by a factor α is tantamount to dilating the configuration ω vertically by a factor of $1/\alpha$. Hence it is natural that only the ratio μ/λ plays a role in determining criticality.

However, for $q \in [1, 4]$, there are reasons to believe that for the specific values

$$\lambda = \frac{4r}{\sqrt{q(4-q)}} \quad \text{and} \quad \mu = \frac{4r\sqrt{q}}{\sqrt{4-q}},$$

the model is rotationally invariant at large scale, as will be apparent from the link to isoradial graphs.

4.2 Discretisation

Fix $\varepsilon > 0$ and consider the isoradial square lattice $\mathbb{G}^\varepsilon := \mathbb{G}_{\alpha,\beta}$ where $\alpha_n = 0$ for all n and $\beta_n = \varepsilon$ if n is even and $\beta_n = \pi - \varepsilon$ if n is odd. This was also defined in Section 1.2.4. See Figure 1.7 for an illustration.

Recall the notation $x_{i,j}$ with $i+j$ even for the primal vertices of $\mathbb{G}^\varepsilon$ (while $x_{i,j}$ with $i+j$ odd are the dual vertices). Also, recall the notation $\mathsf{R}(i, j; k, \ell)$ for the domains of $\mathbb{G}^\varepsilon$ contained between the vertical tracks s_i and s_j and the horizontal tracks t_k and t_ℓ.

Remind that $\mathbb{G}^\varepsilon$ contains two types of edges: those of length $2\sin(\frac{\varepsilon}{2})$ and those of length $2\cos(\frac{\varepsilon}{2})$. As we will take ε to 0, we call the first *short edges* and the latter *long edges*. And the associated critical parameters used to define $\varphi_{\mathbb{G}^\varepsilon}$ are given by (2.2) where we take $\theta_e = \varepsilon$ if e is a short edge; $\theta_e = \pi - \varepsilon$ if e is a long edge.

When $\varepsilon \to 0$, we have the following asymptotic behaviors,

$$\begin{aligned}
\text{if } 1 \leqslant q < 4, \quad & 1 - p_\varepsilon \sim \frac{2r\varepsilon}{\sqrt{q(4-q)}}, && p_{\pi-\varepsilon} \sim \frac{2r\varepsilon\sqrt{q}}{\sqrt{4-q}};\\
\text{if } q = 4, \quad & 1 - p_\varepsilon \sim \frac{\varepsilon}{2\pi}, && p_{\pi-\varepsilon} \sim \frac{2}{\pi}\varepsilon;\\
\text{if } q > 4, \quad & 1 - p_\varepsilon \sim \frac{2r\varepsilon}{\sqrt{q(q-4)}}, && p_{\pi-\varepsilon} \sim \frac{2r\varepsilon\sqrt{q}}{\sqrt{q-4}}.
\end{aligned}$$

Moreover, the length of a long edge converges to 2, while that of short edges decreases as $\varepsilon + o(\varepsilon)$. Thus, in the limit $\varepsilon \to 0$, the measure converges to the quantum FK model on a dilated lattice $2\mathbb{Z} \times \mathbb{R}$ with parameters

$$\begin{aligned} \text{if } 1 \leqslant q < 4, \quad \lambda_0 &= \frac{2r}{\sqrt{q(4-q)}}, & \mu_0 &= \frac{2r\sqrt{q}}{\sqrt{4-q}}; \\ \text{if } q = 4, \quad \lambda_0 &= \frac{1}{2\pi}, & \mu_0 &= \frac{2}{\pi}; \\ \text{if } q > 4, \quad \lambda_0 &= \frac{2r}{\sqrt{q(q-4)}}, & \mu_0 &= \frac{2r\sqrt{q}}{\sqrt{q-4}}. \end{aligned}$$

Note that λ_0 and μ_0 are continuous in q: when q goes to 4 either from above or from below, the common limits of λ_0 and μ_0 are exactly the values given by $q = 4$. A precise statement is given below in Proposition 4.2.

For the rest of the section, unless otherwise stated, we consider the quantum random-cluster model $\varphi^{\xi}_{\mathcal{Q}}$ on $\mathbb{Z} \times \mathbb{R}$ with parameters $\lambda = 2\lambda_0$ and $\mu = 2\mu_0$ and boundary conditions $\xi = 0, 1$. This is simply the limiting model discussed above rescaled by a factor 1/2. The infinite-volume measures with free and wired boundary conditions can be defined via weak limits as in the classical case. The quantum model with these parameters enjoys a self-duality property similar to that of the discrete model on $\mathbb{G}^{\varepsilon}$ with $\beta = 1$.

To distinguish the subgraphs of $\mathbb{G}^{\varepsilon}$ from those of $\mathbb{Z} \times \mathbb{R}$, we shall always put a superscript ε for those of $\mathbb{G}^{\varepsilon}$ and those of $\mathbb{Z} \times \mathbb{R}$ are always written in calligraphic letters.

For any subgraph $\mathcal{R}$ of $\mathbb{Z} \times \mathbb{R}$, we write $\varphi^{\xi}_{\mathcal{Q},\mathcal{R}}$ for the quantum random-cluster measure on $\mathcal{R}$ with boundary conditions $\xi = 0, 1$.

For $1 \leqslant q \leqslant 4$, we need to consider the counterparts of the horizontal and vertical crossing events given in Lemma 3.10, which can be studied via the convergence given in the following proposition.

Proposition 4.2. *For $a, b, c, d > 0$, let $\mathsf{R}^{\varepsilon} = \mathsf{R}(2c, \frac{2d}{\varepsilon})$ be a subgraph of $\mathbb{G}^{\varepsilon}$ and $\mathcal{R} = [-c, c] \times [-d, d]$ be a subgraph of $\mathbb{Z} \times \mathbb{R}$. Consider $\xi = 0, 1$, then*

$$\varphi^{\xi}_{\mathsf{R}^{\varepsilon}}\Big[\mathcal{C}_h(2a; \tfrac{2b}{\varepsilon})\Big] \xrightarrow[\varepsilon \to 0]{} \varphi^{\xi}_{\mathcal{Q},\mathcal{R}}\Big[\mathcal{C}_h(a; b)\Big], \tag{4.1}$$

$$\varphi^{\xi}_{\mathsf{R}^{\varepsilon}}\Big[\mathcal{C}_v(2a; \tfrac{2b}{\varepsilon})\Big] \xrightarrow[\varepsilon \to 0]{} \varphi^{\xi}_{\mathcal{Q},\mathcal{R}}\Big[\mathcal{C}_v(a; b)\Big]. \tag{4.2}$$

For $q \geqslant 4$, the event to consider is that given by (3.33), which is given as follows.

Proposition 4.3. *For any $N, n > 0$, let $\mathsf{R}^{\varepsilon} = \mathsf{R}(2N, \frac{2N}{\varepsilon})$ be a subgraph of $\mathbb{G}^{\varepsilon}$ and $\mathcal{R} = \Lambda(N) = [-N, N]^2$ be a subgraph of $\mathbb{Z} \times \mathbb{R}$. Then,*

$$\varphi^{\xi}_{\mathsf{R}^{\varepsilon}}\Big[0 \leftrightarrow \partial \mathsf{R}(2n; 2\tfrac{n}{\varepsilon})\Big] \xrightarrow[\varepsilon \to 0]{} \varphi^{\xi}_{\mathcal{Q},\mathcal{R}}\Big[0 \leftrightarrow \partial \Lambda(n)\Big] \tag{4.3}$$

Proof of Propositions 4.2 and 4.3. As we described above, short edges in $\mathbb{G}^{\varepsilon}$ are of length $2\sin(\frac{\varepsilon}{2})$, each of whom is closed with probability $\lambda_0 \varepsilon$, where $\lambda_0 = \frac{2r}{\sqrt{q(4-q)}}$. Given $L > 0$ and consider a collection of $N = \frac{L}{\varepsilon}$ such consecutive edges. Consider $(X_i)_{1 \leqslant i \leqslant N}$ a sequence of i.i.d. Bernoulli random variables of parameter $\lambda_0 \varepsilon$: $X_i = 1$ if the i-th edge is closed and $X_i = 0$ otherwise. Denote $S = \sum_{i=1}^{N} X_i$, which counts the number of closed edges in this collection of edges.

Then, for any fixed $k \geqslant 0$ and $\varepsilon \to 0$, we have that

$$\begin{aligned}\mathbb{P}[S = k] &= \binom{N}{k}(\lambda_0\varepsilon)^k(1-\lambda_0\varepsilon)^{N-k} \\ &\sim \frac{N^k}{k!}(\lambda_0\varepsilon)^k e^{-N\lambda_0\varepsilon} \\ &= e^{-L\lambda_0}\frac{(L\lambda_0)^k}{k!},\end{aligned}$$

where the quantity in the last line is the probability that a Poisson variable of parameter $L\lambda_0$ takes the value k. As a consequence, when $\varepsilon \to 0$, the N vertical short edges will converge to a vertical segment of length L, among which closed edges will give us cut points that can be described by a Poisson point process with parameter λ_0.

The same reasoning applies to the long edges too. This shows that the measures $\varphi^{\xi}_{R^\varepsilon}$ converge weakly to $\varphi^{\xi}_{\mathcal{Q},\mathcal{R}}$, up to a scaling factor of $1/2$. □

Let us discuss the case $q \leqslant 4$ for illustration. In order to prove the RSW property for $\varphi_{\mathcal{Q}}$, one needs to bound uniformly the left hand sides of (4.1) and (4.2) for $a = n$ and $b = \rho n$ for any fixed quantity ρ. By duality, we may focus only on lower bounds.

Notice that for any fixed $\varepsilon > 0$, the RSW property obtained in Theorem 3.1 provides us with bounds for $\varphi^{\xi}_{R^\varepsilon}\left[\mathcal{C}_h(2n; 2\rho\frac{n}{\varepsilon})\right]$ and $\varphi^{\xi}_{R^\varepsilon}\left[\mathcal{C}_v(2n; \frac{2n}{\varepsilon})\right]$ which are uniform in n. However, these are not necessarily uniform in ε. Indeed, all estimates of Section 3.3 crucially depend on angles being bounded uniformly away from 0.

Removing this restriction in general is an interesting but difficult problem. However, in the simple case of the lattices $\mathbb{G}^\varepsilon$, this is possible, and is done below.

4.3 The case $1 \leqslant q \leqslant 4$

To show Theorem 4.1 for $1 \leqslant q \leqslant 4$, it is enough to show the RSW property for the quantum model, the rest of the proof follows as in Section 3.3.4. To this end, we proceed in the similar way as for isoradial graphs. More precisely, the following proposition provides us with uniform bounds in $\varepsilon \in (0, \pi)$ for crossing probabilities in $\mathbb{G}^\varepsilon$. Then Proposition 4.2 transfers these results to the quantum model and the same argument as in Lemma 3.13 yields the RSW property for the quantum model.

Proposition 4.4. *There exist $\delta > 0$, constants $a \geqslant 3$ and $b > 3a$ and n_0 such that, for all $\varepsilon \in (0, \pi)$ and $n \geqslant n_0$, there exist boundary conditions ξ on the region $\mathsf{R}^\varepsilon = \mathsf{R}(bn; \frac{bn}{\varepsilon})$ of $\mathbb{G}^\varepsilon$ such that*

$$\begin{aligned}\varphi^{\xi}_{\mathsf{R}^\varepsilon}\left[\mathcal{C}_h(3an, bn; \tfrac{bn}{\varepsilon})\right] \geqslant 1-\delta/2 \quad \text{and} \quad \varphi^{\xi}_{\mathsf{R}^\varepsilon}\left[\mathcal{C}^*_h(3an, bn; \tfrac{bn}{\varepsilon})\right] \geqslant 1-\delta/2, \\ \varphi^{\xi}_{\mathsf{R}^\varepsilon}\left[\mathcal{C}_v(an; \tfrac{2n}{\varepsilon})\right] \geqslant \delta \quad \text{and} \quad \varphi^{\xi}_{\mathsf{R}^\varepsilon}\left[\mathcal{C}^*_v(an; \tfrac{2n}{\varepsilon})\right] \geqslant \delta, \\ \varphi^{\xi}_{\mathsf{R}^\varepsilon}\left[\mathcal{C}_h(an, 3an; \tfrac{n}{\varepsilon})\right] \geqslant \delta \quad \text{and} \quad \varphi^{\xi}_{\mathsf{R}^\varepsilon}\left[\mathcal{C}^*_h(an, 3an; \tfrac{n}{\varepsilon})\right] \geqslant \delta. \end{aligned} \tag{4.4}$$

For the rest of the section, we focus on proving Proposition 4.4; the rest of the arguments used to obtain the RSW property for $\varphi_{\mathcal{Q}}$ are standard.

By symmetry, we may focus on $\varepsilon \leqslant \pi/2$; thus, difficulties only appear as $\varepsilon \to 0$. Fix $\varepsilon > 0$. We shall follow the same ideas as in Section 3.3.2. Recall the construction of the mixed lattice G_{mix}: for $M, N_1, N_2 > 0$, consider the graph obtained by superimposing a horizontal strip of

$\mathbb{G}^\varepsilon$ of height N_2+1 and width $2M+1$ over a horizontal strip of regular square graph $\mathbb{G}_{0,\frac{\pi}{2}}$ of height N_1+1 and same width. Let the lower vertices of this graph be on the line $\mathbb{R}\times\{0\}$, with $x_{0,0}$ at 0. Convexify this graph. The graph thus obtained, together with its reflection with respect to $\mathbb{R}\times\{0\}$, form G_{mix}.

Write $\widetilde{G}_{\text{mix}}$ for the graph with the regular and irregular blocks reversed. See Sections 3.2.1 and 3.3.2 for details on this construction and the track exchanging procedure that allows us to transform G_{mix} into $\widetilde{G}_{\text{mix}}$. Figure 4.1 contains an illustration of G_{mix} and $\widetilde{G}_{\text{mix}}$.

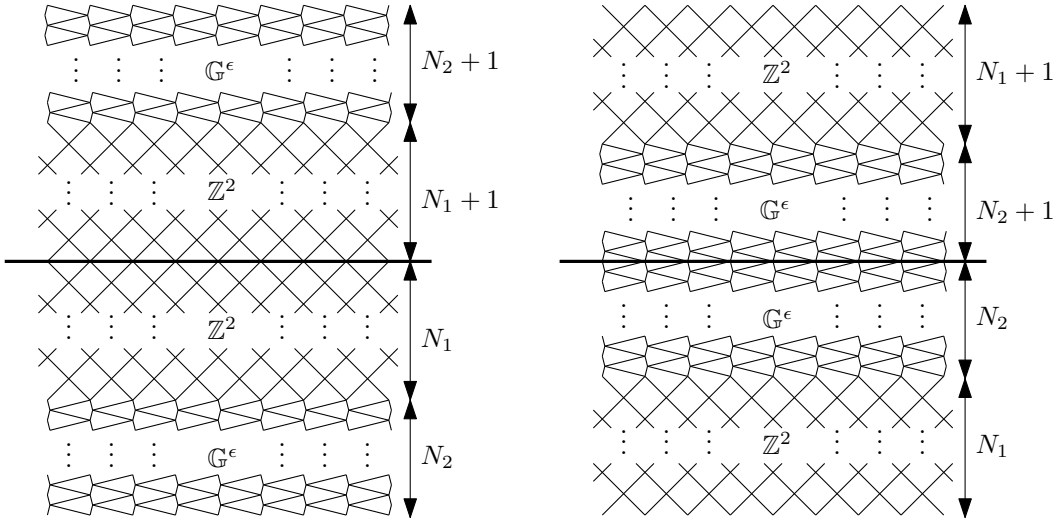

Figure 4.1 – **Left:** The graph G_{mix}. **Right:** The transformed graph $\widetilde{G}_{\text{mix}}$.

Write $\varphi_{G_{\text{mix}}}$ and $\varphi_{\widetilde{G}_{\text{mix}}}$ for the random-cluster measures with $\beta=1$ on G_{mix} and $\widetilde{G}_{\text{mix}}$, respectively, with free boundary conditions. The following adaptations of Propositions 3.15 and 3.16 imply Proposition 4.4 as in Section 3.3.2.2.

Proposition 4.5. *There exist $\lambda_0 := \lambda_0(q) > 0$ and $n_0 \geqslant 1$ such that for all $\lambda > \lambda_0$, $\varepsilon \in (0,\pi/2]$, $\rho_{out} > \rho_{in} > 0$, $n \geqslant n_0$ and sizes $M \geqslant (\rho_{out}+\frac{\lambda}{\varepsilon})n$, $N_1 \geqslant n$ and $N_2 \geqslant \frac{\lambda}{\varepsilon}n$,*

$$\varphi_{\widetilde{G}_{mix}}\Big[\mathcal{C}_h(\rho_{in}n,(\rho_{out}+\tfrac{\lambda}{\varepsilon})n;\lambda\tfrac{n}{\varepsilon})\Big] \geqslant (1-\rho_{out}e^{-n})\varphi_{G_{mix}}\Big[\mathcal{C}_h(\rho_{in}n,\rho_{out}n;n)\Big]. \tag{4.5}$$

The quantities λ_0 and λ above have no relation to the intensity of the Poisson point process used in the definition of $\varphi_{\mathcal{Q}}$.

Proposition 4.6. *There exists $\eta > 0$ and a sequence $(c_n)_n \in (0,1]^{\mathbb{N}}$ with $c_n \to 1$ such that, for all $\varepsilon \in (0,\pi/2]$, $n \geqslant 1$ and sizes $M \geqslant 3n$, $N_1 \geqslant N$ and $N_2 \geqslant \frac{n}{\varepsilon}$,*

$$\varphi_{\widetilde{G}_{mix}}\Big[\mathcal{C}_v(3n;\eta\tfrac{n}{\varepsilon})\Big] \geqslant c_n\varphi_{G_{mix}}\Big[\mathcal{C}_v(n;n)\Big]. \tag{4.6}$$

Proposition 4.5 controls the upward drift of a crossing: it claims that with high probability (independently of ε), this drift (in the graph distance) is bounded by a constant times $\frac{1}{\varepsilon}$. As a result, due to the particular structure of $\mathbb{G}^\varepsilon$, the upward drift in terms of the Euclidean distance is bounded by a constant independent of ε. The proof follows the same idea as that of Proposition 3.15 with the difference that it requires a better control of (3.9), which is obtained by a coarse-graining argument.

Proposition 4.6 controls the downward drift of a vertical crossing. The proof follows the same lines as that of Proposition 3.16, with a substantial difference in the definition (3.12) of

the process H which bounds the decrease in height of a vertical crossing when performing a series of track exchanges. In the proof of Proposition 3.16, H was a sum of Bernoulli random variables; here the Bernoulli variables are replaced by geometric ones. This difference may seem subtle, but is essential in obtaining a bound on the Euclidean downward drift which is uniform in ε.

Proof of Proposition 4.5. We keep the same notations as in the proof of Proposition 3.15. We remind that the process $(H^k)_{0\leqslant k\leqslant n}$ is coupled with the evolution of $(\gamma^{(k)})_{0\leqslant k\leqslant n}$ in such a way that all vertices $x_{i,j}$ visited by $\gamma^{(k)}$ have $(i,j)\in H^k$. Moreover, (H^k) can be seen as a growing pile of sand which grows laterally by 1 at each time step and vertically by 1 independently at each column with probability η. The goal here is to estimate η in the special case of G_{mix} as illustrated in Figure 4.1. More precisely, we want to improve the bound given in (3.10). Let $\lambda>0$ denote a (large) value, we will see at the end of the proof how it needs to be chosen.

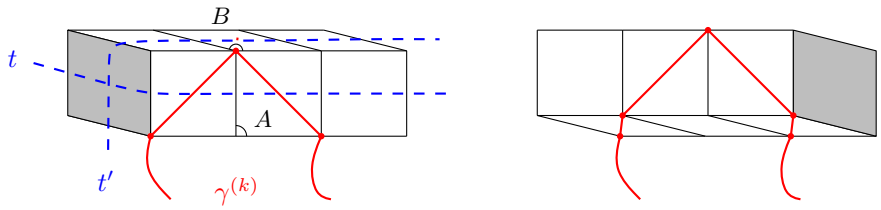

Figure 4.2 – Figure 3.12 adapted to the case of G_{mix} defined above. When we perform star--triangle transformations, we exchange two tracks, one of transverse angle $\frac{\pi}{2}$ and the other $\pi-\varepsilon$ or ε. We assume that we are in the case $A=\frac{\pi}{2}$ and $B=\pi-\varepsilon$.

In the special case of G_{mix} described above, a track exchange is always between tracks with transverse angles $A=\frac{\pi}{2}$ and $B=\pi-\varepsilon$ or ε. This is illustrated in Figure 4.2. The parameter $\eta_{A,B}$ is the probability that the path $\gamma^{(k)}$, as shown in the figure, drifts upwards by 1 when the dashed edge on the left of the figure is open. This can be estimated as follows for $1\leqslant q<4$,

$$\eta_{A,B}=\frac{y_{\pi-A}y_{\pi-(B-A)}}{q}=\begin{cases}\frac{\sin(r(\frac{\pi}{2}-\varepsilon))}{\sin(r(\frac{\pi}{2}+\varepsilon))} & \text{if } 1\leqslant q<4,\\ \frac{\frac{\pi}{2}-\varepsilon}{\frac{\pi}{2}+\varepsilon} & \text{if } q=4.\end{cases}$$

A quick computation then shows that we have

$$\eta:=\sup_{A,B\in[\varepsilon,\pi-\varepsilon]}\eta_{A,B}=1-\zeta(q)\varepsilon,\qquad\text{where }\zeta(q)=\frac{2\sqrt{2+\sqrt{q}}}{\pi^2}.$$

Thus, this value η may be used in the process (H^k) bounding the evolution of $(\gamma^{(k)})$. Hence, we obtain, for $0\leqslant k\leqslant\frac{\lambda}{\varepsilon}$,

$$\mathbb{P}\Big[h(\gamma^{(k)})<\tfrac{\lambda}{\varepsilon}n\Big]\geqslant\mathbb{P}\Big[\max\{j:(i,j)\in H^k\}<\tfrac{\lambda}{\varepsilon}n\Big].$$

A straightforward application of (3.9) is not sufficient to conclude, as it would provide a value of λ of order $\log(\frac{1}{\varepsilon})$ rather than of constant order. We will improve (3.9) slightly by revisiting its proof (given in [GM13a, Lem. 3.11]).

We are interested in the time needed to add a neighboring block from those which are already included by H^k. To be more precise, with each edge e of $\mathbb{Z}\times\mathbb{N}$, we associate a time

t_e: if e is horizontal, set $t_e = 1$; if e is vertical, set t_e to be a geometric random variable with parameter $\zeta(q)\varepsilon$. Moreover, we require that the random variables (t_e) are independent.

For $x, y \in \mathbb{Z} \times \mathbb{N}$, define $\mathcal{P}(x,y)$ to be the set of paths going from x to y, containing no downwards edge. For a path $\gamma \in \mathcal{P}(x,y)$, write $\tau(\gamma) = \sum_{e \in \gamma} t_e$, which is the total time needed to go through all the edges of γ. Also write $\tau(x,y) = \inf\{\tau(\gamma) : \gamma \in \mathcal{P}(x,y)\}$. As such, the sets $(H^k)_{k \geqslant 0}$ can be described by

$$H^k = \{y \in \mathbb{Z} \times \mathbb{N} : \exists x \in H^0, \tau(x,y) \leqslant k\}, \tag{4.7}$$

where we recall the definition of H^0:

$$H^0 = \{(i,j) \in \mathbb{Z} \times \mathbb{N} : -(\rho_{\text{out}} + 1)n \leqslant i - j \text{ and } i + j \leqslant (\rho_{\text{out}} + 1)n \text{ and } j \leqslant n\}.$$

Thus, our goal is to prove that the time needed to reach any point at level $\frac{\lambda}{\varepsilon}n$ is greater than $\frac{\lambda}{\varepsilon}n$ with high probability.

Let $\mathcal{P}_n$ be set of all paths of $\mathcal{P}(x,y)$ with $x \in H^0$, $y = (i,j)$ with $j = \frac{\lambda}{\varepsilon}n$ and which contain at most n horizontal edges. Then, (4.7) implies

$$\mathbb{P}\Big[\max\{j : (i,j) \in H^{\frac{\lambda}{\varepsilon}n}\} \geqslant \tfrac{\lambda}{\varepsilon}n\Big] = \mathbb{P}\Big[\exists \gamma \in \mathcal{P}_n : \tau(\gamma) \leqslant \tfrac{\lambda}{\varepsilon}n\Big]. \tag{4.8}$$

Next comes the key ingredient of the proof. We define the notion of *boxes* as follows. For $(k,\ell) \in \mathbb{Z} \times \mathbb{N}$, set

$$B(k,\ell) = \{(k,j) \in \mathbb{Z} \times \mathbb{N} : \tfrac{\ell - 1}{\varepsilon} \leqslant j < \tfrac{\ell}{\varepsilon}\}.$$

We note that different boxes are disjoint and each of them contains $\frac{1}{\varepsilon}$ vertical edges. A sequence of adjacent boxes is called a *box path*. Note that such a path is not necessarily self-avoiding. Set $\widetilde{\mathcal{P}}_n$ to be the set of box paths from some $B(k,n)$ to some $B(\ell, \lambda n)$, where k and ℓ are such that $-(\rho_{\text{out}} + 1)n \leqslant k \leqslant (\rho_{\text{out}} + 1)n$ and $|k - \ell| \leqslant n$, and in which at most n pairs of consecutive boxes are adjacent horizontally.

With any path $\gamma \in \mathcal{P}_n$, we associate the box path $\widetilde{\gamma} \in \widetilde{\mathcal{P}}_n$ of boxes visited by γ (above level n/ε). Notice that, since γ has at most n horizontal edges, so does $\widetilde{\gamma}$.

Given a box path $\widetilde{\gamma} = (\widetilde{\gamma}_i) \in \mathcal{P}_n$, call $\widetilde{\gamma}_i$ a *vertical* box if $\widetilde{\gamma}_{i-1}, \widetilde{\gamma}_i$ and $\widetilde{\gamma}_{i+1}$ have the same horizontal coordinate. Since any path $\widetilde{\gamma} \in \widetilde{\mathcal{P}}_n$ can only have at most n pairs of consecutives boxes that are adjacent horizontally, there are at least $(\lambda - 3)n$ vertical boxes in $\widetilde{\gamma}$. See Figure 4.3 for an illustration of the above notions.

A box is called *bad* if it contains a vertical edge e such that $t_e \geqslant 2$. We can estimate the probability that a box is bad:

$$\mathbb{P}[\text{a given box is bad}] = 1 - (1 - \zeta\varepsilon)^{1/\varepsilon} \to 1 - e^{-\zeta} \quad \text{as } \varepsilon \to 0.$$

Notice that for a path $\gamma \in \mathcal{P}_n$ such that $\tau(\gamma) \leqslant \frac{\lambda}{\varepsilon}n$, there are at most n vertical bad boxes in $\widetilde{\gamma}$. Indeed, due to the definition, in any bad vertical box of $\widetilde{\gamma}$, γ crosses an edge e with $t_e \geqslant 2$. Therefore,

$$\begin{aligned}\mathbb{P}\Big[\exists \gamma \in \mathcal{P}_n : \tau(\gamma) \leqslant \tfrac{\lambda}{\varepsilon}n\Big] &\leqslant \mathbb{P}\Big[\exists \widetilde{\gamma} \in \widetilde{\mathcal{P}}_n : \text{ there are at most } n \text{ vertical bad boxes in } \widetilde{\gamma}\Big] \\ &\leqslant \sum_{\widetilde{\gamma} \in \widetilde{\mathcal{P}}_n} \mathbb{P}\Big[\text{there are at most } n \text{ vertical bad boxes in } \widetilde{\gamma}\Big] \end{aligned} \tag{4.9}$$

Let us now bound the above. First, note that any path $\widetilde{\gamma} \in \widetilde{\mathcal{P}}_n$ has length at most λn and can have at most n horizontal displacements, which gives

$$|\widetilde{\mathcal{P}}_n| \leqslant 2(\rho_{\text{out}} + 1)n 2^n \binom{\lambda n}{n} \leqslant \rho_{\text{out}}(c\lambda)^n, \tag{4.10}$$

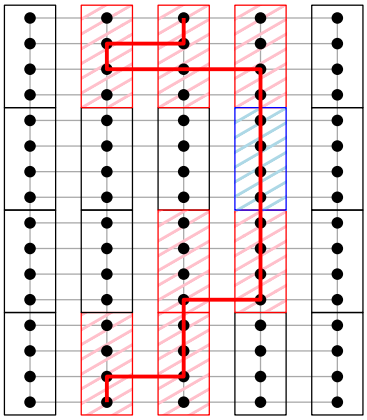

Figure 4.3 – A path $\gamma \in \mathcal{P}_n$ and its associated box path $\widetilde{\gamma} \in \widetilde{\mathcal{P}}_n$. Note that the box path $\widetilde{\gamma}$ might not be self-avoiding. The blue box in the figure is a vertical box for $\widetilde{\gamma}$.

for a constant $c > 0$ independent of all the other parameters. Secondly, recall that any $\widetilde{\gamma} \in \widetilde{\mathcal{P}}_n$ has at least $(\lambda - 3)n$ vertical boxes. Let $X_1, \dots, X_{(\lambda-3)n}$ be i.i.d. Bernoulli random variables with parameter $\delta = 1 - (1 - \zeta\varepsilon)^{1/\varepsilon}$ that indicate whether the $(\lambda - 3)n$ first vertical boxes of $\widetilde{\gamma}$ are bad ($X_i = 1$ if the i^{th} vertical box of $\widetilde{\gamma}$ is bad and $X_i = 0$ otherwise). Then,

$$\begin{aligned}\mathbb{P}\Big[\text{there are at most } n \text{ vertical bad boxes in } \widetilde{\gamma}\Big] &\leqslant \mathbb{P}\Big[X_1 + \cdots + X_{(\lambda-3)n} \leqslant n\Big] \\ &\leqslant \left[\left(\frac{(\lambda-3)\delta}{\lambda-4}\right)^{\lambda-4}(\lambda-3)(1-\delta)\right]^n. \qquad (4.11)\end{aligned}$$

The last inequality is obtained by large deviation theory.

Finally, put (4.8)–(4.11) together, as in [GM13a, Lem. 3.11]. It follows that if λ is chosen larger than some threshold $\lambda_0 > \frac{4-3\delta}{1-\delta}$ that only depends on δ, then

$$\mathbb{P}\Big[\max\{j : (i,j) \in H^{\frac{\lambda}{\varepsilon}n}\} \geqslant \tfrac{\lambda}{\varepsilon}n\Big] \leqslant \rho_{\text{out}} e^{-n}.$$

Recall that $\delta \xrightarrow[\varepsilon\to 0]{} 1 - e^{-\zeta}$ is uniformly bounded in $\varepsilon > 0$, hence λ_0 may also be chosen uniform in ε.

Remark 4.7. We point out that the coarse-graining argument above is essential to the proof due to the reduced combinatorial factor (4.10). In effect, the computation in [GM13a, Lem. 3.11] would have given us a combinatorial factor $(c\lambda/\varepsilon)^n$, and due to the additional ε in the denominator, one can only show that λ should grow as $\log(\frac{1}{\varepsilon})$. This improvement is made possible because when, ε goes to 0, paths in the directed percolation take $\frac{1}{\varepsilon}$ more vertical edges than horizontal ones, and bad edges (those with passage-time greater than 2) are of density proportional to ε. We can therefore "coarse grain" a good number of paths to a unique one, which improves the bound.

□

Proof of Proposition 4.6. We will adapt the proof of Proposition 3.16 to our special setting. The goal is to have a better control of the downward drift of paths when track exchanges are performed. There are two significant differences: (i) a better description of the regions D^k in which vertical paths are contained; (ii) a (stochastic) lower bound on h^k by a sum of geometric random variables rather than a sum of Bernoulli variables as in the aforementioned proof.

In this proof we are only interested in events depending on the graph above the base level, and we will only refer to the upper half-plane henceforth.

Fix $\varepsilon > 0$ and $n \in \mathbb{N}$. Let $M \geqslant 4n$, $N_1 \geqslant n$ and $N_2 \geqslant \frac{n}{\varepsilon}$ where, as illustrated in Figure 4.1, $2M+1$ is the width of the blocks of $\mathbb{G}^{(1)} = \mathbb{Z}^2$ and $\mathbb{G}^{(2)} = \mathbb{G}^{\varepsilon}$, $N_1 + 1$ is the height of the block of $\mathbb{Z}^2$ and N_2 that of $\mathbb{G}^{\varepsilon}$. Recall that the sequence of star-triangle transformations we consider here is $\Sigma^{\uparrow}$, which consists of pulling up tracks of $\mathbb{G}^{(1)}$ one by one above those of $\mathbb{G}^{(2)}$, from the top-most to the bottom-most. We write $\mathbb{P}$ for the measure taking into account the choice of a configuration ω according to the random-cluster measure $\varphi_{G_{\text{mix}}}$ as well as the results of the star-triangle transformations in $\Sigma^{\uparrow}$ applied to the configuration ω.

For $0 \leqslant i \leqslant N_1$, recall from Section 3.2.1 the notation

$$\Sigma_i^{\uparrow} = \Sigma_{t_i, t_{N_1+N_2+1}} \circ \cdots \circ \Sigma_{t_i, t_{N_1+1}},$$

for the sequence of star-triangle transformations moving the track t_i of $\mathbb{G}^{(1)}$ above $\mathbb{G}^{(2)}$. Then, $\Sigma^{\uparrow} = \Sigma_0^{\uparrow} \circ \cdots \circ \Sigma_{N_1}^{\uparrow}$.

We note that $\omega \in \mathcal{C}_v(n;n)$ if and only if $\Sigma_{n+1}^{\uparrow} \circ \cdots \circ \Sigma_{N_1}^{\uparrow}(\omega) \in \mathcal{C}_v(n;n)$, since the two configurations are identical between the base t_0 and t_n. Thus, we can assume that $\Sigma_{N_1}^{\uparrow}, \cdots, \Sigma_{n+1}^{\uparrow}$ are performed and look only at the effect of $\Sigma_n^{\uparrow}, \cdots, \Sigma_0^{\uparrow}$ on such a configuration. Let us define for $0 \leqslant k \leqslant n+1$,

$$\begin{aligned}
G^k &= \Sigma_{n-k+1}^{\uparrow} \circ \cdots \circ \Sigma_{N_1}^{\uparrow}(G_{\text{mix}}),\\
\omega^k &= \Sigma_{n-k+1}^{\uparrow} \circ \cdots \circ \Sigma_{N_1}^{\uparrow}(\omega),\\
D^k &= \{x_{u,v} \in G^k : |u| \leqslant n+2k,\, 0 \leqslant v \leqslant N_2 + n\},\\
h^k &= \sup\{h \leqslant N_2 + n - k : \exists u, v \in \mathbb{Z} \text{ with } x_{u,0} \xleftrightarrow{D^k, \omega^k} x_{v,h}\}.
\end{aligned}$$

That is, h^k is the highest level that may be reached by an ω^k-open path lying in the rectangle D^k. These notions are illustrated in Figure 4.4

Due to the above definitions, if $\omega^0 \in \mathcal{C}_v(n;n)$, then $h^0 \geqslant n$. Hence,

$$\mathbb{P}[h^0 \geqslant n] \geqslant \mathbb{P}[\omega^0 \in \mathcal{C}_v(n;n)] = \varphi_{G_{\text{mix}}}[\mathcal{C}_v(n;n)].$$

Moreover, using the fact that ω^{n+1} follows the law of $\varphi_{\widetilde{G}_{\text{mix}}}$ and the definitions of D^{n+1} and h^{n+1} above, we obtain

$$\varphi_{\widetilde{G}_{\text{mix}}}[\mathcal{C}_v(3n; \eta\tfrac{n}{\varepsilon})] \geqslant \mathbb{P}(h^{n+1} \geqslant \eta\tfrac{n}{\varepsilon}).$$

Therefore, it is enough to show

$$\mathbb{P}\Big[h^{n+1} \geqslant \eta\tfrac{n}{\varepsilon}\Big] \geqslant c_n \mathbb{P}\Big[h^0 \geqslant n\Big], \tag{4.12}$$

for some $\eta \in (0, \frac{1}{2})$ to be specified below and constants c_n with $c_n \to 1$ as $n \to \infty$, all independent of ε.

Fix $0 \leqslant k \leqslant n$ and let us examine the $(N_1 - (n-k) + 1)^{th}$ step of $\Sigma^{\uparrow}$, that is $\Sigma_{n-k}^{\uparrow}$. Write $\Psi_j := \Sigma_{t_{n-k}, t_{N_1+j}} \circ \cdots \circ \Sigma_{t_{n-k}, t_{N_1+1}}$ for $0 \leqslant j \leqslant N_2 + 1$. In other words, Ψ_j is the sequence of star-triangle transformations that applies to G^k and moves the track t_{n-k} above j tracks of $\mathbb{G}^{(2)}$, namely $t_{N_1+1}, \ldots, t_{N_1+j}$. Moreover, $\Psi_{N_2} = \Sigma_{n-k}^{\uparrow}$; hence, $\Psi_{N_2}(G^k) = G^{k+1}$ and $\Psi_{N_2}(\omega^k) = \omega^{k+1}$.

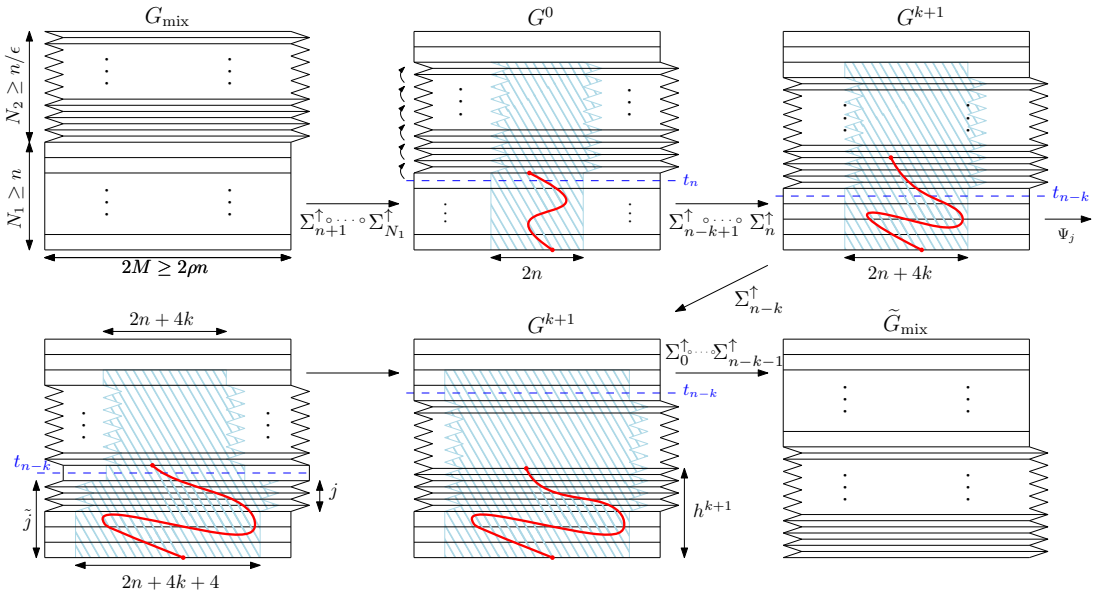

Figure 4.4 – Several stages in the transformation of G_{mix} (only the outlines of the diamond graphs are depicted). Pulling up the top $N_1 - n$ tracks of the regular lattice does not affect the event $\mathcal{C}_v(n;n)$. The red vertical crossing is then affected by the track exchanges. However, it remains in the hashed domains $(D^k)_{0\leqslant k\leqslant n+1}$, and $(D^k_j)_{0\leqslant j\leqslant N_2}$. Its height evolves according to (3.14)–(3.16), (4.13) and (4.14). Notice the asymmetric shape of D^k_j in the fourth diagram, where j is even.

For $0 \leqslant j \leqslant N_2$ write $\widetilde{j} := n-k+j$ and define D^k_j as the subgraph of $\Psi_j(G^k)$ induced by vertices $x_{u,v}$ with $0 \leqslant v \leqslant N_2+n$ and

$$\begin{cases} |u| \leqslant n+2k+2 & \text{if } v \leqslant \widetilde{j}, \\ -(n+2k) \leqslant u \leqslant n+2k+1 & \text{if } v = \widetilde{j}+1 \text{ and } j \text{ odd}, \\ -(n+2k+1) \leqslant u \leqslant n+2k & \text{if } v = \widetilde{j}+1 \text{ and } j \text{ even}, \\ |u| \leqslant n+2k & \text{if } v > \widetilde{j}+1. \end{cases}$$

We note that $D^k \subseteq D^k_0 \subseteq \cdots \subseteq D^k_{N_2} \subseteq D^{k+1}$. Let $\omega^k_j = \Psi_j(\omega^k)$ and

$$h^k_j = \sup\{h \leqslant N_2+n-k : \exists u,v \in \mathbb{Z} \text{ with } x_{u,0} \overset{D^k_j,\omega^k_j}{\longleftrightarrow} x_{v,h}\}.$$

Due to inclusions between the domains, we have $h^k \leqslant h^k_0$ and $h^k_{N_2} \leqslant h^{k+1}$. Next, we aim to obtain similar equations to (3.14)–(3.17).

Fix $0 \leqslant j \leqslant N_2$ and let $\Sigma := \Sigma_{t_{n-k}, t_{N_1+j+1}}$ be the track exchange to be applied to $\Psi_j(G^k)$. Moreover, let $\mathcal{P}_j$ be the set of paths γ of $\Psi_j(G^k)$, contained in D^k_j, with one endpoint at height 0, the other at height $h(\gamma)$, and all other vertices with heights between 1 and $h(\gamma)-1$.

First we claim that, if γ is an ω^k_j-open path of $\mathcal{P}_j$, then $\Sigma(\gamma)$ is ω^k_{j+1}-open and contained in D^k_{j+1} (hence contains a subpath of $\mathcal{P}_{j+1}$ reaching the same height as $\Sigma(\gamma)$). Due to the specific structure of $\mathbb{G}^\varepsilon$, we prove this according to the parity of j. For j even, the transverse angle of the track t_{N_1+j+1} is $\pi-\varepsilon$. Thus, as shown by the blue points in Figure 3.5, Σ induces a possible horizontal drift of γ of $+2$ at level $\widetilde{j}$ and $+1$ at level $\widetilde{j}+1$. By its definition, D^k_{j+1}

indeed contains $\Sigma(\gamma)$. For j odd, the figure is symmetric, thus we get horizontal drifts of -2 and -1 at levels $\widetilde{j}$ and $\widetilde{j}+1$, respectively.

Let us briefly comment on the differences between the above and the general case appearing in Proposition 3.16. In Proposition 3.16, since the directions of the track exchanges are not necessarily alternating, we may repeatedly obtain horizontal drifts of the same sign. This is why the domains D^k_j in Proposition 3.16 grow with slope 1 (see Figure 3.13), and eventually induce a different definition of D^k than the one above. In the present case, due to alternating transverse angles which create alternating positive and negative drifts, D^k may be chosen with vertical sides and D^{k+1} is obtained by adding two columns on the left and right of D^k. While this may seem an insignificant technicality, it allows to bound the horizontal displacement of the vertical crossing by $2n$ rather than a quantity of order $\frac{n}{\varepsilon}$, and this is essential for the proof.

As a consequence of the discussion above, equations (3.14)–(3.16) hold as in the classical case. For this proof, we will improve (3.15) and (3.17) to

$$\mathbb{P}[h^k_{j+1} \geqslant h+1 \,|\, h^k_j = h] \geqslant 1 - C\varepsilon \qquad \text{if } h = \widetilde{j}, \tag{4.13}$$

$$\mathbb{P}[h^k_{j+1} \geqslant h \,|\, h^k_j = h] \geqslant 1 - C\varepsilon \qquad \text{if } h = \widetilde{j}+1, \tag{4.14}$$

for some constant $C > 0$ that does not depend on ε, only on q.

Before going any further, let us explain the meaning of (3.14)–(3.16), (4.13) and (4.14) through a non-rigorous illustration. In applying $\Sigma^{\uparrow}_{n-k}$, the track t_{n-k} (of transverse angle $\pi/2$) is moved upwards progressively. Let us follow the evolution of a path γ reaching height h^k throughout this process. As long as the track t_{n-k} does not reach height h^k, the height reached by γ is not affected. When t_{n-k} reaches height h^k (as in Figure 4.5; left diagram), the height of γ may shrink by 1 or remain the same; (4.14) indicates that the former arrises with probability bounded above by $C\varepsilon$. If γ shrinks, the following track exchanges do not influence γ any more, and we may suppose $h^{k+1} = h^k - 1$. Otherwise, the top endpoint of γ at the following step is just below t_{n-k} (as in Figure 4.5; centre diagram). In the following track exchange, γ may increase by 1 in height. By (4.13), this occurs with probability $1 - C\varepsilon$. If the height of γ does increase, then it is again just below t_{n-k}, and it may increase again. In this fashion, γ is "dragged" upwards by t_{n-k}. This continues until γ fails once to increase. After this moment, γ is not affected by any other track exchange of $\Sigma^{\uparrow}_{n-k}$.

The reasoning above would lead us to believe that $h^{k+1} \geqslant h^k - 2 + Y$ stochastically, where Y is a geometric random variable with parameter $C\varepsilon$. This is not entirely true since the conditioning in (4.13) and (4.14) is not on ω^k_j, but only on h^k_j. However, this difficulty may be avoided as in the proof of Proposition 3.16. Let us render this step rigorous and obtain the desired conclusion (4.12), before proving (4.13) and (4.14).

Let $(Y_k)_{0 \leqslant k \leqslant n}$ be i.i.d. geometric random variables of parameter $C\varepsilon$. Define the Markov process $(H^k)_{0 \leqslant k \leqslant n+1}$ by $H^0 = h^0$ and $H^{k+1} = \min\{H^k + Y_k - 2, n - k + N_2\}$. Then, the comparison argument of [GM13a, Lem. 3.7] proves that h^k dominates H^k stochastically for any k. Precisely, for any k, the processes $(H^j)_{0 \leqslant j \leqslant n+1}$ and $(h^j)_{0 \leqslant j \leqslant n+1}$ may be coupled such that $H^k \leqslant h^k$ a.s.. We insist that we do not claim that there exists a coupling that satisfies the above inequality simultaneously for all k. We do not provide details on how to deduce this inequality from (3.14)–(3.16), (4.13) and (4.14), since this step is very similar to the corresponding argument in [GM14, Lem. 6.9]. Let us simply mention that the cap of $n - k + N_2$ imposed on H^k comes from the fact that a path may not be dragged upwards above the highest track of the irregular block.

By comparing h^{n+1} and H^{n+1}, we find

$$c_n := \frac{\mathbb{P}\Big[h^{n+1} \geqslant \eta\frac{n}{\varepsilon}\Big]}{\Big[h^0 \geqslant n\Big]} \geqslant \mathbb{P}\Big[H^{n+1} \geqslant \eta\frac{n}{\varepsilon}\,\Big|\,H^0 \geqslant n\Big] \geqslant \mathbb{P}\Big[Y_0 + \cdots + Y_n - (n+2) \geqslant \eta\frac{n}{\varepsilon}\Big].$$

The last inequality is due to that, if $H^k + Y_k - 2 = n - k + N_2$ at any point during the process, then $h^{n+1} \geqslant \eta\frac{n}{\varepsilon}$ is sure to arrises. Finally notice that $\mathbb{E}[Y_k - 1] = \frac{1-C\varepsilon}{C\varepsilon} > \eta/\varepsilon$ for $\eta < 1/C$ and ε small enough. The same large deviation argument as in the final step of the proof of Proposition 3.16 allows us to conclude that $c_n \to 1$, uniformly in ε. Thus, we are only left with proving (4.13) and (4.14), which we do next.

First we prove (4.14). This is similar to the argument proving (3.17), with a slight improvement on the estimate of the parameter δ. Fix $0 \leqslant j \leqslant N_2$ and use the notation introduced above. Without loss of generality, assume also that j is even so that the track exchange $\Sigma = \Sigma_{t_{n-k}, t_{N_1+j+1}}$ is performed from left to right. Denote by $\Gamma = \Gamma(\omega_j^k)$ the ω_j^k-open path of $\mathcal{P}_j$ that is the minimal element of $\{\gamma \in \mathcal{P}_j : h(\gamma) = h_j^k, \gamma \text{ is } \omega_j^k\text{-open}\}$ as in Proposition 3.16.

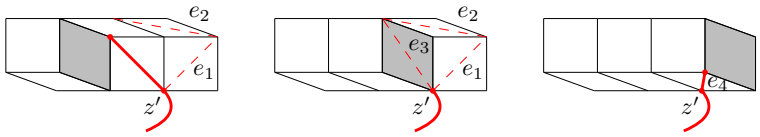

Figure 4.5 – Three star-triangle transformations contributing to Σ slide the gray rhombus from left to right. If the three edges in the middle diagram are all closed, then e_4 is open with probability $\frac{y_{e_1} y_{e_3}}{q}$.

Fix some $\gamma \in \mathcal{P}_j$ of height $\widetilde{j}+1$. Let $z = x_{u,\widetilde{j}+1}$ denote the upper endpoint of γ and let z' denote the other endpoint of the unique edge of γ leading to z. Then either $z' = x_{u+1,\widetilde{j}}$ or $z' = x_{u-1,\widetilde{j}}$.

Conditioning on $\Gamma = \gamma$. If $z' = x_{u-1,\widetilde{j}}$, then it is always the case that $h(\Sigma(\Gamma)) \geqslant \widetilde{j}+1$. Assume that $z' = x_{u+1,\widetilde{j}}$ as in Figure 4.5 and consider the edges $e_1, \dots, e_4$ depicted in the image. If e_1 is open in ω_j^k then it is easy to see that $h_{j+1}^k = \widetilde{j}+1$, for any outcome of the star-triangle transformations. The same is valid for the edge e_3 appearing in the second diagram of Figure 4.5. Assume that both e_1 and e_3 are closed in the second diagram. Then, if in addition e_2 is also closed, by the randomness appearing in the star-triangle transformation leading to the fourth diagram,

$$\mathbb{P}[e_4 \text{ is open} \,|\, e_1, e_2, e_3 \text{ are closed}] \geqslant \frac{y_{e_1} y_{e_3}}{q}.$$

This is due to the transition probabilities of Figure 2.8. Finally, if e_4 is open in the last diagram, then the height of Γ remains at least $\widetilde{j}+1$ for the rest of Σ. In conclusion,

$$\mathbb{P}[h_{j+1}^k \geqslant \widetilde{j}+1 \,|\, \Gamma = \gamma] \geqslant \frac{y_{e_1} y_{e_3}}{q} \mathbb{P}[e_2 \text{ is closed} \,|\, \Gamma = \gamma \text{ and } e_1, e_3 \text{ closed}]$$

Notice that the edge e_2 is above level $\widetilde{j}$, hence the conditioning $\Gamma = \gamma$ and e_1, e_3 closed affects it negatively. Thus, $\mathbb{P}[e_2 \text{ is closed} \,|\, \Gamma = \gamma \text{ and } e_1, e_3 \text{ closed}] \geqslant 1 - p_{e_2}$. Using the fact that $y_{e_1} = \sqrt{q}$, $y_{e_3} \to \sqrt{q}$ and $p_{e_2} \sim C'\varepsilon$ as $\varepsilon \to 0$, with $C' > 0$ depending only on q, and summing over all possibilities on γ, we obtain

$$\mathbb{P}[h_{j+1}^k \geqslant \widetilde{j}+1 \,|\, h_j^k = \widetilde{j}+1] \geqslant 1 - C\varepsilon,$$

for some constant C depending only on q.

Now let us prove (4.13). The argument is very similar to the above. Assume again that the track exchange $\Sigma = \Sigma_{t_{n-k}, t_{N_1+j+1}}$ is performed from left to right. Let Γ be defined as above and call z its top endpoint. Condition on $h_j^k = \widetilde{j}$. Then, as the vertical rhombus is slid through t_{n-k}, t_{N_1+j+1}, it arrives above z as in the second diagram of Figure 4.5. Let e_1, e_2, e_3 and e_4 be defined as in Figure 4.5. If e_1 or e_3 are open in the second diagram, then $h_{j+1}^k = \widetilde{j} + 1$ for any outcome of the star-triangle transformations [1]. Assume that e_1 and e_3 are both closed at this stage. Moreover, since the conditioning only depends on edges below level $\widetilde{j} + 1$, it influences the state of e_2 only via boundary conditions. Hence, $\mathbb{P}[e_2 \text{ is closed} | \Gamma \text{ and } e_1, e_3 \text{ closed}] \geqslant 1 - p_{e_2}$. As discussed above, when e_1, e_2 and e_3 are all closed, the final star-triangle transformation of Figure 4.5 produces an open edge e_4 with probability bounded below by $1 - C\varepsilon$. We conclude as above.

□

4.3.1 The case $q > 4$

We will adapt the proof of the exponential decay of Section 3.4 to the quantum case. More precisely, we only need to do so for the case of isoradial square lattices, that is Section 3.4.1. The argument is very similar to that of Section 3.4.1, with the exception that Propositions 4.5 and 4.6 are used instead of Propositions 3.15 and 3.16.

We recall the notation R^{hp} for half-plane rectangles and the additional subscript ε for domains defined in $\mathbb{G}^\varepsilon$. The key result is the following.

Proposition 4.8. *There exist constants $C, c > 0$ depending only on q such that, for any $\varepsilon > 0$ small enough,*

$$\varphi^0_{\mathsf{R}^{hp,\varepsilon}(N;\frac{N}{\varepsilon})}\Big[0 \leftrightarrow \partial \mathsf{R}^{hp,\varepsilon}(n;\tfrac{n}{\varepsilon})\Big] \leqslant C\exp(-cn), \qquad \forall n < N. \tag{4.15}$$

The above has the following direct consequences.

Corollary 4.9. *There exist constants $C, c > 0$ depending only on q such that for ε small enough,*

$$\varphi^0_{\mathsf{R}^{\varepsilon}(N;\frac{N}{\varepsilon})}\Big[0 \leftrightarrow \partial \mathsf{R}^{\varepsilon}(n;\tfrac{n}{\varepsilon})\Big] \leqslant C\exp(-cn), \qquad \forall n < N. \tag{4.16}$$

Corollary 4.10. *There exist constants $C, c > 0$ depending only on q such that,*

$$\varphi^0_{\mathcal{Q},\Lambda(N)}\Big[0 \leftrightarrow \partial\Lambda(n)\Big] \leqslant C\exp(-cn). \tag{4.17}$$

Corollary 4.9 is an straightforward adaptation of Proposition 3.23. Corollary 4.10 is a consequence of the fact that the constants in (4.16) are uniform, thus we can take $\varepsilon \to 0$ and apply Proposition 4.3.

To conclude, as in Section 3.4.3, Corollary 4.10 implies Theorem 4.1 for $q > 4$.

We will not give more details on the proofs of Corollaries 4.9 and 4.10 and Theorem 4.1. For the rest of the section, we focus on showing Proposition 4.8.

Proof of Proposition 4.8. We follow the idea of the proof of Proposition 3.25.

Fix $\varepsilon > 0$ as in the statement. For $N > n$, let G_{mix} be the mixture of $\mathbb{G}^{(1)} = \mathbb{G}^\varepsilon$ and $\mathbb{G}^{(2)} = \mathbb{Z}^2$, as described in Section 3.2. In this proof, the mixed lattice is only constructed above

[1] Due to the conditioning, e_1 or e_3 may only be open if their top endpoint lies outside D_j^k.

the base level; it has $2N+1$ vertical tracks $(s_i)_{-N\leqslant i\leqslant N}$ of transverse angle 0 and $\frac{N}{\varepsilon}+N+2$ horizontal tracks $(t_j)_{0\leqslant j\leqslant \frac{N}{\varepsilon}+N+1}$, the first $\frac{N}{\varepsilon}+1$ having alternate angles ε and $\pi-\varepsilon$ (we call this the irregular block) and the following $N+1$ having transverse angle $\frac{\pi}{2}$ (we call this the regular block). Finally, G_{mix} is a convexification of the piece of square lattice described above.

Set $\widetilde{G}_{\mathrm{mix}}$ to be the result of the inversion of the regular and irregular blocks of G_{mix} using the sequence of transformations $\Sigma^{\uparrow}$. Let $\varphi_{G_{\mathrm{mix}}}$ and $\varphi_{\widetilde{G}_{\mathrm{mix}}}$ be the random-cluster measures with free boundary conditions on G_{mix} and $\widetilde{G}_{\mathrm{mix}}$, respectively. The latter is then the push-forward of the former by the sequence of transformations $\Sigma^{\uparrow}$.

Let $\delta_0\in(0,1)$ be a constant that will be set below; it will be chosen only depending on q. Write ∂_L, ∂_R and ∂_T for the left, right and top boundaries, respectively, of a rectangular domain $\mathsf{R}^{\mathrm{hp},\varepsilon}(.;.)$.

Consider a configuration ω on G_{mix} such that $0\longleftrightarrow\partial\mathsf{R}^{\mathrm{hp},\varepsilon}(n;\frac{n}{\varepsilon})$. Then, as in (3.40), we have

$$\begin{aligned}\varphi_{G_{\mathrm{mix}}}\Big[0\leftrightarrow\partial\mathsf{R}^{\mathrm{hp},\varepsilon}(n;\tfrac{n}{\varepsilon})\Big]\leqslant{}&\varphi_{G_{\mathrm{mix}}}\Big[0\xleftrightarrow{\mathsf{R}^{\mathrm{hp},\varepsilon}(n;\delta_0\frac{n}{\varepsilon})}\partial_L\mathsf{R}^{\mathrm{hp},\varepsilon}(n;\delta_0\tfrac{n}{\varepsilon})\Big]\\&+\varphi_{G_{\mathrm{mix}}}\Big[0\xleftrightarrow{\mathsf{R}^{\mathrm{hp},\varepsilon}(n;\delta_0\frac{n}{\varepsilon})}\partial_R\mathsf{R}^{\mathrm{hp},\varepsilon}(n;\delta_0\tfrac{n}{\varepsilon})\Big]\\&+\varphi_{G_{\mathrm{mix}}}\Big[0\xleftrightarrow{\mathsf{R}^{\mathrm{hp},\varepsilon}(n;\delta_0\frac{n}{\varepsilon})}\partial_T\mathsf{R}^{\mathrm{hp},\varepsilon}(n;\delta_0\tfrac{n}{\varepsilon})\Big].\end{aligned}\tag{4.18}$$

Moreover, since the graphs G_{mix} and $\mathbb{G}^{\varepsilon}$ are identical in $\mathsf{R}^{\mathrm{hp},\varepsilon}(N;\frac{N}{\varepsilon})$, we obtain,

$$\varphi^{0}_{\mathsf{R}^{\mathrm{hp},\varepsilon}(N;\frac{N}{\varepsilon})}\Big[0\leftrightarrow\partial\mathsf{R}^{\mathrm{hp},\varepsilon}(n;\tfrac{n}{\varepsilon})\Big]\leqslant\varphi_{G_{\mathrm{mix}}}\Big[0\leftrightarrow\partial\mathsf{R}^{\mathrm{hp},\varepsilon}(n;\tfrac{n}{\varepsilon})\Big],\tag{4.19}$$

where we use the comparison between boundary conditions.

In conclusion, in order to obtain (4.15) it suffices to prove that the three probabilities of the right-hand side of (4.18) are bounded by an expression of the form Ce^{-cn}, where the constants C and c depend only on q. We concentrate on this from now on.

Let us start with the last line of (4.18). Recall Proposition 4.6; a straightforward adaptation reads:

Adaptation of Proposition 4.6. *There exist $\tau>0$ and $c_n>0$ satisfying $c_n\to1$ as $n\to\infty$ such that, for all n and sizes $N\geqslant 4n$,*

$$\varphi_{\widetilde{G}_{mix}}\Big[0\xleftrightarrow{\mathsf{R}^{hp,\varepsilon}(4n;\delta_0\tau n)}\partial_T\mathsf{R}^{hp,\varepsilon}(4n;\delta_0\tau n)\Big]\geqslant c_n\varphi_{G_{mix}}\Big[0\xleftrightarrow{\mathsf{R}^{hp,\varepsilon}(n;\delta_0\frac{n}{\varepsilon})}\partial_T\mathsf{R}^{hp,\varepsilon}(n;\delta_0\tfrac{n}{\varepsilon})\Big].\tag{4.20}$$

Indeed, the proof of the above is identical to that of Proposition 4.6 with the only difference that the position of the two graphs are switched, thus the factor ε^{-1} becomes ε. The constant τ and the sequence $(c_n)_n$ only depend on q.

Observe that, in $\widetilde{G}_{\mathrm{mix}}$, the domain $\mathsf{R}^{\mathrm{hp}}(N;N)$ is fully contained in the regular block and contains $\mathsf{R}^{\mathrm{hp}}(4n;\delta_0\tau n)$ if $\delta_0\tau\leqslant1$. Thus, by comparison between boundary conditions,

$$\begin{aligned}&\varphi_{\widetilde{G}_{\mathrm{mix}}}\Big[0\xleftrightarrow{\mathsf{R}^{\mathrm{hp}}(4n;\delta_0\tau n)}\partial_T\mathsf{R}^{\mathrm{hp}}(4n;\delta_0\tau n)\Big]\\&\quad\leqslant\varphi^{1/0}_{\mathsf{R}^{\mathrm{hp}}(N;N)}\Big[0\xleftrightarrow{\mathsf{R}^{\mathrm{hp}}(4n;\delta_0\tau n)}\partial_T\mathsf{R}^{\mathrm{hp}}(4n;\delta_0\tau n)\Big]\\&\quad\leqslant\varphi^{1/0}_{\mathsf{R}^{\mathrm{hp}}(N;N)}\Big[0\leftrightarrow\partial\Lambda(\delta_0\tau n)\Big]\leqslant C_0\exp(-c_0\delta_0\tau n).\end{aligned}$$

where $\mathsf{R}^{\mathrm{hp}}(N;N)$ is the subgraph of $\mathbb{Z}^2$ and the last inequality is given by Proposition 3.24. Note that c_0 and τ depend only on q. Thus, from (4.20) and the above we obtain,

$$\varphi_{G_{\mathrm{mix}}}\Big[0 \xleftrightarrow{\mathsf{R}^{\mathrm{hp}}(4n;\delta_0\tau n)} \partial_T \mathsf{R}^{\mathrm{hp}}(4n;\delta_0\tau n)\Big] \leqslant \frac{1}{c_n} C_0 \exp(-c_0\delta_0\tau n). \tag{4.21}$$

For n large enough, we have $c_n > 1/2$, and the left-hand side of (4.21) is smaller than $2C_0\exp(-c_0\delta_0\tau n)$. Since the threshold for n and the constants c_0, τ and δ_0 only depend on q, the bound is of the required form.

We now focus on bounding the probabilities of connection to the left and right boundaries of $\mathsf{R}^{\mathrm{hp},\varepsilon}(n;\delta_0\frac{n}{\varepsilon})$.

Observe that, for a configuration such that the event $\{0 \xleftrightarrow{\mathsf{R}^{\mathrm{hp},\varepsilon}(n;\delta_0\frac{n}{\varepsilon})} \partial_R \mathsf{R}^{\mathrm{hp},\varepsilon}(n;\delta_0\frac{n}{\varepsilon})\}$ occurs, it suffices to change the state of at most $\delta_0\frac{n}{\varepsilon}$ edges to connect 0 to the vertex $x_{0,n}$ (we will assume here n to be even, otherwise $x_{0,n}$ should be replaced by $x_{0,n+1}$). Moreover, these edges can be chosen to be vertical ones in the irregular block, thus they are all "short" edges with subtended angle ε. By the finite-energy property, there exists a constant $\tau = \tau(\varepsilon, q) \in (0,1)$ such that

$$\varphi_{G_{\mathrm{mix}}}\Big[0 \xleftrightarrow{\mathsf{R}^{\mathrm{hp},\varepsilon}(n;\delta_0\frac{n}{\varepsilon})} \partial_R \mathsf{R}^{\mathrm{hp},\varepsilon}(n;\delta_0\tfrac{n}{\varepsilon})\Big] \leqslant \tau^{-\delta_0\frac{n}{\varepsilon}} \varphi_{G_{\mathrm{mix}}}\Big[0 \leftrightarrow x_{0,n}\Big],$$

where τ can be estimated as follows,

$$\tau = \frac{p_\varepsilon}{p_\varepsilon + (1-p_\varepsilon)q} = \frac{y_\varepsilon}{q + y_\varepsilon} \geqslant 1 - c_1\varepsilon,$$

where $c_1 > 0$ is a constant depending only on q.

The points 0 and $x_{0,n}$ are not affected by the transformations in $\Sigma^{\uparrow}$, therefore

$$\begin{aligned}
\varphi_{G_{\mathrm{mix}}}\Big[0 \leftrightarrow x_{0,n}\Big] &= \varphi_{\widetilde{G}_{\mathrm{mix}}}\Big[0 \leftrightarrow x_{0,n}\Big] \\
&\leqslant \varphi_{\widetilde{G}_{\mathrm{mix}}}\Big[0 \leftrightarrow \partial\Lambda(n)\Big] \\
&\leqslant \varphi^{1/0}_{\mathsf{R}^{\mathrm{hp}}(N;N)}\Big[0 \leftrightarrow \partial\Lambda(n)\Big] \\
&\leqslant C_0\exp(-c_0 n),
\end{aligned}$$

where in the last line, $\mathsf{R}^{\mathrm{hp}}(N;N)$ is the subgraph of $\widetilde{G}_{\mathrm{mix}}$, or equivalently of $\mathbb{Z}^2$ since these two are identical. The last inequality is given by Proposition 3.24. We conclude that,

$$\begin{aligned}
\varphi_{G_{\mathrm{mix}}}\Big[0 \xleftrightarrow{\mathsf{R}^{\mathrm{hp},\varepsilon}(n;\delta_0\frac{n}{\varepsilon})} \partial_R \mathsf{R}^{\mathrm{hp},\varepsilon}(n;\delta_0\tfrac{n}{\varepsilon})\Big] &\leqslant C_0\exp\Big[-(c_0 + \tfrac{\delta_0}{\varepsilon}\log\tau)n\Big] \\
&\leqslant C_0\exp\Big[-(c_0 + \tfrac{\delta_0}{\varepsilon}\log(1-c_1\varepsilon))n\Big].
\end{aligned} \tag{4.22}$$

The same procedure also applies to the event $\Big\{0 \xleftrightarrow{\mathsf{R}^{\mathrm{hp},\varepsilon}(n;\delta_0\frac{n}{\varepsilon})} \partial_L \mathsf{R}^{\mathrm{hp},\varepsilon}(n;\delta_0\tfrac{n}{\varepsilon})\Big\}$.

Now let $\delta_1 = \frac{c_0\varepsilon}{c_0\tau\varepsilon - \log(1-c_1\varepsilon)}$ and $\delta_0 = \min\{\delta_1, \frac{1}{2}\}$. Notice that $\delta_1 \to \frac{c_0}{c_0\tau + c_1} > 0$ when $\varepsilon \to 0$, which gives the following relation,

$$c_0 + \frac{\delta_0}{\varepsilon}\log(1-c_1\varepsilon) \geqslant c_0 + \frac{\delta_1}{\varepsilon}\log(1-c_1\varepsilon) = c_0\delta_1\tau \longrightarrow \frac{c_0^2\tau}{c_0\tau + c_1} > 0,$$

as $\varepsilon \to 0$. Thus, for ε small enough, we can pick a uniform constant δ_0 such that

$$c_0 + \frac{\delta_0}{\varepsilon} \log(1 - c_1 \varepsilon) \geqslant \frac{1}{2} c_0 \delta_1 \tau =: c.$$

Then, Equations (4.18), (4.21) and (4.22) imply that for n larger than some threshold depending only on q,

$$\varphi_{G_{\text{mix}}}\Big[0 \leftrightarrow \partial\Lambda(n)\Big] \leqslant 4C_0 \exp(-cn).$$

Finally, by (4.19), we deduce (4.15) for all $N \geqslant 4n$ and n large enough. The condition on n may be removed by adjusting the constant C. □

Chapter 5

Semi-discrete complex analysis

In this chapter, we construct the main tool of our study: the semi-discrete complex analysis. There is a number of papers dealing with this, see for example [Kur63, Kur64, Kur67]. However, they do not go far enough for our needs. Thereforem, we will investigate deeper and construct the theory needed to study the quantum Ising model.

Pretty often, the notions defined on the square lattice or isoradial graphs [Duf68, Duf56, BMS05, Ken02, CS11, BG15] can be generalized easily, such as derivatives, holomorphicity and harmonicity (Section 5.1.1), Brownian motion (Section 5.2), Dirichlet boundary problem (Section 5.3) and other related objects.

The integration on the primal or dual lattice of a semi-discrete function can also be defined similarly (Section 5.1.2). A minor difficulty could arise when it comes to integrating the product of two semi-discrete functions. We will explain in Section 5.1.3 how to define this so as to have expected properties as in the continuous setting.

Another difficulty appears in the construction of the semi-discrete Green's function (Section 5.4). This can be done by modifying the approach from [Ken02], which makes use of discrete exponential functions. In the discrete case, the Green's function can also be seen as an isomonodromic discrete logarithm [BMS05].

The notion of *s-holomorphicity* was defined in (2.9) and will allow us to show the convergence stated in Theorem 6.1, using the fact that the observable defined in Section 6.2 is s-holomorphic.

5.1 Basic definitions

5.1.1 Derivatives

Let Ω_δ be a primal semi-discrete domain. A function f defined on Ω_δ is said to be *continuous* if $y \mapsto f(x,y)$ is continuous for all $x \in \{x, (x,y) \in \Omega_\delta\}$. The same definition applies to functions defined on a dual domain $\Omega^\star_\delta$, a medial domain $\Omega^\diamond_\delta$ or a mid-edge domain $\Omega^\flat_\delta$. We then define in the same way a differentiable function on these domains, or even $\mathcal{C}^k$ functions, by demanding the property on all the vertical intervals.

Given a vertex $p \in \mathbb{L}^\diamond_\delta$, we denote by $p^\pm$ the right and left neighboring vertices in $\mathbb{L}^\diamond_\delta$, i.e., $p^\pm := p \pm \frac{\delta}{2}$. Similarly, we may write $e^\pm := e \pm \frac{\delta}{2}$ for neighboring mid-edge vertices of $e \in \mathbb{L}^\flat_\delta$.

If $p \in \mathbb{L}^\diamond_\delta$, we denote by $e^\pm_p$ the right and the left neighboring mid-edges, or $e^\pm_p := p \pm \frac{\delta}{4}$. In the same way, given a mid-edge $e \in \mathbb{L}^\flat_\delta$, we denote by $p^\pm_e$ the right and the left neighboring medial vertices, or $p^\pm_e := e \pm \frac{\delta}{4}$.

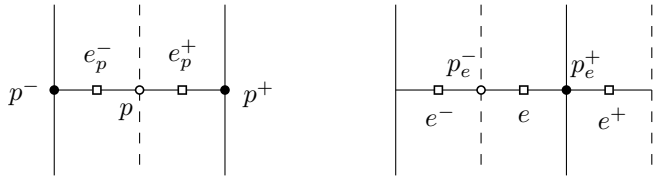

Figure 5.1 – Illustration of the definitions above. *Left*: neighboring mid-edges and vertices of a vertex. *Right*: neighboring vertices and mid-edges of a mid-edge.

For $e \in \mathbb{L}_\delta^\flat$, we may also write u_e (*resp.* w_e) the neighboring primal (*resp.* dual) vertex. In other words,

$$\{u_e\} = \{p_e^+, p_e^-\} \cap \mathbb{L}_\delta,$$
$$\{w_e\} = \{p_e^+, p_e^-\} \cap \mathbb{L}_\delta^\star.$$

See Figure 5.2 for an illustration.

Figure 5.2 – Illustration of the neighboring primal and dual vertices.

The derivatives $D^{(\delta)}$ and $\overline{D}^{(\delta)}$ of a differentiable function on $\mathbb{L}_\delta^\diamond$ or $\mathbb{L}_\delta^\flat$ can be defined by taking the "semi-discrete counterpart". Thus, the notion of holomorphicity and harmonicity will be defined in the same way.

Definition 5.1. Let $f : \mathbb{L}_\delta^\diamond \to \mathbb{C}$ be a complex function defined on the medial lattice. Let $p \in \mathbb{L}_\delta^\diamond$. The *x-derivative* at p is given by

$$D_x^{(\delta)} f(p) := \frac{f(p^+) - f(p^-)}{\delta}.$$

If $p \in \mathbb{L}_\delta^\diamond$, we define the *second x-derivative* at p by

$$D_{xx}^{(\delta)} f(p) := D_x^{(\delta)} \circ D_x^{(\delta)} f(p) = \frac{f(p^{++}) + f(p^{--}) - 2f(p)}{\delta^2}$$

where $p^{++} = (p^+)^+$ and $p^{--} = (p^-)^-$.

Definition 5.2. Let $f : \mathbb{L}_\delta^\diamond \to \mathbb{C}$ be a differentiable complex function defined on a medial lattice $\mathbb{L}_\delta^\diamond$. Its *derivatives* at $p \in \mathbb{L}^\diamond$ are given by

$$D^{(\delta)} f(p) = \frac{1}{2}\left[D_x^{(\delta)} f(p) + \frac{\partial_y f(p)}{\mathrm{i}}\right] = \frac{1}{2}\left[\frac{f(p^+) - f(p^-)}{\delta} + \frac{\partial_y f(p)}{\mathrm{i}}\right], \tag{5.1}$$
$$\overline{D}^{(\delta)} f(p) = \frac{1}{2}\left[D_x^{(\delta)} f(p) - \frac{\partial_y f(p)}{\mathrm{i}}\right] = \frac{1}{2}\left[\frac{f(p^+) - f(p^-)}{\delta} - \frac{\partial_y f(p)}{\mathrm{i}}\right]. \tag{5.2}$$

A semi-discrete function f is said to be (semi-discrete) *holomorphic at* $p \in \mathbb{L}_\delta^\diamond$ if $\overline{D}^{(\delta)} f(p) = 0$, and is said to be *holomorphic in* $\Omega_\delta^\diamond$, where $\Omega_\delta^\diamond$ is a medial domain, if $\overline{D}^{(\delta)} f(p) = 0$ for all $p \in \operatorname{Int} \Omega_\delta^\diamond$.

The same definitions (5.1) and (5.2) could also be used for functions defined on mid-edge domains. Let $f : \mathbb{L}_\delta^\flat \to \mathbb{C}$ be a differentiable complex function defined on the mid-edge lattice, then

$$D^{(\delta)} f(e) = \frac{1}{2}\left[\frac{f(e^+) - f(e^-)}{\delta} + \frac{\partial_y f(e)}{\mathrm{i}}\right], \tag{5.3}$$

$$\overline{D}^{(\delta)} f(e) = \frac{1}{2}\left[\frac{f(e^+) - f(e^-)}{\delta} - \frac{\partial_y f(e)}{\mathrm{i}}\right]. \tag{5.4}$$

Consider a twice differentiable function f defined on a primal (or dual) lattice. We can define its *Laplacian* by

$$\Delta^{(\delta)} f := 4D^{(\delta)}\overline{D}^{(\delta)} f = 4\overline{D}^{(\delta)} D^{(\delta)} f = D_{xx}^{(\delta)} f + \partial_{yy} f. \tag{5.5}$$

A twice differentiable function f defined on the primal domain Ω_δ is said to be

- *harmonic* if $\Delta^{(\delta)} f(p) = 0$, for all $p \in \mathrm{Int}^2\,\Omega_\delta$;
- *subharmonic* if $\Delta^{(\delta)} f(p) \geqslant 0$, for all $p \in \mathrm{Int}^2\,\Omega_\delta$;
- *superharmonic* if $\Delta^{(\delta)} f(p) \leqslant 0$, for all $p \in \mathrm{Int}^2\,\Omega_\delta$.

Here, we take twice interior because in the definition of the Laplacian, the second x-derivative is involved. We extend these definitions to a twice differentiable function defined on a dual domain in the same way.

5.1.2 Integration on primal and dual lattices

Now, we define the notion of *(semi-discrete) complex line integral* for a semi-discrete function f living on $\mathbb{L}_\delta^\diamond$. Let $\mathcal{P} = [k\delta + \mathrm{i}\,a, k\delta + \mathrm{i}\,b]$ be a vertical primal (*resp.* dual) segment, meaning that $k \in \mathbb{Z}$ (*resp.* $k \in \mathbb{Z} + \frac{1}{2}$) and $a < b$. If the segment $\mathcal{P}$ is oriented upwards, we write

$$\int_{\mathcal{P}} f(z)\mathrm{d}z := \mathrm{i}\int_a^b f(\delta k + \mathrm{i}\,y)\mathrm{d}y = \mathrm{i}\int_a^b f_k(y)\mathrm{d}y \tag{5.6}$$

to be the complex line integral along the vertical segment $\mathcal{P}$, where we define $f_k(\cdot) = f(\delta k + \mathrm{i}\cdot)$. Both primal and dual vertical segments are called *medial vertical segments*.

Let $\mathcal{P} = \{\delta k + \mathrm{i}\,t, m \leqslant k \leqslant n, k \in \mathbb{Z}\}$ be a horizontal primal segment for $m, n \in \mathbb{Z}$. We define

$$\int_{\mathcal{P}} f(z)\mathrm{d}z := \delta\sum_{k=m}^{n-1} f\left(\delta\left(k + \frac{1}{2}\right) + \mathrm{i}\,t\right) = \delta\sum_{k=m}^{n-1} f_{k+\frac{1}{2}}(t) \tag{5.7}$$

to be the complex line integral along the horizontal primal segment $\mathcal{P}$ oriented to the right. If we have a horizontal dual segment $\mathcal{P} = \{\delta(k + \frac{1}{2}) + \mathrm{i}\,t, m \leqslant k \leqslant n, k \in \mathbb{Z}\}$, we define in a similar way

$$\int_{\mathcal{P}} f(z)\mathrm{d}z := \delta\sum_{k=m+1}^{n} f(\delta k + \mathrm{i}\,t) = \delta\sum_{k=m+1}^{n} f_k(t) \tag{5.8}$$

the complex line integral along the horizontal dual segment. Both primal and dual horizontal segments are called *medial horizontal segments*.

In both vertical and horizontal cases, we define the semi-discrete complex line integral of a reversed path to be the opposite of the semi-discrete complex line integral of the original path.

The integrals above are called "semi-discrete complex line integrals" is for the following reason: we take into account the direction in which the segment goes, giving factors ± 1 (horizontal segments) or $\pm \mathrm{i}$ (vertical segments). We may also define the integration against $|\mathrm{d}z|$, removing thus these factors. Moreover, our integrals shall be defined additively.

Given a semi-discrete primal domain Ω_δ and a semi-discrete function f on it, we may write its integral on the domain by

$$\int_{\Omega_\delta} f(y)\mathrm{d}y := \delta \sum_{\operatorname{Int}\Omega_\delta} \int_{\alpha_k}^{\beta_k} f_k(y)\mathrm{d}y,$$

where the sum is taken over all the dual vertical lines in $\operatorname{Int}\Omega_\delta$. This can be seen as a double integral, in which one involves horizontal segments and the other one vertical segments. And the complex line integral along horizontal segments gives the factor δ. We may also deduce the same formula for a dual domain $\Omega_\delta^\star$. Here, we note that the integration against $\mathrm{d}y$ should be seen as classical real integration.

An *elementary primal (*resp. *dual) domain* is given by

$$B_k(\alpha,\beta) = \{x + \mathrm{i}\, y, \delta k \leqslant x \leqslant \delta(k+1), \alpha \leqslant y \leqslant \beta\}$$

for $\alpha < \beta$ integers and $k \in \mathbb{Z}$ (*resp.* $k \in \mathbb{Z} + \frac{1}{2}$). Its boundary consists of four primal (*resp.* dual) segments, two vertical ones and two horizontal ones. By convention, we will always orient the boundary counterclockwise. An *elementary medial domain* is either a primal or a dual elementary domain which shall be denoted by $B_k^\diamond(\alpha,\beta)$ for $k \in \frac{1}{2}\mathbb{Z}$ in the rest of this article.

From the complex line integrals along horizontal and vertical segments given by Equations (5.6), (5.7) and (5.8), we can also define the complex line integral along the boundary of any primal or dual domain by linearity. Let us consider an elementary primal or dual domain $B_k(\alpha,\beta)$ as an example. Denote by $\mathcal{C}$ its boundary which is oriented counterclockwise. If f is a semi-discrete function which is piecewise continuous, then its integral along the contour $\mathcal{C}$ is given by

$$\oint_{\mathcal{C}} f(z)\mathrm{d}z := \delta\left[f_{k+\frac{1}{2}}(\alpha) - f_{k+\frac{1}{2}}(\beta)\right] + \mathrm{i}\int_\alpha^\beta [f_{k+1}(y) - f_k(y)]\mathrm{d}y, \tag{5.9}$$

consisting of the four integrals coming from the four sides of the elementary domain. Moreover, if f is piecewise differentiable, this can be rewritten as

$$\oint_{\mathcal{C}} f(z)\mathrm{d}z = \delta\left[f_{k+\frac{1}{2}}\right]_\beta^\alpha + \mathrm{i}\,\delta\int_\alpha^\beta D_x^{(\delta)} f_{k+\frac{1}{2}}(y)\mathrm{d}y \tag{5.10}$$

$$= 2\,\mathrm{i}\,\delta\int_\alpha^\beta \overline{D}^{(\delta)} f_{k+\frac{1}{2}}(y)\mathrm{d}y. \tag{5.11}$$

where in $\overline{D}^{(\delta)} f$, the term $\partial_y f$ is given in the sense of distributions.

Given a primal semi-discrete domain Ω_δ, we define the integral of a semi-discrete function f along its counterclockwise-oriented contour by decomposing its boundary into vertical and horizontal segments and adding them up.

The integral along the contour of a dual domain is defined in a similar way and the corresponding properties can be obtained as well. We note that here we do not define the integral along the contour of a medial domain.

Proposition 5.3 (Green's formula). *Consider a primal domain Ω_δ. Denote by $\mathcal{C}$ its boundary which is oriented counterclockwise. Take a semi-discrete function f which is piecewise differentiable, then its integral along the contour $\mathcal{C}$ satisfies the following relation*

$$\oint_{\mathcal{C}} f(z)dz = 2\mathrm{i}\int_{\Omega_\delta} \overline{D}^{(\delta)} f(y)dy.$$

Proof. We decompose the primal or dual domain into elementary ones and sum up Equation (5.10) corresponding to each of them. On the right hand side, some integrals along the boundary of elementary domains appear twice with opposite sign and cancel out, therefore, the only remaining terms sum up to the complex line integral along the contour $\mathcal{C}$. □

Define a vector operator $\nabla = (D_x^{(\delta)}, \partial_y)$ called *nabla*. The following statement is similar to Green's formula in the continuous setting. This allows us to reduce a 2-dimensional integral into a contour integral on a more general (primal) domain.

Proposition 5.4 (Divergence theorem). *Let Ω_δ be a primal domain with contour $\mathcal{C}$ which is oriented counterclockwise. Let $\overrightarrow{F} = (F_x, F_y)$ be a semi-discrete function which is continuous and takes values in $\mathbb{R}^2$. We have the following equality,*

$$\int_{\Omega_\delta} \nabla \cdot \overrightarrow{F}(y)dy = \oint_{\mathcal{C}} \overrightarrow{F}(z) \cdot \overrightarrow{n}(z)|dz|, \tag{5.12}$$

where $\overrightarrow{n}(z)$ is the vector obtained after a rotation of $-\frac{\pi}{2}$ from the tangent vector (oriented counterclockwise) to $\mathcal{C}$ at z with norm 1.

Proof. As usual, it suffices to show this for an elementary domain, and then sum up over a decomposition of Ω_δ into elementary domains. Let $B_k(\alpha, \beta)$ be an elementary domain. Write $F_{k,x}(\cdot) = F_x(\delta k + \mathrm{i}\cdot)$ and $F_{k,y} = F_y(\delta k + \mathrm{i}\cdot)$. The left-hand side of Equation (5.12) can be rewritten as

$$\begin{aligned}&\delta \int_\alpha^\beta (D_x^{(\delta)} F_{k,x} + \partial_y F_{k,y})(y)\mathrm{d}y \\ &\qquad = \int_\alpha^\beta (F_{k+\frac{1}{2},x} - F_{k-\frac{1}{2},x})(y)\mathrm{d}y + \delta[F_{k,y}(\beta) - F_{k,y}(\alpha)]\end{aligned}$$

which is exactly the right-hand side of Equation (5.12). □

We note again that this proposition is still valid even if $\overrightarrow{F}$ is only piecewise differentiable, as long as we interpret derivatives in the sense of distributions.

5.1.3 Integration of a product of functions

Here, we define the integration of a product of functions and establish the equivalent of Green's theorem in the semi-discrete case.

Let us start again with integration along elementary segments. Consider two functions defined on the semi-discrete lattice f and g, a vertical primal (*resp.* dual) segment $\mathcal{P} = [k\delta + \mathrm{i}\,a, k\delta + \mathrm{i}\,b]$ with $k \in \mathbb{Z}$ (*resp.* $k \in \mathbb{Z} + \frac{1}{2}$) and $a < b$. Recall that $f_k(\cdot) = f(k\delta + \mathrm{i}\cdot)$. If the segment $\mathcal{P}$ is oriented upwards, we write

$$\int_{\mathcal{P}} [f; g]\mathrm{d}z := \int_a^b [f_{k-\frac{1}{2}}(y) g_{k+\frac{1}{2}}(y) - f_{k+\frac{1}{2}}(y) g_{k-\frac{1}{2}}(y)]\mathrm{d}y \tag{5.13}$$

to be the integral along $\mathcal{P}$. If the segment is oriented downwards, we take the opposite of the above quantity.

For $m, n \in \mathbb{Z}$, let $\mathcal{P} = \{k\delta + \mathrm{i}\, t, m \leqslant k \leqslant n, k \in \mathbb{Z}\}$ be a horizontal primal segment. We define

$$\int_{\mathcal{P}} [f;g]\mathrm{d}z := \delta^2 \sum_{k=m}^{n-1} (g_{k+\frac{1}{2}} \partial_y f_{k+\frac{1}{2}} - f_{k+\frac{1}{2}} \partial_y g_{k+\frac{1}{2}})(t) \tag{5.14}$$

the integral along the horizontal primal segment $\mathcal{P}$, oriented towards the right.

In the same way as integration of a semi-discrete function along the (counterclockwise-oriented) contour of a semi-discrete domain, we define the counterpart of a product of functions by decomposing the contour into vertical and horizontal segments and adding them up.

Proposition 5.5 (Green's theorem)**.** *Consider a primal (or dual) domain Ω_δ and denote by $\mathcal{C}$ its counterclockwise-oriented boundary. Given two semi-discrete functions f and g which are piecewise differentiable in Ω'_δ such that $\Omega_\delta \subset \operatorname{Int} \Omega'_\delta$, we have*

$$\oint_{\mathcal{C}} [f;g]dz = \delta \int_{\Omega_\delta} [f_k \Delta^{(\delta)} g_k - g_k \Delta^{(\delta)} f_k](y)dy.$$

Proof. As usual, we start by showing this for an elementary domain since we can superimpose these domains to obtain more general domains and the integration terms simplify. Consider $B_{k-\frac{1}{2}}(\alpha, \beta)$ a dual elementary domain and denote $\mathcal{C}$ its contour with counterclockwise orientation. By definition, we have

$$\begin{aligned}
\oint_{\mathcal{C}} [f;g]\mathrm{d}z &= \int_\alpha^\beta [f_k g_{k+1} - f_{k+1} g_k](y)\mathrm{d}y - \int_\alpha^\beta [f_{k-1} g_k - f_k g_{k-1}](y)\mathrm{d}y \\
&\quad + \delta^2 \left[(g_k \partial_y f_k - f_k \partial_y g_k)(t)\right]_\beta^\alpha \\
&= \int_\alpha^\beta [f_k(\delta^2 D_{xx}^{(\delta)} g_k + 2g_k) - g_k(\delta^2 D_{xx}^{(\delta)} f_k + 2f_k)](y)\mathrm{d}y \\
&\quad + \delta^2 \int_\alpha^\beta \partial_y (f_k \partial_y g_k - g_k \partial_y f_k)(t)\mathrm{d}t \\
&= \delta^2 \int_\alpha^\beta [f_k D_{xx}^{(\delta)} g_k - g_k D_{xx}^{(\delta)} f_k](y)\mathrm{d}y + \delta^2 \int_\alpha^\beta (f_k \partial_{yy} g_k - g_k \partial_{yy} f_k)(t)\mathrm{d}t \\
&= \delta^2 \int_\alpha^\beta (f_k \Delta^{(\delta)} g_k - g_k \Delta^{(\delta)} f_k)(y)\mathrm{d}y.
\end{aligned}$$

□

5.2 Brownian motion, harmonic measure and Laplacian

Let $\delta > 0$. The standard Brownian motion on the semi-discrete lattice $\mathbb{L}_\delta = \delta\mathbb{Z} \times \mathbb{R}$ can be seen as a continuous-time random walk in the horizontal direction; and a standard Brownian motion on $\mathbb{R}$ in the vertical direction. We give a more precise description below.

Definition 5.6. Let $(T_i)_{i\in\mathbb{N}}$ be a family of i.i.d. exponential random variables of rate 1 and $(D_i)_{i\in\mathbb{N}}$ be a family of i.i.d. uniform random variables taking value in $\{+1, -1\}$. We define

$$S_t = \sum_{i=1}^{N(t)} D_i$$

where

$$N(t) = \sup\{n \in \mathbb{N}, T_1 + \cdots + T_n \leqslant t\}.$$

The continuous-time process $(S_t)_{t\in\mathbb{R}}$ is the *standard continuous-time simple random walk* on $\mathbb{Z}$.

Remark 5.7. We can easily compute the expectation and variance of S_t which are respectively 0 and t. It also has good scaling properties and one can show that $(\delta S_{t/\delta^2})$ converges to (B_t) in law when δ goes to 0, where (B_t) is a standard one-dimensional Brownian motion. Here, the process $(\delta S_{t/\delta^2})$ can be seen as the continuous-time random walk with symmetric jumps $\pm\delta$ at exponential rate $\frac{1}{\delta^2}$.

We can now define the *semi-discrete standard Brownian motion* on $\mathbb{L}_\delta$.

Definition 5.8. A *semi-discrete standard Brownian motion* on $\mathbb{L}_\delta$ is given by

$$B_t^{(\delta)} = (X_t, Y_t) = (\delta S_{t/\delta^2}, B_t), \quad \forall t \geqslant 0$$

where (S_t) is a standard one-dimensional continuous-time simple random walk and (B_t) is a standard one-dimensional Brownian motion, both of them being independent of each other. The starting point $B_0^{(\delta)}$ is arbitrary, which is given by the starting points of (S_t) and (B_t).

As in the discrete and continuous cases, we can define the notion of *harmonic measure* via the standard Brownian motion.

Definition 5.9. Given a primal domain Ω_δ and $(B_t^{(\delta)})$ a Brownian motion on Ω_δ starting at some point $(x, y) \in \Omega_\delta$, we define

$$T_{\Omega_\delta} = \inf\{t \geqslant 0, B_t^{(\delta)} \notin \operatorname{Int}\Omega_\delta\} \tag{5.15}$$

The *harmonic measure* of Ω_δ with respect to (x, y), denoted by $\mathrm{d}\omega_{\Omega_\delta}((x, y), \cdot)$, is the law of $B_{T_{\Omega_\delta}}^{(\delta)}$.

Here, we are interested in the harmonic measure on centered elementary rectangular domains $R_\varepsilon = \{-\delta, 0, \delta\} \times [-\varepsilon, \varepsilon]$. On such domains, the harmonic measure with respect to 0, denoted by ρ_ε, is the sum of two Dirac masses at $\pm i\varepsilon$ and two density measures which are symmetric in both discrete and continuous directions on $\{\pm\delta\} \times [-\varepsilon, \varepsilon]$.

We will write $g_\delta(\varepsilon)$ for the probability that the Brownian motion $B_t^{(\delta)}$ leaves R_ε (the first time) from its left or right sides. This can be expressed by using the harmonic measure on R_ε as follows,

$$g_\delta(\varepsilon) = \int_{-\varepsilon}^{\varepsilon} \rho_\varepsilon(-\delta, y)\mathrm{d}y + \int_{-\varepsilon}^{\varepsilon} \rho_\varepsilon(\delta, y)\mathrm{d}y. \tag{5.16}$$

Thus, we can write the Dirac masses at $\pm i\varepsilon$ in this way:

$$\rho_\varepsilon(\pm i\varepsilon) = \rho_\varepsilon(0, \pm\varepsilon) = \frac{1 - g_\delta(\varepsilon)}{2} \cdot \delta_{\pm\varepsilon}.$$

Definition 5.10. Given a primal domain Ω_δ, a function $f : \Omega_\delta \to \mathbb{R}$ is said to satisfy the *mean-value property* on elementary rectangles if for all $(x, y) \in \Omega_\delta$ and $\varepsilon > 0$ such that $R'_\varepsilon = (x, y) + R_\varepsilon \subset \Omega_\delta$, we have

$$f(x, y) = \mathbb{E}_{(x,y)}\left[f\left(B_{T_{R'_\varepsilon}}^{(\delta)}\right)\right]. \tag{5.17}$$

Here, $B_t^{(\delta)}$ is the standard Brownian motion starting at (x, y) and $T_{R'_\varepsilon}$ the stopping time defined in Equation (5.15).

Remark 5.11. In terms of harmonic measure, Equation (5.17) can be reformulated as (without loss of generality, we take $(x, y) = (0, 0)$)

$$\begin{aligned} f(0,0) &= \int_{\partial R_\varepsilon} f(z)\rho_\varepsilon(z)|\mathrm{d}z| \\ &= \int_{-\varepsilon}^{\varepsilon} f(-\delta, y)\rho_\varepsilon(-\delta, y)\mathrm{d}y + \int_{-\varepsilon}^{\varepsilon} f(\delta, y)\rho_\varepsilon(\delta, y)\mathrm{d}y \\ &\quad + \frac{1 - g_\delta(\varepsilon)}{2} \cdot (f(-i\varepsilon) + f(i\varepsilon)). \end{aligned}$$

The following proposition computes the existing probability from the left or right boundary of R_ε. This will be useful later in Proposition 5.13 to show that the mean-value property implies that the Laplcian of a harmonic function is zero.

Proposition 5.12. *The probability that the Brownian motion $B_t^{(\delta)}$ leaves R_ε (the first time) by the left or right boundary is*

$$g_\delta(\varepsilon) = 1 - \frac{1}{\cosh(\sqrt{2}\varepsilon/\delta)} = \left(\frac{\varepsilon}{\delta}\right)^2 + \mathcal{O}_\delta\left(\varepsilon^4\right),$$

where the asymptotic behavior is given for $\varepsilon \to 0$.

Proof. Fix $(B_t^{(\delta)} = (\delta S_{t/\delta}, B_t))_{t\geqslant 0}$ as in Definition 5.8. This probability is exactly $\mathbb{P}[\delta^2 T_1 < \tau]$ where T_1 is an exponential law with parameter 1, which is independent of the stopping time $\tau = \tau_\varepsilon \wedge \tau_{-\varepsilon}$ for the standard 1D Brownian motion. Here

$$\tau_x := \begin{cases} \inf\{t, B_t \geqslant x\} & \text{if } x > 0, \\ \inf\{t, B_t \leqslant x\} & \text{if } x < 0. \end{cases}$$

By Fubini, we have

$$1 - g_\delta(\varepsilon) = \mathbb{P}[\delta^2 T_1 > \tau] = \mathbb{E}[\mathbb{P}[T_1 > \tau/\delta^2 \mid \tau]] = \mathbb{E}[\exp(-\tau/\delta^2)],$$

which is the Laplace transform of τ.

To calculate this, we note that the continuous-time process

$$M_t = \exp\left(\sqrt{2}B_t/\delta - t/\delta^2\right)$$

is a martingale with respect to the canonical filtration. Moreover, by the definition of the stopping time τ, the process $(M_{t\wedge\tau})_t$ is a martingale bounded by $e^{\sqrt{2}\varepsilon/\delta}$. The stopping time being finite almost surely, we can apply Doob's optional stopping theorem, giving us:

$$\begin{aligned} 1 &= \mathbb{E}[M_0] = \mathbb{E}[M_\tau] \\ &= \frac{1}{2}\mathbb{E}[M_\tau|\tau = \tau_\varepsilon] + \frac{1}{2}\mathbb{E}[M_\tau|\tau = \tau_{-\varepsilon}] \\ &= \frac{1}{2}\exp\left(\sqrt{2}\varepsilon/\delta\right)\mathbb{E}\left[\exp(-\tau/\delta^2)|\tau = \tau_\varepsilon\right] \\ &\quad + \frac{1}{2}\exp\left(-\sqrt{2}\varepsilon/\delta\right)\mathbb{E}\left[\exp(-\tau/\delta^2)|\tau = \tau_{-\varepsilon}\right]. \end{aligned} \tag{5.18}$$

Since $(B_t)_t$ and $(-B_t)_t$ are equal in law, we have

$$\mathbb{E}\left[\exp(-\tau/\delta^2)|\tau = \tau_\varepsilon\right] = \mathbb{E}\left[\exp(-\tau/\delta^2)|\tau = \tau_{-\varepsilon}\right].$$

Moreover,

$$\mathbb{E}\left[\exp(-\tau/\delta^2)\right] = \frac{1}{2}\mathbb{E}\left[\exp(-\tau/\delta^2)|\tau = \tau_\varepsilon\right] + \frac{1}{2}\mathbb{E}\left[\exp(-\tau/\delta^2)|\tau = \tau_{-\varepsilon}\right],$$

giving

$$\mathbb{E}\left[\exp(-\tau/\delta^2)\right] = \mathbb{E}\left[\exp(-\tau/\delta^2)|\tau = \tau_\varepsilon\right] = \mathbb{E}\left[\exp(-\tau/\delta^2)|\tau = \tau_{-\varepsilon}\right].$$

Thus, Equation (5.18) becomes

$$1 = \cosh\left(\sqrt{2}\varepsilon/\delta\right) \cdot \mathbb{E}\left[\exp(-\tau/\delta^2)\right],$$

which implies

$$\mathbb{E}\left[\exp(-\tau/\delta^2)\right] = \frac{1}{\cosh\left(\sqrt{2}\varepsilon/\delta\right)}$$

and

$$g_\delta(\varepsilon) = 1 - \mathbb{E}\left[\exp(-\tau/\delta^2)\right] = \frac{\cosh\left(\sqrt{2}\varepsilon/\delta\right) - 1}{\cosh\left(\sqrt{2}\varepsilon/\delta\right)}.$$

□

The following proposition gives two equivalent characteristics for semi-discrete harmonic functions: one using the mean-value property and the other using the Laplacian.

Proposition 5.13. *Let Ω_δ be a primal domain and $h : \Omega_\delta \to \mathbb{R}$ be a $\mathcal{C}^2$ function defined on it. Then, the following two statements are equivalent :*

1. *h satisfies the mean-value property (Definition 5.10) on elementary rectangles;*
2. *$\Delta^{(\delta)}h \equiv 0$ on Ω_δ.*

Proof. Here, we will show that the property 1 implies the property 2. The converse will be discussed later in Section 5.3.

Consider a function f as in the statement. We will apply the mean-value property at a point of Ω_δ and consider elementary rectangles with smaller and smaller height to prove the desired property. Let $\varepsilon > 0$ and consider an elementary rectangle R_ε. Let us first approximate the contribution of $\mathbb{E}_0\left[f\left(B_T^{(\delta)}\right)\right]$ on the left boundary by $h(-\delta, 0)$:

$$\begin{aligned}
&\int_{-\varepsilon}^{\varepsilon} h(-\delta, y)\rho_\varepsilon(-\delta, y)dy - \frac{g_\delta(\varepsilon)}{2} \cdot h(-\delta, 0) \\
&\quad = \int_{-\varepsilon}^{\varepsilon} [h(-\delta, y) - h(-\delta, 0)]\rho_\varepsilon(-\delta, y)\mathrm{d}y \\
&\quad = \int_{-\varepsilon}^{\varepsilon} [y\partial_y h(-\delta, 0) + E_\varepsilon(-\delta, y)]\rho_\varepsilon(-\delta, y)\mathrm{d}y.
\end{aligned}$$

The harmonic measure ρ_ε is symmetric in y, thus the integral of $y\partial_y h$ gives zero. The error term can be expressed as follows

$$E_\varepsilon(-\delta, y) = \int_0^y \partial_{yy} h(-\delta, t)(y - t)\mathrm{d}t$$

giving the upper bound

$$|E_\varepsilon(-\delta, y)| \leqslant C \cdot \frac{y^2}{2}, \quad \forall y \in [-\varepsilon, \varepsilon],$$

where $C = \sup\{\partial_{yy} h(-\delta, y), y \in [-\varepsilon, \varepsilon]\}$. In consequence, we have

$$\left| \int_{-\varepsilon}^{\varepsilon} h(-\delta, y)\rho_\varepsilon(-\delta, y)\mathrm{d}y - \frac{g_\delta(\varepsilon)}{2} \cdot h(-\delta, 0) \right| \leqslant C \int_{-\varepsilon}^{\varepsilon} \frac{\varepsilon^2}{2} \rho_\varepsilon(-\delta, y)\mathrm{d}y = \frac{C\varepsilon^2}{2} \cdot \frac{g_\delta(\varepsilon)}{2},$$

allowing us to write

$$\int_{-\varepsilon}^{\varepsilon} h(-\delta, y)\rho_\varepsilon(-\delta, y)\mathrm{d}y = \frac{g_\delta(\varepsilon)}{2} \cdot \left[h(-\delta, 0) + \mathcal{O}\left(\varepsilon^2\right)\right]. \tag{5.19}$$

Similarly, we also have

$$\int_{-\varepsilon}^{\varepsilon} h(\delta, y)\rho_\varepsilon(\delta, y)\mathrm{d}y = \frac{g_\delta(\varepsilon)}{2} \cdot \left[h(\delta, 0) + \mathcal{O}\left(\varepsilon^2\right)\right]. \tag{5.20}$$

Combining Equations (5.19) and (5.20) and inserting in (5.17), we get

$$\begin{aligned} 0 &= \frac{g_\delta(\varepsilon)}{2} \cdot \left[h(-\delta, 0) + h(\delta, 0) - 2h(0, 0) + \mathcal{O}\left(\varepsilon^2\right)\right] \\ &\quad + \frac{1 - g_\delta(\varepsilon)}{2} \cdot [h(0, \varepsilon) + h(0, -\varepsilon) - 2h(0, 0)] \\ &= \frac{g_\delta(\varepsilon)}{2} \cdot \left[\delta^2 D_{xx}^{(\delta)} h(0, 0) + \mathcal{O}\left(\varepsilon^2\right)\right] + \frac{1 - g_\delta(\varepsilon)}{2} \cdot \left[\varepsilon^2 h_{yy}(0, 0) + \mathcal{O}\left(\varepsilon^2\right)\right]. \end{aligned}$$

We divide everything by ε^2 to get

$$0 = \frac{g_\delta(\varepsilon)}{2\varepsilon^2} \cdot \left[\delta^2 D_{xx}^{(\delta)} h(0, 0) + \mathcal{O}\left(\varepsilon^2\right)\right] + \frac{1 - g_\delta(\varepsilon)}{2} \cdot \left[h_{yy}(0, 0) + \mathcal{O}(1)\right].$$

When ε goes to 0, using Proposition 5.12 we obtain

$$\frac{1}{2}\Delta^{(\delta)} h(0, 0) = \frac{1}{2} D_{xx}^{(\delta)} h(0, 0) + \frac{1}{2}\partial_{yy} h(0, 0) = 0.$$

□

The semi-discrete Laplacian can also be interpreted by means of a generator. The *generator* of a continuous-time Markov process (X_t, Y_t) is the linear operator P such that

$$Pf(x, y) = \lim_{t \to 0} \frac{\mathbb{E}_{(x,y)}[f(X_t, Y_t)] - f(x, y)}{t}$$

for $\mathcal{C}^2$ functions $f : \mathbb{R}^2 \to \mathbb{R}$.

Proposition 5.14. *The generator of $B^{(\delta)}$ is $\frac{1}{2} D_{xx}^{(\delta)} + \frac{1}{2}\partial_{yy}$.*

Proof. We omit the proof here as it is straightforward and we do not need this proposition below. □

In $\mathbb{R}^2$, the generator of the standard 2D Brownian motion is one half of the planar Laplacian, so we may also expect the same connection between the semi-discrete Brownian motion and Laplacian, which actually follows from the above proposition and Equation (5.5).

5.3 Dirichlet boundary problem

Dirichlet boundary problems are of great importance in analysis and can be solved by the Brownian motion. It is one of the simplest boundary value problems one can imagine: given an open domain Ω and a function f defined on its boundary $\partial\Omega$, we look for functions which are harmonic in the Ω which coincides with f on the boundary.

To study the convergence of the observable that we define in Section 6.2, we actually deal with some particular boundary-value problems. Therefore, a good understanding of the *Dirichlet boundary problem* is necessary. The existence of the solution is given by the Brownian motion (Proposition 5.16) and the uniqueness is based on the maximum principle (Proposition 5.15).

Proposition 5.15 (Maximum principle)**.** *Consider a primal semi-discrete domain Ω_δ. Let u be a subharmonic function defined on Ω_δ, i.e., $\Delta^{(\delta)}u(p) \geqslant 0$ for all $p \in \mathrm{Int}^2\,\Omega_\delta$. Then, we have*

$$\sup_{z\in\Omega_\delta} u(z) = \sup_{z\in\partial\Omega_\delta} u(z).$$

In other words, the maximum of u is reached on the boundary.

Proof. First of all, let us assume that u is subharmonic but not harmonic, meaning that $\Delta^{(\delta)}u > 0$ on $\mathrm{Int}^2\,\Omega_\delta$. Take $z \in \mathrm{Int}\,\Omega_\delta$ a point at which u reaches its maximum. Since it is a maximum on vertical axes, we have $\partial_{yy}u(z) \leqslant 0$. And we also have $D^{(\delta)}_{xx}u(z) = u(z+\delta)+u(z-\delta)-2u(z) \leqslant 0$. Thus, the semi-discrete Laplacian satisfies $\Delta^{(\delta)}u(z) = D^{(\delta)}_{xx}u(z)+\partial_{yy}u(z) \leqslant 0$, leading to a contradiction.

In a more general case with $\Delta^{(\delta)}u \geqslant 0$ in $\mathrm{Int}\,\Omega_\delta$, let us consider the family of functions $(u_\varepsilon)_{\varepsilon>0}$ defined by

$$u_\varepsilon(z) = u(z) + \varepsilon y^2,$$

where y is the second coordinate of z. We have $\Delta^{(\delta)}u_\varepsilon = \Delta^{(\delta)}u + 2\varepsilon$, meaning that u_ε is strictly subharmonic. From the first part of the proof, we deduce that

$$\sup_{z\in\Omega_\delta} u_\varepsilon(z) = \sup_{z\in\partial\Omega_\delta} u_\varepsilon(z).$$

Since both terms are finite and decreasing while ε decreases to 0, taking the limit implies the desired result. □

Given a primal semi-discrete domain Ω_δ and a function $g : \partial\Omega_\delta \to \mathbb{R}$, the associated *Dirichlet problem* consists in determining a function $h : \Omega_\delta \to \mathbb{R}$ such that

1. it coincides with g on the boundary, i.e., $g = h_{|\partial\Omega_\delta}$;
2. it is harmonic on $\mathrm{Int}\,\Omega_\delta$, i.e., $(\Delta^{(\delta)}h)_{|\mathrm{Int}\,\Omega_\delta} \equiv 0$.

In such case, we say that h is a *solution* to the Dirichlet boundary problem.

Given a semi-discrete Dirichlet boundary problem, one can establish a solution by considering a semi-discrete Brownian motion, stopped when it touches the boundary. The statement is as follows.

Proposition 5.16 (Existence of solution)**.** *A solution to the Dirichlet boundary problem is given by*

$$h(z) = \mathbb{E}\left[g(B^{(\delta)}_T)\right], \quad \forall z \in \Omega_\delta, \tag{5.21}$$

where

$$T = \inf\{t \geqslant 0, B^{(\delta)}_t \notin \Omega_\delta\}.$$

Proof. We note that Equation (5.21) is well defined because the trajectory of $B_T^{(\delta)}$ is almost surely continuous (in the semi-discrete sense), thus $B_T^{(\delta)} \in \partial\Omega_\delta$.

If h is given by Equation (5.21), then it satisfies the mean-value property on elementary rectangles as well. Indeed, take $z \in \Omega_\delta$ and $\varepsilon > 0$ small enough such that $z + R_\varepsilon \subset \Omega_\delta$. Consider the stopping time

$$T' = \inf\{t \geqslant 0, B_t^{(\delta)} \notin z + R_\varepsilon\}$$

and write

$$h(z) = \mathbb{E}_z\left[g\left(B_T^{(\delta)}\right)\right] = \mathbb{E}_z\left[\mathbb{E}_{B_{T'}}\left[g\left(B_T^{(\delta)}\right)\middle| T'\right]\right] = \mathbb{E}_z\left[h\left(B_{T'}^{(\delta)}\right)\right]$$

which is exactly the mean-value property. Moreover, one can also show that h is $\mathcal{C}^2$ using classical arguments (convolution for example), and the already proved first implication of Proposition 5.13 gives $\Delta^{(\delta)}h \equiv 0$ on Ω_δ. □

Moreover, using the maximum principle (Proposition 5.15), one can show that such a solution is unique.

Proposition 5.17 (Uniqueness)**.** *The solution to the Dirichlet problem is unique.*

Proof. By linearity, it is enough to show uniqueness when the boundary condition is 0. Consider a semi-discrete domain Ω_δ and $h : \overline{\Omega_\delta} \to \mathbb{R}$ which is zero on the boundary $\partial\Omega_\delta$ and harmonic on Ω_δ. Applying the maximum principle to h and $-h$, the function h should reach its maximum and minimum on the boundary. Therefore, it is zero everywhere. □

Proof of Proposition 5.13. Here, we finish the proof of the proposition by using the uniqueness of the solution to the Dirichlet problem. Consider a semi-discrete domain Ω_δ and a function $f : \Omega_\delta \to \mathbb{R}$ satisfying $\Delta^{(\delta)}f \equiv 0$. We want to show that it satisfies the mean-value property on rectangles.

Take $z \in \Omega_\delta$ and $\varepsilon > 0$ such that $z+R_\varepsilon \subset \Omega_\delta$. Consider $g : \partial(z+R_\varepsilon) \to \mathbb{R}$ which coincides with f. There exists a unique function $h : z + R_\varepsilon \to \mathbb{R}$ such that $h_{z+\partial R_\varepsilon} \equiv g$ and $\Delta^{(\delta)}h \equiv 0$ over $z + R_\varepsilon$. Since f satisfies exactly the same conditions, we have $f \equiv h$ on $z + R_\varepsilon$.

By the construction of the solution to the Dirichlet problem (Proposition 5.16), f satisfies the mean-value property on rectangles. □

5.4 Green's function

A Green's function is a function which is harmonic everywhere except at one point, where it has a singularity described by the Dirac mass. It is closely related to the average number of visits of a random walk in the discrete setting and the average time spent by a Brownian motion in the continuous setting. We will explain its construction in the semi-discrete setting, show that it is unique up to an additive constant and derive some of its properties and asymptotic behavior.

Moreover, the Riesz representation (Proposition 5.26) allows us to "decompose" a function into sum of Green's functions. This will be important for the convergence theorem (Theorem 6.20) of semi-discrete s-holomorphic functions.

We note that this construction is the least trivial generalization among all the other notions from the isoradial case. The idea is based on the use of discrete exponential functions introduced in [Ken02] but the computation turns out to be more technical in our case.

5.4.1 Construction and properties

A Green's function is a function $\mathcal{G}_\delta(z,\zeta)$ defined on the semi-discrete (primal) lattice satisfying the following three properties.

1. It is translational invariant, i.e., there exists a function G_δ such that for any $z,\zeta \in \mathbb{L}$, we have $G_\delta(\zeta - z) = \mathcal{G}_\delta(z,\zeta)$.
2. The function $\zeta \mapsto G_\delta(\zeta)$ is $\mathcal{C}^2$ and semi-discrete harmonic except at $\zeta = 0$, where it is only continuous.
3. Behavior around the origin: when $\varepsilon > 0$ is small, the quantities $G_\delta(\mathrm{i}\,\varepsilon)$ and $G_\delta(-\mathrm{i}\,\varepsilon)$ coincide at order $\mathcal{O}(1)$ and order $\mathcal{O}\left(\varepsilon^2\right)$,

$$\lim_{\varepsilon\to 0^+} G_\delta(\mathrm{i}\,\varepsilon) = \lim_{\varepsilon\to 0^+} G_\delta(-\mathrm{i}\,\varepsilon),$$
$$\lim_{\varepsilon\to 0^+} \partial_{yy} G_\delta(\mathrm{i}\,\varepsilon) = \lim_{\varepsilon\to 0^+} \partial_{yy} G_\delta(-\mathrm{i}\,\varepsilon),$$

   whereas at order $\mathcal{O}(\varepsilon)$, we have a jump,

$$\partial_y G_\delta(\mathrm{i}\,0^+) - \partial_y G_\delta(\mathrm{i}\,0^-) = \lim_{\varepsilon\to 0}[\partial_y G_\delta(\mathrm{i}\,\varepsilon) - \partial_y G_\delta(-\mathrm{i}\,\varepsilon)] = \frac{1}{\delta}.$$

   This is called the *normalization* of a Green's function.

If G_δ is a Green's function, we can apply Green's formula (Proposition 5.3) or the Divergence Theorem (Proposition 5.4) to get the usual property that, for a dual domain $\Omega_\delta^\star$ such that $0 \in \operatorname{Int}\Omega_\delta^\star$,

$$\int_{\Omega_\delta^\star} \Delta^{(\delta)} G_\delta(y)\mathrm{d}y = 1$$

and

$$\int_{\Omega_\delta^\star} f(y)\Delta^{(\delta)} G_\delta(y)\mathrm{d}y = f(0)$$

where f is a semi-discrete function on $\Omega_\delta^\star$.

We will show that there exists a unique function (up to an additive constant) having these properties. To achieve this, we generalize the method of discrete exponential functions from [Ken02]. First of all, let us define G_δ for $\delta = 1$ (Proposition 5.18) then for general δ (Proposition 5.21).

Consider a family of meromorphic functions on $\mathbb{C}$ indexed by vertices in $\mathbb{L}_1$ in the following way:

- at the origin: $f_0(z) = \frac{1}{z}$;
- if $t \in \mathbb{R}$, then $f_{\mathrm{i}t}(z) = f_0(z)\cdot\exp\left[2\,\mathrm{i}\,t\left(\frac{1}{z+1} + \frac{1}{z-1}\right)\right]$;
- if $p \in \mathbb{L}_1^\diamond$, then $f_{p^+}(z) = f_p(z)\cdot\frac{z+1}{z-1}$.

In other words, if $\zeta = m + it$ with $m \in \frac{1}{2}\mathbb{Z}$ and $t \in \mathbb{R}$, we can write

$$f_\zeta(z) = \frac{1}{z}\cdot\exp\left[2\,\mathrm{i}\,t\left(\frac{1}{z+1} + \frac{1}{z-1}\right)\right]\cdot\left(\frac{z+1}{z-1}\right)^{2m}. \tag{5.22}$$

Proposition 5.18 (Green's function). *The following function is the Green's function on* $\mathbb{L}_1$

$$G(\zeta) := \frac{1}{8\pi^2\,\mathrm{i}}\int_C f_\zeta(z)\ln(z)dz \tag{5.23}$$

where C is a path in $\mathbb{C}$ depending on ζ, surrounding $\{e^{i\theta}, 0 \leqslant \theta \leqslant \pi\}$ and leaving the origin outside the contour. For the complex logarithm, we define it in $(\theta - \pi, \theta + \pi)$ where θ is an argument of ζ.

Remark 5.19. We can compute the Green's function of Proposition 5.18 with the help of the residue theorem. The possible poles of the function $f_t(z)\ln(z)$ are 1 and -1 and the choice of the branch creates a possible discontinuity only when $t = \operatorname{Im}\zeta = 0$, since elsewhere, we have $\ln(-1) - \ln(1) = \pm i\pi$ with a + sign in the upper half-plane and a − sign in the lower half-plane.

Proof. We start by checking that G given by (5.23) is well-defined. If we change the lift of the logarithm, (equivalent to adding $2k\pi$ to log for an integer k), we need to show that this does not change the value of G, that is to say

$$\int_C f_\zeta(z)\mathrm{d}z = 0$$

for all $\zeta \in \mathbb{L}_1$. This is shown in Appendix, see Proposition A.5.

In each of the half-planes, the function G is $\mathcal{C}^\infty$ because we integrate a smooth function along a path and the branch of the logarithm does not cross 1 or -1 where a discontinuity might be created.

On $\mathbb{Z}\backslash\{0\}$, we can expand the exponential function and see that the residues at 1 and at -1 coincide up to the second order. It is explained in Proposition A.6, telling us that G is $\mathcal{C}^2$ on $\mathbb{L}_1$ except at 0.

Now, let us check that G is semi-discrete harmonic everywhere apart from the origin. Actually, it is sufficient to check that f_ζ is harmonic (with respect to ζ) except at the origin. Writing $\zeta = x + iy$ with $x \in \mathbb{Z}$ and $y \in \mathbb{R}$, we find

$$\begin{aligned}\Delta^{(\delta)}_{xx} f_\zeta &= D^{(\delta)}_{xx} f_\zeta + \partial_{yy} f_\zeta \\ &= \left[(2i)^2\left(\frac{1}{z+1} + \frac{1}{z-1}\right)^2 + \left(\frac{z+1}{z-1}\right)^2 + \left(\frac{z-1}{z+1}\right)^2 - 2\right] f_\zeta \\ &= 0.\end{aligned}$$

Here, it is allowed to add all the terms together since we always consider the same branch of the logarithm.

To conclude the proof, we still need to check the behavior of G around 0. This follows from a direct computation:

$$\begin{aligned}\lim_{\varepsilon\to 0^+} \partial_y G(i\varepsilon) &= \frac{1}{4\pi^2}\int_C \left(\frac{1}{z+1} + \frac{1}{z-1}\right)\frac{\ln(z)}{z}\mathrm{d}z \\ &= \frac{i}{2\pi}\left[\ln(1) - \ln(-1)\right] = \frac{1}{2}\end{aligned}$$

where we use the residue theorem in the second equality. Similarly, we have

$$\lim_{\varepsilon\to 0^-} \partial_y G(i\varepsilon) = -\frac{1}{2}.$$

Lastly, to check that $G(i\varepsilon)$ and $G(-i\varepsilon)$ coincide at order $\mathcal{O}(1)$ and order $\mathcal{O}\left(\varepsilon^2\right)$, we use Lemma A.4.

As a consequence, we get all the properties we were looking for and G is indeed a Green's function on $\mathbb{L}_1$. □

Proposition 5.20 (Asymptotics of Green's function). *Let $\zeta \in \mathbb{L}_1$. When $|\zeta|$ goes to infinity, we have the following asymptotic behavior,*

$$G(\zeta) = \frac{1}{2\pi}\ln(4|\zeta|) + \frac{\gamma_{Euler}}{2\pi} + \mathcal{O}\left(\frac{1}{|\zeta|^2}\right). \tag{5.24}$$

Proof. The proof is similar to the one given in [Ken02] for the discrete Green's function on isoradial graphs. We need to be careful when dealing with the exponential term in f_ζ. To get the improved error term $\mathcal{O}\left(1/|\zeta|^2\right)$, we use the method from [Büc08].

Consider $\zeta = m + \mathrm{i}t \in \mathbb{L}_1$ and write $d = |\zeta|$ and $\arg\zeta = \theta_0$. Take $r = \mathcal{O}\left(1/d^4\right)$ and $R = \frac{1}{r} = \mathcal{O}\left(d^4\right)$. We will consider the path C going as follows:

1. counterclockwise around the ball of radius R around the origin from the angles $\theta_0 - \pi$ to $\theta_0 + \pi$;
2. along the direction $e^{\mathrm{i}\theta_0}$ from $-R$ to $-r$;
3. around the ball of radius r around the origin from angle $\theta_0 + \pi$ back to $\theta_0 - \pi$;
4. along the direction $e^{\mathrm{i}\theta_0}$ from $-r$ to $-R$, back to the starting point.

This path is illustrated in Figure 5.3.

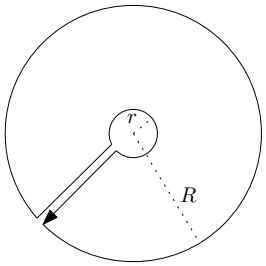

Figure 5.3 – The path along which we integrate in the proof of Proposition 5.20.

We estimate these integrals separately, combining the two integrals along the direction $e^{\mathrm{i}\theta_0}$. First of all, to study the integral around the ball of radius r, we start by expanding f_ζ for $z = re^{\mathrm{i}\theta}$ when r is small:

$$\frac{1}{1+z} - \frac{1}{1-z} = \mathcal{O}(r) \quad \text{and} \quad \frac{1+z}{1-z} = \exp(\mathcal{O}(r)).$$

Due to the invariance of these formulae (up to sign) by $r \leftrightarrow R = \frac{1}{r}$, the same expansions hold for $z = Re^{\mathrm{i}\theta}$ as well. Thus,

$$f_\zeta(z) = \frac{1}{z}\exp(\mathcal{O}(dr)) = \frac{1}{z}(1 + \mathcal{O}(dr)).$$

If we sum up the integrals around the ball of radius r and around the ball of radius R, we obtain

$$\frac{1}{8\pi^2\,\mathrm{i}}\int_{\theta_0-\pi}^{\theta_0+\pi}(1+\mathcal{O}(dr))[(\ln R + \mathrm{i}\theta) - (\ln r + \mathrm{i}\theta)]\,\mathrm{i}\,\mathrm{d}\theta$$
$$= \frac{\ln R - \ln r}{4\pi} + \mathcal{O}\left(\frac{1}{d^2}\right).$$

On the direction $e^{\mathrm{i}\theta_0}$ from $-R$ to $-r$, we also add up the two integrals. Since the logarithm differs by $2\pi\,\mathrm{i}$ on the both sides, by combining we get

$$\frac{e^{\mathrm{i}\theta_0}}{4\pi}\int_{-R}^{-r} f_\zeta(se^{\mathrm{i}\theta_0})\mathrm{d}s.$$

We should split this integral into 3 parts, I_1 for the integral from $-R$ to $-\sqrt{d}$, I_2 from $-\sqrt{d}$ to $-1/\sqrt{d}$ and I_3 from $-1/\sqrt{d}$ to $-r$. For $|z|$ small, we expand f_ζ to order $\mathcal{O}\left(z^3\right)$:

$$f_\zeta(z) = \frac{e^{4\overline{\zeta}z+\mathcal{O}\left(dz^3\right)}}{z}.$$

Thus, I_3 can be rewritten (let $\alpha = 4\overline{\zeta}e^{\mathrm{i}\theta_0} = 4|\zeta| = 4d$)

$$\begin{aligned} I_3 &= \frac{1}{4\pi}\int_{-1/\sqrt{d}}^{-r} \frac{e^{\alpha s+\mathcal{O}\left(ds^3\right)}}{s}\mathrm{d}s = \frac{1}{4\pi}\left(\int_{-\alpha/\sqrt{d}}^{-\alpha r}\frac{e^s}{s}\mathrm{d}s + \int_{-1/\sqrt{d}}^{-r}\mathcal{O}\left(ds^3\right)\frac{e^{\alpha s}}{s}\mathrm{d}s\right) \\ &= \frac{1}{4\pi}\left(\int_{-\alpha/\sqrt{d}}^{-1}\frac{e^s}{s}\mathrm{d}s + \int_{-1}^{-\alpha r}\frac{e^s-1}{s}\mathrm{d}s + \int_{-1}^{-\alpha r}\frac{\mathrm{d}s}{s}\right) + \mathcal{O}\left(\frac{1}{d^2}\right) \\ &= \frac{1}{4\pi}\left(\ln(\alpha r) + \gamma_{\mathrm{E}uler}\right) + \mathcal{O}\left(\frac{1}{d^2}\right), \end{aligned}$$

where in the first line, we expand the exponential; in the second line, the integral with $\mathcal{O}\left(ds^3\right)$ gives $\mathcal{O}\left(1/d^2\right)$; and in the last line, $\ln(\alpha r)$ comes from the third integral and Euler's constant comes from the first two integrals by taking $\alpha r \to 0$ and $\alpha/\sqrt{d} \to \infty$.

In a similar way (or by making the change of variable $s \to 1/s$), we get

$$I_1 = \frac{1}{4\pi}\left(-\ln(R/\alpha) + \gamma_{\mathrm{E}uler}\right) + \mathcal{O}\left(\frac{1}{d^2}\right).$$

To conclude the proof, we need to show that the intermediate term behaves as $\mathcal{O}\left(\frac{1}{d^2}\right)$. Let $z = se^{\mathrm{i}\theta_0}$ for $s \in [-\sqrt{d}, -1/\sqrt{d}]$. For the exponential term in f_ζ, we have

$$\begin{aligned} \exp\left[2\mathrm{i}\,t\left(\frac{1}{z+1}+\frac{1}{z-1}\right)\right] &= \exp\left[-2t\,\mathrm{Im}\left(\frac{1}{z+1}+\frac{1}{z-1}\right)\right] \\ &= \exp\left[2ts\sin\theta_0\left(\frac{1}{|z+1|^2}+\frac{1}{|z-1|^2}\right)\right] \\ &\leqslant \exp\left(-\mathcal{O}\left(\frac{t^2}{d^{3/2}}\right)\right). \end{aligned}$$

Then, for the other one, assume $m \geqslant 0$ (so $\cos\theta_0 \geqslant 0$),

$$\begin{aligned} \left|\frac{z+1}{z-1}\right|^{2m} &= \left(\frac{s^2+1+2s\cos\theta_0}{s^2+1-2s\cos\theta_0}\right)^m \leqslant \left(1+\frac{4s\cos\theta_0}{(s-1)^2}\right)^m \\ &\leqslant \exp\left(\frac{4ms\cos\theta_0}{(s-1)^2}\right) \leqslant \exp\left(-\mathcal{O}\left(\frac{m^2}{d^{3/2}}\right)\right) \end{aligned}$$

and we have the same bound for $m \leqslant 0$. After all, the intermediate term can be bounded by

$$I_2 \leqslant \sqrt{d}e^{-\mathcal{O}\left(\sqrt{d}\right)} \leqslant \mathcal{O}\left(\frac{1}{d^2}\right).$$

Finally, we sum up all the terms and take the limit $r \to 0$ (thus $R \to \infty$) to have

$$G(\zeta) = \frac{1}{2\pi}\left[\ln(4|\zeta|) + \gamma_{\mathrm{E}uler}\right] + \mathcal{O}\left(\frac{1}{d^2}\right). \qquad \square$$

Proposition 5.21. *On $\mathbb{L}_\delta$, there exists a unique Green's function with the following normalization at* 0

$$G_\delta(0) = \frac{1}{2\pi}(\ln\delta - \ln 4 - \gamma_{Euler}).$$

Moreover, its asymptotic behavior when $\frac{|\zeta|}{\delta}$ goes to ∞ is

$$G_\delta(\zeta) = \frac{1}{2\pi}\ln|\zeta| + \mathcal{O}\left(\frac{\delta^2}{|\zeta|^2}\right).$$

We call G_δ the free Green's function on $\mathbb{L}_\delta$.

Proof. To construct a Green's function with such normalization, we can consider

$$G_\delta(\zeta) = G\left(\frac{\zeta}{\delta}\right) + \frac{1}{2\pi}(\ln\delta - \ln 4 - \gamma_{Euler}).$$

To show the uniqueness, assume that G_δ and $\widetilde{G_\delta}$ are two such functions. Let $\mathcal{G}_\delta = G_\delta - \widetilde{G_\delta}$. The first order singularities at zero cancel out due to the same normalization, so the function $\mathcal{G}_\delta$ is $\mathcal{C}^1$ around 0. Since the second order terms of $G_\delta(\mathrm{i}\,\varepsilon)$ and $G_\delta(-\mathrm{i}\,\varepsilon)$ coincide (same for $\widetilde{G_\delta}$), $\mathcal{G}_\delta$ is $\mathcal{C}^2$ around 0. Finally, $\mathcal{G}_\delta$ is harmonic in $\mathbb{L}_\delta$ and is bounded (due to the asymptotic behavior), it should be zero everywhere by Harnack principle (see below, Proposition 5.25). □

Given a primal semi-discrete domain Ω_δ, we can define the *Green's function on* Ω_δ by

$$G_{\Omega_\delta} = G_\delta - H_{\Omega_\delta}$$

where G_δ is the free Green's function on $\mathbb{L}_\delta$ and H_{Ω_δ} the unique solution to the Dirichlet problem on the primal semi-discrete domain Ω_δ whose boundary condition is given by $G_{\delta|\partial\Omega_\delta}$ Here, we note that G_{Ω_δ} is non-positive.

5.4.2 Link with Brownian motion

In the discrete setting, the Green's function gives the average number of visits at each site of a simple random walk; and in the continuous setting, it tells the average time spent by a standard Brownian motion in an infinitesimal region. In the semi-discrete setting, we can also establish a similar result.

Proposition 5.22. *Let Q_δ be a semi-discrete primal domain. Consider $B^{(\delta)}$ a Brownian motion started at $x \in Q_\delta$ as defined in Section 5.2, stopped at τ, the first exiting time of the domain Q_δ. Then, we have the following asymptotic behavior which is independent of δ,*

$$\mathbb{E}[\tau] \asymp \int_{Q_\delta} |G_{\Omega_\delta}(x,y)|dy,$$

where the left-hand side is the average time spent by the semi-discrete Brownian motion $B^{(\delta)}$ in Q_δ; and the right-hand side is the integral of the Green's function on the same domain.

On a discrete graph, the expectation of the number of visits of a random walk (stopped after an exponential time if it is recurrent) is given by the negative of its associated Green's function. Similarly, the average time spent by a Brownian motion in a continuous space ($\mathbb{R}^d$ for example) is also given by the opposite of its associated Green's function (again stopped

after an exponential time if it is recurrent). Here in the semi-discrete setting, we should interpret the Green's function in the continuous direction as the average time spent by the Brownian motion; whereas in the discrete direction, the expectation of the number of "visits", which justifies the factor δ in the definition of $\int_{Q_\delta}$.

Proof. The semi-discrete Brownian motion $B^{(\delta)}$ converges in law to its continuous 2D counterpart, so does the semi-discrete Green's function, which converges uniformly on every compact not containing 0 to the 2D Green's function. As such, the integral of semi-discrete Green's function converges to the integral of 2D Green's function on every compact not containing 0. Moreover, $\ln y$ is integrable on $[0, \varepsilon]$, so the integral of the semi-discrete Green's function on a small rectangular domain around 0 can be well controlled, and this quantity goes to 0 when $\varepsilon \to 0$. □

If the Green's funcion is tightly linked to the Brownian motion, it is also the case for the harmonic measure. Actually, the following proposition allows us to write down equations associating the harmonic measure to the Green's function.

Proposition 5.23 (Link with harmonic measure)**.** *Consider a semi-discrete primal domain Ω_δ with $u_0 \in \operatorname{Int}\Omega_\delta$. Let $a \in \partial\Omega_\delta := \mathcal{C}_h \cup \mathcal{C}_v$ be a point on the boundary, where $\mathcal{C}_h$ and $\mathcal{C}_v$ denote respectively the horizontal and vertical parts. Write $\omega_{\Omega_\delta}(u_0, \{a\})$ for the harmonic measure with respect to u_0. We note that it should be seen as a density when $a \in \mathcal{C}_v$ and a Dirac mass when $a \in \mathcal{C}_h$. Then,*

- *if $a \in \mathcal{C}_v$, we have $\omega(u_0, \{a\}) = -\frac{1}{\delta} G_{\Omega_\delta}(u_0, a_{int})$;*
- *if $a \in \mathcal{C}_h$, we have $\omega(u_0, \{a\}) = \pm \partial_y G_{\Omega_\delta}(u_0, a)$,*

where a_{int} is the unique vertex in $\{a \pm \delta\} \cap \operatorname{Int}\Omega_\delta$, ∂_y is the vertical derivative with respect to the second coordinate and we take the + sign if the boundary is oriented to the left at a and the − sign otherwise.

Proof. It is immediate from Green's Theorem (Proposition 5.5) by taking $f = \omega_{\Omega_\delta}(\cdot, \{a\})$ and $g = G_{\Omega_\delta}(u_0, \cdot)$ and the fact that $\int_{\Omega_\delta} f \Delta^{(\delta)} g = 1$. □

Lemma 5.24. *We keep the same notation as above and take $\Omega_\delta = B_\delta(u_0, R)$. There exist two positive constants c_1 and c_2, independent of δ, such that*

- *if $a \in \mathcal{C}_v$, we have $c_1 \leqslant \omega(u_0, \{a\}) \leqslant c_2$;*
- *if $a \in \mathcal{C}_h$, we have $c_1 \delta \leqslant \omega(u_0, \{a\}) \leqslant c_2 \delta$.*

Proof. We link the harmonic measure to Green's function via Proposition 5.23, which can be estimated more easily by its asymptotic behavior given in Proposition 5.21. We can write

$$G_{\Omega_\delta}(u_0, u) - \frac{1}{2\pi} \ln \frac{|u - u_0|}{R} = \left[G_\delta(u_0, u) - \frac{1}{2\pi} \ln |u - u_0| \right] - \left[H_{\Omega_\delta}(u, u_0) - \frac{1}{2\pi} \ln R \right].$$

The first term is $\mathcal{O}\left(\frac{\delta^2}{|u-u_0|^2}\right)$. The second term is harmonic in $B_\delta(u_0, R)$, thus by the maximum principle, we get

$$\begin{aligned} \left| H_{\Omega_\delta}(u, u_0) - \frac{1}{2\pi} \ln R \right| &\leqslant \sup_{v \in \partial B_\delta(u_0, R)} \left| G_\delta(v, u_0) - \frac{1}{2\pi} \ln R \right| \\ &\leqslant \frac{\delta}{\pi R} + \mathcal{O}\left(\frac{\delta^2}{R^2}\right), \end{aligned}$$

where we use the fact that $R - 2\delta \leqslant |v - u_0| \leqslant R$ since $v \in \partial B_\delta(u_0, R)$. In summary, for all $u \in B_\delta(u_0, R)$,

$$\left| G_{\Omega_\delta}(u_0, u) - \frac{1}{2\pi} \ln \frac{|u - u_0|}{R} \right| = \frac{\delta}{\pi R} + \mathcal{O}\left(\frac{\delta^2}{|u - u_0|^2} + \frac{\delta^2}{R^2} \right).$$

By taking $u = a_{int}$ with $a \in \mathcal{C}_v$, we get the first part of the proposition. By taking $u \in B_\delta(u_0, R)$ closer and closer to $a \in \mathcal{C}_h$, we get the second part. □

5.5 Harnack Principle and convergence theorems

This part deals mostly with analysis of semi-discrete harmonic functions. We give the semi-discrete version of Harnack Lemma (Proposition 5.25) which is useful to show a convergence theorem for harmonic functions (Theorem 5.27). We also discuss the Riesz representation for semi-discrete functions (Proposition 5.26). In Section 6.5, we will apply these propositions to Theorem 6.1.

Proposition 5.25 (Semi-discrete Harnack Lemma). *Let $u_0 \in \Omega_\delta$ and $0 < r < R$ such that $B_\delta(u_0, R) \subset \Omega_\delta$. Consider a non-negative semi-discrete harmonic function $H : B_\delta(u_0, R) \to \mathbb{R}$. Let $M = \max H$ on Ω_δ. If $u, u^+ \in B_\delta(u_0, r)$, then*

$$|H(u^+) - H(u)| \leqslant const \cdot \frac{\delta M}{R - r},$$
$$\partial_y H(u) \leqslant const \cdot \frac{M}{R - r}.$$

Proof. We adapt the proof from the classical setting, which is based on the mean-value property (5.17) and coupling between semi-discrete Brownian motions.

For the first part, we consider a semi-discrete Brownian motion (X_t) issued from u and define T to be the exiting time of (X_t) from the ball $B_\delta(u_0, R)$. Write τ_1 for the first moment (before T) at which X_t and u_+ are on the same vertical primal line:

$$\tau_1 = \inf\{T \geqslant t \geqslant 0, \operatorname{Re} X_t = \operatorname{Re} u_+\}.$$

If $\tau_1 < \infty$, define $v = X_{\tau_1}$ and l to be the (horizontal) perpendicular bisector of the segment $[u_+, v]$. Write σ for the reflection with respect to l and define $Y_t = \sigma(X_{\tau_1 + t})$ up to τ_2, the time at which X_t touches l, and then $Y_t = X_{\tau_1 + t}$ afterwards. If $\tau_1 = \infty$, define (Y_t) to be a semi-discrete Brownian motion issued from u_+. Finally, define T' to be the exiting time of (Y_t) from the ball $B_\delta(u_0, R)$. As such, we have

$$|H(u^+) - H(u)| = |H(Y_{T'}) - H(X_T)| \leqslant 2M \mathbb{P}(X_T \neq Y_{T'}).$$

Using the coupling described above, one can compute the probability on the right-hand side. We find

$$\mathbb{P}(X_T \neq Y_{T'}) \leqslant \mathbb{P}(\tau_1 = \infty) + \mathbb{P}(\tau_2 = \infty \mid \tau_1 < \infty),$$

where both terms on the right-hand side are of order $\frac{\delta}{R-r}$ from gumbler's ruin theorem.

For the second inequality concerning the derivative in y, we use the same method by taking two points u and $v = u + \mathrm{i}\,\varepsilon$ on the same primal line which are at distance ε going to 0. The difference between $H(u)$ and $H(v)$ can be bounded by $\text{const} \cdot \frac{\varepsilon M}{R-r}$ and by dividing everything by ε and taking the limit, we obtain what we look for. □

Proposition 5.26 (Riesz representation). *Let f be a function on Ω_δ vanishing on the boundary $\partial\Omega_\delta$. Then, for all $y \in \Omega_\delta$,*

$$f(y) = \int_{\Omega_\delta} \Delta^{(\delta)} f(x) G_{\Omega_\delta}(x, y) dx.$$

Moreover, if f is not differentiable, we can define the integral in the sense of distributions.

Proof. The function $f - \int_{\Omega_\delta} \Delta^{(\delta)} f(x) G_{\Omega_\delta}(x, \cdot) \mathrm{d}x$ is harmonic and zero on the boundary, thus zero everywhere. □

Theorem 5.27 (Convergence theorem for harmonic functions). *Let $(h_\delta)_{\delta>0}$ be a family of semi-discrete harmonic functions on Ω_δ. It forms a precompact family for the uniform topology on compact subsets of Ω if one of the following conditions is satisfied.*

1. *The family (h_δ) is uniformly bounded on any compact subset of Ω.*
2. *For any compact $K \subset \Omega$, there exists $M = M(K) > 0$ such that for all $\delta > 0$, we have*

$$\int_{K_\delta} |h_\delta(x)|^2 dx \leqslant M.$$

Proof. The first point comes from Arzelà-Ascola since (h_δ) is uniformly Lipschitz (Proposition 5.25).

It remains to show that the second point implies the first one. Start by choosing a compact subset $K \subset \Omega$. Denote by $d = d(D, \partial\Omega)$ the distance between K and the boundary of Ω. Let K' be the $d/2$-neighborhood of K.

Let $0 < \delta < d/2$ and $x \in \operatorname{Int} K_\delta$. Choose Q to be a rectangular domain in K' which is centered at x. Write $Q_\delta = (x + [-r\delta, r\delta] \times [-s, s]) \cap \mathbb{L}_\delta$, $r \in \mathbb{N}$, for its semi-discrete counterpart. It is possible to have $r\delta > d/4$ and $s > d/4$ due to the assumption on the distance, and we assume so in the following.

If we write $H_k = \{k\delta\} \times [-s, s]$, the hypothesis implies

$$\sum_{k=\frac{r}{2}}^{r} \delta \left(\int_{H_{-k}} + \int_{H_k} \right) |h_\delta(y)|^2 \mathrm{d}y \leqslant M(K') =: M$$

for a certain constant M which is uniform in δ. Take $k \in [\![r/2, r]\!]$ such that the summand is minimum, and denoting this value of k by p, we get

$$\left(\int_{H_{-p}} + \int_{H_p} \right) |h_\delta(y)|^2 \mathrm{d}y \leqslant \frac{1}{\delta} \frac{M}{r/2} \leqslant c_1,$$

where c_1 is a uniform constant in δ.

For $t \in [0, s]$, denote $H_p^t = \{p\delta\} \times [-t, t]$. We can write, by linearity, h_δ as linear combination of harmonic measures,

$$h_\delta(x) = \left(\int_{H_{-p}^t} + \int_{H_p^t} \right) h_\delta(y) \omega_t(x, y) \mathrm{d}y + \sum_{\substack{k=-p+1 \\ y=k\delta \pm \mathrm{i}t}}^{p-1} h_\delta(y) \omega_t(x, y), \tag{5.25}$$

where ω_t is the harmonic measure in $[-p\delta, p\delta] \times [-t, t]$.

We integrate Equation (5.25) from $t = s/2$ to $t = s$ and get

$$h_\delta(x) = \frac{2}{s}\int_{s/2}^{s}\left(\int_{H_{-p}^t} + \int_{H_p^t}\right) h_\delta(y)\omega_t(x,y)\mathrm{d}y\mathrm{d}t + \frac{2}{s}\int_{s/2}^{2}\sum_{\substack{k=-p+1\\ y=k\delta\pm \mathrm{i}\,t}}^{p-1} h_\delta(y)\omega_t(x,y)\mathrm{d}t.$$

We want to show that $h_\delta(x)$ is uniformly bounded in x and in δ. We will take its square and apply Cauchy-Schwarz.

Below, denote respectively the first and second integrals A and B. First of all, note that $h_\delta(x)^2 \leqslant 2(A^2 + B^2)$, so we just need to show that A and B are bounded. We have,

$$\begin{aligned} A^2 &\leqslant \left(\frac{2}{s}\right)^2 \int_{s/2}^{s}\left(\int_{H_{-p}^t} + \int_{H_p^t}\right) h_\delta(y)^2\mathrm{d}y\mathrm{d}t \int_{s/2}^{s}\left(\int_{H_{-p}^t} + \int_{H_p^t}\right)\omega_t(x,y)^2\mathrm{d}y\mathrm{d}t \\ &\leqslant \left(\int_{H_{-p}^s} + \int_{H_p^s}\right) h_\delta(y)^2\mathrm{d}y \left(\int_{H_{-p}^t} + \int_{H_p^t}\right)\omega_s(x,y)^2\mathrm{d}y \end{aligned}$$

where $(2/s)^2$ is distributed once in the first term and once in the second, normalizing the integrals. (The length of the segment along which we integrate is $s/2$.) Then, for x and y fixed, $\omega_t(x,y) \leqslant \omega_s(x,y)$ for $t \leqslant s$. Here, the first term is bounded by c_1 by hypothesis, and the second by another constant c_2 from Lemma 5.24.

For the second term, Cauchy-Schwarz gives

$$B^2 \leqslant \left(\frac{2}{s}\right)^2 \int_{s/2}^{s}\sum_{\substack{k=-p+1\\ y=k\delta+\mathrm{i}\,t}}^{p-1} \delta h_\delta(y)^2\mathrm{d}t \int_{s/2}^{s}\sum_{\substack{k=-p+1\\ y=k\delta+\mathrm{i}\,t}}^{p-1} \frac{\omega_t(x,y)^2}{\delta}\mathrm{d}t.$$

On the right-hand side, the first term is bounded by M by assumption and the second term bounded by a uniform constant c_3 because $\omega_t(x,y)$ can be bounded by $c_4\delta$ uniformly (in a similar manner as before) in δ and in $y - x$, and there are $\mathcal{O}(1/\delta)$ terms in the sum. □

Proposition 5.28 (Estimate of the derivative of the Green's function). *Let $Q \subset \Omega_\delta$ such that $9Q \subset \Omega_\delta$. There exists $C > 0$ such that for all $\delta > 0$ and $y \in 9Q_\delta$, we have*

$$\int_{Q_\delta} |D_x^{(\delta)} G_{9Q_\delta}(x,y)|dx \leqslant C\int_{Q_\delta} |G_{9Q_\delta}(x,y)|dx.$$

Proof. For $y \in 9Q_\delta \backslash 3Q_\delta$, we estimate the Green's function in terms of the Brownian motion, or more precisely, the harmonic measure. We recall that $G_{9Q_\delta}(\cdot, y)$ is non positive, so that we can write for $x \in 2Q_\delta$,

$$|G_{9Q_\delta}(x,y)| = \int_{\mathcal{C}_v} |G_{9Q_\delta}(z,y)|\omega_{2Q_\delta}(z,y)|\mathrm{d}z| + \frac{1}{\delta}\int_{\mathcal{C}_h} |G_{9Q_\delta}(z,y)|\omega_{2Q_\delta}(z,y)|\mathrm{d}z|$$

where we denote the vertical and horizontal parts of the boundary $\partial(2Q_\delta)$ by $\mathcal{C}_v$ and $\mathcal{C}_h$. We can assume that

$$H := \int_{\mathcal{C}_h} |G_{9Q_\delta}(z,y)||\mathrm{d}z| \geqslant V := \int_{\mathcal{C}_v} |G_{9Q_\delta}(z,y)||\mathrm{d}z|.$$

The estimations of ω_{9Q_δ} in Lemma 5.24 gives us the lower and upper bounds easily

$$|G_{9Q_\delta}(x,y)| \leqslant c_2 \oint_{\partial(2Q_\delta)} |G_{9Q_\delta}(z,y)||\mathrm{d}z| = c_2(H+V) \leqslant 2c_2 H$$

and

$$\begin{aligned} |G_{9Q_\delta}(x,y)| &\geqslant c_1 \oint_{\partial(2Q_\delta)} |G_{9Q_\delta}(z,y)||\mathrm{d}z| \\ &\geqslant c_1 \int_{\mathcal{C}_h} |G_{9Q_\delta}(z,y)||\mathrm{d}z| = c_1 H. \end{aligned}$$

Thus, for $x, x' \in 2Q_\delta$,

$$\frac{1}{c_3}|G_{9Q_\delta}(x,y)| \leqslant |G_{9Q_\delta}(x',y)| \leqslant c_3 |G_{9Q_\delta}(x,y)|$$

with $c_3 = 2c_2/c_1$. Knowing that $G_{9Q_\delta}(\cdot, y)$ is harmonic in Q_δ, we apply Proposition 5.25 and the above inequality to get

$$|D_x^{(\delta)} G_{9Q_\delta}(x,y)| \leqslant c_4 \max_{x' \in Q_\delta} |G_{9Q_\delta}(x',y)| \leqslant c_3 c_4 |G_{9Q_\delta}(x,y)|.$$

For $y \in 3Q_\delta$, from Proposition 5.22, the average time spent by the Brownian motion, stopped when touching $\partial 9Q_\delta$, in Q_δ is proportional to

$$\int_{Q_\delta} |G_{9Q_\delta}(x,y)|\mathrm{d}x.$$

This quantity can be bounded from below by a constant c_5 because the semi-discrete Brownian motion converges to its continuous counterpart in $\mathbb{R}^2$.

Now it remains to show that the left-hand side can be bounded from above by a constant.

We write

$$G_{9Q_\delta}(x,y) = [G_{9Q_\delta}(x,y) - G_\delta(x,y)] + G_\delta(x,y),$$

where G_δ is the Green's function on $\mathbb{L}_\delta$ defined in Proposition 5.21. The first part $G_{9Q_\delta}(\cdot,y) - G_\delta(\cdot,y)$ is harmonic in $9Q_\delta$ (the singularities cancel out); moreover, on the boundary $\partial 9Q_\delta$, G_{9Q_δ} is zero and G_δ is bounded by a constant depending only on the domain Q by using the asymptotic behavior of the free Green's function in Proposition 5.21. The Harnack principle (Proposition 5.25) gives

$$|D_x^{(\delta)}[G_{9Q_\delta}(x,y) - G_\delta(x,y)]| \leqslant c_6.$$

Thus,

$$\int_{Q_\delta} |D_x^{(\delta)}[G_{9Q_\delta}(x,y) - G_\delta(x,y)]|\mathrm{d}x \leqslant \delta \cdot \frac{c_7}{\delta} \cdot c_6 = c_6 c_7.$$

Concerning $|D_x^{(\delta)} G_\delta(x,y)|$, we can look at its asymptotic behavior and show that, for $\zeta = m + \mathrm{i}\,t \in Q_\delta$ with $|\zeta| \gg \delta$,

$$\begin{aligned} D_x^{(\delta)} G_\delta(\zeta, y) &= \frac{1}{\delta}\left[G_\delta(\zeta + \frac{\delta}{2}, y) - G_\delta(\zeta - \frac{\delta}{2}, y)\right] \\ &= \frac{1}{2\pi\delta}\left[\ln\left(\frac{(m+\frac{\delta}{2})^2 + t^2}{m^2+t^2}\right) - \ln\left(\frac{(m-\frac{\delta}{2})^2 + t^2}{m^2+t^2}\right)\right] \\ &= \frac{1}{2\pi\delta}\left[\frac{2\delta m}{m^2+t^2} + \mathcal{O}\left(\delta^2\right)\right] = \frac{1}{\pi}\frac{m}{m^2+t^2} + \mathcal{O}(\delta). \end{aligned}$$

Thus, by integrating along vertical axes in Ω_δ, we get some quantity with the same asymptotic behavior (independent of δ but on Q_δ),

$$\int_{Q_\delta} |D_x^{(\delta)} G_\delta(x,y)| \mathrm{d}x \leqslant c_8.$$

The proof follows readily. □

5.6 Convergence to continuous Dirichlet problem

In this section, we study the convergence of semi-discrete harmonic functions when the mesh size of the lattice goes to 0.

Lemma 5.29. *Let Ω be a domain and (Ω_δ) its semi-discretized approximations converging to Ω in the Carathéodory sense. For each $\delta > 0$, consider a semi-discrete harmonic function h_δ on Ω_δ. Assume that h_δ converges uniformly on any compact subset of Ω to a function h, then h is also harmonic.*

Proof. From Proposition 5.25 and Theorem 5.27, we know that the family $(D_x^{(\delta)} h_\delta)$ is precompact thus we can extract from it a converging subsequence. Since $\partial_x h$ is the only possible sub-sequential limit, $(D_x^{(\delta)} h_\delta)$ converges. Similarly, one can also prove that $\Delta^{(\delta)} h_\delta = 0$ converges to Δh, which is also zero. □

Proposition 5.30. *Let Ω be a domain with two marked points on the boundary $a, b \in \partial\Omega$. Consider f a bounded continuous function on $\partial\Omega \backslash \{a,b\}$ and h the solution associated to the Dirichlet boundary value problem with boundary condition f. For each $\delta > 0$, let Ω_δ be the semi-discretized counterpart of the domain Ω, a_δ and b_δ approximating a and b. Let $f_\delta : \partial\Omega_\delta \to \mathbb{R}$ be a sequence of uniformly bounded functions converging uniformly away from a and b to f and h_δ be the solution of the semi-discrete Dirichlet boundary problem with f_δ as boundary condition. Then,*

$$h_\delta \to h$$

uniformly on compact subsets of Ω.

Proof. We first note that the semi-discretized domains converge in the Carathéodory sense to (Ω, a, b). Since (f_δ) is uniformly bounded, it is the same for the family (h_δ). Theorem 5.27 says that (h_δ) is a precompact family. Let $\widetilde{h}$ be a subsequential limit, which should also be harmonic inside Ω by Lemma 5.29. To show that $h = \widetilde{h}$, we need to prove that $\widetilde{h}$ can be extended to the boundary by f in a continuous way.

Let $x \in \partial\Omega \backslash \{a,b\}$ and $\varepsilon > 0$. By uniform convergence of $(f_\delta)_{\delta>0}$, there exists $R > 0$ such that for $\delta > 0$ small enough,

$$|f_\delta(x') - f_\delta(x)| < \varepsilon$$

for all $x' \in \partial\Omega_\delta \cap B_\delta(x, R)$. Let $r < R$ whose value is to be chosen later. For all $y \in B_\delta(x, r)$, we have

$$\begin{aligned} |h_\delta(y) - f_\delta(x)| &= \mathbb{E}[f_\delta(X_\tau) - f_\delta(x)] \\ &\leqslant \varepsilon + 2M\mathbb{P}[X_\tau \notin B_\delta(x, R)], \end{aligned}$$

where X is a semi-discrete Brownian motion started at y and τ its hitting time of the boundary $\partial\Omega_\delta$. In the last line, we decompose according to B_τ, the position of the Brownian motion at the hitting time: whether it is inside $B_\delta(x, R)$ or not. Lemma 5.31 gives the upper

bound $\mathbb{P}[X_\tau \notin B_\delta(x,R)] \leqslant (r/R)^\alpha$ for some independent constant $\alpha > 0$. We may choose $r = R(\varepsilon/2M)^{1/\alpha}$ and let δ go to 0 to obtain $|\widetilde{h}(y) - f(x)| \leqslant 2\varepsilon$ for all $y \in B_\delta(x,r)$. □

Lemma 5.31 (Weak Beurling's estimate). *For $a > 0$, write $\mathbb{D}(a) = [-a,a]^2$. There exists $\alpha > 0$ such that for any $r \in (0, \frac{1}{2})$ and any curve inside $\mathbb{D}(1)$ from $\partial\mathbb{D}(1)$ to $\partial\mathbb{D}(r)$, the probability that a semi-discrete random walk on $\mathbb{D}_\delta(1)$ starting at 0 exits $\mathbb{D}_\delta(1)$ without crossing γ is smaller than r^α uniformly in $\delta > 0$.*

Proof. This proof is classical, so we do not give all the details here. The idea is to decompose the annulus $\mathbb{D}(1)\backslash\mathbb{D}(r)$ into disjoint annuli $A_x = \mathbb{D}(2x)\backslash\mathbb{D}(x)$ and use the fact that the probability that a semi-discrete Brownian motion closes the loop in each annulus is of constant probability (which is a consequence of the RSW property, see Section 6.4.1). □

5.7 S-holomorphicity

The notion of *s-holomorphicity* will turn out to be important for the convergence theorem (Theorem 6.20). Actually, the semi-discrete holomorphicity provides us only with half of Cauchy-Riemann equations and fortunately, the rest of the information can be "recovered" by s-holomorphicity.

Roughly speaking, in Section 6.2.3, we will define a primitive of $\operatorname{Im} f^2$ where f is s-holomorphic and the convergence of this primitive provides us with additional information for the convergence of f. We will discuss this in more details in Sections 6.2 and 6.5.

We define the notion of s-holomorphicity on the mid-edge lattice (Definition 5.32) and on the medial lattice (Definition 5.33). And they can be proved to be equivalent in Proposition 5.34.

Definition 5.32. Let $f : \Omega_\delta^\flat \to \mathbb{C}$ be a function defined on the mid-edge semi-discrete lattice. It is said to be *s-holomorphic* if it satisfies the two following properties.

1. Parallelism: for $e \in \Omega_\delta^\flat$, we have $f(e) /\!\!/ \tau(e)$ where $\tau(e) = [\mathrm{i}(w_e - u_e)]^{-1/2}$, u_e and w_e denote respectively the primal and the dual extremities of the mid-edge e. In other words,
   - $f(e) \in \nu\mathbb{R}$ if p_e^+ is a dual vertex, and
   - $f(e) \in \mathrm{i}\,\nu\mathbb{R}$ if p_e^+ is a primal vertex,

   where $\nu = \exp(-\mathrm{i}\,\pi/4)$.
2. Holomorphicity: for all vertex e on the mid-edge lattice $\Omega_\delta^\flat$, we have $\overline{D}^{(\delta)} f(e) = 0$.

Definition 5.33. Let $g : \Omega_\delta^\diamond \to \mathbb{C}$ be a function defined on the medial semi-discrete domain. It is said to be *s-holomorphic* if it satisfies the two following properties.

1. Projection: for every $e = [p_e^- p_e^+] \in \Omega_\delta^\flat$, we have
$$\operatorname{Proj}[g(p_e^-), \tau(e)] = \operatorname{Proj}[g(p_e^+), \tau(e)] \tag{5.26}$$
   where $\operatorname{Proj}(X, \tau)$ denotes the projection of X in the direction of τ :
$$\operatorname{Proj}[X, \tau] = \frac{1}{2}\left[X + \frac{\tau}{\overline{\tau}} \cdot \overline{X}\right].$$
2. Holomorphicity: for all vertex e on medial lattice $\Omega_\delta^\diamond$, we have $\overline{D}^{(\delta)} f(e) = 0$.

These definitions may be linked to their counterparts in the setting of isoradial graphs. To be more precise, one can use the definitions provided in [CS11] on the lattice $\mathbb{G}^\varepsilon$, which is illustrated in Figure 1.7, and recover the above definitions by taking $\varepsilon \to 0$.

We have a correspondence between s-holomorphic functions on $\Omega_\delta^\diamond$ and those on $\Omega_\delta^\flat$.

Proposition 5.34. *Given an s-holomorphic function $f : \Omega_\delta^\flat \to \mathbb{C}$, one can define $g : \Omega_\delta^\diamond \to \mathbb{C}$ by:*

$$g(p) = f(e_p^-) + f(e_p^+), \quad p \in \Omega_\delta^\diamond.$$

Then, the new function g is still s-holomorphic.

Conversely, given an s-holomorphic function $g : \Omega_\delta^\diamond \to \mathbb{C}$, one can define $f : \Omega_\delta^\flat \to \mathbb{C}$ by:

$$f(e) = \mathrm{Proj}[g(p_e^-), \tau(e)] = \mathrm{Proj}[g(p_e^+), \tau(e)], \quad e \in \Omega_\delta^\flat.$$

Then, the new function f is still s-holomorphic.

Proof. Assume that $f : \Omega_\delta^\flat \to \mathbb{C}$ is s-holomorphic. Let us show that g as defined above is s-holomorphic on $\Omega_\delta^\diamond$. The projection property is satisfied from the parallelism of f and so is the holomorphicity.

Assume that $g : \Omega_\delta^\diamond \to \mathbb{C}$ is s-holomorphic. Let us show that f as defined above is s-holomorphic on $\Omega_\delta^\flat$. The parallelism is clearly satisfied by the definition. We just need to check the holomorphicity of f. Let $e \in \Omega_\delta^\flat$. We can assume that p_e^+ is primal and p_e^- dual such that $\tau(e) /\!\!/ e^{\mathrm{i}\pi/4}$. We want to calculate $\partial_y f(e)$.

$$\begin{aligned}
\partial_y f(e) &= \partial_y \mathrm{Proj}[g(p), \tau(e)] \\
&= \frac{1}{2}\partial_y[g(p) + \mathrm{i}\overline{g(p)}] \\
&= \frac{1}{2}\left[\frac{\mathrm{i}}{\delta}(g(p^+) - g(p^-)) + \mathrm{i}\left(-\frac{\mathrm{i}}{\delta}\right)(\overline{g(p^+)} - \overline{g(p^-)})\right] \\
&= \frac{\mathrm{i}}{\delta}[f(e^+) - f(e^-)]
\end{aligned}$$

where we use $\tau(e)/\overline{\tau(e)} = \mathrm{i}$ and $\tau(e^+)/\overline{\tau(e^+)} = \tau(e^-)/\overline{\tau(e^-)} = -\mathrm{i}$. □

Chapter 6

Scaling limit of the quantum Ising model

6.1 The quantum random-cluster model

We remind that the semi-discrete lattice and semi-discrete domains were defined in Section 1.2.1. Here, we talk about the semi-discretization of domains in $\mathbb{R}^2$, on which we define the quantum Ising model.

6.1.1 Semi-discretization of a continuous domain

A set in $\mathbb{R}^2$, or $\mathbb{C}^2$, is called a *domain* if it is open, bounded and simply connected. A *Dobrushin domain* is a domain with two distinct marked points a, b on the boundary. It is often denoted by a triplet (Ω, a, b) where Ω is a domain and $a, b \in \partial\Omega$.

Here, we explain how to *semi-discretize* such a domain to get its semi-discrete counterpart, on which the FK-representation of the quantum Ising model will be defined. Consider a Dobrushin domain (Ω, a, b) in $\mathbb{C}$ or $\mathbb{R}^2$ and $\delta > 0$. Let us denote by $[a^w_\delta a^b_\delta]$ and $[b^b_\delta b^w_\delta]$ two mid-edges with $a^b_\delta, b^b_\delta \in \mathbb{L}_\delta$, $a^w_\delta, b^w_\delta \in \mathbb{L}^\star_\delta$ and mid-points $a^\flat_\delta$ and $b^\flat_\delta$ given by minimizing the distances between a and $a^\flat_\delta$ and between b and $b^\flat_\delta$ over all possible such mid-edge segments contained in Ω. Once we get these two distinguished edges $[a^w_\delta a^b_\delta]$ and $[b^b_\delta b^w_\delta]$, we complete the semi-discrete domain by making approximation with primal horizontal and vertical segment of the arc $(a_\delta b_\delta)$ then with dual horizontal and vertical segments of the arc $(b_\delta a_\delta)$. Moreover, we ask that these segments to be inside Ω. This semi-discrete domain lies in Ω and is denoted by $(\Omega^\diamond_\delta, a_\delta, b_\delta)$. See Figure 6.1 for an example.

We write $\partial\Omega^\diamond_\delta$ for the boundary of this Dobrushin domain. This consists of four components:

$$\begin{aligned}
[a^w_\delta a^b_\delta] &\quad \text{an horizontal edge}\\
(a_\delta b_\delta) := (a^b_\delta b^b_\delta) &\quad \text{the arc going from } a^b_\delta \text{ to } b^b_\delta\\
[b^b_\delta a^w_\delta] &\quad \text{an horizontal edge}\\
(b_\delta a_\delta) := (b^w_\delta a^w_\delta) &\quad \text{the arc going from } b^w_\delta \text{ to } a^w_\delta\ .
\end{aligned}$$

They are ordered counterclockwise in Figure 6.1. Then, the quantum Ising model can be defined on such discretized domains and we also obtain the loop representation of the model

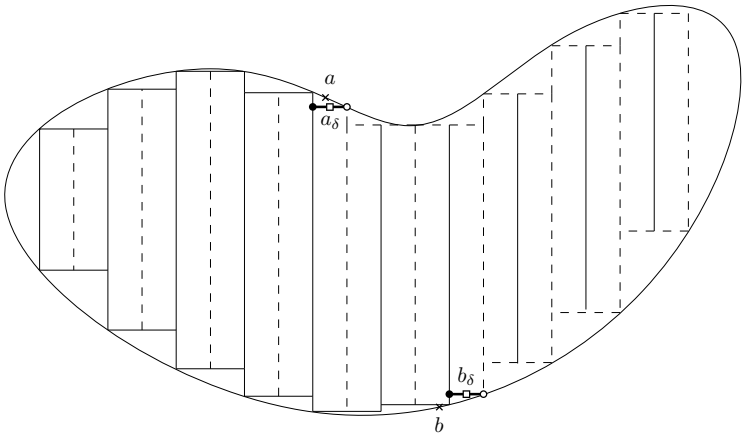

Figure 6.1 – An example of approximation of a continuous Dobrushin domain by a semi-discrete one with mesh size δ.

at the criticality as mentioned in Section 1.2.5, adapted to the case $q = 2$,

$$\mathrm{d}\mathbb{P}^{\mathrm{QI}}_{\lambda,\mu}(D,B) \propto \sqrt{2}^{l(D,B)}\mathrm{d}\mathbb{P}_{\rho,\rho}(D,B) \tag{6.1}$$

where $l(D,B)$ denotes the number of loops in a given configuration (D,B) and $\rho = \sqrt{\lambda\mu}$.

Note that semi-discrete domains $(\Omega^\diamond_\delta, a_\delta, b_\delta)$ defined above converge to the continuous domain (Ω, a, b) in the Carathéodory topology.

6.1.2 Main result

The result that we will show in this artical concerns the conformal invariance of the interface of the loop representation of the quantum Ising model. Since the conformal invariance also implies the rotational invariance, the parameters λ and μ should be chosen such that the model is isotropic. The good choice of such parameters are given by $\lambda = \frac{1}{2\delta}$ and $\mu = \frac{1}{\delta}$ (thus, $\rho = \frac{1}{\sqrt{2}\rho}$). In Section 6.2, or more precisely, Equation (6.4), we will see that it is actually a necessary and sufficient condition to get an observable with nice properties.

We are ready to give a formal statement of the main theorem.

Theorem 6.1. *Let (Ω, a, b) a Dobrushin domain. For $\delta > 0$, semi-discretize the domain to get a semi-discrete Dobrushin domain $(\Omega^\diamond_\delta, a_\delta, b_\delta)$ and consider the FK-representation of the critical quantum Ising model with parameters $\lambda = \frac{1}{2\delta}$ and $\mu = \frac{1}{\delta}$ on it. Denote by γ_δ the interface going from a_δ to b_δ in $(\Omega^\diamond_\delta, a_\delta, b_\delta)$, which separates the primal cluster connected to the wired boundary $(a_\delta b_\delta)$ and the dual cluster connected to the free boundary $(b_\delta a_\delta)$. Then, the law of γ_δ converges weakly to the chordal Schramm-Löwner Evolution $SLE_{16/3}$ running from a to b in Ω.*

6.2 Observable and properties

6.2.1 Definition and illustration

Let us take a Dobrushin domain (Ω, a, b) in $\mathbb{R}^2$. Consider $\delta > 0$ and the semi-discretized domain $(\Omega^\diamond_\delta, a_\delta, b_\delta)$ with mesh size δ, on which we put the loop representation of the critical quantum Ising model given by (6.1) with parameter ρ, which is the intensity of the Poisson point processes on both primal and dual vertical lines.

The intensity ρ should be chosen to be proportional to $\frac{1}{\delta}$, which is the factor that appears in the intensity of a Poisson point process when we scale it by δ in space. Moreover, we should consider $\rho = \frac{1}{\sqrt{2}\delta}$, the constant $\frac{1}{\sqrt{2}}$ being chosen to make the model isotropic. A heuristic of such a choice is as follows.

A special case of the conformal invariance is the rotational invariance, so in particular, the invariance by rotation of $\frac{\pi}{2}$. The relation that we obtain later in (6.4) shows that only for the choice of $\rho = \frac{1}{\sqrt{2}\delta}$, the observable defined in (6.2) is (semi-discrete) holomorphic. And the holomorphicity should be interpreted as follows: the observable varies in the same way in the horizontal (discrete) direction and the vertical (continuous) direction. This justifies why the choice of ρ is important, and that there is only one possible value satisfying this property.

The loop representation of the quantum Ising model gives an interface going from a_δ to b_δ. If $e \in \Omega_\delta^\flat$ is a mid-edge vertex of the Dobrushin domain $(\Omega_\delta^\diamond, a_\delta, b_\delta)$, we can define our observable at this point by

$$F_\delta(e) := F_{(\Omega_\delta^\diamond, a_\delta, b_\delta)}(e) = \frac{\nu}{\sqrt{\delta}} \cdot \mathbb{E}\left[\exp\left(\frac{\mathrm{i}}{2} W(e, b_\delta)\right) \mathbb{1}_{e \in \gamma_\delta}\right] \tag{6.2}$$

where γ_δ denotes the (random) interface going from a_δ to b_δ and $W(e, b_\delta)$ its winding from e to b_δ and $\nu = \exp(-\mathrm{i}\,\pi/4)$.

Remark 6.2. For the readers who might have read [CS12], since here the graph is oriented differently, the multiplicative factor ν is chosen so that we can keep the same notations for properties that follow later.

Remark 6.3. Since the domain we consider here is simply connected, the winding $W(e, e_b^\delta)$ for a mid-edge vertex e on the boundary does not depend on the random configuration. Following the interface, we always have the primal vertical line on the right and the dual vertical line on the left. As a consequence, we have two cases:

- If $p_e^- \in \Omega_\delta$ and $p_e^+ \in \Omega_\delta^\star$, then the winding $W(e, b_\delta)$ is a multiple of 2π and $F_\delta(e)$ is parallel to ν.
- If $p_e^- \in \Omega_\delta^\star$ and $p_e^+ \in \Omega_\delta$, then the winding $W(e, b_\delta)$ is a multiple of 2π plus π and $F_\delta(e)$ is parallel to $\mathrm{i}\,\nu$.

This says that F_δ satisfies the first property in Definition 5.32.

Figure 6.2 – Local relative position of primal / dual vertices with the direction of F_δ in blue.

We can notice that the winding at e_b is $W(e_b, e_b) = 0$, thus $F_\delta(e_b) = \frac{\nu}{\sqrt{\delta}}$, which is called the *normalizing constant*.

Then, we define the observable $\mathcal{F}_\delta$ on $\Omega_\delta^\diamond$ for all $p \in \Omega_\delta^\diamond$ by

$$\mathcal{F}_\delta(p) = F_\delta(e_p^+) + F_\delta(e_p^-). \tag{6.3}$$

If $p \in \partial\Omega_\delta^\diamond$, one of the e_p^+ and e_p^- is not defined. We then take the undefined term to be 0. As such, the function $\mathcal{F}_\delta$ is defined everywhere on $\Omega_\delta^\diamond$. We notice that $\mathcal{F}_\delta$ satisfies the projection property (5.26).

Let p be a point on ∂_{ab} or on $\partial_{ba}^\star$. We denote by $\tau(p)$ the tangent vector to $\partial\Omega_\delta$ oriented from b_δ^b to a_δ^b in the former case, and oriented from b_δ^w to a_δ^w in the latter case.

Proposition 6.4. *For $p \in \partial_{ab} \cup \partial^{\star}_{ba}$, we have $\mathcal{F}_\delta(p) /\!\!/ \tau(p)^{-1/2}$.*

Proof. We can assume that $p \in \partial_{ab}$ since the proof is similar in the other case. In this case, we get two types of tangent vector: $\tau(p)$ is horizontal when p is a dual vertex and vertical when p is a primal vertex.

1. Assume that the tangent vector $\tau(p)$ is horizontal. We may assume that $\tau(p)$ is oriented from left to right, then the paths counted in $F_\delta(e_p^+)$ are exactly those counted in $F_\delta(e_p^-)$, because the interface going through e_p^+ is forced to turn left and go through e_p^-. Thus, the observable $\mathcal{F}_\delta(p)$ at p can be written as

$$\mathcal{F}_\delta(p) = (1 - \mathrm{i})F_\delta(e_p^+).$$

   The quantity $F_\delta(e_p^+)$ being parallel to $\mathrm{i}\,\nu$, we have $\mathcal{F}_\delta(p) \in \mathbb{R}$. Also, we know that $\tau(p)^{-1/2}$ is parallel to 1. The case where $\tau(p)$ is oriented from right to left can be treated in the same way.

2. Assume that the tangent vector $\tau(p)$ is vertical which can be oriented either upwards or downwards. If $\tau(p)$ is oriented downwards, $\mathcal{F}_\delta(p)$ takes the same value as $F_\delta(e_p^-)$, which belongs to $\mathrm{i}\,\nu\mathbb{R}$ due to Remark 6.3. Moreover, $\tau(p)^{-1/2}$ is parallel to $\mathrm{i}\,\nu$. It is similar if $\tau(p)$ is oriented upwards.

□

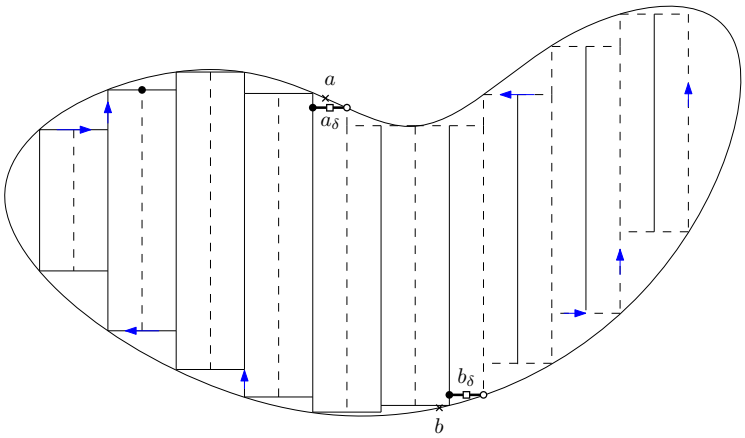

Figure 6.3 – The Dobrushin domain shown in Figure 6.1 with tangent vectors τ drawn in blue with arrows on the boundary.

6.2.2 Relations and holomorphicity

To study the observables F_δ and $\mathcal{F}_\delta$, we start by establishing local bijections between configurations which will give us local relations for F_δ and $\mathcal{F}_\delta$. Our goal is to get relations between the observable F_δ and its derivative $\partial_y F_\delta$.

To achieve this, we fix a *local window* with height equal to ε and width covering three columns, as shown in Figure 6.4. We notice that, in the loop representation, if we reverse the role of primal and dual lines, the loops and interfaces are kept the same but with opposite orientations. Thus, it is enough to fix an arbitrary choice of primal and dual lines.

By studying the difference between different contributions of $\exp(\frac{\mathrm{i}}{2}W(e,b_\delta))$ in the expectation of (6.2) at different vertical positions (at the top and the bottom of the local window), and by making ε go to 0, we will get the derivative. Since the number of points given by point Poisson processes is proportional to the length of the interval, thus to ε in our case. And actually, in our computation, we will take into account terms up to the order ε since higher-order terms will disappear in the limit. In consequence, only configurations containing a single Poisson point in the local window will count.

Some abbreviations are introduced below to lighten our notations. We denote the north-/southwest/middle/east mid-edge vertices by taking their initials: nw, nm, ne, sw, sm and se. We denote by b_n the primal extremity shared between nw and nm and by b_s the one shared between sw and sm. Similarly for w_n and w_s. See again Figure 6.4.

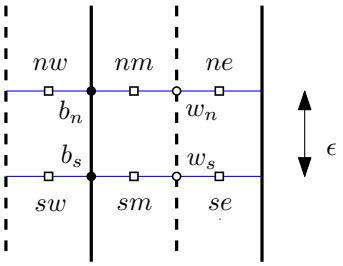

Figure 6.4 – A local window with height ε. The same notations are used in the following figures and tables of this section.

To understand the bijections between configurations, the reader is invited to have a look at Figure 6.5 while reading the following explanation. The bijections are obtained by starting with an interface going through the middle column, which is not a loss of generality. In our case, it goes down due to the choice of the local window. We assume that there is not any Poisson points in this local window.

We will then analyze different possibilities. Once the interface goes out of the local window, it may never come back to the neighboring columns (i.e., west and east), which is the case of (1a). Otherwise, the interface may come back to one of the neighboring mid-edge columns. In (2a), it comes back through the East column and in (3a), through the West column.

Now we can consider Poisson points in our configurations. As we mentioned earlier, we are only interested in configurations with at most one such point. In (1b), (2b) and (3b), we add one Poisson point between b_s and b_n whereas in (1c), (2c) and (3c), we add one between w_s and w_n. The configurations (1a), (1b) and (1c) are in bijection, same for (2a), (2b) and (2c) or (3a), (3b) and (3c). Notice that these configurations do not have the same weight, but we know the ratio between their weights, which will allow us to get linear relations between the contribution of $\exp(\frac{\mathrm{i}}{2}W(e,b_\delta))\mathbb{1}_{e\in\gamma_\delta}$ to f at nw, sw, nm, sm, ne and se.

First of all, we write down different contributions in Table 6.1. Its last column contains the weight of each configuration up to a multiplicative constant depending on the original configuration in (1a), (2a) and (3a). However, the fact that this multiplicative constant is unknown does not raise any difficulty since we only need linear relations between values of F_δ at different mid-edge vertices.

We take the difference of contributions between the north mid-edge and the south mid-edge in each of the three columns to get Table 6.2. After this, we get $F_\delta(w)$, $F_\delta(m)$ and $F_\delta(e)$ from

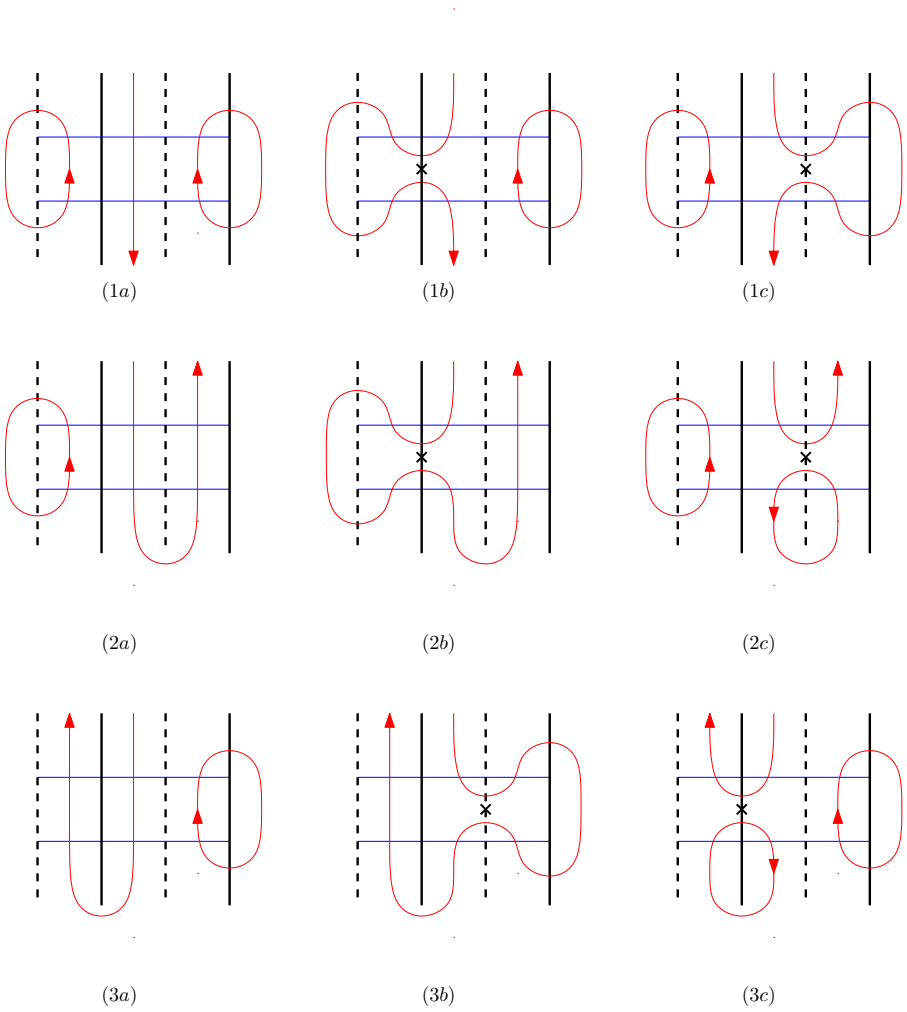

Figure 6.5 – Bijection between configurations in a local window chosen above.

Table 6.1 by ignoring terms of order higher than ε; and $\partial_y F_\delta(w)$, $\partial_y F_\delta(m)$ and $\partial_y F_\delta(e)$ by dividing the quantities in Table 6.2 by ε and then making it go to 0.

The quantities in the first and the second lines of Table 6.3 satisfy

$$(F_\delta(e) - F_\delta(w)) \cdot \mathrm{i}\sqrt{2}\rho = \partial_y F_\delta(m). \tag{6.4}$$

Moreover, those in the first and the third line satisfy also the same equation. By summing over the possible local configurations and by gathering them together, we obtain that for each $m \in \Omega_\delta^\flat$

$$\overline{D}^{(\delta)} F_\delta(m) = \frac{1}{2}\left[\frac{F_\delta(e) - F_\delta(w)}{\delta} - \frac{\partial_y F_\delta(m)}{\mathrm{i}}\right] = 0. \tag{6.5}$$

Gathering all the above computations and using Proposition 5.34, we obtain the following proposition about the s-holomorphicity of the observables F_δ and $\mathcal{F}_\delta$.

Proposition 6.5. *The observables F_δ and $\mathcal{F}_\delta$ satisfy the following properties.*

1. *The observable F_δ is s-holomorphic on $\Omega_\delta^\flat$.*
2. *The observable $\mathcal{F}_\delta$ is s-holomorphic on $\Omega_\delta^\diamond$.*

	nw	sw	nm	sm	ne	se	weights
1a	0	0	1	1	0	0	$\sqrt{2}$
1b	$e^{\mathrm{i}\frac{\pi}{2}}$	$e^{-\mathrm{i}\frac{\pi}{2}}$	1	1	0	0	$\varepsilon\rho$
1c	0	0	1	1	$e^{-i\frac{\pi}{2}}$	$e^{i\frac{\pi}{2}}$	$\varepsilon\rho$
2a	0	0	1	1	$e^{-i\frac{\pi}{2}}$	$e^{-i\frac{\pi}{2}}$	$\sqrt{2}$
2b	$e^{i\frac{\pi}{2}}$	$e^{-i\frac{\pi}{2}}$	1	1	$e^{-i\frac{\pi}{2}}$	$e^{-i\frac{\pi}{2}}$	$\varepsilon\rho$
2c	0	0	1	0	$e^{-i\frac{\pi}{2}}$	0	$2\varepsilon\rho$
3a	$e^{i\frac{\pi}{2}}$	$e^{i\frac{\pi}{2}}$	1	1	0	0	$\sqrt{2}$
3b	$e^{i\frac{\pi}{2}}$	0	1	0	0	0	$2\varepsilon\rho$
3c	$e^{i\frac{\pi}{2}}$	$e^{i\frac{\pi}{2}}$	1	1	$e^{-i\frac{\pi}{2}}$	$e^{i\frac{\pi}{2}}$	$\varepsilon\rho$

Table 6.1 – Contributions of the exponential term in each configuration at different positions.

	$nw-sw$	$nm-sm$	$ne-se$
1	$2i\varepsilon\rho$	0	$-2i\varepsilon\rho$
2	$2i\varepsilon\rho$	$2\varepsilon\rho$	$-2i\varepsilon\rho$
3	$2i\varepsilon\rho$	$2\varepsilon\rho$	$-2i\varepsilon\rho$

Table 6.2 – Computation of the difference between the contributions of North and South.

	$F_\delta(w)$ $\partial_y F_\delta(w)$	$F_\delta(m)$ $\partial_y F_\delta(m)$	$F_\delta(e)$ $\partial_y F_\delta(e)$
1	0 $2i\rho$	$\sqrt{2}$ 0	0 $-2i\rho$
2	0 $2i\rho$	$\sqrt{2}$ 2ρ	$-\mathrm{i}\sqrt{2}$ $-2i\rho$
3	$\mathrm{i}\sqrt{2}$ $2i\rho$	$\sqrt{2}$ 2ρ	0 $-2i\rho$

Table 6.3 – By considering order 0 and order 1 terms in ε, we get F_δ and $\partial_y F_\delta$.

By Proposition 5.34, the observables F_δ and $\mathcal{F}_\delta$ encode the same information. We will then sometimes work with F_δ, sometimes with $\mathcal{F}_\delta$, according to our convenience.

6.2.3 Primitive of $\mathcal{F}_\delta^2$

In Section 6.3.2, we will see that the observable $\mathcal{F}_\delta$ is the solution to some boundary value problem and we will prove that it converges, when $\delta \to 0$, to its counterpart in the continuum (Theorem 6.22). To achieve this, we define a primitive of $\mathcal{F}_\delta^2$ which is "almost" harmonic (Proposition 6.10) and relate the whole problem to the Dirichlet boundary problem studied earlier (Section 5.3).

The approach is exactly the same as that in [CS12]

Given v a site on the lattice, we denote by e_v^+ and e_v^- the mid-edges having v as extremity on the right side and the left side of v, as illustrated in Figure 6.6. In a similar way, we denote by e_v^{++} and e_v^{--} the second on the right or left.

Let us define H_δ, a "primitive" of $\mathcal{F}_\delta^2$ in the following way. Since $\mathcal{F}_\delta$ and F_δ can be related, in the definitions below we only work with F_δ first.

1. If b and b' are primal vertices such that $\operatorname{Re} b = \operatorname{Re} b'$ and $[bb'] \subset \Omega_\delta^\diamond$, define

$$H_\delta(b') - H_\delta(b) = 2 \cdot \operatorname{Im} \int_b^{b'} F_\delta(e_v^-)\overline{F_\delta}(e_v^+)\mathrm{d}v \tag{6.6}$$

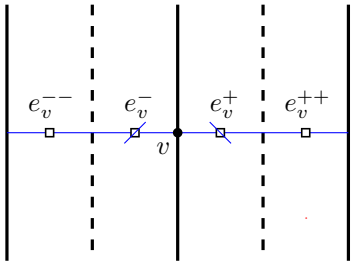

Figure 6.6 – Notations for neighboring mid-edges.

2. If w and w' are dual vertices such that $\operatorname{Re} w = \operatorname{Re} w'$ and $[ww'] \subset \Omega_\delta^\diamond$, define

$$H_\delta(w') - H_\delta(w) = -2 \cdot \operatorname{Im} \int_w^{w'} F_\delta(e_v^-)\overline{F_\delta}(e_v^+)\mathrm{d}v. \tag{6.7}$$

3. If b and w are neighboring primal and dual vertices in $\Omega_\delta^\diamond$, define

$$H_\delta(b) - H_\delta(w) = \delta |F_\delta(bw)|^2. \tag{6.8}$$

Proposition 6.6. *The primitive H_δ is well-defined up to an additive constant.*

Proof. It is sufficient to check that the difference of H_δ along cycles is always 0, or equivalently, the difference along elementary rectangles is always 0. Let u_1, u_2, v_2, v_1 be a rectangle as shown in Figure 6.7. We denote by e_{m_i} the mid-edge between u_i and v_i for $i = 1, 2$.

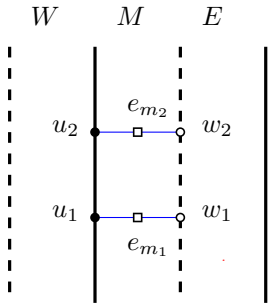

Figure 6.7 – An elementary rectangle $u_1u_2w_2w_1$.

We need to show that the difference of H_δ along u_1u_2, u_2w_2, w_2w_1 and w_1u_1 gives 0. We apply directly the definitions from Equations (6.6), (6.7) and (6.8).

$$\begin{aligned}
&H_\delta(u_2) - H_\delta(u_1) + H_\delta(w_2) - H_\delta(u_2) + H_\delta(w_1) - H_\delta(w_2) + H_\delta(u_1) - H_\delta(w_1) \\
&= 2\operatorname{Im} \int_{u_1}^{u_2} F_\delta(e_v^-)\overline{F_\delta}(e_v^+)\mathrm{d}v - \delta|F_\delta(u_2w_2)|^2 + 2\operatorname{Im} \int_{w_1}^{w_2} F_\delta(e_v^-)\overline{F_\delta}(e_v^+)\mathrm{d}v + \delta|F_\delta(u_1w_1)|^2 \\
&= 2\operatorname{Im} \int_{m_1}^{m_2} [F_\delta(e_m^-)\overline{F_\delta}(e_m) + F_\delta(e_m)\overline{F_\delta}(e_m^+)]\mathrm{d}m - \delta(|F_\delta(u_2w_2)|^2 - |F_\delta(u_1w_1)|^2).
\end{aligned}$$

The first term can be rewritten as:

$$2\,\mathrm{Im}\int_{m_1}^{m_2}[F_\delta(e_m^-)\overline{F_\delta}(e_m)+F_\delta(e_m)\overline{F_\delta}(e_m^+)]\mathrm{d}m = 2\,\mathrm{Im}\int_{m_1}^{m_2}[F_\delta(e_m^-)-F_\delta(e_m^+)]\overline{F_\delta}(e_m)\mathrm{d}m,$$

and the second term as:

$$\begin{aligned}-\delta(|F_\delta(u_2w_2)|^2-|F_\delta(u_1w_1)|^2) &= -\delta\,\mathrm{Re}\int_{m_1}^{m_2}2\partial_y F_\delta(e_m)\overline{F_\delta}(e_m)\mathrm{d}m\\ &= -\,\mathrm{Re}\int_{m_1}^{m_2}2\,\mathrm{i}(F_\delta(e_m^+)-F_\delta(e_m^-))\overline{F_\delta}(e_m)\mathrm{d}m\\ &= 2\,\mathrm{Im}\int_{m_1}^{m_2}[F_\delta(e_m^+)-F_\delta(e_m^-)]\overline{F_\delta}(e_m)\mathrm{d}m\end{aligned}$$

where we use the holomorphic relation (6.5) in the second line. Thus, the quantity we were looking for is indeed 0. □

From the previous proposition, we can fix $H_\delta(b_\delta^w)$ to be zero, thus fixing the additive constant. Now, we can really talk about *the* primitive H_δ.

We will reformulate the definitions above to get relations for H_δ between different points on the same axis (Proposition 6.7) and neighboring points on medial lattice (Proposition 6.8). This will give us a simpler expression: $H_\delta = \mathrm{Im}\int^\delta(\mathcal{F}_\delta(z))^2\mathrm{d}^\delta z$.

Proposition 6.7. *Let $p,p'\in\Omega_\delta^\diamond$ such that $\mathrm{Re}\,p=\mathrm{Re}\,p'$ and $[pp']\subset\Omega_\delta^\diamond$. Then we have*

$$H_\delta(p')-H_\delta(p)=\mathrm{Im}\int_p^{p'}\mathrm{i}\cdot(\mathcal{F}_\delta(v))^2\,dv. \tag{6.9}$$

Proof. We first assume that $p,p'\in\Omega_\delta$. Given $v\in[pp']$, since $F_\delta(e_v^-)\in\mathrm{i}\,v\mathbb{R}$ and $F_\delta(e_v^+)\in v\mathbb{R}$, we have

$$\begin{aligned}\mathrm{Im}\left[\mathrm{i}\cdot\mathcal{F}_\delta(v)^2\right] &= \mathrm{Re}\left[F_\delta(e_v^-)^2+F_\delta(e_v^+)^2+2F_\delta(e_v^-)F_\delta(e_v^+)\right]\\ &= 2\,\mathrm{Re}\left[F_\delta(e_v^-)F_\delta(e_v^+)\right]\\ &= 2\,\mathrm{Im}\left[F_\delta(e_v^-)\overline{F_\delta}(e_v^+)\right].\end{aligned}$$

The same computation for $p,p'\in\Omega_\delta^\star$ and $v\in[pp']$ leads to

$$\mathrm{Im}\left[\mathrm{i}\cdot\mathcal{F}_\delta(v)^2\right]=-2\,\mathrm{Im}\left[F_\delta(e_v^-)\overline{F_\delta}(e_v^+)\right].$$

Using Equations (6.6) and (6.6), we get the result. □

Proposition 6.8. *Let $p\in\Omega_\delta^\diamond$ such that $p^-,p^+\in\Omega_\delta^\diamond$. Then,*

$$H_\delta(p^+)-H_\delta(p^-)=\mathrm{Im}[\mathcal{F}_\delta(p)^2(p^+-p^-)]. \tag{6.10}$$

Proof. We can assume that $p\in\Omega_\delta^\star$ and $p^-,p^+\in\Omega_\delta$. The other case when $p\in\Omega_\delta$ can be treated in the same way.

From the parallelism property, we know that $F_\delta(e_p^-) \in \nu\mathbb{R}$ and $F_\delta(e_p^+) \in \mathrm{i}\,\nu\mathbb{R}$. A simple computation gives

$$\begin{aligned}\operatorname{Im}\left[\mathcal{F}_\delta(p)^2\right] &= \operatorname{Im}\left[F_\delta(e_p^-)^2 + F_\delta(e_p^+)^2 + 2F_\delta(e_p^-)F_\delta(e_p^+)\right] \\ &= |F_\delta(e_p^+)|^2 - |F_\delta(e_p^-)|^2.\end{aligned}$$

Since $p^+ - p^- = \delta$, this completes the proof. □

Corollary 6.9. *The primitive H_δ is constant on both arcs ∂_{ab} and $\partial^\star_{ba}$. Moreover,*

$$H_{\delta|\partial_{ab}} = 1 \quad \text{and} \quad H_{\delta|\partial^\star_{ba}} = 0. \tag{6.11}$$

Proof. Proposition 6.4 gives the direction of $\mathcal{F}_\delta$ and Equations (6.9) and (6.10) give its relation to H_δ on each part of the two arcs. We conclude easily that $\mathcal{F}_\delta(p)$ is constant on both arcs. The difference of these constants can be obtained by estimating H_δ at, for example, $b_\delta = [b_\delta^b b_\delta^w]$:

$$H_\delta(b_\delta^b) = H_\delta(b_\delta^b) - H_\delta(b_\delta^w) = \delta|F_\delta(b_\delta)|^2 = 1.$$

□

Proposition 6.10. *The primitive H_δ is subharmonic on primal axes and superharmonic on dual axes, i.e.,*

$$\Delta^{(\delta)}H_\delta(u) \geqslant 0 \quad \text{and} \quad \Delta^{(\delta)}H_\delta(w) \leqslant 0$$

for all $u \in \Omega_\delta$ and $w \in \Omega^\star_\delta$.

Proof. We remind that in a semi-discrete lattice, the Laplacian is defined as follows:

$$\Delta^{(\delta)}_{xx}H_\delta(u) = D^{(\delta)}_{xx}H_\delta(u) + \partial_{yy}H_\delta(u)$$

for u a vertex in primal or dual axis.

First, we assume that u is a primal vertex. By using the definition of H_δ, the second derivative along x can be reformulated,

$$D^{(\delta)}_{xx}H_\delta(u) = \frac{1}{\delta}\left[|F_\delta(e_u^{++})|^2 - |F_\delta(e_u^+)|^2 - |F_\delta(e_u^-)|^2 + |F_\delta(e_u^{--})|^2\right].$$

Similarly, the second derivative along y can be rewritten as:

$$\begin{aligned}\partial_{yy}H_\delta(u) &= 2\operatorname{Im}[\partial_y(F_\delta(e_u^-)\overline{F_\delta}(e_u^+))] \\ &= 2\operatorname{Im}[\partial_y F_\delta(e_u^-)\overline{F_\delta}(e_u^+) + F_\delta(e_u^-)\overline{\partial_y F_\delta}(e_u^+)] \\ &= 2\operatorname{Im}[\partial_y F_\delta(e_u^-)\overline{F_\delta}(e_u^+) - \overline{F_\delta}(e_u^-)\partial_y F_\delta(e_u^+)] \\ &= 2\operatorname{Im}\left[\frac{\mathrm{i}}{\delta}\left[F_\delta(e_u^+) - F_\delta(e_u^{--})\right]\cdot\overline{F_\delta}(e_u^+) - \overline{F_\delta}(e_u^-)\cdot\frac{\mathrm{i}}{\delta}\left[F_\delta(e_u^{++}) - F_\delta(e_u^-)\right]\right] \\ &= \frac{2}{\delta}\operatorname{Re}[(F_\delta(e_u^+) - F_\delta(e_u^{--}))\overline{F_\delta}(e_u^+) - \overline{F_\delta}(e_u^-)(F_\delta(e_u^{++}) - F_\delta(e_u^-))] \\ &= \frac{2}{\delta}\left[|F_\delta(e_u^+)|^2 + |F_\delta(e_u^-)|^2 - \operatorname{Re}[F_\delta(e_u^{--})\overline{F_\delta}(e_u^+) + \overline{F_\delta}(e_u^-)F_\delta(e_u^{++})]\right].\end{aligned}$$

Finally, we notice that

$$\begin{aligned}
&|F_\delta(e_u^{++}) - F_\delta(e_u^{-})|^2 + |F_\delta(e_u^{+}) - F_\delta(e_u^{--})|^2 \\
&\qquad = |F_\delta(e_u^{++})|^2 + |F_\delta(e_u^{+})|^2 + |F_\delta(e_u^{-})|^2 + |F_\delta(e_u^{--})|^2 \\
&\qquad\qquad - 2\,\mathrm{Re}\left[\overline{F_\delta}(e_u^{-})F_\delta(e_u^{++}) + F_\delta(e_u^{--})\overline{F_\delta}(e_u^{+})\right] \\
&\qquad = \delta D_{xx}^{(\delta)} H_\delta(u) + \delta \partial_{yy} H_\delta(u) \\
&\qquad = \delta \Delta^{(\delta)} H_\delta(u).
\end{aligned}$$

In consequence, the primitive H_δ is subharmonic on primal axes.

The proof for the superharmonicity on dual axes is similar. We do the same calculation and obtain the above equation with a minus sign. □

6.3 Boundary-value problems

6.3.1 Boundary modification trick

In [CS12], the boundary modification trick is introduced to enlarge an isoradial Dobrushin domain into an isoradial primal domain; and in the same manner, a function defined on a Dobrushin domain can also be extended to the enlarged primal domain. The goal of this is to associate a boundary value problem on a Dobrushin domain to its counterpart on the enlarged primal domain, on which we have a better understanding of such a problem. The same procedure can also be made in the semi-discrete setting that we describe below.

The primal (*resp.* dual) domain extended from a Dobrushin domain is given by keeping the primal boundary ∂_{ab} and by adding an extra layer ∂_{ba} to the dual boundary $\partial_{ba}^\star$. More precisely, on the arc $\partial_{ba}^\star$ we change the horizontal parts from dual to primal and add one more primal layer *outside* (in the sense defined below) the original domain. The same procedure applies similarly if we want to get an extended dual domain: we get $\partial_{ab}^\star$ from ∂_{ab} and keep $\partial_{ba}^\star$. We will denote by $\widetilde{\Omega}_\delta$ and $\widetilde{\Omega}_\delta^\star$ these two modified domains. See Figure 6.8a and Figure 6.8b for examples.

In an algebraic way, each dual point $p \in \partial_{ba}^\star$ on the dual boundary possesses two primal neighbors p^- and p^+. One of them is in $\operatorname{Int}\Omega_\delta^\diamond$ and the other is not (although it may lie on the boundary ∂_{ab}). We include the one which is not in $\operatorname{Int}\Omega_\delta^\diamond$, providing us with the new boundary.

We notice that some points may be added twice (red part in Figure 6.8b) and some points may overlap the other part of its own boundary ∂_{ab} (red part in Figure 6.8a). In this way, the boundary of the extended domain is not described by a Jordan curve anymore. However, this is not a problem: we just keep these double points and consider that they are situated on the two different sides of the same boundary and all the theorems concerning boundary value problem will still be valid. We can also see this as a domain minus a slit.

The following lemma tells us how to extend the primitive H_δ to the extended domain after boundary modification trick, keeping its sub- and superharmonicity properties.

Lemma 6.11. *Let $w \in \partial_{ba}^\star$ be a dual vertex on the arc $(b_\delta a_\delta)$. Assume u_{int} to be the neighboring primal vertex of w which is in the domain $\Omega_\delta^\diamond$ and u_{ext} the primal one to be added via the boundary modification trick. Then, if we set $H_\delta(u_{ext}) = H_\delta(w)$, the function H_δ remains subharmonic at u_{int}. We can also extend H_δ on $\widetilde{\Omega}_\delta^\star$ in a similar way, giving a similar result.*

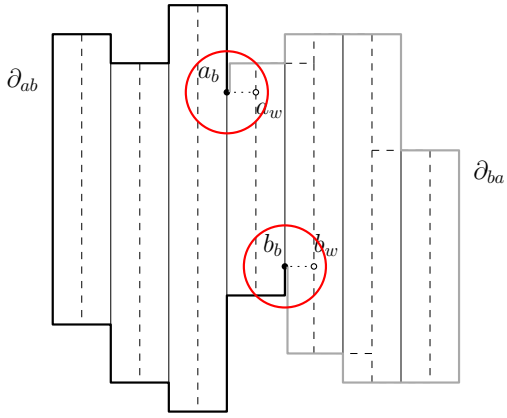

(a) The enlarged primal domain.

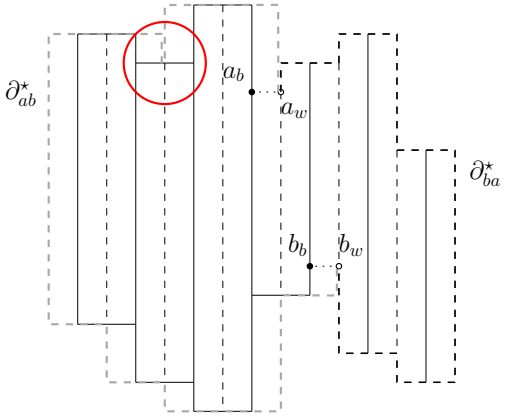

(b) The enlarged dual domain.

Figure 6.8 – The primal and the dual domains enlarged from the Dobrushin domain illustrated in Figure 1.5. The red part indicates the overlapping part of the enlarged domain with the original boundary.

Proof. By abusing the notation, we continue writing F_δ, $\mathcal{F}_\delta$ and H_δ on the extended domain $\widetilde{\Omega}_\delta$. We notice that if we let $F_\delta(u_{ext}w) = 0$ and $\mathcal{F}_\delta(w) = F_\delta(wu_{int})$, the properties in Proposition 6.5 are still satisfied. This can be computed by establishing a similar table as Table 6.3 on the boundary. Then, by setting $H_\delta(u_{ext}) = H(w)$, we get a primitive H_δ which always satisfies Equations (6.7) and (6.8). In such a way, the Proposition 6.10 still holds. □

6.3.2 Riemann-Hilbert boundary value problem

We studied the semi-discrete Dirichlet problem in Section 5.3. In this section, we introduce the semi-discrete Riemann-Hilbert boundary value problem, which is similar to the Dirichlet problem, but whose resolution is a bit more technical. However, the boundary modification trick mentioned in the previous section along with the knowledge of the Dirichlet problem may help us achieve this.

In a semi-discrete Dobrushin domain $(\Omega^\diamond_\delta, a_\delta, b_\delta)$, we say that a function F_δ defined on $\Omega^\flat_\delta$ is a solution to the *(semi-discrete) Riemann-Hilbert boundary value problem* with respect to the Dobrushin domain $(\Omega^\diamond_\delta, a_\delta, b_\delta)$ if the following three conditions are satisfied:

(A) s-holomorphicity: $\mathcal{F}_\delta$ is s-holomorphic in $\Omega^\diamond_\delta$;

(B) boundary conditions: for $p \in (a_\delta b_\delta) \cup (b_\delta a_\delta)$, $\mathcal{F}_\delta(p)$ is parallel to $\tau(p)^{-1/2}$;
(C) normalization: $F_\delta(e_b^\delta) = \mathrm{Proj}[\mathcal{F}_\delta(b_\delta^w), \nu] = \frac{\nu}{\sqrt{\delta}}$,

where $\mathcal{F}_\delta$ is defined via Equation (6.3).

Existence of such a solution has been shown already. In effect, the observable we introduced earlier satisfies these three conditions, as shown in Section 6.2.2. When it comes to uniqueness, we will use the primitive H_δ we constructed in Section 6.2.3 along with the boundary modification trick.

Proposition 6.12 (Existence of solution)**.** *The observable F_δ defined in (6.2) is a solution to the above boundary value problem.*

Proof. It is direct from the properties of the observable as shown in Propositions 6.4 and 6.5. □

Proposition 6.13 (Uniqueness of solution)**.** *For each semi-discrete Dobrushin domain $(\Omega_\delta^\diamond, a_\delta, b_\delta)$, the semi-discrete boundary value problem has a unique solution.*

Proof. Assume that there are two solutions $F_{\delta,1}$ and $F_{\delta,2}$ to the boundary value problem mentioned above. Let $F_\delta := F_{\delta,1} - F_{\delta,2}$. Note that F_δ is still s-holomorphic being difference of two such functions. Define $\mathcal{F}_\delta$ as in Equation (6.3). Consider $H_\delta := \mathrm{Im} \int (\mathcal{F}_\delta(z))^2 \mathrm{d}z$ the primitive defined in Section 6.2.3. The function H_δ is constant on the arcs $(a_\delta b_\delta)$ and $(b_\delta a_\delta)$ respectively due toe the property (B). Moreover, the identity $F_\delta(e_b^\delta) = 0$ says that these two constants should be the same. Apply the boundary modification trick to extend $\Omega_\delta^\diamond$ into the primal domain $\widetilde{\Omega}_\delta$.

Extend the primitive H_δ to the new boundary of $\widetilde{\Omega}_\delta$ as in Lemma 6.11. The lemma also says that H_δ stays subharmonic in $\mathbb{L}_\delta \cap \widetilde{\Omega}_\delta$ and superharmonic in $\mathbb{L}_\delta^\star \cap \widetilde{\Omega}_\delta$. This gives us that $0 \geqslant (H_\delta)_{|\mathbb{L}_\delta^\star \cap \widetilde{\Omega}_\delta} \geqslant (H_\delta)_{|\mathbb{L}_\delta^\star \cap \widetilde{\Omega}_\delta^\star} \geqslant 0$. By uniqueness of the Dirichlet problem (Proposition 5.17), we know that H_δ is constant everywhere.

The fact that H_δ is constant everywhere tells us that F_δ is zero everywhere on $\Omega_\delta^\flat$. Thus, these two solutions are equal. □

6.4 RSW on the quantum model

In Chapter 4, we showed the RSW property on the critical quantum random-cluster model for $1 \leqslant q \leqslant 4$, thus in particular, on the random-cluster representation of the quantum Ising model. Here, we provide an alternative using the fermionic observable (6.2) and the second--moment method.

6.4.1 RSW property: second-moment method

In the previous section, we established the conformal invariance of the limit of our semi-discrete observables. To show that the interface can be identified with an SLE curve in the limit and to determine its parameter, we need the so-called Russo-Seymour-Welsh (RSW) property. This provides the hypothesis needed in [KS12] which, along with Theorem 6.22, shows the main Theorem 6.1.

The goal of this section is to show the following property.

Proposition 6.14 (RSW property). *Fix $\alpha > 0$. Consider the rectangular domain $R_{n,\alpha} = [-n, n] \times [-\alpha n, \alpha n]$ and write $R^{\delta}_{n,\alpha}$ for its semi-discretized counterpart (primal domain). Let ξ be a boundary condition on $R^{\delta}_{n,\alpha}$. Then, there exists $c(\alpha) > 0$ which is independent of n and δ such that*

$$c \leqslant \mathbb{P}^{\xi}(\mathcal{C}_h(R^{\delta}_{n,\alpha})) \leqslant 1 - c,$$
$$c \leqslant \mathbb{P}^{\xi}(\mathcal{C}_v(R^{\delta}_{n,\alpha})) \leqslant 1 - c,$$

where $\mathcal{C}_h$ and $\mathcal{C}_v$ denote the events "having a horizontal / vertical crossing".

The proof of Proposition 6.14 is based on the use of the same fermionic observable introduced in Section 6.2 and the second moment method to estimate the crossing probabilities. This is inspired from [DCHN11] where the classical Ising case is treated and here we adapt the proof to the case of quantum Ising.

To show the RSW property in Proposition 6.14, we only need to show the lower bound for free boundary condition by duality [DCHN11]. In this section, we will just show the property for the horizontal crossing, since the proof to estimate the probability of the vertical crossing is similar.

We recall that $(\Omega^{\diamond}_{\delta}, a_{\delta}, b_{\delta})$ is a Dobrushin domain, meaning that the arc $(a_{\delta}b_{\delta})$ is wired and the arc $(b_{\delta}a_{\delta})$ is free. In Section 6.3.1, we introduced the notion of modified primal and dual domains of a Dobrushin domain, which are denoted by $\widetilde{\Omega}_{\delta}$ and $\widetilde{\Omega}^{\star}_{\delta}$ respectively. Let us write $\mathrm{HM}_{\bullet}$ and $\mathrm{HM}_{\circ}$ the harmonic functions on modified domains $\widetilde{\Omega}_{\delta}$ and $\widetilde{\Omega}^{\star}_{\delta}$ having boundary conditions 1 on the (extended) wired arc (∂_{ab} for $\widetilde{\Omega}_{\delta}$ and $\partial^{\star}_{ab}$ for $\widetilde{\Omega}^{\star}_{\delta}$) and 0 on the (extended) free arc (∂_{ba} for $\widetilde{\Omega}_{\delta}$ and $\partial^{\star}_{ba}$ for $\widetilde{\Omega}^{\star}_{\delta}$).

We start by noticing that the connection probability of a vertex next to the free arc $(b_{\delta}a_{\delta})$ to the wired arc $(a_{\delta}b_{\delta})$ can be written in a simple way by using the parafermionic observable.

Proposition 6.15. *Let $u \in \Omega_{\delta}$ such that $\{u^+, u^-\} \cap (b_{\delta}a_{\delta}) \neq \varnothing$ (equivalently, u is next to the free arc). Write e for the mid-edge between u and the free arc $(b_{\delta}a_{\delta})$. Then, we have*

$$\mathbb{P}_{(\Omega^{\diamond}_{\delta}, a_{\delta}, b_{\delta})}(u \leftrightarrow (a_{\delta}b_{\delta}))^2 = \delta |F(e)|^2.$$

Proof. We take the definition of F,

$$\begin{aligned}\delta |F(e)|^2 &= \left| \mathbb{E}_{(\Omega^{\diamond}_{\delta}, a_{\delta}, b_{\delta})} \left[\exp\left(\frac{\mathrm{i}}{2} W(e, b_{\delta}) \right) \mathbb{1}_{e \in \gamma_{\delta}} \right] \right|^2 \\ &= |\mathbb{E}_{(\Omega^{\diamond}_{\delta}, a_{\delta}, b_{\delta})}[\mathbb{1}_{e \in \gamma_{\delta}}]|^2 = \mathbb{P}_{(\Omega^{\diamond}_{\delta}, a_{\delta}, b_{\delta})}(e \in \gamma_{\delta})^2\end{aligned}$$

where the winding $W(e, b_{\delta})$ is always a constant if e is adjacent to the boundary. We also notice that $e \in \gamma_{\delta}$ is equivalent to u connected to the wired arc $(a_{\delta}b_{\delta})$. □

By using harmonic functions $\mathrm{HM}_{\bullet}$ and $\mathrm{HM}_{\circ}$, we can get easily the following proposition.

Proposition 6.16. *Let $u \in \Omega_{\delta}$ next to the free arc. Write $w \in \{u^+, u^-\}$ which is not on the free arc. We have*

$$\sqrt{\mathrm{HM}_{\circ}(w)} \leqslant \mathbb{P}_{(\Omega^{\diamond}_{\delta}, a_{\delta}, b_{\delta})}(u \leftrightarrow (a_{\delta}b_{\delta})) \leqslant \sqrt{\mathrm{HM}_{\bullet}(u)}$$

Proof. Write w_{∂} the neighbor of u which is on the free arc. We have

$$H(u) = H(u) - H(w_{\partial}) = \delta |F(e)|^2 = \mathbb{P}_{(\Omega^{\diamond}_{\delta}, a_{\delta}, b_{\delta})}(u \leftrightarrow (a_{\delta}b_{\delta}))^2.$$

Moreover, by Lemma 6.11, H is subharmonic on $\widetilde{\Omega}_\delta$, we get $H(u) \leqslant \mathrm{HM}_\bullet(u)$. Similarly, writing $e = (uw)$,

$$H(w) = \delta|F(e)|^2 - \delta|F(e')|^2 \leqslant \delta|F(e)|^2 = \mathbb{P}_{(\Omega_\delta^\diamond, a_\delta, b_\delta)}(u \leftrightarrow (a_\delta b_\delta))^2$$

and we conclude by superharmonicity of H on $\widetilde{\Omega}_\delta^\star$. □

Now, we are ready to show the RSW property. We keep the same notation as in the statement of Proposition 6.14. We write ∂_- and ∂_+ for the left and right (primal) borders of $R_{n,\alpha}^\delta$. We define the random variable N given by the 2D Lebesgue measure of the subset of $\partial_- \times \partial_+ \subset \mathbb{R}^2$ consisting of points which are connected in $R_{n,\alpha}^\delta$. More precisely,

$$N = \iint_{\substack{x\in\partial_- \\ y\in\partial_+}} \mathbb{1}_{x\leftrightarrow y}\mathrm{d}x\mathrm{d}y.$$

To show Proposition 6.14, we use the second moment method. In other words, by using Cauchy-Schwarz, we need to show that the lower bound of

$$\mathbb{P}^0(N > 0) = \mathbb{E}^0[\mathbb{1}_{N>0}^2] \geqslant \frac{\mathbb{E}^0[N]^2}{\mathbb{E}^0[N^2]} \tag{6.12}$$

is uniform in n and δ. First, we get a lower bound for $\mathbb{E}^0[N]$.

Lemma 6.17. *There exists a uniform constant c independent of n and δ such that*

$$\mathbb{E}^0[N] \geqslant cn.$$

Proof. We decompose the right boundary into $m = \lfloor n/\delta \rfloor$ parts,

$$\partial_+ = \bigcup_{i=0}^{m-1} \partial_+^i \text{ where } \partial_+^i = \left(\{\alpha n\} \times \left(-n + i\cdot\frac{2n}{m}, -n + (i+1)\cdot\frac{2n}{m}\right)\right).$$

We expand the expectation,

$$\begin{aligned}\mathbb{E}^0[N] &= \iint_{\substack{x\in\partial_- \\ y\in\partial_+}} \mathbb{P}^0(x\leftrightarrow y)\mathrm{d}x\mathrm{d}y \\ &= \int_{x\in\partial_-}\sum_{i=0}^{m-1}\mathbb{P}^0(x\leftrightarrow\partial_+^i)\mathrm{d}x.\end{aligned}$$

By Proposition 6.16, each $\mathbb{P}^0(x\leftrightarrow\partial_+^i)$ can be bounded from below by $\mathrm{HM}_\circ(w)$ where w is a neighbor of x which is not on the free arc, and the harmonic measure is with respect to the modified domain $\widetilde{\Omega}_\delta^\star$ where the Dobrushin domain $(\Omega_\delta^\diamond, a_\delta, b_\delta)$ is given by $\Omega_\delta^\diamond = R_{n,\alpha}^\delta$, a_δ and b_δ such that $\partial_+^i = (a_\delta b_\delta)$. Moreover, from the local central limit theorem and gambler's ruin-type estimate, we have that $\mathrm{HM}_\circ(w) \geqslant c(\delta/n)^2$ for a $c > 0$ uniform in n, δ and i.

Finally, we get

$$\mathbb{E}^0[N] \geqslant \int_{x\in\partial_-} m\cdot\sqrt{c}\frac{\delta}{n}\mathrm{d}x \geqslant c'n$$

where c' is a uniform constant. □

To estimate $\mathbb{E}^0[N^2]$, we need Proposition 6.18, a consequence of Lemma 6.19. Both of them make use of the so-called *exploration path*, which is the interface between the primal wired cluster and the dual free cluster. The proof in the discrete case [DCHN11] can be easily adapted to the semi-discrete case, since the interface is well-defined and we have similar estimates on harmonic functions, by means of semi-discrete Brownian motion, local central limit theorem and gambler's ruin-type estimates. Therefore, we will just give the proof of Lemma 6.19.

For any given α, n and δ, let us consider $R_{n,\alpha}$ as before and $(R^\delta_{n,\alpha}, a_\delta, b_\delta)$ the semi-discretized Dobrushin domain obtained from $R_{n,\alpha}$ with the right boundary $\partial_+ = (a_\delta b_\delta)$ which is wired.

Proposition 6.18 ([DCHN11, Proposition 14]). *There exists a constant $c > 0$ which is uniform in α and n such that for any rectangle $R^\delta_{n,\alpha}$ and any two points $x, z \in \partial_-$, we have*

$$\mathbb{P}_{(R^\delta_{n,\alpha}, a_\delta, b_\delta)}(x, z \leftrightarrow \partial_+) = \mathbb{P}^0_{R^\delta_{n,\alpha}}(x, z \leftrightarrow \partial_+) \leqslant \frac{c}{\sqrt{|x-z|n}}$$

Lemma 6.19 ([DCHN11, Lemma 15]). *There exists a constant $c > 0$ which is uniform in α, n, δ and $x \in \partial_-$ such that for any rectangle $R^\delta_{n,\alpha}$ and all $k \geqslant 0$,*

$$\mathbb{P}_{(R^\delta_{n,\alpha}, a_\delta, b_\delta)}(B_\delta(x,k) \leftrightarrow (a_\delta b_\delta)) \leqslant c\sqrt{\frac{k}{n}}.$$

Proof. Let $n, k, \delta, \alpha > 0$, the rectangular domain $R^\delta_{n,\alpha}$ and its semi-discrete counterpart, the Dobrushin domain $(R^\delta_{n,\alpha}, a_\delta, b_\delta)$ where $\partial_+ = (a_\delta b_\delta)$ is the wired arc. Consider $x \in \partial_-$. For $k \geqslant n$, the inequality is trivial, so we can assume $k < n$.

Since the probability $\mathbb{P}_{(R^\delta_{n,\alpha}, a_\delta, b_\delta)}(B_\delta(x,k) \leftrightarrow (a_\delta b_\delta))$ is non-decreasing in α, we can bound it by above by replacing α by $\alpha + 1$, which we bound by above by a longer wired arc $(c_\delta d_\delta)$, where c_δ and d_δ are respectively the left-bottom and the left-top points of the rectangular domain $R^\delta_{n,\alpha}$. See Figure 6.9 for notations.

$$\begin{aligned}\mathbb{P}_{(R^\delta_{n,\alpha}, a_\delta, b_\delta)}(B_\delta(x,k) \leftrightarrow (a_\delta b_\delta)) &\leqslant \mathbb{P}_{(R^\delta_{n,\alpha+1}, a_\delta, b_\delta)}(B_\delta(x,k) \leftrightarrow (a_\delta b_\delta)) \\ &\leqslant \mathbb{P}_{(R^\delta_{n,\alpha+1}, c_\delta, d_\delta)}(B_\delta(x,k) \leftrightarrow (c_\delta d_\delta))\end{aligned}$$

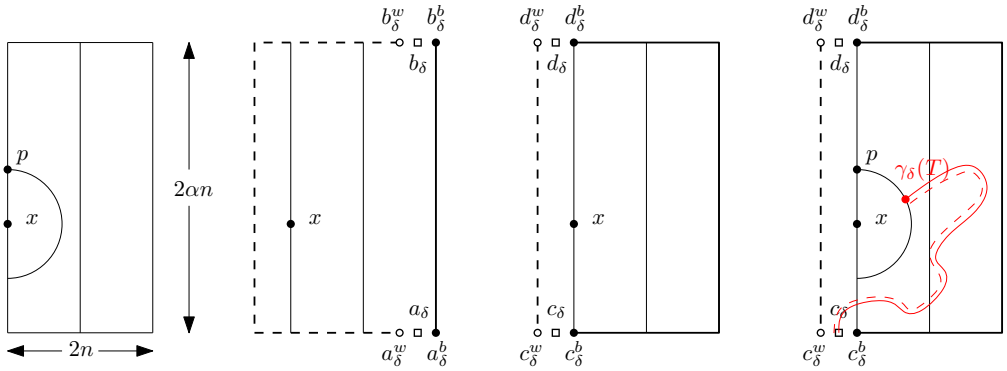

Figure 6.9 – *First:* The primal domain $R^\delta_{n,\alpha}$. *Second:* The Dobrushin domain $(R^\delta_{n,\alpha}, a_\delta, b_\delta)$. *Third:* The Dobrushin domain $(R^\delta_{n,\alpha}, c_\delta, d_\delta)$. *Third:* The Dobrushin domain $(R^\delta_{n,\alpha}, c_\delta, d_\delta)$. *Fourth:* The exploration path starting at c_δ and touching $B_\delta(x,k)$ at time T.

Let γ_δ be the interface as defined in Section 1.2.5 and used in Section 6.2 to define the fermionic observable. The definition of γ_δ tells us that the ball $B_\delta(x,k)$ is connected to the wired arc if and only if γ_δ goes through a mid-edge which is adjacent to the ball. We parameterize γ_δ by its length and denotes T the hitting time of the set of the mid-edges adjacent to the ball $B_\delta(x,k)$. Therefore, $B_\delta(x,k)$ is connected to the wired arc if and only if $T<\infty$.

Write p for the top-most point of $B_\delta(x,k)$. We can rewrite the probability of $\{p \leftrightarrow (c_\delta d_\delta)\}$ by conditioning on $\gamma_\delta[0,T]$ and using Markov domain property to obtain

$$\begin{aligned}\mathbb{P}_{(R^\delta_{n,\alpha+1},c_\delta,d_\delta)}(p \leftrightarrow (c_\delta d_\delta)) &= \mathbb{E}_{(R^\delta_{n,\alpha+1},c_\delta,d_\delta)}[\mathbb{1}_{T<\infty}\mathbb{P}_{(R^\delta_{n,\alpha+1},c_\delta,d_\delta)}(p \leftrightarrow (c_\delta d_\delta) \mid \gamma_\delta[0,T])]\\ &= \mathbb{E}_{(R^\delta_{n,\alpha+1},c_\delta,d_\delta)}[\mathbb{1}_{T<\infty}\mathbb{P}_{(R^\delta_{n,\alpha+1}\setminus\gamma_\delta[0,T],\gamma_\delta(T),d_\delta)}(p \leftrightarrow (c_\delta d_\delta))].\end{aligned}$$

We estimate this quantity in two different ways to get the desired inequality. Firstly, since p is at distance at least n from the wired arc, we have

$$\mathbb{P}_{(R^\delta_{n,\alpha+1},c_\delta,d_\delta)}(p \leftrightarrow (c_\delta d_\delta)) \leqslant \frac{c_1}{\sqrt{n}},$$

which follows from Proposition 6.16 and the fact that $\mathrm{HM}_\bullet \leqslant \frac{c}{n}$. Secondly, we can write $\gamma_\delta(T)$ as $z+(s,-r,s)$ where $0\leqslant s\leqslant k$ and $0\leqslant r\leqslant 2k$. Thus, the line $z+\mathbb{Z}\times\{-r\}$ disconnects a from the free arc, we estimate the harmonic function and we obtain a.s.

$$\mathbb{P}_{(R^\delta_{n,\alpha+1}\setminus\gamma_\delta[0,T],\gamma_\delta(T),d_\delta)}(p \leftrightarrow (c_\delta d_\delta)) \geqslant \frac{c_2}{\sqrt{r}} \geqslant \frac{c_2}{\sqrt{2k}}$$

which again comes from Proposition 6.16 and the estimate $\mathrm{HM}_\circ \geqslant \frac{c}{r}$. This final estimate being uniform in $\gamma_\delta[0,T]$, we get

$$\frac{c_2}{\sqrt{2k}}\mathbb{P}_{(R^\delta_{n,\alpha+1},c_\delta,d_\delta)}(T<\infty) \leqslant \mathbb{P}_{(R^\delta_{n,\alpha+1},c_\delta,d_\delta)}(p \leftrightarrow (c_\delta d_\delta)) \leqslant \frac{c_1}{\sqrt{n}}.$$

which implies the statement. □

Now, we can complete the proof of the RSW property.

Proof of Proposition 6.14. From Equation (6.12) and Lemma 6.17, we just need to show that

$$\mathbb{E}^0[N^2] = \iiiint \mathbb{P}^0(x\leftrightarrow y, z\leftrightarrow t)\mathrm{d}x\mathrm{d}y\mathrm{d}z\mathrm{d}t \tag{6.13}$$

is $\mathcal{O}\left(n^2\right)$.

Consider $x,z\in\partial_-$, $y,t\in\partial_+$ and l the middle vertical line separating them, we get

$$\mathbb{P}^0(x\leftrightarrow y, z\leftrightarrow t) \leqslant \mathbb{P}^0(x,z\leftrightarrow l)\mathbb{P}^0(y,t\leftrightarrow l)$$

because the left-hand side of l and the right-hand side of l are independent. Therefore, the integral in Equation (6.13) can be cut into two independent parts, each of whom gives the same contribution,

$$\begin{aligned}&\iiiint_{\substack{x,z\in\partial_-\\ y,t\in\partial_+}} \mathbb{P}^0(x\leftrightarrow y, z\leftrightarrow t)\mathrm{d}x\mathrm{d}y\mathrm{d}z\mathrm{d}t\\ &\quad= \left(\iint_{x,z\in\partial_-}\mathbb{P}^0(x,z\leftrightarrow l)\mathrm{d}x\mathrm{d}z\right)\left(\iint_{y,t\in\partial_+}\mathbb{P}^0(y,t\leftrightarrow l)\mathrm{d}y\mathrm{d}t\right)\\ &\quad= \left(\iint_{x,z\in\partial_-}\mathbb{P}^0(x,z\leftrightarrow l)\mathrm{d}x\mathrm{d}z\right)^2\\ &\quad\leqslant \left(\iint_{x,z\in\partial_-}\frac{c}{\sqrt{|x-z|n}}\mathrm{d}x\mathrm{d}z\right)^2 \leqslant (4cn)^2\end{aligned}$$

where in the last line we use Proposition 6.18.

The proof is thus complete. □

6.5 Convergence of the interface

In this section, we prove Theorem 6.1 which consists of the two following parts:

- Theorem 6.22 determines the limit of the observables F_δ.
- Proposition 6.14 gives an RSW-type estimate on crossing events. Thus, the condition G2 required in [KS12] is fulfilled and the tightness of the family of interfaces (γ_δ) is guaranteed for the weak convergence.

The first point can be done by using similar arguments as in [Smi06, Smi10, DCS12, CS12] and the second point by the second-moment method introduced in [DCHN11]. Once these two technical points are proven, one may follow the classical argument of martingales to identify the limiting curve, see [DCS12, DC13].

6.5.1 Convergence theorem

Theorem 6.20 (Convergence theorem for s-holomorphic functions)**.** *Let $Q \subset \Omega$ be a rectangular domain such that $9Q \subset \Omega$. Let $(\mathcal{F}_\delta)_{\delta>0}$ be a family of s-holomorphic functions on $\Omega_\delta^\diamond$ and $H_\delta = \mathrm{Im} \int \mathcal{F}_\delta^2$. If $(H_\delta)_{\delta>0}$ is uniformly bounded on $9Q_\delta$, then $(\mathcal{F}_\delta)$ is precompact on Q_δ.*

Remark 6.21. For each $z \in \mathrm{Int}\,\Omega$, we can find a neighborhood Q of z small enough such that $9Q \subset \Omega$ to have precompactness of $(\mathcal{F}_\delta)$ near z. Then we can use a diagonal argument to extract a subsequence of $(\mathcal{F}_\delta)$ converging uniformly on all compacts of Ω.

Proof. It is sufficient to show the second point in Theorem 5.27. We write

$$\delta \int_{Q_\delta^\diamond} |\mathcal{F}_\delta(v)|^2 \mathrm{d}v = \delta \int_{Q_\delta} |D_x^{(\delta)} H_\delta(x)| \mathrm{d}x + \delta \int_{Q_\delta^\star} |D_x^{(\delta)} H_\delta(x)| \mathrm{d}x$$

which is exactly the definition of H_δ in Proposition 6.8. These two terms can be treated in a similar way. We will thus just look at the first one and show that it is bounded by a constant uniformly in δ.

On the primal semi-discretized domain $9Q_\delta$, write $H_\delta = S_\delta + R_\delta$ where S_δ is semi-discrete harmonic with boundary values $H_{\delta|\partial 9Q_\delta}$ on $\partial 9Q_\delta$.

$$\begin{aligned}\int_{Q_\delta} |D_x^{(\delta)} S_\delta(x)| \mathrm{d}x &\leqslant \int_{Q_\delta} c_1 \cdot \sup_{9Q_\delta} |S_\delta| \leqslant \frac{c_2}{\delta} \cdot c_1 \cdot \sup_{9Q_\delta} |S_\delta| \\ &= \frac{c_1 c_2}{\delta} \sup_{\partial(9Q_\delta)} |S_\delta| = \frac{c_3}{\delta} \sup_{\partial(9Q_\delta)} |H_\delta| \leqslant \frac{c_4}{\delta}.\end{aligned}$$

Here, we use Proposition 5.25 in the first inequality; the total length of axes in Q_δ is proportional to δ^{-1} in the second; the maximum principle (Proposition 5.15) in the third; H_δ and S_δ coincide on the boundary $\partial 9Q_\delta$ in the fourth ; and finally, H_δ is bounded by hypotheses. Moreover, the constants c_i may depend on the domain Ω but are uniform in δ.

We will now do something similar to R_δ. First, we write (Proposition 5.26)

$$R_\delta(x) = \int_{9Q_\delta} \Delta^{(\delta)} R_\delta(y) G_{9Q_\delta}(x, y) \mathrm{d}y.$$

Since H is subharmonic, it is the same for R_δ. Thus, $\Delta^{(\delta)} R_\delta \geqslant 0$ in $9Q_\delta$. Then, we have

$$\begin{aligned}
\int_{Q_\delta} |D_x^{(\delta)} R_\delta(x)| \mathrm{d}x &\leqslant \int_{Q_\delta} \int_{9Q_\delta} \Delta^{(\delta)} R_\delta(y) |D_x^{(\delta)} G_{9Q_\delta}(x,y)| \mathrm{d}y \mathrm{d}x \\
&= \int_{9Q_\delta} \Delta^{(\delta)} R_\delta(y) \int_{Q_\delta} |D_x^{(\delta)} G_{9Q_\delta}(x,y)| \mathrm{d}x \mathrm{d}y \\
&\leqslant \int_{9Q_\delta} c_5 \cdot \Delta^{(\delta)} R_\delta(y) \int_{Q_\delta} G_{9Q_\delta}(x,y) \mathrm{d}x \mathrm{d}y \\
&= c_5 \int_{Q_\delta} \int_{9Q_\delta} \Delta^{(\delta)} R_\delta(y) G_{9Q_\delta}(x,y) \mathrm{d}y \mathrm{d}x \\
&= c_5 \int_{Q_\delta} R_\delta(x) \mathrm{d}x \\
&\leqslant c_5 \cdot \frac{c_6}{\delta} = \frac{c_5 c_6}{\delta}
\end{aligned}$$

where we use the triangular inequality in the first line; Fubini in the second line (all the terms are non-negative); Proposition 5.28 in the third; Fubini again in the fourth, Riesz representation (Proposition 5.26) again in the fifth; and finally R_δ is bounded in the last one (because H_δ and S_δ are bounded). □

With all what we have done so far, we can determine the uniform limit of H_δ and $\mathcal{F}_\delta$ when δ goes to 0. First of all, we need to describe the continuous version of the boundary value problem. Given a continuous Dobrushin domain (Ω, a, b), we say that a function f defined on Ω is a solution to the *Riemann-Hilbert boundary value problem* if the following three conditions are satisfied:

(a) holomorphicity: f is holomorphic in Ω with singularities at a and b;
(b) boundary conditions: $f(\zeta)$ is parallel to $\tau(\zeta)^{-1/2}$ for $\zeta \in \partial\Omega \backslash \{a, b\}$, where $\tau(\zeta)$ denotes the tangent vector to Ω oriented from a to b (on both arcs);
(c) normalization: the function $h := \operatorname{Im} \int (f(\zeta))^2 \mathrm{d}\zeta$ is uniformly bounded in Ω and

$$h_{|(a_\delta b_\delta)} = 0, \quad h_{|(b_\delta a_\delta)} = 1.$$

Note that (a) and (b) guarantee that h is harmonic in Ω and constant on both boundary arcs (ab) and (ba). Thus, if we write Φ the conformal mapping from Ω onto the infinite strip $\mathbb{R} \times (0,1)$ sending a and b to $\mp\infty$, the function $h \circ \Phi^{-1}$ is still harmonic. Moreover, the only harmonic function on the strip $\mathbb{R} \times (0,1)$ with boundary condition 1 on $\mathbb{R} \times \{1\}$ and 0 on $\mathbb{R} \times \{0\}$ is $z \mapsto \operatorname{Im}(z)$, we obtain that $h(z) = \operatorname{Im} \Phi(z)$ And from the definition of h in (c), we get

$$h(v) - h(u) = \operatorname{Im}(\Phi(v) - \Phi(u)) = \operatorname{Im} \int_u^v (f(\zeta))^2 \mathrm{d}\zeta$$

for $u, v \in \Omega$. At u fixed, since $\Phi(v) - \Phi(u)$ and $\int_u^v (f(\zeta))^2 \mathrm{d}\zeta$ are both holomorphic in v and have the same imaginary part, they differ only by a real constant. By taking the derivative, we can deduce that

$$\Phi'(v) = f(v)^2$$

or equivalently,

$$f = \sqrt{\Phi'}.$$

Since Φ is a conformal map, its derivative is never 0 on Ω, we can define the square root in a continuous manner (with respect to Ω), and the solution f is well-defined up to the sign.

Moreover, this tells us that $f(\zeta) = c(\zeta)\tau(\zeta)^{-1/2}$ for all $\zeta \in \partial\Omega\backslash\{a,b\}$ where c keeps the same sign all along the boundary. Therefore, we can choose the branch of the logarithm such that $\sqrt{\Phi'}$ corresponds to c positive and $-\sqrt{\Phi'}$ corresponds to c negative. Actually, if we look around b, this branch is given by $\sqrt{1} = 1$.

Theorem 6.22. *The solutions F_δ of the semi-discrete boundary value problems are uniformly close on any compact subset of Ω to their continuous counterpart f defined by (a), (b) and (c). In other words, F_δ converges uniformly as $\delta \to 0$ on all compact sets of Ω to $\sqrt{\Phi'}$ where Φ is any conformal map from Ω to $\mathbb{R} \times (0,1)$ mapping a and b to $\mp\infty$ respectively.*

Proof. We start by showing the convergence of the discrete primitive $H_\delta := \operatorname{Im} \int_\delta (\mathcal{F}_\delta(\zeta))^2 \mathrm{d}\zeta$, using the boundary modification trick introduced in Section 6.3.1. We extend H_δ on $\widetilde{\Omega}_\delta$ and denote its restriction on the primal axes $\widetilde{H_\delta^\bullet}$. By Lemma 6.11, $\widetilde{H_\delta^\bullet}$ is still subharmonic, thus it is smaller than the harmonic function $h_\delta^\bullet$ with boundary condition 0 on $(a_\delta b_\delta)$ and 1 on $(b_\delta a_\delta)$. Proposition 5.30 tells that $h_\delta^\bullet$ converges to the solution H of the continuous Dirichlet boundary problem with boundary conditions 0 on ∂_{ab} and 1 on ∂_{ba}. We can deduce that

$$\limsup_{\delta\to 0} \widetilde{H_\delta^\bullet} \leqslant h$$

on any compact subset of Ω. In a similar manner, denote $\widetilde{H_\delta^\circ}$ the function H_δ extended on $\widetilde{\Omega}_\delta^\star$ which is restricted on dual axes. As before, this time by superharmonicity, we deduce that

$$\liminf_{\delta\to 0} \widetilde{H_\delta^\circ} \geqslant h$$

on any compact subset of Ω. By definition (Equation (6.8)), for a sequence of w_δ and b_δ neighbors in Ω_δ, both approximating $u \in \Omega$ (i.e., $w_\delta \to u$, $b_\delta \to u$), we have

$$h(u) \leqslant \liminf_{\delta\to 0} \widetilde{H_\delta^\circ}(w_\delta) \leqslant \limsup_{\delta\to 0} \widetilde{H_\delta^\circ}(b_\delta) \leqslant h(u).$$

Since the convergence to h on $\widetilde{\Omega}_\delta$ and $\widetilde{\Omega}_\delta^\star$ is uniform on compact subsets, it is the same for the convergence of both $\widetilde{H_\delta^\bullet}$ and $\widetilde{H_\delta^\circ}$.

Consider $Q \subset \Omega$ such that $9Q \subset \Omega$. By the uniform convergence of H_δ, the family (H_δ) is bounded uniformly in $\delta > 0$ on $9Q$. Theorem 6.20 implies that $\mathcal{F}_\delta$ is a precompact family of semi-discrete s-holomorphic functions on Q.

Consider δ_n a subsequence such that $\mathcal{F}_{\delta_n}$ converges uniformly on all compact subsets of Ω_δ to $\mathcal{F}$. For $u, v \in \Omega_\delta$ and converging subsequences $u_n \to u$ and $v_n \to v$, we have

$$\begin{aligned} h(v) - h(u) &= \lim_{n\to\infty} (H_{\delta_n}(v_n) - H_{\delta_n}(u_n)) \\ &= \lim_{n\to\infty} \operatorname{Im} \int_{v_n}^{u_n} \mathcal{F}_{\delta_n}(z)^2 \mathrm{d}z \\ &= \operatorname{Im} \int_v^u \mathcal{F}(z)^2 \mathrm{d}z. \end{aligned}$$

Same as the discussion just above, the limit $\mathcal{F}$ is given by $\sqrt{\Phi'}$ where Φ is any conformal map from Ω to $\mathbb{R} \times (0,1)$ mapping a and b to $\mp\infty$. □

Here we give a brief idea to the proof for the vertical crossing. To start with, we need to establish propositions similar to Propositions 6.15 and 6.16. We will get $\sqrt{\partial_y \mathrm{HM}_\bullet}$ and

$\sqrt{\partial_y \mathrm{HM}_\circ}$ in the statement. And to estimate these harmonic functions, we can use Harnack Principle (Proposition 5.25) to get the correct orders. Then, the end of the story is the same, since we can always define the exploration path and get the same estimates (Lemmas 6.17 and 6.18).

6.5.2 Conclusion: proof of the Main Theorem

Now we have all the necessary ingredients to conclude the proof of the Main Theorem:

1. The RSW property shown in the previous section gives the G2 condition mentioned in [KS12], giving as conclusion that the family of interfaces (γ_δ) is tight for the weak convergence.
2. The fact that the fermionic observable (seen as an exploration process) is a martingale and is conformally invariant allows us to identify the limit via Itô's formula. More precisely, if γ is a subsequential limit of the interface parameterize by a Löwner chain W, from property of martingales and Itô's formula, we prove that (W_t) and $(W_t^2 - \kappa t)$ are both martingales ($\kappa = 16/3$ for quantum FK-Ising). The computation is exactly the same as in the limit of the classical FK-Ising since we have the same Riemann-Hilbert Boundary value problem in continuum and same martingales. Readers who are interested in more details, see [DCS12, DC13].

6.5.3 Going further: quantum random-cluster model

In the paper in preparation [DCLM17], the quantum random-cluster measure with parameters $\lambda, \mu > 0$, cluster weight $q \geqslant 1$ and boundary condition ξ can be defined on any open semi-discrete domain Ω_δ. Its definition is given by (1.15) that we recall here

$$\mathrm{d}\varphi^{\xi}_{\mathcal{Q},\Omega_\delta}(D,B) \propto q^{k^\xi(D,B)} \mathrm{d}\mathbb{P}_{\mathcal{Q},\Omega_\delta}(D,B),$$

where D (resp. B) is a finite set of points on primal (resp. dual) vertical lines. In the above definition, $\mathbb{P}_{\mathcal{Q},\Omega_\delta}$ is the measure of the family of independent Poisson point processes with parameter λ on primal vertical lines and parameter μ on dual vertical lines. The quantity $k^\xi(D,B)$ counts the number of connected components in the configuration (D,B) with respect to the boundary condition ξ on the domain Ω_δ.

It is proven in the same paper that this model exhibits a phase transition for parameters $\lambda, \mu > 0$ such that $\mu/\lambda = q$. Moreover, for these values, we may write the measure associated with the loop representation of the model as follows:

$$\mathrm{d}\varphi^{\xi}_{\mathcal{Q},\Omega_\delta}(D,B) \propto \sqrt{q}^{l^\xi(D,B)} \mathrm{d}\mathbb{P}_{\mathcal{Q},\Omega_\delta}(D,B),$$

where $l^\xi(D,B)$ denotes the number of loops in the configuration (D,B). And if we look at the model defined on a Dobrushin domain $(\Omega_\delta^\diamond, a_\delta, b_\delta)$ as we studeid in Section 6.2, we get a collection of loops and an interface γ_δ going from a_δ to b_δ.

In particular, using the approach of isoradial graphs [DCLM17, Sec. 1], one can see that there are reasons to believe that for the following parameters

$$\lambda = \frac{4r}{\delta\sqrt{q(4-q)}} \quad \text{and} \quad \mu = \frac{4r\sqrt{q}}{\delta\sqrt{4-q}}, \quad \text{where } r = \frac{1}{\pi}\arccos\Big(\frac{\sqrt{q}}{2}\Big),$$

the quantum random-cluster model is isotropic. Therefore, a result on the conformal invariance of the interface could be expected: γ_δ should converge to SLE_κ with $\kappa = 4\pi/\arccos(-\sqrt{q}/2)$

as δ goes to 0 as in the discrete setting [Sch07]. This might be achieved by using the so-called *parafermionic observable*, which is a modified version of the one used here,

$$F_\delta(e) = \frac{\nu}{\sqrt{\delta}} \cdot \mathbb{E}\Big[\exp\big(\mathrm{i}\,\sigma\, W(e, b_\delta)\big)\, \mathbb{1}_{e\in\gamma_\delta}\Big], \quad \text{where } \sigma = \frac{2}{\pi}\arcsin\Big(\frac{\sqrt{q}}{2}\Big). \tag{6.14}$$

However, as for the discrete setting mentioned in [Smi10], only half of the Cauchy-Riemann relations are known, which is not enough to establish the conformal invariance.

Appendix A

Computation of residues

For a non-negative integer k and an integer m, define the following meromorphic function on $\mathbb{C}$,

$$g_{k,m}(z) := \frac{1}{z}\left(\frac{1}{z+1}+\frac{1}{z-1}\right)^k\left(\frac{z+1}{z-1}\right)^{2m} = \frac{2^k z^{k-1}}{(z-1)^{k+2m}(z+1)^{k-2m}}.$$

We notice that the possible singularities are at 0, 1 and -1.

Lemma A.1. *When $k = 0$, we have $\operatorname{Res}(g_{k,m}, 1) = \operatorname{Res}(g_{k,m}, -1) = 0$ for all integer m.*

Proof. We fix $k = 0$. When $m = 0$, the result is trivial. For $m \geqslant 1$, the function $g_{k,m}$ does not have any pole at -1, so it is clear that $\operatorname{Res}(g_{k,m}, -1) = 0$. The residue of $g_{k,m}(z)$ at $z = 1$ is the residue of $g_{k,m}(y+1)$ at $y = 0$. We have

$$\begin{aligned} g_{k,m}(y+1) &= \frac{1}{y+1}\left(1+\frac{2}{y}\right)^{2m} \\ &= \left[\sum_{k\geqslant 0}(-y)^k\right]\left[\sum_{l=0}^{2m}\binom{2m}{l}\left(\frac{2}{y}\right)^l\right], \end{aligned}$$

where the coefficient of $\frac{1}{y}$ is given by

$$\sum_{l=1}^{2m}\binom{2m}{l}2^l(-1)^{l-1} = -[(1-2)^{2m}-1] = 0.$$

When m is negative, the proof is similar. □

Lemma A.2. *For $k \geqslant 1$, we have $\operatorname{Res}(g_{k,m}, 1) + \operatorname{Res}(g_{k,m}, -1) = 0$.*

Proof. When $k \geqslant 1$, the singularity at 0 is removable. We observe that $|g_{k,m}(z)|$ behaves like $|z|^{-k-1} \leqslant |z|^{-2}$ when $|z|$ is large, giving

$$\lim_{R\to\infty}\frac{1}{2\pi\,\mathrm{i}}\int_{\partial B(0,R)} g_{k,m}(z)\mathrm{d}z = 0.$$

Moreover, when $R > 1$, we have

$$\frac{1}{2\pi\,\mathrm{i}}\int_{\partial B(0,R)} g_{k,m}(z)\mathrm{d}z = \operatorname{Res}(g_{k,m}, -1) + \operatorname{Res}(g_{k,m}, 1).$$

Thus, we get the desired result. □

Lemma A.3. *For $k \geqslant 1$ and $k \leqslant 2|m|$, $\mathrm{Res}(g_{k,m}, 1) = \mathrm{Res}(g_{k,m}, -1) = 0$.*

Proof. The previous lemma tells us that it is enough to show that the residue is zero at either 1 or -1. If m is positive, we notice that $g_{k,m}(z)$ does not have any pole at -1, thus the residue at -1 is zero. If m is negative, the residue at 1 is zero. □

Lemma A.4. *More generally, for all $k \in 2\mathbb{N}$,*

$$\mathrm{Res}(g_{k,m}, 1) = \mathrm{Res}(g_{k,m}, -1) = 0.$$

Proof. Assume that $k = 2l > m \geqslant 0$ for a positive integer l. Look at the residue of $g_{k,m}(z)$ around $z = 1$ is equivalent to looking at the residue of $g_{k,m}(y+1)$ around $y = 0$,

$$\mathrm{Res}(g_{k,m}(z), z = 1) = \mathrm{Res}(g_{k,m}(y+1), y = 0).$$

We have the following equivalent relations

$$\begin{aligned} & \mathrm{Res}(g_{2l,m}(y+1), y = 0) = 0 \\ \Leftrightarrow \quad & \mathrm{Res}\left(\frac{(y+1)^{2l-1}}{y^{2l+2m}(y+2)^{2l-2m}}, y = 0\right) = 0 \\ \Leftrightarrow \quad & \frac{(1+y)^{2l-1}}{(1+\frac{y}{2})^{2l-2m}}[y^{2l+2m-1}] = 0 \end{aligned} \tag{A.1}$$

where the notation $R(y)[y^k]$ gives the coefficient of y^k in the Laurent series of $R(y)$.

We expand the rational fraction to evaluate this coefficient by applying the three following identities,

$$\binom{2m-2l}{2m+p} = (-1)^{2m+p}\binom{2l+p-1}{2m+p} \tag{A.2}$$

$$\binom{2l+p-1}{2m+p} = \sum_{q=0}^{2l-1}\binom{p}{q}\binom{2l-1}{2m+p-q}, \tag{A.3}$$

$$\sum_{k=0}^{n}\binom{n}{k}\binom{k}{r}(-x)^k = (-x)^r(1-x)^{n-r}\binom{n}{r}. \tag{A.4}$$

Equation (A.2) comes from the general definition of binomial coefficients, and in our case, we have $2m - 2l < 0$. Equation (A.3) is an easy combinatorial identity and Equation (A.4) a

simple expansion. Then, the left-hand side of Equation (A.1) equals

$$\begin{aligned}
&\sum_{p=0}^{2l-1}\binom{2l-1}{p}\left(\frac{1}{2}\right)^{2l+2m-1-p}\binom{2m-2l}{2l+2m-1-p}\\
(p\rightsquigarrow 2l-1-p)\quad &=\sum_{p=0}^{2l-1}\binom{2l-1}{p}\left(\frac{1}{2}\right)^{2m+p}\binom{2m-2l}{2m+p}\\
&=\sum_{p=0}^{2l-1}\binom{2l-1}{p}\left(-\frac{1}{2}\right)^{2m+p}\binom{2l+p-1}{2m+p}\\
(\text{Equation (A.3)})\quad &=\sum_{p=0}^{2l-1}\binom{2l-1}{p}\left(-\frac{1}{2}\right)^{2m+p}\sum_{q=0}^{2l-1}\binom{p}{q}\binom{2l-1}{2m+p-q}\\
(q\rightsquigarrow p-q)\quad &=\sum_{p=0}^{2l-1}\binom{2l-1}{p}\left(-\frac{1}{2}\right)^{2m+p}\sum_{q=0}^{2l-1}\binom{p}{q}\binom{2l-1}{2m+q}\\
&=\left(\frac{1}{2}\right)^{2m}\sum_{q=0}^{2l-1}\binom{2l-1}{2m+q}\sum_{p=0}^{2l-1}\binom{2l-1}{p}\binom{p}{q}\left(-\frac{1}{2}\right)^{p}\\
(\text{Equation (A.4)})\quad &=\left(\frac{1}{2}\right)^{2m}\sum_{q=0}^{2l-1}\binom{2l-1}{2m+q}\left(-\frac{1}{2}\right)^{q}\left(\frac{1}{2}\right)^{2l-1-q}\binom{2l-1}{q}\\
&=\left(\frac{1}{2}\right)^{2m+2l-1}\sum_{q=0}^{2l-1}(-1)^{q}\binom{2l-1}{2m+q}\binom{2l-1}{2l-1-q}=0
\end{aligned}$$

where the sum in the last line is the coefficient in front of $x^{2m+2l-1}$ in $(1-x)^{2l-1}(1+x)^{2l-1} = (1-x^2)^{2l-1}$, which is zero because the polynomial only contains monomials of even degree. □

Proposition A.5. *For $\zeta = m + \mathrm{i}\,t \in \mathbb{L}_1$ with $m \in \frac{1}{2}\mathbb{Z}$ and $t \in \mathbb{R}$, let f_ζ as defined in (5.22). Consider C the path defined in Proposition 5.18. Then,*

$$\int_C f_\zeta(z)dz = 0.$$

Proof. We will expand the exponential into series and show that this integral is zero for all terms. We can do this because the series converges uniformly on all compacts to the exponential function. Therefore, it makes sense to exchange the integral and the series. After expanding, we get

$$f_\zeta(z) = \sum_{k\geqslant 0}\frac{(2\,\mathrm{i}\,t)^k}{k!}g_{k,m}(z)$$

and the residue theorem along with Lemma A.1 and Lemma A.2 allows us to conclude. □

The previous proposition is important because it shows that the Green's function as defined by (5.23) does not depend on the lift of the logarithm.

Proposition A.6. *Around $\zeta = m \in \mathbb{Z}\backslash\{0\}$, the function G is $\mathcal{C}^{2|m|}$.*

Proof. To show this, we need to check that for all $k \leqslant 2|m|$, we have

$$\int_C g_{k,m}(z)\ln_1(z)\mathrm{d}z = \int_C g_{k,m}(z)\ln_2(z)\mathrm{d}z$$

where $\ln_i$ is chosen such that $\ln_i(1) - \ln_i(-1) = (-1)^i\,\mathrm{i}\,\pi$. Here, $\ln_1$ corresponds to the logarithm chosen in the upper half-plan and $\ln_2$ in the lower half-plane. From Proposition A.5, we can fix a lift of the logarithm such that $\ln_1 - \ln_2$ is non zero around 1 and -1, for example $\ln_1(1) = 2\,\mathrm{i}\,\pi$, $\ln_1(-1) = 3\,\mathrm{i}\,\pi$, $\ln_2(1) = 0$ and $\ln_2(-1) = -\,\mathrm{i}\,\pi$.

Let I_1 be the integral on the left-hand side and I_2 be the one on the right-hand side. Since $\ln_1 - \ln_2$ is non zero at 1 and -1, we can write

$$I_1 - I_2 = 2\,\mathrm{i}\,\pi[2\,\mathrm{i}\,\pi\,\mathrm{Res}(g_{k,m}(z), z = 1) + 4\,\mathrm{i}\,\pi\,\mathrm{Res}(g_{k,m}(z), z = -1)] = 0$$

due to Lemma A.3. □

Proposition A.6 provides us with the regularity of Green's function; in particular, the second condition giving in Section 5.4.1 is satisfied. This comes to complete the proof of Proposition 5.18.

Appendix **B**

RSW theory and applications

In this part of Appendix, we provide proofs concerning different equivalent formulations of the RSW property. In the case of Bernoulli percolation, these proofs are classical and readers are referred to [Gri99] for a good reference. In our current case of random-cluster model, the boundary conditions count, thus more care is needed and proofs are slightly more technical; however, the main idea remains the same.

We start by proving Lemma 3.10 then Lemma 3.14.

Proof of Lemma 3.10. Fix a doubly-periodic graph $\mathbb{G}$ with grid $(s_n)_{n\in\mathbb{N}}$, $(t_n)_{n\in\mathbb{N}}$.

Let $\rho > 1$ and $\nu > 0$. Assume that (BXP(ρ, ν)) is satisfied and we want to show the strong (Euclidean) RSW property. The converse can be proven in a similar manner, so we omit the proof here.

We start by saying that we can assume $\rho \geqslant 2$ and $\nu \leqslant 1$. Indeed, if $\rho < 2$, in the first part of the proof, we show that it is possible to create longer horizontal and vertical crossings, knowing only (BXP(ρ, ν)), to obtain (BXP(ρ', ν)) for $\rho' \geqslant 2$. The same method can also be applied to reduce the value of ν. Finally, we note that this also allows us to deduce (BXP(ρ, ν)) for any value of $\rho > 1$ and $\nu > 0$.

The first step is to show that if (BXP(ρ, ν)) is true for some $\rho < 2$, then we also have (BXP(2, ν)). Let $\delta := \delta_1(\rho, \nu)$ and $K = (\rho - \frac{1}{\rho})^{-1}$. For $-K \leqslant k \leqslant K$, consider

$$\mathsf{R}_k^v := \mathsf{R}\Big(2\tfrac{k}{K}n, 2(\tfrac{k}{K} + \tfrac{1}{\rho})n; -n, n\Big), \qquad \mathcal{V}_k := \mathcal{C}_v(\mathsf{R}_k^v),$$
$$\mathsf{R}_k^h := \mathsf{R}\Big(2\tfrac{k}{K}n, 2(\tfrac{k}{K} + \rho)n; -n, n\Big), \qquad \mathcal{H}_k := \mathcal{C}_h(\mathsf{R}_k^h),$$

where $\mathcal{V}_k$ (resp. $\mathcal{H}_k$) is the event that there is an vertical (resp. horizontal) crossing in R_k^v (resp. R_k^h). If for all $-K \leqslant k \leqslant K$, both $\mathcal{V}_k$ and $\mathcal{H}_k$ occur, then there is an horizontal crossing in the domain $\mathsf{R}(2n; n)$. See Figure B.1 for the overlapping between domains that ensures a longer crossing. Thus, we have

$$\varphi^0_{\mathsf{R}_n}\Big[\mathcal{C}_h(2n; n)\Big] \geqslant \prod_{k=-K}^{K} \varphi^0_{\mathsf{R}_n}[\mathcal{H}_k]\,\varphi^0_{\mathsf{R}_n}[\mathcal{V}_k] \geqslant \delta^{2(2K+1)},$$

where $\mathsf{R}_n = \mathsf{R}((2+\nu)n; (1+\nu)n)$. The above inequality is a consequence of the FKG inequality, comparison between boundary conditions and the fact that for all $-K \leqslant k \leqslant K$, the translated domain $\mathsf{R}((\rho+\nu)n; (\rho+1)n)$ centered at R_k^h or $\mathsf{R}((1+\frac{\nu}{\rho})n; (1+\frac{1}{\rho})n)$ centered at R_k^v is included in R_n. The same construction works for the vertical crossing in $\mathsf{R}(n; 2n)$ with respect to the measure $\varphi^0_{\mathsf{R}'_n}$ where $\mathsf{R}'_n = \mathsf{R}((1+\nu)n; (2+\nu)n)$.

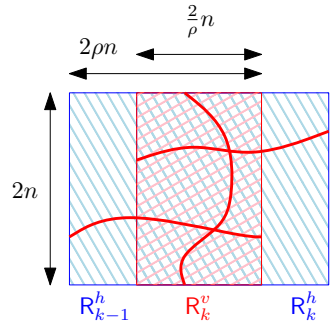

Figure B.1 – The overlapping between successive rectangular domains ensures a longer horizontal crossing. Horizontal rectangular domains R^h_{k-1} and R^h_k (in blue) are of size $2n \times 2\rho n$; the vertical one R^v_k (in red) is of size $2n \times \frac{2}{\rho}n$. To create this overlapping, we shift domains by $2\rho n - \frac{2}{\rho}n = \frac{2}{K}n$ each time.

By considering larger domains with crossings in rectangles of same ratio, one can also reduce the value of ν. We only refer readers to Figure B.2 without providing details here.

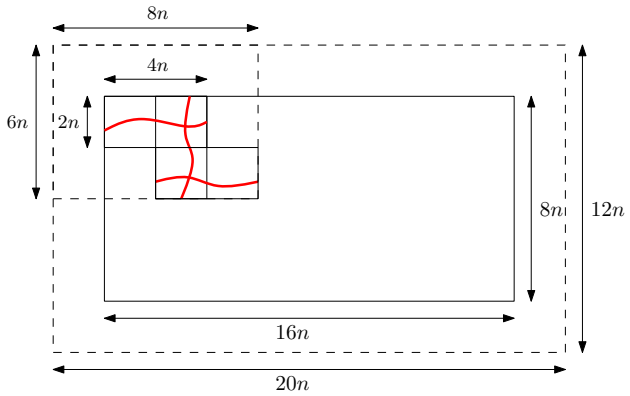

Figure B.2 – We apply (BXP(2, 2)) in smaller rectangular domains to create (BXP(2, $\frac{1}{2}$)) in a bigger rectangular domain. Smaller domains are of the form $\mathsf{R}(2n; n)$ with boundary $\mathsf{R}(4n; 3n)$ and the bigger one is of the form $\mathsf{R}(8\cdot 2n; 8n)$ with boundary $\mathsf{R}(8(2+\frac{1}{2})n; 8(1+\frac{1}{2})n)$.

Now, assume that (BXP(ρ, ν)) is true with $\rho \geqslant 2$ and $\nu \leqslant 1$ and show the strong (Euclidean) RSW property. Let K be a fundamental domain of $\mathbb{G}$ which is bordered by s_0, s_c, t_0 and t_d with s_0 and t_0 included in K; s_c and t_d excluded. This implies that (s_n) is c-periodic and (t_n) is d-periodic. Moreover, up to a rotation, we may assume that (t_n) has asymptotic direction $(1, 0)$, which also means that the graph $\mathbb{G}$ is invariant by a horizontal vector.

Let $n \in \mathbb{N}$. For $i, j \in \mathbb{Z}$, the cell $C_{i,j}$ is defined to be the translated square domain enclosed by $s_{(2i-1)cdn}$, $s_{(2i+1)cdn}$, $t_{(2j-1)cdn}$ and $t_{(2j+1)cdn}$ with the bottom and the left tracks included; the top and the right tracks excluded. Note that $C_{i,j}$ contains d (resp. c) periods in the horizontal (resp. vertical) direction.

For $k > 0$, let $R_k = [-2k, 2k] \times [-k, k]$ be a Euclidean rectangular domain. Also write $\overline{R}_k = [-3k, 3k] \times [-2k, 2k]$. The goal then is to show that for k large enough, $\varphi^0_{\overline{R}_k}[\mathcal{C}_h(R_k)] \geqslant \delta$, where δ is independent of k.

For $\mu > 0$, let $\mathsf{R}^\mu_n = \mathsf{R}(\mu n + 2cdn; 2cdn)$ and $\overline{\mathsf{R}}^\mu_n = \mathsf{R}(\mu n + 3cdn; 3cdn)$. Write $C_i = C_{i,0}$ and $K = \lceil \frac{\mu}{2cd} \rceil + 1$. If for $-K \leqslant i \leqslant K - 1$, $C_i \cup C_{i+1}$ is crossed horizontally and for $-K \leqslant i \leqslant K$,

C_i is crossed vertically, then the event $\mathcal{C}_h(\mathsf{R}_n^\mu)$ occurs. Hence, by the FKG inequality,

$$\varphi^0_{\overline{\mathsf{R}}_n^\mu}\Big[\mathcal{C}_h(\mathsf{R}_n^\mu)\Big] \geqslant \delta^{2K}, \tag{B.1}$$

where $\delta = \delta_1(2,1)$ is provided by BXP(2,1).

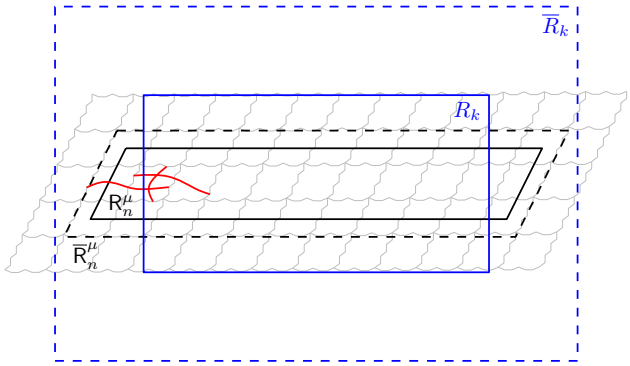

Figure B.3 – The graph $\mathbb{G}$ is in grey. Black domains are rectangular domains with respect to a grid of $\mathbb{G}$; blue domains are Euclidean rectangular domains. Domains with overline are those in which we define random-cluster measures. A horizontal crossing in R_n^μ induces a horizontal crossing in R_k.

To conclude, it is sufficient to show that for k large enough (corresponding to specific values of μ and n),

$$\varphi^0_{\overline{R}_k}\left[\mathcal{C}_h(R_k)\right] \geqslant \varphi^0_{\overline{\mathsf{R}}_n^\mu}\Big[\mathcal{C}_h(\mathsf{R}_n^\mu)\Big]. \tag{B.2}$$

To this end, we need to fix a value of μ such that for all k large enough, we can choose n properly such that (i) R_k is higher and shorter than R_n^μ and (ii) $\overline{\mathsf{R}}_n^\mu$ is included in $\overline{R}_k$ as shown in Figure B.3. These conditions can be rewritten as

$$\begin{cases} k \geqslant 2cd\ell n, \\ 2k \leqslant \mu n, \end{cases} \qquad \begin{cases} 2k \geqslant 3cd\ell n, \\ 3k \geqslant (\mu + 6cd\ell)n. \end{cases}$$

Thus, we may choose $\mu = 12cd\ell$ and $k = 6cd\ell n$.

The above shows that the probability of crossings in $\mathbb{R}^2$ can be bounded from below uniformly, depending only on the ratio of the rectangle, in both asymptotic directions given by (s_n) and (t_n). Then to show that it is the case for any direction, the proof is quite similar as above and we only refer readers to Figure B.4.

□

Proof of Lemma 3.14. Fix $a > 1$ and take $b > 3a$ whose value is to be chosen later. Assume that the condition (BXP(ρ, ν)) is true for all $\rho > 1$ and $\nu > 0$. We show (3.5) only for primal crossings since the proof is exactly the same for dual ones. First of all, we have,

$$\varphi^0_{\Lambda(bn)}\Big[\mathcal{C}_v(\tfrac{an}{2};\tfrac{an}{2})\Big] \geqslant \varphi^0_{\mathsf{R}(an;\frac{3}{2}an)}\Big[\mathcal{C}_v(\tfrac{an}{2};an)\Big] \geqslant \delta_1(2,1),$$

whenever $b \geqslant \frac{3}{2}an$.

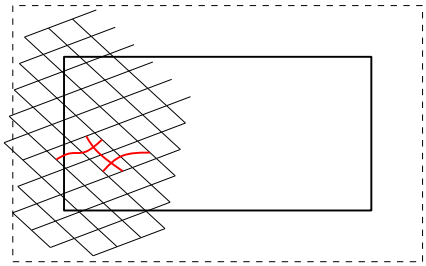

Figure B.4 – Small rhombi indicate Euclidean domains in which we have the RSW property. By putting crossings together in this way, we create a horizontal crossing in the bigger box. Since we the rhombi and the domain can be scaled together, the number of rhombi needed depends only on the ratio, thus the RSW property.

Then, consider the following rectangles and crossing events (see Figure B.5),

$$\begin{aligned} \mathsf{R}^1 &= \mathsf{R}(-2an, 2an; \tfrac{n}{2a}, \tfrac{n}{a}), & \mathcal{H}^1 &= \mathcal{C}_h(\mathsf{R}^1), \\ \mathsf{R}^2 &= \mathsf{R}(-2an, 2an; -\tfrac{n}{a}, -\tfrac{n}{2a}), & \mathcal{H}^2 &= \mathcal{C}_h(\mathsf{R}^2), \\ \mathsf{R}^3 &= \mathsf{R}((2a-\tfrac{1}{a})n, 2an; -\tfrac{n}{a}, \tfrac{n}{a}), & \mathcal{V}^3 &= \mathcal{C}_v(\mathsf{R}^3), \\ \mathsf{R}^4 &= \mathsf{R}(-2an, -(2a-\tfrac{1}{a})n; -\tfrac{n}{a}, \tfrac{n}{a}), & \mathcal{V}^4 &= \mathcal{C}_v(\mathsf{R}^4). \end{aligned}$$

We note that if $\mathcal{H}^1$, $\mathcal{H}^2$, $\mathcal{V}^3$ and $\mathcal{V}^4$ occur, then so does $\mathcal{C}(an, 2an; \frac{n}{a})$. Hence,

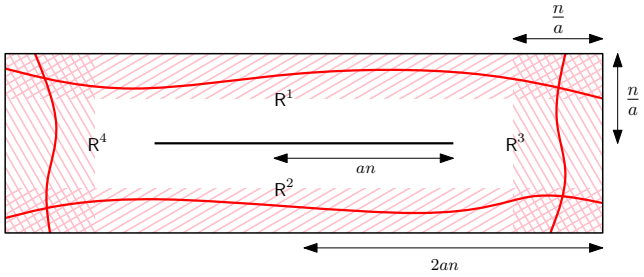

Figure B.5 – The rectangles $\mathsf{R}^1, \dots, \mathsf{R}^4$ are hashed and crossing events $\mathcal{H}^1$, $\mathcal{H}^2$, $\mathcal{V}^3$ and $\mathcal{V}^4$ are drawn in thick red lines.

$$\begin{aligned} \varphi^0_{\Lambda(bn)}\left[\mathcal{C}_h(an, 2an; \tfrac{n}{a})\right] &\geqslant \varphi^0_{\Lambda(3an)}\left[\mathcal{H}^1 \cap \mathcal{H}^2 \cap \mathcal{V}^3 \cap \mathcal{V}^4\right] \\ &\geqslant \delta_1(4a^2, 1)^2 \delta_1(2, 1)^2, \end{aligned}$$

where in the last inequality we use the FKG inequality, comparison between boundary conditions and the following facts:

- The rectangles R^1 and R^2 are translations of $\mathsf{R}(2an; \frac{n}{4a})$ of ratio $8a^2$.
- The rectangles R^3 and R^4 are translations of $\mathsf{R}(\frac{n}{2a}; \frac{n}{a})$ of ratio 2.
- Inclusion of rectangles: translated rectangles $\mathsf{R}((8a^2+1)\frac{n}{4a}; (1+1)\frac{n}{4a})$ having the same center as R^1 and R^2 are included in $\Lambda(3an)$; so are translated rectangles $\mathsf{R}(\frac{n}{a}; \frac{3n}{2a})$ having the same center as R^3 and R^4.

In consequence, we may choose $\delta_v = \frac{1}{2}\min\{\delta_1(2,1), \delta_1(4a^2,1)^2\delta_1(2,1)^2\}$.

Finally, let us show that as $b \to \infty$, we have

$$\varphi^0_{\Lambda(bn)}\Big[\mathcal{C}(3an, bn; bn)\Big] \to 1.$$

Consider $b > 3a$ and an integer k such that $3a^k \leqslant b < 3a^{k+1}$. For any $j \geqslant 0$, define the square domain $\Lambda_j = \Lambda(3a^j n)$, the annulus $\mathsf{A}_j = \Lambda_{j+1} \setminus \Lambda_j$ and the event $\mathcal{C}^*_j = \{\partial\Lambda_j \overset{*}{\longleftrightarrow} \partial\Lambda_{j+1} \text{ in } \mathsf{A}_j\}$, where $\overset{*}{\longleftrightarrow}$ denotes the connection in the dual model. Then, we have

$$\begin{aligned}
\varphi^0_{\Lambda(bn)}\Big[\mathcal{C}_h(3an, bn; bn)^c\Big] &= \varphi^0_{\Lambda(bn)}\Big[\mathsf{R}(3an; 0) \overset{*}{\longleftrightarrow} \partial\Lambda(bn)\Big] \\
&\leqslant \varphi^0_{\Lambda_k}\Big[\bigcap_{j=0}^{k-1} \mathcal{C}^*_j\Big] \\
&= \prod_{j=0}^{k-1} \varphi^0_{\Lambda_k}\Big[\mathcal{C}^*_j \,\Big|\, \bigcap_{j<i<k} \mathcal{C}^*_i\Big] \\
&\leqslant \prod_{j=0}^{k-1} \varphi^0_{\mathsf{A}_j}\Big[\mathcal{C}^*_j\Big],
\end{aligned}$$

where in the last line we use again the argument of exploration from outside and the comparison between boundary conditions. The complement of $\mathcal{C}^*_j$ is exactly the event $\mathcal{A}_j$ that there exists a (primal) circuit in the annulus A_j. Consider four rectangles R^i_j with $i = 1, \dots, 4$ and associated crossing events $\mathcal{H}^1_j = \mathcal{C}_h(\mathsf{R}^1_j)$, $\mathcal{H}^2_j = \mathcal{C}_h(\mathsf{R}^2_j)$, $\mathcal{V}^3_j = \mathcal{C}_v(\mathsf{R}^3_j)$ and $\mathcal{V}^4_j = \mathcal{C}_v(\mathsf{R}^4_j)$ as shown in Figure B.6.

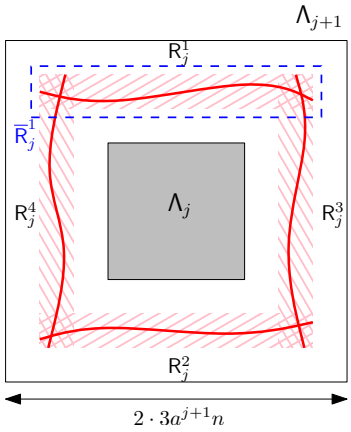

Figure B.6 – The annulus A_j and the four crossings events $\mathcal{H}^1_j$, $\mathcal{H}^2_j$, $\mathcal{V}^3_j$ and $\mathcal{V}^4_j$ creating $\mathcal{A}_j$.

Note that if the crossing events $\mathcal{H}^1_j$, $\mathcal{H}^2_j$, $\mathcal{V}^3_j$ and $\mathcal{V}^4_j$ occur, then so does $\mathcal{A}_j$. Moreover, we may also find $\overline{\mathsf{R}}^i_j$ (having the same center as R^i_j) which are included in Λ_{j+1} such that (BXP(ρ, ν)), for some fixed $\rho > 1$ and $\nu > 0$ independent of j, can be applied on them. These rectangular domains R^i_j and $\overline{\mathsf{R}}^i_j$ can also be chosen such that from scale j to scale $j+1$, they are enlarged by factor a. Thus, for $j \geqslant j_0$, where j_0 is a threshold provided by the RSW property,

$$\varphi^0_{\mathsf{A}_j}[\mathcal{A}_j] \geqslant \varphi^0_{\mathsf{A}_j}\Big[\mathcal{H}^1_j \cap \mathcal{H}^2_j \cap \mathcal{V}^3_j \cap \mathcal{V}^4_j\Big] \geqslant \delta_1(\rho, \nu)^4 =: c, \tag{B.3}$$

where c only depends on ρ and ν which are chosen to depend only on a. In the above inequality, we use the FKG inequality and the comparison between boundary conditions. In summary, we have

$$\varphi^0_{\Lambda(bn)}\Big[\mathcal{C}_h(3an, bn; bn)^c\Big] \leqslant \prod_{j=j_0}^{k-1}(1-c) \leqslant \exp\Big[\ln(1-c)\Big(\tfrac{\ln b - \ln 3}{\ln a} - j_0\Big)\Big] \to 0,$$

as $b \to \infty$. This concludes the proof. □

Appendix C

Proof of phase transition for $1 \leqslant q \leqslant 4$: Theorem 3.1 and Corollary 3.3

We give details of the proof of Theorem 3.1. To show the first point of the theorem, the uniqueness of the measure, we can for instance adapt the proof from [DC13, Cor. 4.40], where only the condition $\varphi^1_G\big[0 \leftrightarrow \infty\big] = 0$ is needed. This is also explained in the upcoming Proposition C.1, with a sketch of proof. This condition is an immediate consequence of the second point of the theorem.

The second point concerning the polynomial decay. Actually, we show that there exist $A, B, \alpha, \beta > 0$ such that for all n large enough,

$$An^{-\alpha} \leqslant \varphi^0_{\mathbb{G}}\big[0 \leftrightarrow \partial\Lambda(n)\big] \leqslant \varphi^1_{\mathbb{G}}\big[0 \leftrightarrow \partial\Lambda(n)\big] \leqslant Bn^{-\beta}. \tag{C.1}$$

Then, we can pick $A = B = 1$ by adjusting constants α and β.

Finally, the last point of the theorem, the RSW property, can be deduced from Corollary 3.12.

Proposition C.1. *If* $\varphi^1_{\mathbb{G},\beta,q}\big[0 \leftrightarrow \infty\big] = 0$, *then* $\varphi^0_{\mathbb{G},\beta,q} = \varphi^1_{\mathbb{G},\beta,q}$.

Proof. Let A an increasing event depending on a finite number of edges of $\mathbb{G}$. We can assume that these edges are all in $\Lambda(k)$ for a certain k. For $N \geqslant n \geqslant k$,

$$\begin{aligned}
&\varphi^1_{\Lambda(N),\beta,q}\big[A \cap \{\partial\Lambda(k) \nleftrightarrow \partial\Lambda(n)\}\big] \\
&\quad = \varphi^1_{\Lambda(N),\beta,q}\big[A \,\big|\, \partial\Lambda(k) \nleftrightarrow \partial\Lambda(n)\big]\varphi^1_{\Lambda(N),\beta,q}\big[\partial\Lambda(k) \nleftrightarrow \partial\Lambda(n)\big] \\
&\quad \leqslant \varphi^0_{\Lambda(n),\beta,q}[A] \cdot \varphi^1_{\Lambda(N),\beta,q}\big[\partial\Lambda(k) \nleftrightarrow \partial\Lambda(n)\big]
\end{aligned}$$

where in the last line we compare the boundary conditions by using the fact that $\{\partial\Lambda(k) \nleftrightarrow \partial\Lambda(n)\}$ is exactly the event that there exists a dual circuit in the annulus $\Lambda(n)\backslash\Lambda(k)$.

Taking $N \to \infty$, we get

$$\varphi^1_{\mathbb{G},\beta,q}\big[A \cap \{\partial\Lambda(k) \nleftrightarrow \partial\Lambda(n)\}\big] \leqslant \varphi^0_{\Lambda(n),\beta,q}[A] \cdot \varphi^1_{\mathbb{G},\beta,q}\big[\partial\Lambda(k) \nleftrightarrow \partial\Lambda(n)\big].$$

Then, taking $n \to \infty$ and using the fact that $\varphi^1_{\mathbb{G},\beta,q}\big[\partial\Lambda(k) \leftrightarrow \infty\big] = 0$ (recall that k is fixed), we obtain

$$\varphi^1_{\mathbb{G},\beta,q}[A] \leqslant \varphi^0_{\mathbb{G},\beta,q}[A],$$

which implies $\varphi^1_{\mathbb{G},\beta,q} = \varphi^0_{\mathbb{G},\beta,q}$. □

Then, we go to the proof of the polynomial decay, or equivalently, (C.1). The upper bound is shown by saying that if a path can go to the boundary $\partial\Lambda(n)$, then it also crosses all the annuli $\Lambda(2^j)\backslash\Lambda(2^{j-1})$ for $1 \leqslant j \leqslant \lfloor \ln n \rfloor$. The lower bound is shown by making crossings of boxes of ration 2 which garantee the existence of a path going to the boundary $\partial\Lambda(n)$. More details are given below.

Proof of (C.1). Fix n and consider an integer k such that $2^k \leqslant n < 2^{k+1}$. For $j \geqslant 1$, define Euclidean annuli $A_j = \Lambda(2^j)\backslash\Lambda(2^{j-1})$ and crossings of annuli $\mathcal{C}_j = \{\partial\Lambda(2^j) \leftrightarrow \partial\Lambda(2^j) \text{ in } A_j\}$. Then, we have

$$\varphi^1_{\mathbb{G}}\Big[0 \leftrightarrow \partial\Lambda(n)\Big] \leqslant \varphi^1_{\mathbb{G}}\Big[\bigcap_{j=1}^{k} \mathcal{C}_j\Big] = \prod_{j=1}^{k} \varphi^1_{\mathbb{G}}\Big[\mathcal{C}_j \,\Big|\, \bigcap_{i>j} \mathcal{C}_i\Big] \leqslant \prod_{j=1}^{k} \varphi^1_{A_j}\big[\mathcal{C}_j\big],$$

where in the last inequality we use again the argument of exploration from outside and the comparison between boundary conditions. The complement of $\mathcal{C}_j$ is exactly the event that there exists a (primal) circuit in the annulus A_j. Hence, from Lemma 3.19, there exists a constant $c > 0$ such that for $j \geqslant J$, where J is a constant,

$$\varphi^1_{A_j}\big[\mathcal{C}_j\big] \leqslant 1 - c.$$

In conclusion, we have,

$$\varphi^1_{\mathbb{G}}\Big[0 \leftrightarrow \partial\Lambda(n)\Big] \leqslant \exp\Big[\ln(1-c)\Big(\tfrac{\ln n}{\ln 2} - J + 1\Big)\Big].$$

Hence, we may take $\beta = -\frac{\ln(1-c)}{\ln 2}$.

For the lower bound, let $R_i = [0, 2^{i-1}] \times [0, 2^i]$ for i odd and $R_i = [0, 2^i] \times [0, 2^{i-1}]$ for i even. We also write $\mathcal{C}_i = \mathcal{C}_v(R_i)$ for i odd and $\mathcal{C}_i = \mathcal{C}_h(R_i)$ for i even. The RSW property (3.1) gives δ such that for $i \geqslant I_0$, we have

$$\varphi^0_{2R_i}\big[\mathcal{C}_i\big] \geqslant \delta.$$

Take $n > 0$ and integer k such that $2^{k-1} \leqslant n < 2^k$. If $\mathcal{C}_i$ occurs for all $I_0 \leqslant i \leqslant k$, then we have a crossing from v to $\partial\Lambda(2^k)$ with $|v| \leqslant 2^{I_0}$. Hence, by the FKG inequality and the comparison between boundary conditions

$$\varphi^0_{\mathbb{G}}\Big[0 \leftrightarrow \partial\Lambda(n)\Big] \geqslant \prod_{i=I_0}^{k} \varphi^0_{2R_i}\big[\mathcal{C}_i\big] \geqslant \exp\Big[\ln\delta\Big(\tfrac{\ln n}{\ln 2} - I_0 + 1\Big)\Big].$$

To finish the proof, we choose $\alpha = -\frac{\ln\delta}{\ln 2}$. □

Proof of Corollary 3.3. We prove the corollary for $1 \leqslant q \leqslant 4$. Since $\varphi^1_{\mathbb{G},1,q}[0 \leftrightarrow \infty] = 0$ from Theorem 3.1, we also have $\varphi^1_{\mathbb{G},\beta,q}[0 \leftrightarrow \infty] = 0$ for all $\beta < 1$. Then Proposition C.1 implies the uniqueness of the measure for $\beta \leqslant 1$. For $\beta > 1$, we use the duality $\varphi^{\xi}_{\mathbb{G},\beta,q} = \varphi^{1-\xi}_{\mathbb{G}^*,1/\beta,q}$ for $\xi = 0, 1$ and apply what we just said above to $\mathbb{G}^*$. Hence, the uniqueness also follows for $\beta > 1$.

For the two remaining points, we use the fact that the unique measure $\varphi^0_{\mathbb{G},1,q} = \varphi^1_{\mathbb{G},1,q}$ satisfies the RSW property. Then, we can follow the same strategy as in [GM13b, Prop. 4.1 and 4.2]: the polynomial decay, Russo's formula and the theory of influence. □

Appendix **D**

Separation Lemma and Consequences

Fix $\eta > 0$ small enough and below we define the η-separated k-arm event using a grid of $\mathbb{G}$.

Cut the top boundary of $\partial\Lambda(n)$ into $2k+1$ parts $I_1^\eta, \dots, I_{2k+1}^\eta$ from left to right such that the intervals of the same parity have the same length: even ones are of length $2\eta n$ and odd ones $\frac{1-2k\eta}{k+1} n$. Repeat the same procedure to the top boundary of $\partial\Lambda(N)$ by replacing n by N and denote the resulting intervals by $J_1^\eta, \dots, J_{2k+1}^\eta$.

The *η-separated k-arm event* $A_k^\eta(n,N)$ is the event $A_k(n,N)$ with the following additional constraints:

- Each $\mathcal{P}_i$ connects I_{2i}^η to J_{2i}^η. We write $(x_i, N) \in J_{2i}^\eta$ for the endpoint on the outer boundary $\partial\Lambda(N)$.
- In the box $[x_i - \eta N, x_i + \eta N] \times [(1+\eta^{3/4})N, (1+\sqrt{\eta})N]$ there is a horizontal crossing of the same type as $\mathcal{P}_i$.
- The two above crossings are connected in $(x_i, N) + \Lambda(\sqrt{\eta}N)$.
- The same thing for the inner boundary.

The first item says that we can decide the position of each path $\mathcal{P}_i$ on the inner and the outer boundaries of the annulus $\mathcal{A}(n,N)$; the second and the third say that these crossings have a *η-fence* that will allow us to extend the arm events outwards; the last one states the same thing but inwards. This is illustrated in Figure D.1.

The following lemma says that the η-separated k-arm event is comparable to the k-arm event in probability. We remind that the random-cluster measure on $\mathbb{G}$ is unique for $1 \leqslant 1 \leqslant 4$ at $\beta = 1$, so we will simply write $\varphi_{\mathbb{G}}$ without any boundary conditions. However, on any finite domain R, there is not uniqueness: $\varphi_R^0 \neq \varphi_R^1$.

Lemma D.1 (Separation Lemma)**.** *Fix $k \in \mathbb{N}$ and $\eta \in (0,1)$. Then there exists $c > 0$ such that for all $N > n$ large enough, we have*

$$\varphi_{\mathbb{G}}[A_k^\eta(n,N)] \geqslant c\, \varphi_{\mathbb{G}}[A_k(n,N)].$$

To show the above separation lemma, we start by stating the following proposition about the extension of arms in larger boxes.

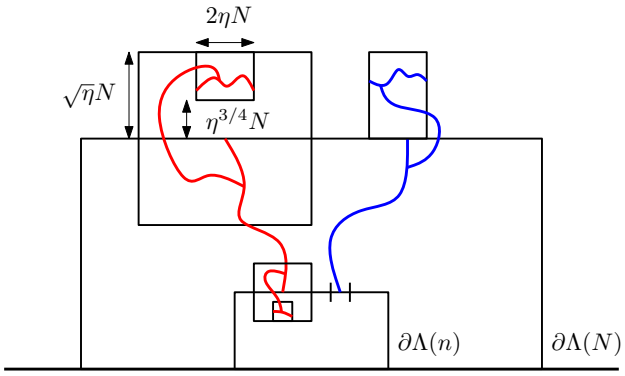

Figure D.1 – The η-separated 2-arm event that we draw only in the upper half-plane. The primal arm is drawn in red and the dual arm in blue. The η-fences on the exterior boundary are drawn but on the interior boundary, only the primal one is drawn, the dual one is omitted.

Proposition D.2 (Arms-extension Lemma). *There exists $c > 0$ such that for $N > 2n$ large enough,*

$$\varphi_{\mathbb{G}}[A_k(n,2N)] \geqslant c\,\varphi_{\mathbb{G}}[A_k(n,N)],$$
$$\varphi_{\mathbb{G}}[A_k(\tfrac{n}{2},N)] \geqslant c\,\varphi_{\mathbb{G}}[A_k(n,N)].$$

The proof of the Arms-extension Lemma is given below, and that of the Separation Lemma later. We note that in the case of the random-cluster model, we do not have independence between disjoint regions, but by comparing boundary conditions, we can still get rid of this constraint and proceed in a similar way as for the classical Bernoulli percolation.

Proof of Proposition D.2. We just show the first point, the second being similar.

Consider, for $1 \leqslant i \leqslant k$, the two following domains

$$R_i = (\tfrac{1}{2}J_{2i}^{\eta}) \times [(1+\eta^{3/4})N, 2N] \text{ and}$$
$$R_i' = J_{2i}^{\eta} \times [N, (2+\eta^{3/4})N].$$

Then, write $\mathcal{V}_i$ for the event that there exists a primal (for i odd) or a dual (for i even) vertical crossing in R_i. In other words, $\mathcal{V}_i = \mathcal{C}_v[R_i]$ for i odd and $\mathcal{V}_i = \mathcal{C}_v^*[R_i]$ for i even. See Figure D.2 for an illustration of the case $k = 2$.

Moreover, if $A_k^{\eta}(n,N)$ and $\mathcal{V}_i$ for $1 \leqslant i \leqslant k$ all occur, then so does $A_k(n,2N)$ due to the η-fences provided by $A_k^{\eta}(n,N)$ that grow on the boundary. Then,

$$\begin{aligned}\varphi_{\mathbb{G}}[A_k(n,2N)] &\geqslant \varphi_{\mathbb{G}}\Big[A_k^{\eta}(n,N) \cap (\mathcal{V}_1 \cap \cdots \cap \mathcal{V}_k)\Big] \\ &= \varphi_{\mathbb{G}}[A_k^{\eta}(n,N)] \cdot \prod_{i=1}^{k} \varphi_{\mathbb{G}}\Big[\mathcal{V}_i \,\Big|\, A_k^{\eta}(n,N) \cap \bigcap_{j<i} \mathcal{V}_j\Big]. \end{aligned} \tag{D.1}$$

By comparing boundary conditions and the RSW property, we get

$$\varphi_{\mathbb{G}}\Big[\mathcal{V}_i \,\Big|\, A_k^{\eta}(n,N) \cap \bigcap_{j<i} \mathcal{V}_j\Big] \geqslant \varphi_{R_i'}^{0}[\mathcal{V}_i] \geqslant c_1, \text{ for } i \text{ odd;} \tag{D.2}$$

$$\varphi_{\mathbb{G}}\Big[\mathcal{V}_i \,\Big|\, A_k^{\eta}(n,N) \cap \bigcap_{j<i} \mathcal{V}_j\Big] \geqslant \varphi_{R_i'}^{1}[\mathcal{V}_i] \geqslant c_1, \text{ for } i \text{ even,} \tag{D.3}$$

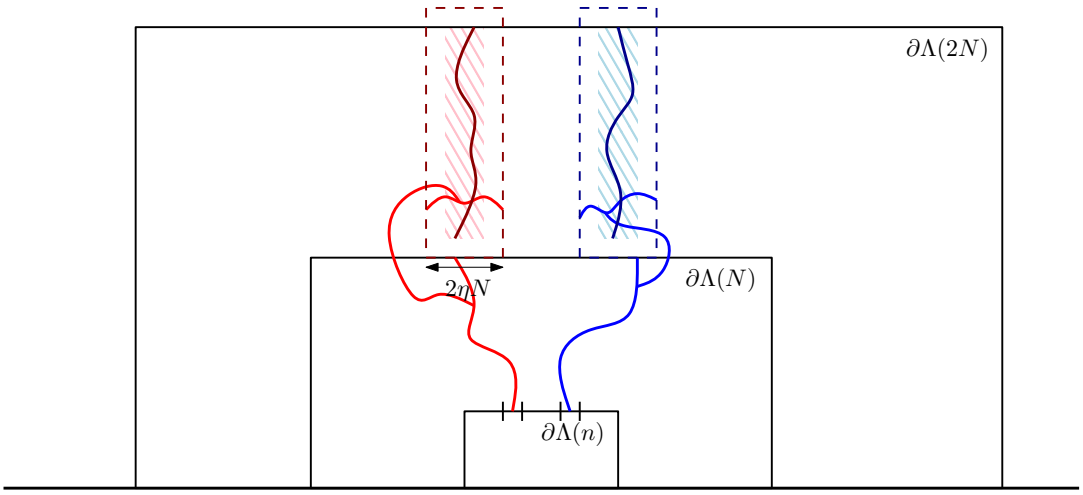

Figure D.2 – From the η-separated 2-arm event $A_2^\eta(n,N)$, we can add one vertical primal (darkred) and one vertical dual (darkblue) crossings such that $A_2(n,2N)$ is realized. In the figure we only draw the upper-half plane.

where $c_1 > 0$ does not depend on i. From Lemma D.1, we get $c_2 > 0$ such that

$$\varphi_{\mathbb{G}}[A_k^\eta(n,N)] \geqslant c_2\, \varphi_{\mathbb{G}}[A_k(n,N)]. \tag{D.4}$$

We replace (D.2)–(D.4) in (D.1) to conclude that

$$\varphi_{\mathbb{G}}^\xi[A_k(n,2N)] \geqslant c_1^k c_2\, \varphi_{\mathbb{G}}^\xi[A_k(n,N)].$$

□

The proof of the Separation Lemma (Lemma D.1) is based on the RSW property. It is almost identical to the one in the case of Bernoulli percolation, with the main difference that the random-cluster measure is not a product measure, thus no independence between disjoint domains. However, we can overcome this problem by means of the RSW property and the comparison between different boundary conditions. We start by introducing some notations and lemmas before showing Lemma D.1 in the end of this section.

Write $B_N = [0,8N]\times[0,N]$. For $\eta > 0$, the box B_N is said to be η-separable if any sequence of disjoint bottom-top crossings $(\Gamma_i)_i$ of alternating colors in B_N can be modified into $(\widetilde{\Gamma}_i)_i$ such that

- Each $\widetilde{\Gamma}_i$ has the same bottom-endpoint as Γ_i and is a bottom-top crossing of the same type as Γ_i.
- The endpoints of $\widetilde{\Gamma}_i$ are separated by at least $\sqrt{\eta}N$ from each other and from corners.
- At the top-endpoint of each $\widetilde{\Gamma}_i$, there is a η-fence. The definition of a η-fence is the same as above.

Unlike the definition of the η-separated k-arm event $A_k^\eta(n,N)$, we do not ask the crossings to land in some particular intervals.

To show Lemma D.1, we start with the following lemma.

Lemma D.3. *For $\nu > 0$, there exists $\eta' = \eta'(\nu) > 0$ and $N_0 = N_0(\nu) \in \mathbb{N}$ such that for any boundary conditions ξ and all $N \geqslant N_0$,*

$$\varphi^{\xi}_{2B_N}\Big[B_N \text{ is } \eta'\text{-separable}\Big] > 1 - \frac{\nu}{4}.$$

We note that the boundary conditions ξ here may be random, as in Lemma 3.13.

Lemma D.4. *There exist $C_1, C_2 > 0$ such that for $\nu > 0$ and $\eta' = \eta'(\nu)$ as given by Lemma D.3, for $N > n \geqslant N_0(\nu)$ and $\xi = 0, 1$, we have*

$$\varphi_{\mathbb{G}}\Big[A_k(2^n, 2^N)\Big] \leqslant C_1 \varphi_{\mathbb{G}}\Big[A_k^{\eta'}(2^n, 2^{N+1})\Big] + \nu \varphi_{\mathbb{G}}\Big[A_k(2^n, 2^{N-1})\Big]$$

and

$$\begin{aligned}\varphi_{\mathbb{G}}\Big[A_k(2^n, 2^N)\Big] &\leqslant \sum_{0 \leqslant j < N-n} C_1 \nu^j \varphi_{\mathbb{G}}\Big[A_k^{\eta'}(2^n, 2^{N-j+1})\Big] \\ &\leqslant \sum_{0 \leqslant j < N-n} C_1 C_2^j \nu^j \varphi_{\mathbb{G}}\Big[A_k^{\eta'}(2^n, 2^{N+1})\Big]. \end{aligned} \tag{D.5}$$

Proof. This lemma includes Lemmas 2.3.5–2.3.8 from [Man12].

We cut the event $A_k(2^n, 2^N)$ into two disjoint subsets A_k^1 and A_k^2. The subset A_k^1 is such that one of the four rectangles forming the annulus $\mathcal{A}(2^{N-1}, 2^N)$ is not η'-separable. We write

$$\begin{aligned} R_1 &= [-2^{N+1}, 2^{N+1}] \times [3 \cdot 2^{N-1}, 2^{N+1}], \\ R_2 &= [-2^{N+1}, 2^{N+1}] \times [-2^{N+1}, -3 \cdot 2^{N-1}], \\ R_3 &= [3 \cdot 2^{N-1}, 2^{N+1}] \times [-2^{N+1}, 2^{N+1}], \\ R_4 &= [-2^{N+1}, -3 \cdot 2^{N-1}] \times [-2^{N+1}, 2^{N+1}]. \end{aligned}$$

See Figure D.3.

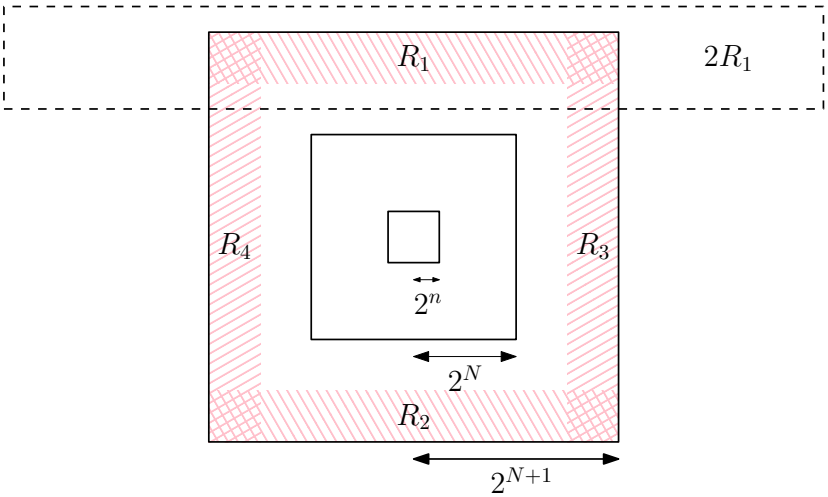

Figure D.3 – Boxes R_i are shaded in red. Each arm coming from $\partial\Lambda(2^n)$ should go through one of R_i before reaching $\partial\Lambda(2^N)$.

This gives

$$\begin{aligned}\varphi_{\mathbb{G}}[A_k^1] &= \varphi_{\mathbb{G}}[\text{one of } R_1,\dots R_4 \text{ is not } \eta'\text{-separable and } A_k(2^n,2^N)]\\ &\leqslant 4\varphi_{\mathbb{G}}[R_1 \text{ is not } \eta'\text{-separable and } A_k(2^n,2^N)]\\ &= 4\varphi_{\mathbb{G}}[A_k(2^n,2^N)]\varphi_{\mathbb{G}}[R_1 \text{ is not } \eta'\text{-separable}|A_k(2^n,2^N)]\\ &\leqslant \nu\varphi_{\mathbb{G}}[A_k(2^n,2^N)],\end{aligned}$$

where we apply Lemma D.3 in the last line, by choosing ξ the boundary conditions induced by $\varphi_{\mathbb{G}}$ on R_1 knowing $A_k(2^n,2^N)$.

Concerning A_k^2, it is the event that all the four rectangles $R_1,\dots,R_4$ are η'-separable, but the endpoints of the arms might not distributed as we wish as in $A_k^{\eta'}(2^n,2^N)$. However, [Man12, Lem. 2.3.6] is a combinatorial lemma, allowing us to pick a sequence of intervals in which the endpoints have the highest probability to land in. Then, from this sequence, one can extend the arms to the next scale and ask the position of these endpoints to be distributed as in $A_k^{\eta'}(2^n,2^{N+1})$ [Man12, Lem. 2.3.7]. The second step is basically what we did in the proof of Proposition D.2. These two steps together give the constant $C_1>0$. The first inequality has been shown.

For the recurrence step, one uses the same technique to extend arms to get $C_2>0$ which is the cost to make the arms distributed as in $A_k^{\eta'}$ at all the scales. This is Lemma 2.3.8 from [Man12].

□

Proof of Lemma D.3. Fix $\nu>0$ and we show the lemma in three steps:

- with high probability, the number of crossings cannot be too large;
- the crossings can be made to be far from each other and from the corners;
- we can construct fences from the endpoints of the crossings.

The proof is based on circuits in concentric annuli and more precisely, on Lemma 3.19.

Let I be the number of disjoint horizontal crossings of B_N with alternating colors. Write $\mathcal{E}_1,\dots,\mathcal{E}_I$ for the existence of such crossings from left to right. If they exist, denote the crossings by $\Gamma_1,\dots,\Gamma_I$ and their right endpoints $z_1,\dots,z_I$. Then, we can write

$$\varphi^{\xi}_{2B_N}[I\geqslant T]\leqslant\varphi^{\xi}_{2B_N}\Big[\bigcap_{i=1}^{T}\mathcal{E}_i\Big]=\prod_{i=1}^{T}\varphi^{\xi}_{2B_N}\Big[\mathcal{E}_i\Big|\bigcap_{j=1}^{i-1}\mathcal{E}_j\Big].$$

We estimate the probability in the product above as follows. We start by exploring the crossings from the left of B_N knowing $\cap_{j=1}^{i-1}\mathcal{E}_j$. Assume for example that $\mathcal{E}_i$ is a primal crossing. Then,

$$\varphi^{\xi}_{2B_N}\Big[\mathcal{E}_i\Big|\bigcap_{j=1}^{i-1}\mathcal{E}_j\Big]\leqslant\varphi^{1}_{2B_N}[\mathcal{E}_i]\leqslant 1-c,$$

where $c>0$ is a uniform constant in i provided by the RSW property. See Figure D.4 for an illustration. Hence,

$$\varphi^{\xi}_{2B_N}[I\geqslant T]\leqslant(1-c)^T.$$

Take $T\geqslant T_0(\nu)=\frac{\ln\nu}{\ln(1-c)}$ so we have $(1-c)^T\leqslant\nu$.

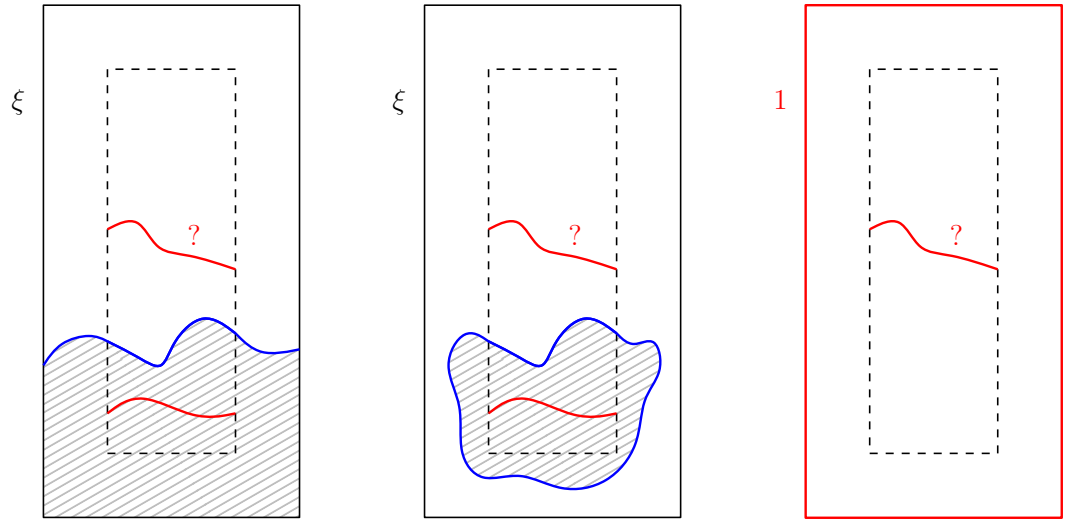

Figure D.4 – (a) (b) We explore the horizontal crossings from the bottom of B_N. Explored area is shaded in grey. In any of these two cases, the induced boundary conditions are less favaroable than that in (c).

Denote Z^- (resp. Z^+) the upper left (resp. upper right) corner of B_N. Now we show the two following points.

- With high probability, the corners Z^- and Z^+ are far from all the other endpoints z_i.
- Let $\nu' = \frac{\nu}{T}$. The probability that each crossing of B_N may be made into a η-fence is greater than $1 - \nu'$.

The proofs work exactly in the same way as in the case of the Bernoulli percolation once Lemma 3.19 is at our disposition. We will just give a sketch here.

For $\eta > 0$, we say that Z^- is η-protected if there exist one primally-open and one dually-open path both at distance at least $\sqrt{\eta}N$ from Z^-, separating Z^- from the bottom of B_N. See Figure D.5 for an illustration. The same definition also applies to Z^+ with Z^- replaced.

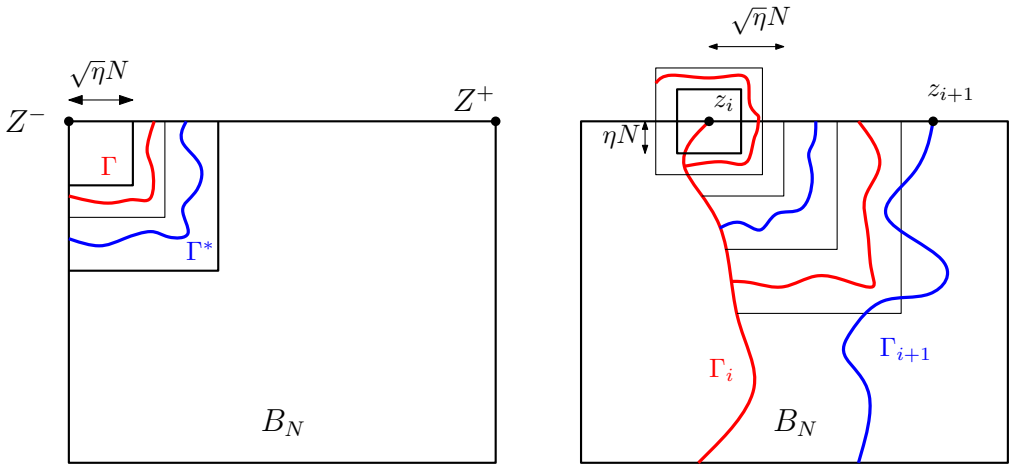

Figure D.5 – **Left:** The corner Z^- is η-protected. **Right:** The endpoint z_i is η-protected and there is a η-fence for the path Γ_i.

Write $A_i = Z^- + \mathcal{A}(\sqrt{\eta}N2^i, \sqrt{\eta}N2^{i+1})$ for the annulus centered at Z^- with outer radius $\sqrt{\eta}N2^{i+1}$ and inner radius $\sqrt{\eta}N2^i$. The number of such annuli is given by maximal K such that $\sqrt{\eta}2^{K+1} < 1$, or $K = -\frac{1}{2}\frac{\ln \eta}{\ln 2} - 1$. We also denote by Γ and Γ^* the outmost primal and the dual circuit at distance at least $\sqrt{\eta}N$ from Z^-. This gives

$$\varphi^{\xi}_{2B_N}\Big[Z^- \text{ is not } \eta\text{-protected}\Big] \leqslant \varphi^{\xi}_{2B_N}\Big[\Gamma \text{ does not exist}\Big] + \varphi^{\xi}_{2B_N}\Big[\Gamma^* \text{ does not exist}\Big].$$

Consider $c > 0$ as given by Lemma 3.19. We explore the configuration from outside annulus by annulus and use the classic argument of conditioning, then we get

$$\varphi^{\xi}_{2B_N}\Big[\Gamma \text{ does not exist}\Big] \leqslant (1-c)^K.$$

For K large enough (η small enough), this quantity can be made smaller than ν. More precisely, we need the following condition

$$\eta \leqslant \exp\left[-\frac{2\ln \nu}{\ln(1-c)}\ln 2 - 2\ln 2\right] =: \eta_1(\nu)$$

The same bound can also be obtained for the non-existence of Γ^*. In conclusion, we have

$$\varphi^{\xi}_{2B_N}\Big[Z^+ \text{ is not } \eta\text{-protected}\Big] \leqslant 2\nu \qquad \text{and}$$
$$\varphi^{\xi}_{2B_N}\Big[Z^- \text{ is not } \eta\text{-protected}\Big] \leqslant 2\nu.$$

We come to the endpoints of vertical crossings Γ_i. Recall that $\nu' = \frac{\nu}{T}$ and we will show that for η small enough, the probability that each Γ_i can be made into a η-fence is greater than $1-\nu'$.

For $K \in \mathbb{N}$ to be chosen later, an endpoint z_i is said to be η-protected if:

- One of the annuli $\mathcal{A}(\eta N2^k, \eta N2^{k+1})$, $\frac{K}{2} \leqslant i \leqslant K$, contains a circuit of the same color as Γ_i. See the inner-most annulus around z_i on the right-hand side of Figure D.5.
- There are two annuli among $\mathcal{A}(\sqrt{\eta}N2^k, \sqrt{\eta}N2^{k+1})$, $1 \leqslant i \leqslant K$ such that one contains a primally-open (resp. dually-open) path connecting Γ_i to $\{N\} \times \mathbb{R}$.

We will take η and K such that $\sqrt{\eta}2^{K+1} < 1 < \sqrt{\eta}2^{K+2}$. As such, if z_i is η-protected, the first point guarantees that there is a circuit of the same color as Γ_i in $\mathcal{A}(\eta^{3/4}N, \sqrt{\eta}N)$, which creates a η-fence. Then, the second point ensures that different z_i's are separated by distance larger than $\sqrt{\eta}N$.

As before with an exploration process from below and the comparison between boundary conditions, we can show that

$$\varphi^{\xi}_{2B_N}\Big[z_i \text{ is not } \eta\text{-protected}\Big] \leqslant 3(1-c)^K,$$

where $c > 0$ is again given by Lemma 3.19 which only depends on the RSW property. Finally, choose

$$\eta \leqslant \exp\left[-\frac{2\ln \nu'}{\ln(1-c)}\ln 2 - 2\ln 2\right] =: \eta_2(\nu),$$

and we have

$$\varphi^{\xi}_{2B_N}\Big[z_i \text{ is not } \eta\text{-protected}\Big] \leqslant 3\nu',$$

In summary, we have

$$\begin{aligned}\varphi^{\xi}_{2B_N}[B_N \text{ is not } \eta\text{-separable}] &\leqslant \varphi^{\xi}_{2B_N}[I > T] \\ &\quad + \varphi^{\xi}_{2B_N}\Big[Z^+ \text{ is not } \eta\text{-protected}\Big| I \leqslant T\Big] \\ &\quad + \varphi^{\xi}_{2B_N}\Big[Z^- \text{ is not } \eta\text{-protected}\Big| I \leqslant T\Big] \\ &\quad + \varphi^{\xi}_{2B_N}\Big[\text{one of the } z_i\text{'s is not } \eta\text{-protected}\Big| I \leqslant T\Big] \\ &\leqslant \nu + 2\nu + 2\nu + 3\nu' T = 7\nu.\end{aligned}$$

□

Now we are ready to show the separation lemma in the case of the random-cluster model.

Proof of Lemma D.1. It is a consequence of Lemma D.4. We take $C_1, C_2 > 0$ as given in the lemma. Pick $\nu = \frac{C_2}{2}$ and η' as given by Lemma D.3. Then, Equation (D.5) gives

$$\varphi_{\mathbb{G}}\Big[A_k(2^n, 2^N)\Big] \leqslant 2C_1 \varphi_{\mathbb{G}}\Big[A_k^{\eta'}(2^n, 2^{N+1})\Big].$$

□

Bibliography

[ABF87] Aizenman, M., Barsky, D. J., and Fernández, R. The phase transition in a general class of Ising-type models is sharp. *J. Statist. Phys.*, 47(3-4):343–374, 1987.

[Bax82] Baxter, R. J. *Exactly solved models in statistical mechanics.* Academic Press, Inc. [Harcourt Brace Jovanovich, Publishers], London, 1982.

[BD12] Beffara, V. and Duminil-Copin, H. The self-dual point of the two-dimensional random-cluster model is critical for $q \geqslant 1$. *Probab. Theory Related Fields*, 153(3-4):511–542, 2012.

[BDC12] Beffara, V. and Duminil-Copin, H. The self-dual point of the two-dimensional random-cluster model is critical for $q \geqslant 1$. *Probab. Theory Related Fields*, 153(3-4):511–542, 2012.

[BDCS15] Beffara, V., Duminil-Copin, H., and Smirnov, S. On the critical parameters of the $q \leqslant 4$ random-cluster model on isoradial graphs. *J. Phys. A*, 48(48):484003, 25, 2015.

[BG09] Björnberg, J. E. and Grimmett, G. R. The phase transition of the quantum Ising model is sharp. *J. Stat. Phys.*, 136(2):231–273, 2009.

[BG15] Bobenko, A. I. and Günther, F. Discrete complex analysis on planar quad-graphs. *arXiv:1505.05673*, 2015.

[BH16] Benoist, S. and Hongler, C. The scaling limit of critical Ising interfaces is cle (3). *arXiv:1604.06975*, 2016.

[Bjö13] Björnberg, J. E. Infrared bound and mean-field behaviour in the quantum Ising model. *Comm. Math. Phys.*, 323(1):329–366, 2013.

[BMS05] Bobenko, A. I., Mercat, C., and Suris, Y. B. Linear and nonlinear theories of discrete analytic functions. Integrable structure and isomonodromic Green's function. *J. Reine Angew. Math.*, 583:117–161, 2005.

[BPZ84a] Belavin, A. A., Polyakov, A. M., and Zamolodchikov, A. B. Infinite conformal symmetry in two-dimensional quantum field theory. *Nuclear Phys. B*, 241(2):333–380, 1984.

[BPZ84b] Belavin, A. A., Polyakov, A. M., and Zamolodchikov, A. B. Infinite conformal symmetry of critical fluctuations in two dimensions. *J. Statist. Phys.*, 34(5-6):763–774, 1984.

[Büc08] Bücking, U. Approximation of conformal mappings by circle patterns. *Geom. Dedicata*, 137:163–197, 2008.

[Car92] Cardy, J. L. Critical percolation in finite geometries. *J. Phys. A*, 25(4):L201–L206, 1992.

[Car96] Cardy, J. *Scaling and renormalization in statistical physics*, volume 5. Cambridge university press, 1996.

[CDCH+14] Chelkak, D., Duminil-Copin, H., Hongler, C., Kemppainen, A., and Smirnov, S. Convergence of Ising interfaces to Schramm's SLE curves. *C. R. Math. Acad. Sci. Paris*, 352(2):157–161, 2014.

[CHI15] Chelkak, D., Hongler, C., and Izyurov, K. Conformal invariance of spin correlations in the planar Ising model. *Ann. of Math. (2)*, 181(3):1087–1138, 2015.

[CS11] Chelkak, D. and Smirnov, S. Discrete complex analysis on isoradial graphs. *Adv. Math.*, 228(3):1590–1630, 2011.

[CS12] Chelkak, D. and Smirnov, S. Universality in the 2D Ising model and conformal invariance of fermionic observables. *Invent. Math.*, 189(3):515–580, 2012.

[DC13] Duminil-Copin, H. *Parafermionic observables and their applications to planar statistical physics models*, volume 25. Ensaios Matemáticos, 2013.

[DCHN11] Duminil-Copin, H., Hongler, C., and Nolin, P. Connection probabilities and RSW-type bounds for the two-dimensional FK Ising model. *Comm. Pure Appl. Math.*, 64(9):1165–1198, 2011.

[DCLM17] Duminil-Copin, H., Li, J.-H., and Manolescu, I. Universality for random-cluster model on isoradial graphs. *In preparation*, 2017.

[DCM16] Duminil-Copin, H. and Manolescu, I. The phase transitions of the planar random-cluster and Potts models with $q \geqslant 1$ are sharp. *Probability Theory and Related Fields*, 164(3):865–892, 2016.

[DCS12] Duminil-Copin, H. and Smirnov, S. Conformal invariance of lattice models. In *Probability and statistical physics in two and more dimensions*, volume 15 of *Clay Math. Proc.*, pages 213–276. Amer. Math. Soc., Providence, RI, 2012.

[DCST17] Duminil-Copin, H., Sidoravicius, V., and Tassion, V. Continuity of the Phase Transition for Planar Random-Cluster and Potts Models with $1 \leqslant q \leqslant 4$. *Comm. Math. Phys.*, 349(1):47–107, 2017.

[DGH+16] Duminil-Copin, H., Gagnebin, M., Harel, M., Manolescu, I., and Tassion, V. Discontinuity of the phase transition for the planar random-cluster and Potts models with $q > 4$. *ArXiv e-prints*, November 2016.

[Don51] Donsker, M. D. An invariance principle for certain probability linit theorems. *Mem. Amer. Math. Soc.*, 1951.

[Don52] Donsker, M. D. Justification and extension of doob's heuristic approach to the kolmogorov-smirnov theorems. *The Annals of mathematical statistics*, pages 277–281, 1952.

[DRT16] Duminil-Copin, H., Raoufi, A., and Tassion, V. A new computation of the critical point for the planar random-cluster model with $q \geqslant 1$. *ArXiv e-prints*, April 2016.

[DRT17] Duminil-Copin, H., Raoufi, A., and Tassion, V. Sharp phase transition for the random-cluster and Potts models via decision trees. *ArXiv e-prints*, May 2017.

[DS12] Duminil-Copin, H. and Smirnov, S. Conformal invariance of lattice models. In *Probability and statistical physics in two and more dimensions*, volume 15 of *Clay Math. Proc.*, pages 213–276. Amer. Math. Soc., Providence, RI, 2012.

[Duf56] Duffin, R. J. Basic properties of discrete analytic functions. *Duke Math. J.*, 23:335–363, 1956.

[Duf68] Duffin, R. J. Potential theory on a rhombic lattice. *J. Combinatorial Theory*, 5:258–272, 1968.

[Dum17] Duminil-Copin, H. Lectures on the Ising and Potts models on the hypercubic lattice. *ArXiv e-prints*, July 2017.

[ES88] Edwards, R. G. and Sokal, A. D. Generalization of the Fortuin-Kasteleyn-Swendsen-Wang representation and Monte Carlo algorithm. *Phys. Rev. D (3)*, 38(6):2009–2012, 1988.

[FK72] Fortuin, C. M. and Kasteleyn, P. W. On the random-cluster model. I. Introduction and relation to other models. *Physica*, 57:536–564, 1972.

[GG11] Graham, B. and Grimmett, G. Sharp thresholds for the random-cluster and Ising models. *Ann. Appl. Probab.*, 21(1):240–265, 2011.

[GHP16] Gheissari, R., Hongler, C., and Park, S. Ising model: Local spin correlations and conformal invariance. *arXiv:1312.4446*, 2016.

[GM13a] Grimmett, G. R. and Manolescu, I. Inhomogeneous bond percolation on square, triangular and hexagonal lattices. *Ann. Probab.*, 41(4):2990–3025, 2013.

[GM13b] Grimmett, G. R. and Manolescu, I. Universality for bond percolation in two dimensions. *Ann. Probab.*, 41(5):3261–3283, 2013.

[GM14] Grimmett, G. R. and Manolescu, I. Bond percolation on isoradial graphs: criticality and universality. *Probab. Theory Related Fields*, 159(1-2):273–327, 2014.

[GOS08] Grimmett, G. R., Osborne, T. J., and Scudo, P. F. Entanglement in the quantum Ising model. *J. Stat. Phys.*, 131(2):305–339, 2008.

[Gri99] Grimmett, G. *Percolation.* Springer, Berlin. Math. Review 2001a, 1999.

[Gri06] Grimmett, G. *The random-cluster model*, volume 333 of *Grundlehren der Mathematischen Wissenschaften [Fundamental Principles of Mathematical Sciences]*. Springer-Verlag, Berlin, 2006.

[Gri10] Grimmett, G. *Probability on Graphs: Random Processes on Graphs and Lattices*. Institute of Mathematical Statistics Textbooks. Cambridge University Press, 2010.

[Hol74] Holley, R. Remarks on the FKG inequalities. *Comm. Math. Phys.*, 36:227–231, 1974.

[HS13] Hongler, C. and Smirnov, S. The energy density in the planar Ising model. *Acta Math.*, 211(2):191–225, 2013.

[HVK17] Hongler, C., Viklund, F. J., and Kytölä, K. Conformal field theory at the lattice level: Discrete complex analysis and virasoro structure. *arXiv:1307.4104v2*, 2017.

[Iof09] Ioffe, D. Stochastic geometry of classical and quantum Ising models. In *Methods of contemporary mathematical statistical physics*, volume 1970 of *Lecture Notes in Math.*, pages 87–127. Springer, Berlin, 2009.

[Isi25] Ising, E. Beitrag zur theorie des ferromagnetismus. *Zeitschrift für Physik A Hadrons and Nuclei*, 31(1):253–258, 1925.

[Ken99] Kennelly, A. E. The equivalence of triangles and three-pointed stars in conducting networks. *Electrical world and engineer*, 34(12):413–414, 1899.

[Ken93] Kenyon, R. Tiling a polygon with parallelograms. *Algorithmica*, 9(4):382–397, 1993.

[Ken02] Kenyon, R. The Laplacian and Dirac operators on critical planar graphs. *Invent. Math.*, 150(2):409–439, 2002.

[KS05] Kenyon, R. and Schlenker, J.-M. Rhombic embeddings of planar quad-graphs. *Trans. Amer. Math. Soc.*, 357(9):3443–3458, 2005.

[KS12] Kemppainen, A. and Smirnov, S. Random curves, scaling limits and Loewner evolutions. *arXiv preprint arXiv:1212.6215*, 2012.

[KS15] Kemppainen, A. and Smirnov, S. Conformal invariance of boundary touching loops of FK Ising model. *arXiv:1509.08858*, 2015.

[KS16] Kemppainen, A. and Smirnov, S. Conformal invariance in random cluster models. II. Full scaling limit as a branching SLE. *arXiv:1609.08527*, 2016.

[Kur63] Kurowski, G. J. Semi-discrete analytic functions. *Trans. Amer. Math. Soc.*, 106:1–18, 1963.

[Kur64] Kurowski, G. J. On the convergence of semi-discrete analytic functions. *Pacific J. Math.*, 14:199–207, 1964.

[Kur67] Kurowski, G. J. A convolution product for semi-discrete analytic functions. *J. Math. Anal. Appl.*, 20:421–441, 1967.

[KW41] Kramers, H. A. and Wannier, G. H. Statistics of the two-dimensional ferromagnet. I. *Phys. Rev. (2)*, 60:252–262, 1941.

[Len20] Lenz, W. Beitrag zum verständnis der magnetischen erscheinungen in festen körpern. *Z. Phys.*, 21:613–615, 1920.

[Man12] Manolescu, I. *Universality for planar percolation.* PhD thesis, University of Cambridge, 2012.

[Mer01] Mercat, C. Discrete Riemann surfaces and the Ising model. *Comm. Math. Phys.*, 218(1):177–216, 2001.

[Ons44] Onsager, L. Crystal statistics. I. A two-dimensional model with an order-disorder transition. *Phys. Rev. (2)*, 65:117–149, 1944.

[Pei36] Peierls, R. On Ising's model of ferromagnetism. In *Mathematical Proceedings of the Cambridge Philosophical Society*, volume 32, pages 477–481. Cambridge University Press, 1936.

[Pfe70] Pfeuty, P. The one-dimensional Ising model with a transverse field. *Annals of Physics*, 57(1):79–90, 1970.

[Rus78] Russo, L. A note on percolation. *Z. Wahrscheinlichkeitstheorie und Verw. Gebiete*, 43(1):39–48, 1978.

[Sch00] Schramm, O. Scaling limits of loop-erased random walks and uniform spanning trees. *Israel J. Math.*, 118:221–288, 2000.

[Sch07] Schramm, O. Conformally invariant scaling limits: an overview and a collection of problems. In *International Congress of Mathematicians. Vol. I*, pages 513–543. Eur. Math. Soc., Zürich, 2007.

[Smi01] Smirnov, S. Critical percolation in the plane: conformal invariance, Cardy's formula, scaling limits. *C. R. Acad. Sci. Paris Sér. I Math.*, 333(3):239–244, 2001.

[Smi06] Smirnov, S. Towards conformal invariance of 2D lattice models. In *International Congress of Mathematicians. Vol. II*, pages 1421–1451. Eur. Math. Soc., Zürich, 2006.

[Smi10] Smirnov, S. Conformal invariance in random cluster models. I. Holomorphic fermions in the Ising model. *Ann. of Math. (2)*, 172(2):1435–1467, 2010.

[SW78] Seymour, P. D. and Welsh, D. J. A. Percolation probabilities on the square lattice. *Ann. Discrete Math.*, 3:227–245, 1978. Advances in graph theory (Cambridge Combinatorial Conf., Trinity College, Cambridge, 1977).

[ZJ07] Zinn-Justin, J. *Phase transitions and renormalization group.* Oxford University Press on Demand, 2007.